Energy Harvesting Potential of a Micro-Thermal Network Using a Nodal Approach to Reduce GHG Emissions in Mixed Electrical Grids

Energy Harvesting Potential of a Micro-Thermal Network Using a Nodal Approach to Reduce GHG Emissions in Mixed Electrical Grids

By Ahmed Abdalla, M.A.Sc., B.A.Sc.

A Thesis Submitted to the School of Graduate Studies in Partial Fulfillment of the Requirements for the Degree

Doctor of Philosophy

in Mechanical Engineering

McMaster University

Doctor of Philosophy (2023) McMaster University

Mechanical Engineering Hamilton, Ontario

TITLE: Energy Harvesting Potentials in Energy Intensive Communities and the Impact of Integrating Thermal and Electrical Energy Systems on the Reduction of GHG Emissions and Regional Electrical Grids

AUTHOR: Ahmed Abdalla

B.A.Sc. (October 6 University)

M.A.Sc. (Cairo University)

SUPERVISORS: Dr. James S. Cotton, Professor, Department of Mechanical Engineering

Dr. Scott Bucking, Associate Professor, Department of Civil and Environmental Engineering, Carleton University

NUMBER OF PAGES: xix, 198

Abstract

Integrating the electrical and thermal community buildings' energy systems can play an important role in harvesting wasted energy resources and reduction of carbon emissions from buildings and electricity generation sectors. It also increases demand management flexibility by minimizing the curtailed electricity on the grid through electrified heating without increasing the electricity peak demand. The current work examines Integrated Community Energy and Harvesting systems (ICE-Harvest), a new generation of distributed energy resources systems (DERs). They prioritize the harvesting of community waste energy resources—for example, heat rejected from cooling processes and distributed peak electricity fossil-fuel-fired generators, as well as energy from curtailed clean grid electricity resources—to help in satisfying the heating demands of commercial and residential buildings. As such, ICE-Harvest systems provide a solution that can minimize greenhouse gas emissions from high-energy-consumption buildings in cold-climate regions such as North America and Northern Europe.

In the current research, a thermal energy sharing model was developed to provide a dynamic characterization of the potential benefits of integrating and harvesting energy within a community of any number of buildings. The proposed model estimates the amount of rejected heat from cooling and refrigeration systems that can be simultaneously collected and used to heat other nearby buildings connected with a low temperature microthermal network (MTN). It also determines the proper timing and quantity of electricity used by the heat pumps in low-temperature MTNs as well as the reduction of both GHG emissions and the energy required from the EMC relative to conventional stand-alone systems. For an energy-balanced community cluster, the model showed that, over the course of a year, the energy harvesting would reduce this node’s GHG

emissions by 74% and cover approximately 82% of the heating requirements compared to the BAU system.

The results also revealed that the diversity in thermal demand between the connected buildings increases the harvesting potential. This research develops two clustering methods for the ICE-Harvest system. The proposed methods are clustering around anchor building and density-based (DB) clustering with post-processing by adding the closest anchor building to each cluster that focuses on the diversity of the buildings in each cluster. The energy sharing model is used to examine these techniques in comparison with the density-based clustering technique, the commonly used technique in the literature on a large database of 14000 high energy consumption buildings collected in Ontario, Canada. The results of this case study reveal that DB clustering with post-processing resulted in the largest emission reduction per unit piping network length of 360 t CO_{2eq} /km/year. In addition, this research identified seven different cluster categories based on the total and simultaneous cooling-to-heating ratios of each cluster.

The ICE harvest system integrates the thermal and electrical networks to add more flexibility to the electricity grid and schedule the electrification of heating (EoH). Current research provides a reduced model for the ICE-Harvest system to study its impact for over 1100 clusters of different categories on a provincial scale on the GHG emission and electricity demand from the grid. The use of ICE-Harvest systems at this scale can displace the energy required from the gas-fired heating resources by 11 TWh, accounting for over 70% of the clusters' total heating requirements. This results in a 1.9 Mt CO_{2eq} reduction in total GHG emissions, which represents around 60% of the clusters' emissions.

Operating conditions of the thermal network (TN) in the integrated community energy systems affect the ability to harvest waste energy and the reduction of GHG emissions as well as the

electricity peak demand and consumption. In the current research, modeling of different thermal distribution network operating scenarios was performed for the different community energy profile clusters. These operation scenarios include low-temperature (fourth generation), ultra-low (fifth generation), a binary range-controlled temperature modulating thermal network operating between Low and Ultra-low temperatures (ICE-Harvest), and a new proposed scenario wherein a continuous range-controlled temperature modulating micro-thermal network. The continuous range-controlled temperature scenario shows the most benefits with the large implementation on the identified clusters. It adds more flexibility to balance the electricity grid as well as results in large GHG emission savings while controlling the increase in site electricity peak demand.

The load profile of the cluster affects the selection of the most beneficial energy integrated system. This research shows that, for most of the heating-dominated clusters, it is better to employ the continuous range-controlled temperature TN with peak control and CHP on sites to serve the high heating demands along with short term and seasonal thermal storage. For the majority of balanced and /or cooling-dominated clusters, it is better to implement more carbon-free resources to the electricity grid or on-site that produce electricity but are not associated with heat such as wind, hydro, and solar PV panels. Parametric studies were performed in this research including changing the CHP size, the CHP utilization efficiency, and the grid gas-fired generators usage conditions to show their impact on the GHG emissions reduction from the clustered buildings.

The analysis was implemented on a fleet of 1139 sites in Ontario and the results showed that the CHP size and operating hours have a measurable impact on GHG emission saving. The system can reach up to 58% and 66.5% emission savings of the total sites' emissions with 93% and 39% operating hours respectively following the Ontario grid natural gas peaking power plants for the

years of 2016 and 2017 with larger CHP sizes. The largest share of GHG emission saving in 2016 is by the CHP (61%) as opposed to 30% in 2017.

The reduced models introduced in this research for the thermal energy sharing, the ICE-harvest system operation and sizing, and the MTN operation aid the investigation of the impact of the large implementation of the ICE-Harvest systems on the GHG emissions and electricity grid.

Dedication

This Thesis is dedicated to the following special people in my life:

To my late father **Saber Abdalla**, Dad, I wish you were here to be proud of your son. I miss you each and every day, you were my hero, and you always believed in me. Your endless love, guidance, and the good you instilled in me continue to bless my life. O Allah forgive and have mercy upon him, excuse him and pardon him, make honorable his reception, and grant him paradise, next to your beloved prophet Muhammad (Peace be upon him).

To my mother **Nabilahanem**, Mom, I owe you my life, I can't imagine my life without you. I will never be able to fulfill your rights upon me, you have always been there for me in time of need, you gave me the most precious feeling in the world, and you BELIEVED in me. You are always my inspiration. You are a great example of hard work, patience, and kindness above all. I am truly indebted to you and dad for who I am today.

My brothers, **Mohamed and Galal**, you are like fathers to me. You always have my back. You are my lifeboat when I am drowning. My sister, **Fatma**, you used to push me forward to start this journey, without you I wouldn't have accomplished any of that. My brother-in-law, **Saber**, I owe you too much, you were always like a brother to me, thank you for your support and guidance. The apple of my eye, my sister **Nehal**, you are ardently loved and missed.

Love You!!

Acknowledgments

In the name of Allah, the Most Gracious and the Most Merciful, all praise is due to Allah alone for blessing me with patience, knowledge, and strength to complete this work and granting me everything in my life.

I would like to express my gratitude toward my supervisors; Dr. Cotton and Dr. Bucking. No words can describe my gratitude toward Dr. Cotton. His critical organized way of thinking and revision throughout this program was the key to having the work in its present form. Dr. Cotton is a great leader, his suggestions and fruitful discussions were a motivation throughout the course of this work. Thank you, Dr. Bucking for guiding me and supporting me all the time. I would have never accomplished this without the mentorship of Dr. Cotton and Dr. Bucking.

I am also grateful to my supervisory committee members, Dr. Lightstone and Dr. Adams for their suggestions and comments during our annual meetings.

Special thanks to Dr. Saber, Dr. Yasser, Dr. Vick, Dr. Chebeir, Dr. Shady, Dr. Marin, Dr. Heidari, Dr. Elhameh, Kelton, and Jeff, you never hesitate to offer help and guidance.

Thank you to the ICE-Harvest amazing team, Ryan, Brenden, Chantel, Briana, Alireza, Joshua, Jessica, Nina, Mina, Jacob, Max, Stacey, and Farid, I learned a lot from you.

Thank you to Mechanical Engineering administrators, Nicole, Lily, and Leslie. Whenever I ask for help you instantly do your best to help, you always make it easy for us.

Special thanks to Safy, you always make everything easy for me, your very helpful person. Thank you for being such a good friend and helping me through this challenging Ph.D. journey.

Special thanks to my dear friend Hassan, I always loved our gatherings and chatting. You are a great friend that I am glad to have.

Thank you to my lab friends Abdelnabi, Hamouda, and Saksham, I had a wonderful time with you that I will never forget.

Thank you to my Egyptian friends Ahmed Ali, Ahmed Teamah, Samy, Hammouda, Abdelaltif, Waraky, and Fathalla.

I would like to thank my lifetime friends; Ahmed Hisham, Ahmed Adel, Mahmoud Gamal, Ahmed Abdella, Ahmed Shaaban, Mahmoud Shehata, Eslam Hussien, Youssef, Shika, Mohamed Ramzi, Mostafa Ramzi, and Samy Bakry.

Table of Contents

List of Tables

List of Figures

Notations and Abbreviations

Nomenclature

Q	Heat flow rate [kW]
T	Temperature [°C]
L	Length [m]
W	Electric work (kW]
E	Electricity demand [kW]

Subscripts

B	Relating to a building
boiler	Relating to the boiler
C	Relating to a cooling process
CHP	Relating to a CHP
Conv	Relating to conventional system
Elec	Related to electricity
H	Relating to a heating process
HP	Relating to a heat pump
max	Maximum allowed or expected value
min	Minimum allowed or expected value
rej	Heat rejection from cooling systems
rej-s	Surplus heat rejection from cooling systems
Sh	Related to thermal energy sharing
TES	Relating to the thermal Energy Storage
th	Relating to thermal energy

Abbreviations

1GDHS	1st Generation District Heating System
2GDHS	2nd Generation District Heating System
3GDHS	3rd Generation District Heating System

4GDHS	4th Generation District Heating System
5GDHCS	5th Generation District Heating and Cooling System
AEF	Average Emission Factor
AFUE	Annual Fuel Utilization Efficiency
ATD	Aggregate Thermal Demand
ATES	Aquifer Thermal Energy Storage
BHP	Boost Heat Pump
BAU	Business as Usual
Bal	Balanced
BH	Balanced High-Concurrent
BL	Balanced Low-Concurrent
CDD	Cooling Degree Days
CD	Cooling Dominant
CHP	Combined Heat and Power
CH	Cooling High-Concurrent
CL	Cooling Low-Concurrent
CO2e	Carbon Dioxide Equivalent
COP	Coefficient of Performance
DB	Density-Based
DER	Distributed Energy Resources
DHS	District Heating Systems
DR	Demand Response
EF	Emission Factor
EAC	Equivalent Annual Cost
EMC	Energy Management Center
EoH	Electrification of Heating
ETS	Energy Transfer Station
ExH	Extra-Heating

GSHP	Ground Source Heat Pump
HDD	Heating Degree Days
HD	Heating Dominant
HH	Heating High-Concurrent
HL	Heating Low-Concurrent
HAEF	Hourly Average Emission Factor
HRHP	Heat Recovery Heat Pump
HVAC	Heating Ventilation and Air Conditioning
ICE	Integrated Community Energy
IEA	International Energy Agency
IESO	Independent Electricity System Operator
IPCC	Intergovernmental Panel on Climate Change
LHD	Linear Heat Density
LTTN	Low Temperature Thermal Network
LTS	Long-Term Storage
MEF	Marginal Emission Factor
NG	Natural Gas
OPTICS	Ordering Points to Identify the Clustering Structure
PV	Photovoltaic
RHP	Recovery Heat Pump
SMTN	Smart Thermal Network
STS	Short-Term Storage
SOM	Self-Organizing Map
TN	Thermal Network
TTD	Terminal Temperature Difference
ULTTN	Ultra Low Temperature Thermal Network
UN	United Nations
VT	Variable Temperature

Chapter 1

Introduction

1.1. Introduction and literature review

To limit global warming, the Paris Agreement [1], which has been ratified by the 55 countries responsible for 55% of global greenhouse gas emissions, was implemented to keep global temperatures below 1.5^{o}C above pre-industrial levels [2]. One of the major sources of GHG emissions is the building sector, according to the United Nations' Global Status Report 2017 which indicates that the building operation and construction sectors account for 36% of global end-energy use and 39% of carbon dioxide (CO2) emissions [3]. In cold-climate countries such as Canada, most of these emissions are produced by building heating demands. In 2019 the GHG emissions from space and water heating in residential and commercial buildings in Canada were 88 Mt CO_{2eq} [4]. These figures are notable, as continued growth in the global population will be accompanied by a corresponding growth in the building sector and its associated energy demands. In order for Canada to meet the global climate targets outlined in the Paris Agreement by 2030, it will need to reduce the energy intensity of its buildings sector by an average of 30% (compared to 2015 values) [5]. This will be a challenge, as building energy consumption is higher in cold-climate countries like Canada, largely due to the high number of heating degree days per year. It is possible to mitigate climate change by reducing GHG emissions from buildings' energy systems while still providing desirable levels of service by harvesting buildings' wasted energy, and electricity grid curtailed non-fossil fuel energy resources such as nuclear and renewable energy systems, especially with the vast range of renewable technologies currently available [6].

The main objective of this research is to develop energy models that can evaluate the impacts of large scale implementation of the harvesting of these community waste energy resources on the regional electricity grid and the associated reduction of GHG emissions.

The current work investigates the Integrated Community Energy and Harvesting systems (ICE-Harvest), that prioritize the harvesting of community waste energy resources. As such, ICE-Harvest systems provide a solution that can minimize GHG emissions from high-energy-consumption buildings in cold-climate regions such as North America and Northern Europe. The ICE-Harvest system connects a group of high energy consumption buildings to allow for energy exchange between buildings thus harvesting the cooling processes heat rejected from buildings with high cooling demands to heat nearby buildings with high heating demands.

In the next subsection 1.1, the different ways of harvesting energy between buildings are discussed showing the benefits and disadvantages as well as the need for a thermal network to connect buildings and allow for energy exchange. In order to achieve a large opportunity for harvesting waste thermal energy, buildings with diverse requirements i.e. cooling dominated buildings with high process cooling and heating dominated ones with high heating requirements are grouped. Section 1.2 show the previous techniques used in clustering buildings for energy integration in district heating systems. In order to connect buildings via a thermal network the energy density of the buildings, defined as the ratio of the aggregated annual energy demand of the whole cluster buildings' over the trench length of the thermal network, shall be more than 0.5MWh/m/year to overcome the thermal and mechanical losses and to maintain the economic feasibility of the integrated energy systems. As a result, the current research targets high energy consumption buildings relatively close to each other to achieve high linear heat densities.

The recent generations of district heating networks are focused on low temperature operation of the thermal network to harvest low grade heat sources and to allow for electrification of heating via heat pump technology as well as to reduce the network thermal losses. The different district heating network generations' development is presented in Section 1.3. However full electrification

of heating, adds more challenges to electrical grids, section 1.4 and section 1.5 discuss these challenges and previous techniques proposed to increase grid flexibility. The last section shows the ICE-Harvest system which is the focus of this research with a novel thermal network operation schedule that allows harvesting the buildings' and grid waste energy resources while maintaining balance for the electricity grid.

1.1.1. Building waste heat and thermal energy sharing

High energy consumption buildings are large energy consumers and carbon dioxide (CO_2) emitters per unit floor area. Some of these buildings, such as grocery stores, ice rinks, IT servers, and data centers, have high year-round cooling loads (i.e., refrigeration and air conditioning), which produce a large amount of heat rejection to the environment and low heating demand. There are around 5,368 grocery stores and small convenience stores and around 575 ice rinks in Ontario. Ontario rejects a waste heat of 21TWh from cooling processes of which 13TWh from grocery stores, 0.7 Ice-arenas, 3TWh from data centers, and 4.3TWh from residential towers' air conditioning systems [7]. On the other hand, heating-dominated buildings require year-round heating, such as residential towers, hotel buildings, and swimming pools. Ontario consumes 191 TWh of natural gas for building heating [8]. There are many different attempts in harvesting the waste heat from these buildings in the literature. Most of the systems focus on recovering the waste heat within the same building, such as harvesting the heat rejection from cooling to power an absorption chiller [9], [10]. Escriva et al., [11] studied recovering the heat rejected from supermarkets' refrigeration systems in the UK to be used for the supermarket space and domestic hot water heating, resulting in a 62% reduction in the supermarkets' heating energy consumption and over 50% GHG emissions savings. Nall [12] offered a guide for different ways to reduce the

energy consumption of grocery stores by 50% through heat recovery from their refrigeration systems. In another study on an ice rink Piché et al., [13] found that harvesting the heat rejected from the air-cooled condenser of the rink refrigeration system can lead to 60% savings in heating energy consumption.

Other trials showed that harvesting the rejected heat from the cooling dominant buildings can be used for heating other nearby heating-dominated buildings. Recently, Murphy et al., examined to recovers of waste heat between two buildings of a data center and a residential building wherein a simultaneous heating and cooling heat pump is used to heat the residential building on one side while cooling the data center on the other side. Although the study results in large energy savings exceeding 50% of the buildings' energy demand, the methodology is only applicable to space cooling and heating demands of the buildings. However, most of the waste heat of the cooling dominant buildings results from refrigeration systems. For example, around 60% of grocery stores' end energy use is for refrigeration systems [14], [15] which ultimately ends up as cooling process waste heat.

Recently research has focused on thermal energy sharing, which refers to the harvesting of waste heat from refrigeration and space cooling systems of cooling-dominant buildings to provide thermal energy to other nearby heating-dominant buildings, wherein a thermal network is used to redistribute thermal energy within a group of buildings with diverse energy demands [16]–[19]. The 2017 UN Report [20] detailed a number of trials wherein harvested waste heat from different resources. In one of these trials, the waste heat energy from a data center was used as a heat source for a high-temperature district heating system in Paris. Wahlroos et al. [19] used a case study in Finland to perform a simulation where waste heat from a data center was captured and used as an energy source in a low-temperature DH system thermal network. The simulation results

showed that this approach provided a cost reduction of approximately 0.6% to 7.3% based on the amount of waste heat used, from 18.7 MW to 85.5 MW.

With the potential interest in energy sharing and integration between buildings, the need for high-resolution energy sharing models increased. A model that can evaluate the amount of energy that can be simultaneously shared among buildings and how it could be affected by the thermal distribution network conditions.

1.1.2. Clustering

Connecting buildings to create integrated energy communities (building clusters) varies from the electrical grid to the DHS networks. The electricity grid is fully connected while microthermal networks are usually detached. The diversity inside a thermal cluster is more important than from one cluster to another, as in the electricity grid situation.

The integration of buildings with diverse energy demands improves the efficiency of the district heating systems [17], [19], [21], [22]**.** For example, Pass et al. [17] studied the energy demands of some German cities' buildings and showed that a certain combination of specific building archetypes with certain floor areas leads to a yearly cooling to heating ratio of one (i.e. a balanced thermal load), with such buildings as a hospital with a grocery store. The results showed that the perfect density would mean the community has equal heating and cooling load at any given time. Using a low-temperature thermal distribution network with that balanced node maximizes the benefits of energy harvesting. In other studies, Brange et al. and Kauko et al. [23], [24] studied the application of connecting cooling-dominated buildings as prosumers to a high-temperature district heat network in Sweden and Norway, respectively. They both concluded that taking the waste heat

from such buildings to a high-temperature DHS reduced the total energy required from the central heating network but significantly increased the buildings' overall electricity consumption.

District heating systems have always tried to connect the largest number of consumers to the same thermal network to increase the economic feasibility of the system. In the past, spatial clustering of buildings in a DHS has been done based on administrative boundaries. Recently, many clustering methods have been employed such as k-means [25], [26], self-organizing map (SOM) [27], and density-based clustering algorithms [28], [29]. The *k*-mean clustering algorithm is used to optimize the number of connected buildings and the total piping length for certain objective functions such as minimizing the operating cost [26], [27], [30]. Solving optimization problems at an hourly resolution over a whole year is computationally difficult. Common approaches select "typical days" to overcome this issue [31]–[33].

Marquant et al., [28] applied an OPTICS density-based clustering algorithm to a mixture of building types. Specifically, they ran an optimization problem for each cluster and identified the building with the highest heating demand, which was then selected as the anchor building of the cluster. The district heating network size was iteratively increased by adding the closest building to the anchor one up to the nearest N buildings, and the shortest distance for the connection pipe was estimated using the minimum spanning tree from a graph theory algorithm as shown in Figure 0-1 The optimal number of buildings around the anchor building for each cluster was estimated to minimize the equivalent annual costs (EAC) function.

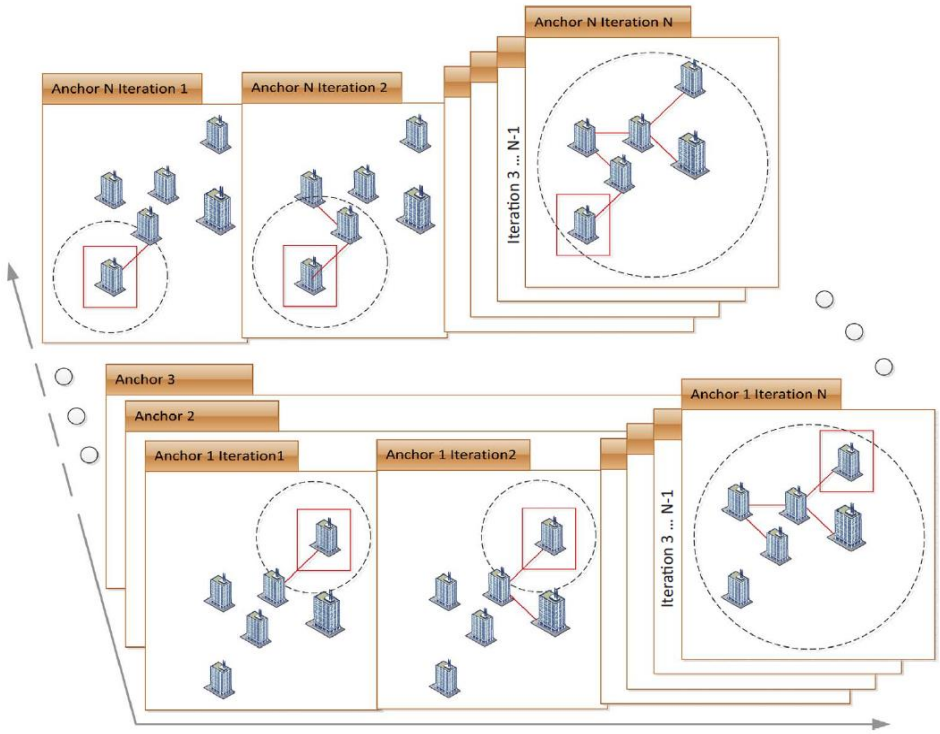

Figure 0-1: Clustering iterations around anchor building in district heating systems [34].

Talebe et al. [35] conducted a review of DH systems. In this review, the DH systems were classified based on the linear heating density (LHD) of a network, which is defined as the ratio of its total annual heating demand over trench length [36]. In systems with higher heat density, the importance of thermal and mechanical losses is less significant [37]. Rosa and Christensen [38] studied a low heat density district heating system (less than 0.2 MWh/meter/year) in a German city. In this case study, they found that the heat density of 0.05 MWh/m/year caused almost 50% thermal losses of the produced thermal energy in the central plant, while increasing the heat density to 0.2 MWh/m/year reduced the piping thermal losses to around 20% as shown in Figure 0-2 It also showed that the operating cost of the system reduced as the LHD increased.

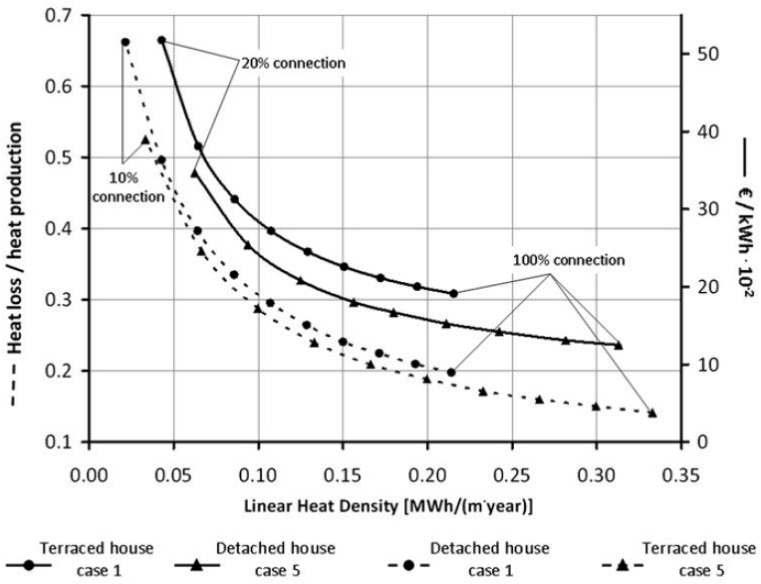

Figure 0-2: The effect of LHD on the DHS thermal losses and operating cost [38].

According to Talebe et al. [35] review, the economic effect of the LHD depends on the heat generation source. The feasible value of the LHD varies from 1 MWh/m for district heating systems with a biomass heat source to 0.2 MWh/m for combined heat and power (CHP)-based systems [36], [37].

Although different buildings' clustering techniques were used for DHS with certain specific characteristics for the connected buildings, assessing or modifying these techniques and characteristics in thermal networks with thermal energy sharing is not studied yet.

1.1.3. Thermal distribution network evolution

Energy distribution from resources to consumers requires energy networks (grid). In electricity, the electricity generators are usually centralized and then a single electricity network distributes the electricity to the different buildings (customers). For thermal energy, the resources could be centralized at a city level, or decentralized to a neighborhood or community level as community energy systems. The centralized approach in thermal networks faces a lot of challenges as it reaches 1000s of km of thermal piping which required pre-development in the infrastructure of the

cities, and it will require a high cost to implement it later or replace it in an existing city. It also causes substantive thermal losses as the distance between the energy source and consumers are far as well as relatively large mechanical pumping power, especially in low-building density cities [39], [40]. The community energy systems that connect a cluster of buildings' has gained interest recently [41]–[45]. It shows more flexibility, modularity, and low risk in investment. It also has lower thermal losses and requires less mechanical power [41]–[45].

Community energy systems consist of two main sections. The first section is the thermal piping network (TN) which is required to serve, harvest, and share energy between the clustered buildings in the community and distribute the energy resources to the consumers. The second section is the main resources hub or the energy management center (EMC) that is mainly responsible for the generation of the required energies [7], [21], [46]. In addition, there are energy transfer stations that transfer energy between the EMC and the TN and between the TN and the individual buildings. The TN operation temperature plays an important role in the ability of the system to serve the integrated community buildings. It affects the thermal losses, the ability of waste energy harvesting, and the amount of electricity required for this energy sharing and harvesting.

According to the TN operation temperature, Buffa et al., [47] classified the thermal network of District heating systems DHS into five generations. 1st generation (1GDHS) was using steam with a temperature higher than 100^{o}C and in the 2nd generation (2GDHS), pressurized water was used with an operating temperature higher than 100^{o}C while the third generation used pressurized water with about 80-90^{o}C [48]–[50]. All of these three generations were used on large scale over a city size which made them suffer from high thermal losses that reach 30% of the heating demands in some cases [47], [51], [52]. The 4th generation district heating system (4GDHS) reduced the operating temperature to around 60^{o}C to reduce the thermal losses. Also, the 4GDHS goes toward

more decentralization with community-size systems [50], [53]–[56]. There are many advantages of using the 4GDHS that make it a focus of many researchers recently. From 2014 to 2017, 298 papers are talking about the 4GDHS according to Lund et al. [50]. Using the low-temperature 4GDHS also allows for harvesting solar energy for heating requirements, Solar energy with aid of thermal storage and good building insulation was able to cover almost 95% of the heating demand in the study by Flynn et al.[56].

Recently, more carbon-free resources have been implemented in the electricity generation systems which has led to a greater focus on the electrification of heating using water or air source heat pumps. This strategy has evolved to the concept of a 5th generation district heating and cooling system (5GDHCS) that operates at an ultra-low temperature from 6-30^{o}C [47], [55]–[59]. The ultra-low operation temperature has less thermal losses than the 4GDHS, it also allows for more harvesting of low-temperature waste resources such as process cooling, data centers rejected heat, and solar thermal systems. Buffa et al., [47] made a survey on 40 networks using the 5GDHCS, wherein 29 of the 40 systems supply energy to the network from a regenerative energy source such as open loop systems like lakes, oceans, geothermal fields, and aquifer thermal energy storage (ATES). There are some open loop systems applications of the 5GDHCS that use deep lakes water as a heat sink in summer and a heat source in winter such as “Genève-Lac-Nations”, and “La Tour-de-Peilz [60]. Other open systems use river streams such as Ohrberg, Germany, which provides energy for 82 building units [61], and Leuven, Belgium [62]. If there is no open source or sink, the 5GDHCS will require a more balanced load between heating and cooling and it depends on fossil fuel-based resources. Pass et al., [17] showed that the exergy efficiency of the 5GDHCS is low as it depends more on electricity for heating purposes. In addition, Ultra-low temperature thermal

network U-LTTN operation as 5GDHCS leads to high electricity peaks, especially on extremely cold winter days.

This research studied the integrated community energy and harvesting system [7] which is considered a hybrid operation between the 4th and 5th GDHS. The TN temperature of this system is controlled to operate at low temp during some times and ultra-low temp during other times. Operating with this schedule is an approach to maximize the benefits of energy harvesting and reduce the impact on the electricity grid. Table 0-1 summarizes the differences between all five generations of DHS.

Table 0-1: Comparison between different generations of DHS and ICE-Harvest systems.

	1GDHS	**2GDHS**	**3GDHS**	**4GDHS**	**5GDHCS**	**ICE-Harvest**
Thermal network temperature	Steam >100ºC	Pressurized hot water mostly over 100°C	Pressurized hot water often below 100°C	Hot water often below 50-70°C	Hot water 6-30°C	Water varies from 20-70°C
Thermal network length	Large (City Size)	Large (City Size)	Large (City Size)	Large & Medium (Campus)	Medium & Small (neighborhood)	Small (neighborhood)
Thermal losses	High	High	High	Medium	Low	Low
Capability for low temp source heat pump harvesting	Difficult	Difficult	Difficult	Medium	High	High
Connected building thermal profile	Heating dominant	Heating dominant	Heating dominant	Heating dominant	Balanced or near heating medium (lake or ground source)	Balanced and heating dominant
Electricity utilization	-	-	-	-	High	Controllable
Exergy utilization from high temperature sources	High	High	High	High	Low	High

As the recent generations of the TN operate at a low temperature, this leads to more electrification of heating. thus, the study of the electricity grid operation is presented in the next section.

1.1.4. Electrical grid

To mitigate climate change most developed countries are planning to reach 100% carbon-free electricity generation in their grids by 2050. Ontario Canada took the lead, where more than 90% of its electricity generation comes from carbon-free resources such as nuclear, hydro, wind, and solar which can be considered the grid of the future [63], [64]. However, the large increase in renewable energy in the electricity grid with its intermittent behavior led to a challenge for the grid due to the mismatch between the electricity available generation resources times and the demand times [64]–[67]. Electricity is curtailed during periods of surplus generation from carbon-free resources, while in other periods, the grid suffers from high demand and low carbon-free generation from renewable resources [63], [68].

Figure 0-3 presents Ontario's electricity generation from different resources for a week in March 2021 [69], during periods of high available wind generation resources but with low demand such as March 13, and 14, the grid curtails carbon-free electricity as a result of the surplus electricity generation from the carbon-free resources [69]. On the other hand, during periods of high demand and low available carbon-free electricity generation resources, the grid utilizes natural gas (NG) peaking generators to rapidly respond to these demand fluctuations, as the case on March 16th, and 17th.

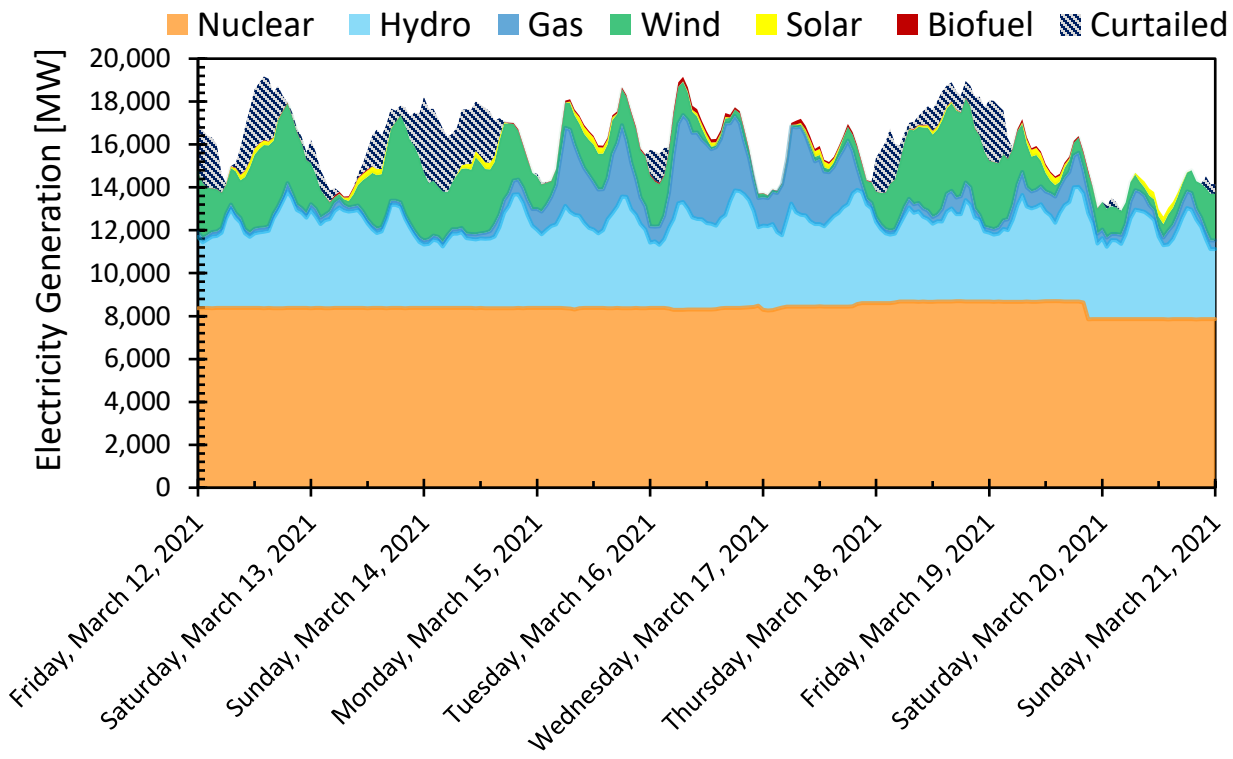

Figure 0-3: Ontario electricity grid generation from different resources for a week in March 2021 [69].

In total, Table 0-2 shows the annual curtailed electricity by source for four years in Ontario from 2015 to 2018. Ontario curtailed electricity increased and peaked in 2017 with 10.2 TWh of curtailed carbon-free electricity. The curtailment sources can be hydro, wind and solar, and nuclear maneuvers.

In the electrical system in Ontario, NG generators are the main dispatchable generation type where 9.5TWh (around 6.5% of the supplied electricity) is produced by NG generators, which account for 26% (11,317 MW) of the installed capacity [63]. As a backup plan for other generators in case of failure or repairs, a large capacity of NG generators is maintained to stabilize the grid. These NG generators have low overall electrical efficiencies of around 42% where the remaining energy is rejected to the ambient as waste heat [70], [71].

Table 0-3 presents the annual NG generation and operating hours for the years 2015, 2016, 2017, and 2018. When the total output of the gas generators reaches 1000 MW or around 10% of the installed gas generator capacity, they are regarded as being "ON". This cutoff was set because 1000 MW of capacity is enough to allow for the coordination of demand response actions.

It can be seen that the NG generation changes from one year to another, where in 2015, and 2017 the NG generation was high around 15.4 and 13.2 respectively with a large number of operating hours (On-Peak) more than 90% of the year. The figure dropped to less than half in 2017 (5.6TWh) with low operating hours lower than 40% of the year being On-Peak hours. In 2018 the NG generation increased again to almost double the value. Tables 2, and 3 show a reverse correlation between the NG generation and the curtailment. During the years with high natural gas generation, the curtailed electricity is low and vice versa, either way, the grid losses energy just more in the form of curtailment in years of high carbon-free generation or waste more heat from the NG generator in the years of higher gas generation supply and lower carbon-free generation.

Table 0-2: Curtailed electricity by source for different years in Ontario [63], [68].

Curtailment by source	**2015**	**2016**	**2017**	**2018**
Wind & Solar (TWh)	0.7	2.3	3.3	2.1
Hydro (TWh)	3.2	4.7	5.9	3.5
Nuclear (TWh)	0.9	0.7	1.0	0.2
Total (TWh)	4.8	7.6	10.2	5.8

Table 0-3: Electricity generation from NG for different years in Ontario [63].

	2015	2016	2017	2018
Electricity generated from gas/Oil (TWh)	15.4	13.2	6.4	10
Number of operating hours (% of annual hours)	8528 (97%)	8205 (93%)	3347 (38%)	4820 (55%)

Impact of Electrification of Heating (EoH):

Ultra-low temperature thermal network as a means to electrify heating leads to challenges to the electrical grid, especially in cold climate countries. Full electrification of heating in cold climate countries will significantly increase electricity consumption and peak demand. Waite and Modi [72] studied the impact on the grid levels in all US states grids showing that the utilization of air source heat pumps to electrify heating energy results in a large increase of around 70% in the aggregated peak electricity demands, wherein the figure rises to more than twice in 23 states. Fawcett et al., [73] studied the situation in the UK grid showing that a 100% use of heat pumps would increase national electricity demand by 25%, and peak electricity demand by 65%. Harvesting energy between buildings can reduce the EoH, but still increase the challenge during the grid peak periods. As a result, recent studies focused on the integration between the thermal and electrical grids.

1.1.5. Electrical grid flexibility and the integration of thermal and electrical grids

There are several techniques in the literature to meet the electricity grid challenges and increase the electricity system's flexibility. The most promoted ways in the literature are demand side management, building fabric and well insulation play an important role in balancing the electricity

grid as well as minimizing buildings' energy demand [74], [75]. EoH when coordinated can provide additional flexibility to the electrical grid. Cooper et al., [76] found that using heat pumps for heating will double the peak electricity demand in the UK and suggested using demand management and energy storage as a solution to reduce the peak demand. Romanchenko et al., [77] investigated the effect of demand response (DR) on the heating energy demand for space heating via controlling the indoor temperature with and without thermal energy storage TES for DHS in Europe. The results indicate that DR provides great potential for reducing the heating energy demand, especially in high energy consumption buildings. Also investigated the effect of adding TES and concluded that DR with TES results in the lowest space heating running cost (11% reduction). Other techniques have focused on the generation side, with energy storage techniques such as electric battery storage [78]–[82], and hydro storage [83].

According to Olauson et al. [84], a successful system flexibility strategy should not only depend on the time scale variability between the loads and generations (e.g. hourly, daily, or monthly), but also on the limitations of the electricity transmission and electrification of heating. Recently integrated thermal and electrical grids have gained focus as it provides additional flexibility to the electrical grid especially when there is a high share of renewable energy penetration to achieve the climate goal. Most of the cases focused on using electrothermal resources such as CHPs as a supply source for DHS centralized and decentralized while balancing the electrical grid. Denmark was able to reach 43% of its power from wind energy. DH in Denmark is responsible for providing 60% of the household heating energy consumption wherein CHP supplies around 70% [85] of DH generation and provides approximately 50% of the electricity generation. Wang et al., [86] performed an investigation on the flexibility in terms of using CHP for supplying DH to balance the electrical grid as well as minimizing heat cost. Thermal storage is used in this study to balance

the CHP production and the network demand resulting in a reduction of 11% in the daily heat cost and reducing the system power imbalance by almost 50%.

As the electrical grid adds more renewables with less dependence on the gas generators (such as Ontario), the dependency on EoH will increase as well as more challenges to the electrical grid due to the intermittency nature of the renewable resources. As a result, the research focus turned towards utilizing heat pumps and electric boilers alongside CHPs and thermal and electrical energy storage systems [74], [87].

Most of the previous studies focused on increasing the flexibility of the system by scheduling the equipment with the aid of battery storage. However, the current study focuses on the ICE-Harvest system that harvests wasted energy resources as well as provides more flexibility via novel network and system operation.

1.1.6. ICE-Harvest System

The integrated community energy and harvesting system (ICE-Harvest) is a decentralized energy system that improves demand flexibility by integrating the thermal and electrical networks between a group of high-energy intensified buildings. It harvests wasted energy from buildings' cooling systems and utilizes the wasted heat from the decentralized dispatchable generators. Its operation is oriented toward GHG emission reduction. Electrification of heating in this system is allowed in times of surplus generation from carbon-free resources on the electricity grid.

The ICE-Harvest system consists of three main components; a microthermal network MTN that connects the buildings cluster; an energy transfer station to transfer the energy to and from the network to the buildings' heating distribution systems; and a centralized energy management center EMC that contains the energy resources as shown in Figure 0-4 The MTN is a unidirectional High-Density Polyethylene (HDPE) thermal network that operates dynamically between the 4th

and 5th generation operating temperature conditions. The working fluid is water. As the flow circulates in the MTN, it works as a heat source for the individual building heating systems as well as a heat sink for the rejected heat from the building cooling systems. According to the energy balance on the MTN, the MTN temperature is controlled by the EMC resources. The MTN runs at a low temperature during peak periods and gets most of the heat from the EMC while operating at an ultra-low temperature during off-peak periods and depends more on EoH via the ETS heat pump, which is favorable during these periods to harvest the grid curtailed electricity.

The energy transfer stations ETSs are responsible for transferring the thermal energy between the MTN and the buildings. This energy transfer can be by only a direct heat exchange via the ETS heat exchanger if the MTN temperature is higher than the building heating distribution system's required temperature ($T_{MTN} > T_B$) and a heat pump is utilized in the opposite case. To harvest the cooling processes' waste heat a recovery heat pump is used to boost the heat rejection from the cooling systems to serve the network when operating at a temperature level higher than the rejection temperature ($T_{MTN} > T_{rej}$) and the ETS heat exchanger is utilized to exchange the heat directly in the opposite case ($T_{MTN} < T_{rej}$).

The EMC in the ICE-harvest systems contains different resources to supply the network heating requirements as well as the site's electricity needs such as CHP that is backed by the electricity grid and natural gas boilers to fulfill the demands depending on the CHP size and operation schedule. In the EMC, the CHP is only used to provide the remaining heat to the MTN to maintain or increase its temperature in times of peak electricity demand on the grid in order to replace the peak natural gas generators on the central grid with the advantage of waste heat utilization from the CHP toward the heating demand. In addition, the EMC also includes short and long-term thermal storage systems to aid in the mismatch between the generation and demand times.

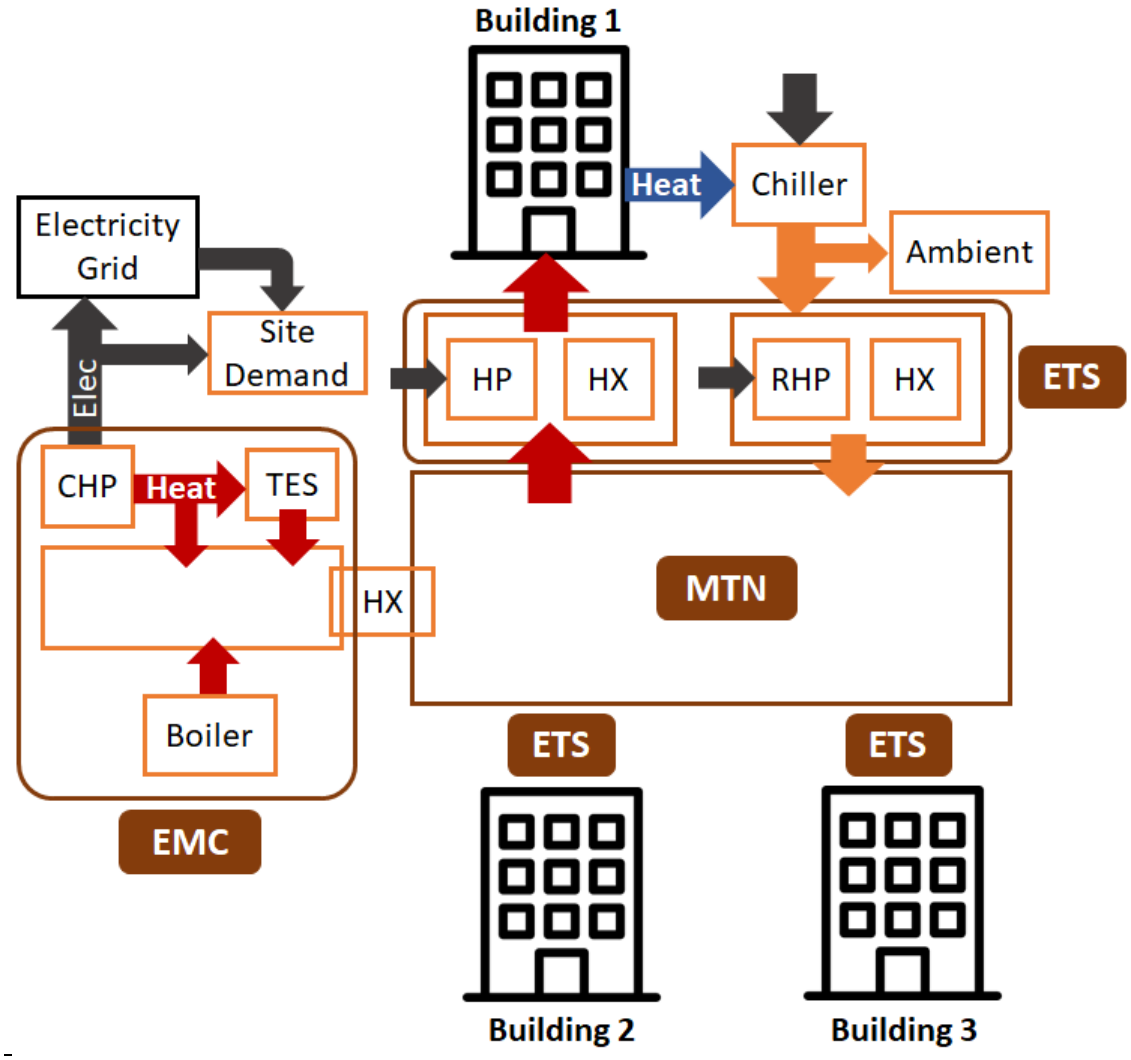

Figure 0-4: Simplified representation of the ICE-Harvest system. Note: the system is not to scale.

1.2. Summary of previous studies' gaps:

After studying the literature in the six subcategories in sections 1.1.1-1.1.6, there are many gaps in the literature as follows:

- Although many studies in the literature discussed harvesting the waste heat between buildings, most of them are focused on space heating and cooling using dynamic simulations for selected case studies. In addition, the literature did not provide a reduced model that can evaluate the

energy harvesting from any building's cooling systems through a low-temperature thermal network with high time resolution within the integrated building community.

- Harvesting waste heat using electric heat pumps is a better way to electrify heating. However, the previous studies did not link the usage of extra electricity to the source of this electricity which might be coming from fossil fuel sources that could globally increase the total GHG emissions. Also, previous researchers did not consider the effects of this electricity increase on the peak demand of the electricity grid, which is a major constraint on the feasibility of buildings' energy systems.
- Although different buildings' clustering techniques were used for DHS with certain specific characteristics for the connected buildings, no prior works have attempted to assess or modify these techniques and characteristics for the ICE-Harvest system with thermal energy sharing.
- There is no reduced model for integrated energy systems that can be applied to any number of clusters on a municipal or provincial/state scale which is necessary to show the impact of fleet deployment of these systems.
- Most prior studies on low-temperature thermal networks that targeted energy harvesting between buildings were focused on balanced or near thermally balanced demand clusters.
- Most prior studies that promoted 5GDHCS for networks were using clusters with thermally energy-balanced buildings [17], [47], [57], [58]. but the benefits of balanced load profiles cannot be guaranteed on the different clusters' load profiles. In addition, the balanced load sites usually have a low effect on the electricity peak, however, for heating dominant sites, the impact is greater which represents the majority of the sites in cold climate regions.
- Previous researchers proposed the integration of CHP as a decentralization for grid natural gas generators to balance the electricity grid and heat the thermal network however none of these

studies investigates the impacts of different CHP sizes, the CHP operation schedule time relative to the electricity grid conditions wherein the model is implemented on a fleet of ICE-Harvest sites, where the CHP's accumulated generation shall be constrained to not exceed the grid natural gas generation.

1.3. Scope of research

1.3.1. Objective and contributions

The main objectives of the current research can be summarized in the following points:

1- Investigate the potential benefits of thermal energy sharing via integrating diverse demand community buildings on the reduction of GHG emissions and energy harvesting between buildings.

2- Quantify the potential performance improvements from the large-scale implementation of a fleet of ICE-Harvest systems (state/provincial level) vs. conventional systems.

3- Investigate the effects of the different building clustering techniques and energy densities on the overall GHG emissions reduction for integrated electrical and thermal energy systems.

4- Investigate the impact of different thermal network temperature operations for different communities' load profiles on the electricity demand and peak, as well as GHG emissions.

5- Study the impact of different CHP sizes, the CHP operation schedule time relative to the electricity grid conditions, as well as the use of thermal storage and the load profile category on the site peak demands, and the overall GHG emissions.

6- Investigate the appropriate selection of energy resources to be used in the EMC according to the dominant load profile category. Also presents the impacts of different CHP sizes, and the CHP operation schedule time relative to peak electricity grid demand.

The contributions of this Ph.D. work, which are fully documented in the three journal publications presented in this thesis, can be summarized in the following:

- A thermal energy sharing model that can provide the amount of simultaneously shared heat energy between the connected integrated community buildings on a high-resolution basis and its impact on the buildings' energy consumption and GHG emissions.
- New clustering methods focus on the diversity in the buildings connected in each cluster to maximize the harvesting of waste energy, wherein buildings with high heat rejection from their cooling system were clustered with other buildings with high heating demand to create a large opportunity for harvesting wasted energy.
- Reduced model for the ICE-Harvest system to calculate the potential of large-scale implementation of a fleet of ICE-Harvest systems (state/provincial level) and the impacts on the total reduction of the GHG emissions, the buildings' energy requirement, and the electricity grid.
- Modeling the different thermal distribution network temperature operating scenarios for different community energy profiles including; low-temperature (fourth generation), ultra-low (fifth generation), smart network (ICE-Harvest) a hybrid between low and ultra-low, and smart network with a variable network temperature and evaluate their impacts on the annual electricity consumption and peak demand, as well as GHG emissions considering harvesting residual heat from cooling processes.
- Study the effect of the integration of combined heat and power as a decentralization of the peaking natural gas plants on the grid as a balance to the renewable resources.
- Study the impacts of different sizes of the CHP, the operation schedule time relative to the electricity grid conditions, and the integration of thermal energy storage for different cluster load profile categories on the site energy consumption and the overall GHG emissions.

Below is a brief description of the main contributions of each publication.

Paper I: Ahmed Abdalla, Saber Mohamed, Scott Bucking, James S. Cotton "Modeling of thermal energy sharing in integrated energy communities with micro-thermal networks,". Published in the Journal of Energy and Buildings

The novelty of this manuscript is investigating the impact of harvesting the heat rejected from the cooling and refrigeration systems of buildings that have high year-round cooling and refrigeration demand such as ice arenas and grocery stores to be used for the heating of other nearby buildings integrated with a micro-thermal network on the reduction of GHG emissions and thermal energy sharing between buildings by developing a high-resolution reduced thermal energy sharing model. This model can provide the amount of simultaneously shared heat energy between the connected integrated community buildings on a high-resolution basis. The model also evaluates the changes in greenhouse gas (GHG) emissions and the amount of energy that is still required from supplemental heating sources after harvesting relative to conventional stand-alone building systems. It also shows the effect of changing the operating temperature of the micro-thermal network on the reduction of both GHG emissions and energy consumption considering the building cooling and heating equipment performance.

Paper II: Ahmed Abdalla, Saber Mohamed, Friedrich Kelton, Scott Bucking, James S. Cotton "The impact of clustering strategies to site integrated community energy and harvesting systems on electrical demand and regional GHG reductions,". Submitted to the journal of Energy Conversion and Management.

This manuscript develops new clustering methods for the Integrated Community Energy and Harvesting systems (ICE-Harvest) that prioritize the harvesting of waste heat rejected from cooling

processes to help satisfy the heating demands of commercial and residential buildings. The clustering approaches focus on the diversity in the buildings connected in each cluster wherein buildings with high heat rejection from their cooling system were clustered with other buildings with high heating demand to create a large opportunity for harvesting wasted energy. Clustering around anchor building and density-based (DB) clustering with post-processing by adding the nearest anchor building to each cluster are developed and compared to the full DB clustering technique. This work also provides a reduced model for the ICE-Harvest system that focuses on harvesting wasted energy from three main resources heat rejected from cooling processes and peak electricity fossil-fuel fired generators, as well as energy from curtailed clean grid electricity resources that can be applied to a fleet of clusters on a municipal or provincial/state scale to show the impact of these systems on GHG emission and electricity demand from the grid.

Paper III: Ahmed Abdalla, Saber Mohamed, Friedrich Kelton, Scott Bucking, James S. Cotton "The impact of the thermal distribution network's operating temperature and system design on different communities' energy profiles," Submitted to the journal of Sustainable Cities and Society.

This article investigates four different network operating scenarios of thermal distribution network low-temperature (fourth- generation), ultra-low (fifth generation), smart network (ICE-Harvest) a hybrid between Low and ultra-low, and a proposed smart network with peak control scenario that variably changes the network temperature to avoid significant increase of the peak electricity demand and to maintain system feasibility for different network profiles. In addition, studying the integration of combined heat and power into the system for a fleet of sites as a decentralization of the peaking natural gas plants on the grid as a balance to the renewable resources. It also presents the large-scale impacts of different CHP sizes and schedule of operation time relative to the electricity grid conditions, as well as the integration of short and long-term thermal storage for the

different clusters' load profile categories on the site peak demands, and the overall GHG emissions.

1.4. Thesis organization

This thesis is organized into 5 chapters:

Chapter 1 presents an introduction and literature review of this dissertation. It also highlights the objective and contributions of this research.

Chapter 2 presents the first journal paper titled: "Modeling of thermal energy sharing in integrated energy communities with micro-thermal networks"

Chapter 3 presents the second journal paper titled: "The impact of clustering strategies to site integrated community energy and harvesting systems on electrical demand and regional GHG reductions"

Chapter 4 presents the third paper titled: "The impact of the thermal distribution network's operating temperature and system design on different communities' energy profiles"

Chapter 5 presents conclusions and recommendations for future work.

1.5. References

[1] United Nations Climate Change, "Paris Agreement - Status of Ratification," 2017. [Online]. Available: https://unfccc.int/process/the-paris-agreement/status-of-ratification. [Accessed: 09-May-2022].

[2] C. J. Rhodes, "The 2015 Paris Climate Change Conference : COP21," 2017, vol. 99, no. 2016, pp. 97–104, doi: 10.3184/003685016X14528569315192.

[3] International Energy Agency (IEA), "Towards a zero-emission, efficient, and resilient buildings and construction sector," *Global Status Report*, 2017. [Online]. Available: www.globalabc.org.

[4] Natural Resources Canada, "Comprehensive Energy Use Database," 2019.

[5] "Canada's 4th Biennial Report to the United Nations Framework Convention on Climate Change (UNFCCC)," 2020.

[6] D. Arvizu *et al.*, *Renewable Energy Sources and Climate Change Mitigation. Special Report of the Intergovernmental Panel on Climate Change*. Cambridge University, 2012.

[7] M. Y. Abdelsalam *et al.*, "Integrated Community Energy and Harvesting Systems: A Climate Action Strategy for Cold Climates," *Appl. Energy*, 2022.

[8] Canada Energy Regulator, "Canada's Energy Future Data Appendices," 2020. [Online]. Available: https://doi.org/10.35002/zjr8-8x75.

[9] V. Minea, "Supermarket refrigeration system with completely secondary loops," *ASHRAE J.*, vol. 49, no. 9, p. 40+, 2007.

[10] K. Ebrahimi, G. F. Jones, and A. S. Fleischer, "Thermo-economic analysis of steady state waste heat recovery in data centers using absorption refrigeration," *Appl. Energy*, vol. 139, pp. 384–397, 2015, doi: 10.1016/j.apenergy.2014.10.067.

[11] E. J. Sarabia Escriva, M. Hart, S. Acha, V. Soto Francés, N. Shah, and C. N. Markides, "Techno-economic evaluation of integrated energy systems for heat recovery applications in food retail buildings," *Appl. Energy*, vol. 305, no. May 2021, 2022, doi: 10.1016/j.apenergy.2021.117799.

[12] D. H. Nall, "Integration of refrigeration and HVAC in grocery stores," *ASHRAE J.*, vol. 59, no. 1, pp. 48–54, 2017.

[13] O. Piché and N. Galanis, "Thermal and economic evaluation of heat recovery measures for indoor ice rinks," *Appl. Therm. Eng.*, vol. 30, no. 14–15, pp. 2103–2108, 2010, doi: 10.1016/j.applthermaleng.2010.05.019.

[14] Z. Mylona, M. Kolokotroni, and S. A. Tassou, "Frozen food retail: Measuring and modelling energy use and space environmental systems in an operational supermarket," *Energy Build.*, vol. 144, pp. 129–143, 2017, doi: 10.1016/j.enbuild.2017.03.049.

[15] Y. Suzuki, Y. Yamaguchi, K. Shiraishi, D. Narumi, and Y. Shimoda, "ANALYSIS AND MODELING OF ENERGY DEMAND OF RETAIL STORES Division of Sustainable

Energy and Environmental Engineering , Graduate School of Graduate School of Environment and Information Science , Yokohama National University , Kanagawa , Japan ABSTRACT," no. January 2011, pp. 14–16, 2011.

[16] A. Abdalla, S. Mohamed, S. Bucking, and J. S. Cotton, "Modeling of thermal energy sharing in integrated energy communities with micro-thermal networks," *Energy Build.*, p. 111170, Jun. 2021, doi: 10.1016/j.enbuild.2021.111170.

[17] R. Z. Pass, M. Wetter, and M. A. Piette, "A thermodynamic analysis of a novel bidirectional district heating and cooling network," *Energy*, vol. 144, pp. 20–30, 2018, doi: 10.1016/j.energy.2017.11.122.

[18] R. Rogers, V. Lakhian, M. Lightstone, and J. S. Cotton, "Modeling of Low Temperature Thermal Networks Using Historical Building Data from District Energy Systems," *Proc. 13th Int. Model. Conf. Regensburg, Ger. March 4–6, 2019*, vol. 157, pp. 543–550, 2019, doi: 10.3384/ecp19157543.

[19] M. Wahlroos, M. Pärssinen, J. Manner, and S. Syri, "Utilizing data center waste heat in district heating – Impacts on energy efficiency and prospects for low-temperature district heating networks," *Energy*, vol. 140, pp. 1228–1238, 2017, doi: 10.1016/j.energy.2017.08.078.

[20] L. Riahi, C. Martinez, P. Lapuente, R. Savickas, Z. Chen, and Š. Prieskienis, "Waste for heating and cooling : How district energy tranforms losses into gains," UN environment, Paris, 2017.

[21] M. Wirtz, L. Kivilip, P. Remmen, and D. Müller, "5th Generation District Heating: A novel design approach based on mathematical optimization," *Appl. Energy*, vol. 260, no. July 2019, p. 114158, 2020, doi: 10.1016/j.apenergy.2019.114158.

[22] A. R. Murphy and A. S. Fung, "Techno-economic study of an energy sharing network comprised of a data centre and multi-unit residential buildings for cold climate," *Energy Build.*, 2019, doi: 10.1016/j.enbuild.2019.01.012.

[23] L. Brange, J. Englund, and P. Lauenburg, "Prosumers in district heating networks - A Swedish case study," *Appl. Energy*, vol. 164, pp. 492–500, 2016, doi: 10.1016/j.apenergy.2015.12.020.

[24] H. Kauko, K. H. Kvalsvik, D. Rohde, N. Nord, and Å. Utne, "Dynamic modeling of local district heating grids with prosumers: A case study for Norway," *Energy*, vol. 151, pp. 261–271, 2018, doi: 10.1016/j.energy.2018.03.033.

[25] Y. Yan, J. Yan, M. Song, X. Zhou, H. Zhang, and Y. Liang, "Design and optimal siting of regional heat-gas-renewable energy system based on building clusters," *Energy Convers. Manag.*, vol. 217, no. May, p. 112963, 2020, doi: 10.1016/j.enconman.2020.112963.

[26] S. Fazlollahi, L. Girardin, and F. Maréchal, *Clustering urban areas for optimizing the design and the operation of district energy systems*, vol. 33, no. 2011. Elsevier, 2014.

[27] R. Jafari-Marandi, M. Hu, and O. F. A. Omitaomu, "A distributed decision framework for building clusters with different heterogeneity settings," *Appl. Energy*, vol. 165, pp. 393–404, 2016, doi: 10.1016/j.apenergy.2015.12.088.

[28] J. F. Marquant, R. Evins, L. A. Bollinger, and J. Carmeliet, "A holarchic approach for multi-scale distributed energy system optimisation," *Appl. Energy*, vol. 208, no. May, pp. 935–953, 2017, doi: 10.1016/j.apenergy.2017.09.057.

[29] J. F. Marquant, L. A. Bollinger, R. Evins, and J. Carmeliet, "A new combined clustering method to Analyse the potential of district heating networks at large-scale," *Energy*, vol. 156, pp. 73–83, 2018, doi: 10.1016/j.energy.2018.05.027.

[30] J. A. Fonseca and A. Schlueter, "Integrated model for characterization of spatiotemporal building energy consumption patterns in neighborhoods and city districts," *Appl. Energy*, vol. 142, pp. 247–265, 2015, doi: 10.1016/j.apenergy.2014.12.068.

[31] F. Domínguez-Muñoz, J. M. Cejudo-López, A. Carrillo-Andrés, and M. Gallardo-Salazar, "Selection of typical demand days for CHP optimization," *Energy Build.*, vol. 43, no. 11, pp. 3036–3043, 2011, doi: 10.1016/j.enbuild.2011.07.024.

[32] S. Fazlollahi, G. Becker, and F. Maréchal, "Multi-objectives, multi-period optimization of district energy systems: III. Distribution networks," *Comput. Chem. Eng.*, vol. 66, pp. 82–97, 2014, doi: 10.1016/j.compchemeng.2014.02.018.

[33] E. D. Mehleri, H. Sarimveis, N. C. Markatos, and L. G. Papageorgiou, "A mathematical programming approach for optimal design of distributed energy systems at the neighbourhood level," *Energy*, vol. 44, no. 1, pp. 96–104, 2012, doi: 10.1016/j.energy.2012.02.009.

[34] J. F. Marquant, R. Evins, L. A. Bollinger, and J. Carmeliet, "A holarchic approach for multi-scale distributed energy system optimisation," *Appl. Energy*, vol. 208, no. August, pp. 935–953, 2017, doi: 10.1016/j.apenergy.2017.09.057.

[35] B. Talebi, P. A. Mirzaei, A. Bastani, and F. Haghighat, "A review of district heating systems: Modeling and optimization," *Front. Built Environ.*, vol. 2, no. October 2016, pp. 1–14, 2016, doi: 10.3389/fbuil.2016.00022.

[36] C. Reidhav and S. Werner, "Profitability of sparse district heating," *Appl. Energy*, vol. 85, no. 9, pp. 867–877, 2008, doi: 10.1016/j.apenergy.2008.01.006.

[37] T. Nuytten, B. Claessens, K. Paredis, J. Van Bael, and D. Six, "Flexibility of a combined heat and power system with thermal energy storage for district heating," *Appl. Energy*, vol. 104, pp. 583–591, 2013, doi: 10.1016/j.apenergy.2012.11.029.

[38] A. Dalla Rosa and J. E. Christensen, "Low-energy district heating in energy-efficient building areas," *Energy*, vol. 36, no. 12, pp. 6890–6899, 2011, doi: 10.1016/j.energy.2011.10.001.

[39] "European Commission"District heating system of the municipality of Bucharest"." [Online]. Available: https://ec.europa.eu/commission/presscorner/detail/fr/ip_21_762.

[40] S. Werner, "International review of district heating and cooling," *Energy*, vol. 137, pp. 617–631, 2017, doi: 10.1016/j.energy.2017.04.045.

[41] F. Bouffard and D. S. Kirschen, "Centralised and distributed electricity systems," *Energy Policy*, vol. 36, no. 12, pp. 4504–4508, Dec. 2008, doi: 10.1016/J.ENPOL.2008.09.060.

[42] F. Li *et al.*, "Smart Transmission Grid: Vision and Framework," *IEEE Trans. Smart Grid*, vol. 1, no. 2, pp. 168–177, 2010, doi: 10.1109/TSG.2010.2053726.

[43] K. Kok *et al.*, "Smart houses for a smart grid," in *20th International Conference on Electricity Distribution*, 2009, pp. 1–4.

[44] Peter W. Newton, *Transitions: Pathways Towards Sustainable Urban Development in Australia*. Springer Science & Business Media, 2008.

[45] H. Ren and W. Gao, "A MILP model for integrated plan and evaluation of distributed energy systems," *Appl. Energy*, vol. 87, no. 3, pp. 1001–1014, Mar. 2010, doi: 10.1016/J.APENERGY.2009.09.023.

[46] A. Abdalla, S. Mohamed, F. Kelton, S. Bucking, and J. S. Cotton, "The impact of clustering strategies to site integrated community energy and harvesting systems on electrical demand and regional GHG reductions," *Energy*.

[47] S. Buffa, M. Cozzini, M. D. Antoni, M. Baratieri, and R. Fedrizzi, "5th generation district heating and cooling systems : A review of existing cases in Europe," *Renew. Sustain. Energy Rev.*, vol. 104, no. October 2018, pp. 504–522, 2019, doi: 10.1016/j.rser.2018.12.059.

[48] L. T. Cooper, "An Evaluation of District Energy Systems in North America : Lessons Learned from Four Heating Dominated Cities in the U . S . and Canada," pp. 60–72, 2012.

[49] B. Rezaie and M. A. Rosen, "District heating and cooling: Review of technology and potential enhancements," *Appl. Energy*, vol. 93, pp. 2–10, May 2012, doi: 10.1016/J.APENERGY.2011.04.020.

[50] H. Lund *et al.*, "4th Generation District Heating (4GDH). Integrating smart thermal grids into future sustainable energy systems.," *Energy*, vol. 68, pp. 1–11, 2014, doi: 10.1016/j.energy.2014.02.089.

[51] S. Werner, "District Heating and Cooling," *Ref. Modul. Earth Syst. Environ. Sci.*, 2013.

[52] D. Prando, A. Prada, F. Ochs, A. Gasparella, and M. Baratieri, "Analysis of the energy and economic impact of cost-optimal buildings refurbishment on district heating systems," *Sci. Technol. Built Environ.*, vol. 21, no. 6, pp. 876–891, 2015, doi: 10.1080/23744731.2015.1040343.

[53] H. Lund *et al.*, "The status of 4th generation district heating: Research and results," *Energy*, vol. 164, pp. 147–159, 2018, doi: 10.1016/j.energy.2018.08.206.

[54] H. Lund, N. Duic, P. A. Østergaard, and B. V. Mathiesen, "Future district heating systems and technologies: On the role of smart energy systems and 4th generation district heating," *Energy*, vol. 165, pp. 614–619, 2018, doi: 10.1016/j.energy.2018.09.115.

[55] J. Ziemele, A. Gravelsins, A. Blumberga, and D. Blumberga, "Combining energy efficiency at source and at consumer to reach 4th generation district heating: Economic and system dynamics analysis," *Energy*, vol. 137, pp. 595–606, 2017, doi: 10.1016/j.energy.2017.04.123.

[56] C. Flynn and K. Sirén, "Influence of location and design on the performance of a solar district heating system equipped with borehole seasonal storage," *Renew. Energy*, vol. 81, pp. 377–388, 2015, doi: 10.1016/j.renene.2015.03.036.

[57] F. Bünning, M. Wetter, M. Fuchs, and D. Müller, "Bidirectional low temperature district energy systems with agent-based control: Performance comparison and operation optimization," *Appl. Energy*, no. October, pp. 502–515, 2018, doi: 10.1016/j.apenergy.2017.10.072.

[58] J. von Rhein, G. P. Henze, N. Long, and Y. Fu, "Development of a topology analysis tool for fifth-generation district heating and cooling networks," *Energy Convers. Manag.*, vol. 196, no. November 2018, pp. 705–716, 2019, doi: 10.1016/j.enconman.2019.05.066.

[59] S. Boesten, W. Ivens, S. C. Dekker, and H. Eijdems, "5Th Generation District Heating and Cooling Systems As a Solution for Renewable Urban Thermal Energy Supply," *Adv. Geosci.*, vol. 49, pp. 129–136, 2019, doi: 10.5194/adgeo-49-129-2019.

[60] Energieschweiz, "Fallbeispiele „ Thermische Netze "," pp. 1–136, 2017.

[61] V. K. Vanoli, D. Christoffers, and G. Rockendorf, *Solarsiedlung am Ohrberg*. 2000.

[62] I. P. Pattijn and A. Baumans, "Fifth-generation thermal grids and heat pumps: A pilot project in Leuven, Belgium," *HPT Mag.*, vol. 35, no. 2, pp. 53–57, 2017.

[63] "The Independent Electricity System Operator (IESO) of Ontario's power system." [Online]. Available: https://www.ieso.ca/en/Corporate-IESO/Media/Year-End-Data.

[64] D. Saxe, "2018 Energy Conservation Progress Report," *Environmental Commissioner of Ontario*, 2018. [Online]. Available: https://www.auditor.on.ca/en/content/reporttopics/envreports/env18/Making-Connections.pdf.

[65] "The Power of Transformation: Wind, Sun and the Economics of Flexible Power Systems," 2014. [Online]. Available: https://www.oecd-ilibrary.org/energy/the-power-of-transformation_9789264208032-en. [Accessed: 25-Jul-2021].

[66] L. Hirth and I. Ziegenhagen, "Balancing power and variable renewables: Three links," *Renew. Sustain. Energy Rev.*, vol. 50, pp. 1035–1051, 2015, doi: 10.1016/j.rser.2015.04.180.

[67] H. Kondziella and T. Bruckner, "Flexibility requirements of renewable energy based electricity systems - A review of research results and methodologies," *Renew. Sustain. Energy Rev.*, vol. 53, pp. 10–22, 2016, doi: 10.1016/j.rser.2015.07.199.

[68] Ontario Power Generation, "The future of Pickering Generating Station." [Online]. Available: https://www.opg.com/powering-ontario/our-generation/nuclear/pickering-nuclear-generation-station/future-of-pickering/. [Accessed: 18-Aug-2021].

[69] "The Independent Electricity System Operator (IESO) of Ontario's power system." [Online]. Available: https://www.ieso.ca/en/Power-Data/Data-Directory.

[70] Cortes Currents, "Transmission Grid Loss," 2022. [Online]. Available:

https://cortescurrents.ca/transmission-grid-loss/. [Accessed: 24-Oct-2022].

[71] Ontario Energy Board, "Ontario Wholesale Electricity Market Price Forecast," 2020. [Online]. Available: https://www.oeb.ca/sites/default/files/rpp-wholesale-electricity-market-price-forecast-20201013.pdf.

[72] M. Waite and V. Modi, "Electricity Load Implications of Space Heating Decarbonization Pathways," *Joule*, vol. 4, no. 2, pp. 376–394, 2020, doi: 10.1016/j.joule.2019.11.011.

[73] T. Fawcett, R. Layberry, and N. Eyre, "Electrification of heating : the role of heat pumps," *BIEE Conf.*, no. September, pp. 1–13, 2014.

[74] N. Good and P. Mancarella, "Flexibility in Multi-Energy Communities with Electrical and Thermal Storage: A Stochastic, Robust Approach for Multi-Service Demand Response," *IEEE Trans. Smart Grid*, vol. 10, no. 1, pp. 503–513, 2019, doi: 10.1109/TSG.2017.2745559.

[75] J. Langevin *et al.*, "US building energy efficiency and flexibility as an electric grid resource," *Joule*, vol. 5, no. 8, pp. 2102–2128, 2021, doi: 10.1016/j.joule.2021.06.002.

[76] S. J. G. Cooper, G. P. Hammond, M. C. McManus, and D. Pudjianto, "Detailed simulation of electrical demands due to nationwide adoption of heat pumps, taking account of renewable generation and mitigation," *IET Renew. Power Gener.*, vol. 10, no. 3, pp. 380–387, 2016, doi: 10.1049/iet-rpg.2015.0127.

[77] D. Romanchenko, E. Nyholm, M. Odenberger, and F. Johnsson, "Impacts of demand response from buildings and centralized thermal energy storage on district heating systems," *Sustain. Cities Soc.*, vol. 64, no. July 2020, p. 102510, 2021, doi: 10.1016/j.scs.2020.102510.

[78] M. S. Ziegler *et al.*, "Storage Requirements and Costs of Shaping Renewable Energy Toward Grid Decarbonization," *Joule*, vol. 3, no. 9, pp. 2134–2153, 2019, doi: 10.1016/j.joule.2019.06.012.

[79] J. A. Dowling *et al.*, "Role of Long-Duration Energy Storage in Variable Renewable Electricity Systems," *Joule*, vol. 4, no. 9, pp. 1907–1928, 2020, doi: 10.1016/j.joule.2020.07.007.

[80] O. J. Guerra, J. Zhang, J. Eichman, P. Denholm, J. Kurtz, and B.-M. Hodge, "The value of seasonal energy storage technologies for the integration of wind and solar power," *Energy Environ. Sci.*, vol. 13, no. 7, pp. 1909–1922, 2020, doi: 10.1039/D0EE00771D.

[81] M. A. Pellow, C. J. M. Emmott, C. J. Barnhart, and S. M. Benson, "Hydrogen or batteries for grid storage? A net energy analysis," *Energy Environ. Sci.*, vol. 8, no. 7, pp. 1938–1952, Jul. 2015, doi: 10.1039/C4EE04041D.

[82] N. A. Sepulveda, J. D. Jenkins, A. Edington, D. S. Mallapragada, and R. K. Lester, "The design space for long-duration energy storage in decarbonized power systems," *Nat. Energy*, vol. 6, no. 5, pp. 506–516, May 2021, doi: 10.1038/s41560-021-00796-8.

[83] J. P. Hoffstaedt *et al.*, "Low-head pumped hydro storage: A review of applicable technologies for design, grid integration, control and modelling," *Renew. Sustain. Energy*

Rev., vol. 158, p. 112119, Apr. 2022, doi: 10.1016/J.RSER.2022.112119.

[84] J. Olauson *et al.*, "Net load variability in Nordic countries with a highly or fully renewable power system," *Nat. Energy*, vol. 1, no. 12, 2016, doi: 10.1038/nenergy.2016.175.

[85] ENERGINET, "Environmental report for Danish electricity and CHP for 2017 status year," 2017.

[86] J. Wang, S. You, Y. Zong, H. Cai, C. Træholt, and Z. Y. Dong, "Investigation of real-time flexibility of combined heat and power plants in district heating applications," *Appl. Energy*, vol. 237, no. January, pp. 196–209, 2019, doi: 10.1016/j.apenergy.2019.01.017.

[87] S. M. Kazemi-Razi, H. Askarian Abyaneh, H. Nafisi, Z. Ali, and M. Marzband, "Enhancement of flexibility in multi-energy microgrids considering voltage and congestion improvement: Robust thermal comfort against reserve calls," *Sustain. Cities Soc.*, vol. 74, no. February, p. 103160, 2021, doi: 10.1016/j.scs.2021.103160.

Chapter 2

Modeling of Thermal Energy Sharing in Integrated Energy Communities With Micro-Thermal Networks

Modeling of thermal energy sharing in integrated energy communities with micro-thermal networks

Ahmed Abdalla[1], Saber Mohamed[1], Scott Bucking[2], James S. Cotton[1*],

[1]McMaster University, Department of Mechanical Engineering, Hamilton, Ontario, Canada

[2]Carleton University, Department of Civil and Environmental Engineering and the Azrieli School of Architecture and Urbanism, Ontario, Canada

*Corresponding Author: cottonjs@mcmaster.ca

Abstract

This investigation focuses on the potential of harvesting heat rejected from the cooling and refrigeration systems of buildings with high year-round cooling and refrigeration demand (e.g., ice arenas and grocery stores) and using it to heat other nearby buildings. Integrating a small group of buildings with diverse thermal demands via a low-temperature micro-thermal network effectively allows wasted thermal energy to be harvested and shared among the buildings with minimal thermal and mechanical losses. This paper presents a reduced model that shows the potential of harvesting thermal energy between buildings by calculating the amount of heat energy simultaneously shared between the connected buildings on a five-minute time resolution. The model also evaluates changes in greenhouse gas (GHG) emissions and the amount of energy that is still required from supplemental heating sources after harvesting relative to conventional stand-alone building systems. This study shows that changing the operating temperature of the micro-thermal network when primarily sharing between diverse thermal demand buildings has a minor effect on GHG emissions but can have a larger effect on electrical energy consumption. The model is applied using actual utility energy consumption at one of the potential clusters in Ontario, with results showing that approximately 48% of the cluster's total heating requirements can be covered by instantaneous sharing between buildings, and an additional 12% can be covered by daily short-

term thermal storage. This reduced heating demand results in an approximately 74% reduction in total GHG emissions.

Keywords: *Thermal energy sharing, Integrated energy communities, High intensity energy buildings, Waste heat, Low temperature micro-thermal network, GHG emissions*

2.1. Introduction

According to the 2017 United Nations Global Status Report, the operation, and construction of buildings account for 36% of global end-energy use, and 39% of energy-related carbon dioxide (CO_2) emissions when upstream power generation is included [1]. These figures are notable, as continued growth in the global population will be accompanied by a corresponding growth in the building sector and its attendant energy demands. In order for Canada to meet the global climate targets outlined in the Paris Agreement by 2030, it will need to find a way to reduce the energy intensity of its buildings sector by an average of 30% (compared to 2015 values) [1]. This will be a challenge, as building energy consumption is higher in cold-climate countries like Canada, largely due to the high number of heating degree days each year. According to Canada's Fourth Biennial Report on Climate Change 2019 [2], governments at all levels are working on a "net-zero energy ready" model building code to be implemented by 2030, as well as new codes for existing buildings to be implemented by 2022. These new codes will lead to buildings with smaller energy footprints, as they will force the designers of new buildings and operators of existing buildings to devise plans to reduce their buildings' energy consumption.

Over the last few decades, many techniques have been employed to reduce overall building energy consumption. For example, the use of systems designed to recover energy from the air in the ventilation system has become a requirement in Canadian building energy codes [3]. Another

effective energy-reduction method is to harvest the waste heat energy produced by refrigeration system components such as economizer cycles, desuperheaters, and compressor cooling jackets in order to heat retail spaces [4]. Indeed, Minea et al. [5] demonstrated that it is possible to use waste heat recovered from vapor-absorption refrigeration systems as a heat source for space heating. Similarly, Ebrahimi et al.'s [6] study of waste heat recovery in a data center showed that it is possible to use recovered waste heat to power one of the building's absorption chillers. Although these studies presented useful methods for improving energy savings, they only focused on harvesting waste heat for reuse in the same building. Some buildings such as wholesale warehouses and ice skating arenas produce large amounts of waste heat energy, but have low heating requirements. As a result, the excess waste heat produced by these buildings is released into the surrounding environment.

Recently research has focused on thermal energy sharing, which refers to the harvesting of waste heat from the refrigeration and space cooling systems of cooling-dominant buildings to provide thermal energy to other nearby heating-dominant buildings. The 2017 UN Report [7] detailed a number of trials wherein harvested waste heat from different resources (eg., sewage water, industrial process, solid municipal waste,…etc.) was used as a thermal source in district heating systems. In one of these trials, the waste heat energy from a data center was used as a heat source for a high-temperature district heating system in Paris.

While the thermal piping network used in district heating systems has existed since the 19th century, Lund et al. [8] have identified four distinct generations of district heating and cooling (DHC) systems. The first three generations of DHC systems used long distributed steam/hot water pipes for heating and chilled water pipes for cooling [8]. In these earlier-generation systems, the thermal network temperature is high (often 100^{o}C), which makes the harvesting of waste heat from

lower-temperature sources very difficult. Moreover, these systems often experience large amounts of heat loss from the high-temperature heating pipes and heat gain to chilled water pipes [9], [10], as well as low utilization rates in off-season times. As a result, researchers have increasingly turned their focus toward lower temperature networks in recent years.

Fourth generation district heating (4GDH) systems address the challenges associated with previous-generation systems by replacing the high-temperature thermal with a lower temperature network of approximately 50^{o}C/20^{o}C for supply and return, respectively[6, 9, 10, 11]. Flynn et al. [14] concluded that the combination of a low-temperature DH system, building insulation, and borehole thermal energy storage could enable solar energy to account for 95% of the system's total energy heating. Lund et al. [11] reported that, from the beginning of 2014 through the end of 2017, the term, "4GDH system," was mentioned in 298 papers, either as part of the study detailed in the paper, or as part of its literature review. They suggested that the high number of references to 4GDH systems may be due to their low temperatures networks, which allow for the harvesting of low-grade waste heat resources and renewable resources, such as solar thermal energy. Fifth generation district heating and cooling (5GDHC) systems use a lower-temperature thermal network than 4GDH systems, which allows them to recover lower-grade waste heat. The 5GDHC system's use of thermal network temperatures that are lower than the required building supply temperature, near the ambient temperature (15-25^{o}C), allows it to recover more waste heat resources [13-16]. Since the 5GDHC system's thermal network temperature is lower than the building heating requirement (~50-60^{o}C), a heat pump is required at each building to lift the temperature. Talebe et al. [19] classified DH systems based on the linear heating density of their networks, which is defined as the ratio of the network's total annual heating demand to its trench

length [20]. In systems with higher heat density, the impact of thermal and mechanical losses is less significant [21].

The introduction of each generation of DHC system has been accompanied by changes not only to the temperature requirements, but also to the piping infrastructure. For example, the four-pipe system (heating supply, heating return, cooling supply, and cooling return) used in the first four generations was replaced by a two-pipe [18] or even a single-pipe [22] system in the 5GDHC. In addition, the 5GDHC system's use of electrical energy to power its heat pumps significantly reduces GHG emissions, provided the electricity is not produced via fossil fuels. However, this benefit remains largely unrealized; since electricity prices in many countries, including Canada, are higher than natural gas prices, thus most heating systems continue to use natural-gas-fired equipment such as boilers. Nonetheless, low-temperature thermal networks' superior waste-heat harvesting abilities can offset a large portion of the heating requirements if the buildings connected to the network have diverse cooling and heating demands year-round.

Zarin et al. [23] analyzed a low-temperature thermal network district system that is capable of recovering low-grade heat rejected from the building's cooling systems. However, their results indicated that the system's large thermal network resulted in high mechanical and thermal energy losses. To aid in their analysis, Zarin et al. [22] used a correlation to measure whether the district system was more efficient than the stand alone system for a certain combination of buildings. Ultimately, they concluded that buildings with different energy demands should be connected in order to benefit from load diversity.

Wirtz et al. [24] developed an optimization model for a bidirectional low-temperature network that changes the flow direction according to the thermal cooling or heating mode. In this study, buildings with diverse thermal energy demands were connected to a centralized energy hub that

included a variety of cooling and heating resources, such as chillers, pumps, heat exchangers, boilers, thermal energy storage, cold storage, and batteries, as well as renewable energy resources, such as solar photovoltaics (PV). Their results showed that this configuration resulted in a 56% reduction in GHG emissions, and about a 42% reduction in cost.

Wahlroos et al. [25] used a case study in Finland to perform a simulation where waste heat from a data center was captured and used as an energy source in a low-temperature DH system thermal network. The simulation results showed that this approach provided a cost reduction of approximately 0.6% to 7.3% based on the amount of waste heat used, from 18.7 MW to 85.5 MW.

Murphy et al. [25] conducted a study wherein a simultaneous heating and cooling pump was used to capture waste heat from the cooling system of a data center that requires year-round cooling and share it with a multi-unit residential building (MURB) that requires year-round heating. The heat pump was connected to an evaporator, which cooled the data center on one side and heated the MURB on the other. Murphy et al.'s [25] results showed that energy sharing reduced the MURB's heating requirements by 55%, and its GHG emissions by 53%. Similarly, energy sharing reduced the data center's cooling requirements and GHG emissions by 50% and 51%, respectively.

Previous studies on low-temperature thermal networks have largely focused on buildings with high year-round space cooling (e.g., data centers) and heating loads (e.g., residential towers). These energy-saving techniques are only applicable in buildings that require space cooling (5 and 10^{o}C for supply and return, respectively) ***throughout the entire year***, with data centers being one of the few viable options for implementation in cold climates.

The current work proposes an energy sharing model wherein waste heat is harvested from high-cooling-energy-intensive buildings that require both space cooling (e.g., data centers) and

refrigeration cooling (e.g., ice hockey arenas and grocery stores) year-round. However, Datacenter, ice arena, and grocery store cooling systems reject heat similarly at about 25-35^{o}C which can be used with the aid of the ETS heat pump integrated into the buildings' heating systems. The major difference is in the cooling product. In data centers, as it is a space cooling, waste heat can be simultaneously cooled using the same heat pump that provides heating on the condenser side. However, in an ice arena, the lower required temperature is between -30 and -10 ^{o}C for the cooling product which will require a separate system. Ice arenas, and grocery stores are among the most energy intensive buildings. A large portion of their energy consumption is used for cooling and refrigeration. As a result, the heat rejected from the condensers of such cooling and refrigeration systems is usually released into the surrounding environment through a cooling tower or evaporative condenser.

Whereas many European cities have existing DH system pipes that service most of their buildings and houses, DH systems are less common in Canadian cities due to the comparatively large geographical scope of urbanization, extreme temperatures, and low natural gas prices. Indeed, high-energy-intensive buildings are usually clustered into groups (e.g., plazas) in Canadian cities.

The current work presents an Integrated Community Energy and Harvesting System (ICE-Harvest) [26] designed to connect a small number of closely situated high-energy-intensive buildings that have diverse thermal demands, with at least one requiring a cooling load year-round. As shown in Figure 2-1, a group of buildings, known as an integrated community energy node, is connected by a Micro-Thermal Network (MTN). There are more than 1,000 grocery stores and ice arenas in Ontario that could be clustered with other nearby heating-dominant buildings to create integrated community energy nodes. The MTN is a single unidirectional thermal pipe filled with low-temperature water (T_{MTN}); this low-temperature water is used to harvest the heat rejected from the

refrigeration and cooling systems of the cooling-dominant buildings, which is then used to satisfy the simultaneous heating requirements of the other heating-dominant buildings within the node. Each building is connected to the MTN through an energy transfer station (ETS), which includes a lift heat pump (HP) and a heat exchanger (HX). The lift heat pump is used to raise the MTN's temperature to satisfy the building's required heating temperature, while the heat exchanger is used to directly exchange the heat rejected from the cooling and refrigeration systems to the MTN. The energy management center (EMC) is a community facility that provides the remaining energy needs of the connected buildings to maintain the MTN at a constant temperature. For meeting thermal demands, it contains different heating energy resources (e.g., boiler, CHP operated as a marginal electricity generator, and thermal energy storage) equipment that provides the remaining heating energy requirements not met by thermal sharing.

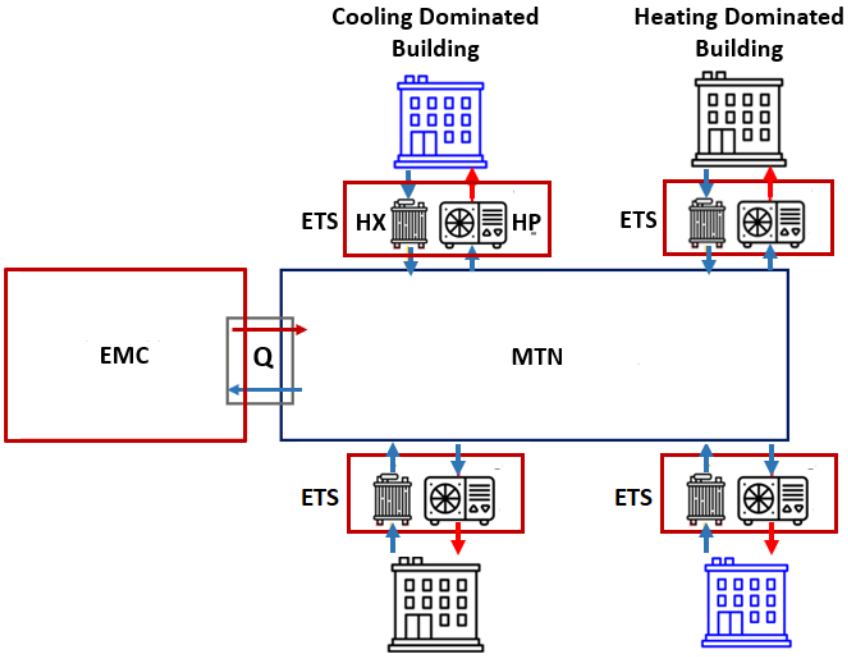

Figure 2-1: An ICE-Harvest system node composed of an Energy Management Center (EMC), Micro-Therm Network (MTN), and Energy Transfer Stations (ETS) that interface with the connected buildings.

In traditional stand-alone building systems, peak demand and a capacity factor are used to size the equipment. In contrast, sizing and control in ICE-Harvest systems require knowing the high resolution energy demands (measured at least hourly) of each building in the node, how much energy can be shared simultaneously, and when and how much energy needs to be stored or discharged from thermal storage.

This paper uses a reduced high-resolution integrated thermal energy sharing model to evaluate the benefits of using an MTN to harvest waste heat rejected from condensers in air conditioning (AC) and other refrigeration systems. While this approach allows for the evaluation of the MTN on its own, it does not allow for the evaluation of a full ICE-Harvest system, which can incorporate different technologies into the EMC and an advanced control system. Benefits of utilizing this model include: (1) allowing engineers to predict how much rejected heat energy from cooling-dominant buildings can be collected and used to heat other buildings in the node; (2) enabling the

prediction of the amount of electricity required to drive lift heat pumps to meet the building's heating loads at specific times.; and (3) quantifying the reduction in both the GHG emissions and the energy required to provide heating, cooling, and electricity of integrated systems relative to conventional stand-alone buildings systems. In the next section, the methodology and flow chart of the model is presented.

2.2. Methodology

2.2.1. Model Description

This section presents a mathematical model for evaluating energy utilization in an ICE-Harvest system. The model utilizes the following inputs: the high-resolution cooling, heating, and electricity aggregated energy consumption of a community node (a group of buildings in relatively close proximity); the coefficient of performance, or efficiencies, of the cooling and heating systems; the buildings' heating system temperature requirements; and the cooling system heat-rejection temperatures for all buildings in the ICE node. These inputs are shown in Figure 2-2.

The model's outputs include: the amount of thermal energy that can be instantaneously shared between the connected buildings (Q_{sh}); the surplus heat energy that can be harvested for later use with the aid of thermal short term storage (Q_{SH_STS}); the electric energy required by the heat pumps needed to harvest waste energy from the cooling and refrigeration processes (W_{HP}); the supplemental thermal energy required from the energy management center (Q_{EMC}); and the reduction in GHG emissions compared to conventional standalone systems. The model is capable of evaluating all of these outputs for different time intervals (e.g., 5 minutes, hourly, daily, weekly, monthly, etc.) according to the input data resolution. The model uses the following assumptions:

- Since the thermal network is short in length, it is considered to have a high linear heat density and a low operating temperature; thus, the model assumes minor effects of mechanical and thermal losses and thermal network mass.
- The model assumes that any imbalance in the node's thermal demands throughout the day can be met via a perfectly insulated short-term thermal storage (STS) of infinite capacity. As a first preliminary sizing approach, the STS is sized to be enough to store excess rejection heat over a 24-hour period and use it on the same day toward sharing (Equation (4)). It is considered a perfectly insulated storage with no losses. At any time interval, if the heat rejected is more than the required heat, the extra heat will be charged to the STS and vice versa. In the current study, no limitation on rate or storage size was implemented. The maximum capacity of the largest STS usage in a peak day for a given year is tracked so that the STS size needed to achieve this can be estimated at the end of the simulation.

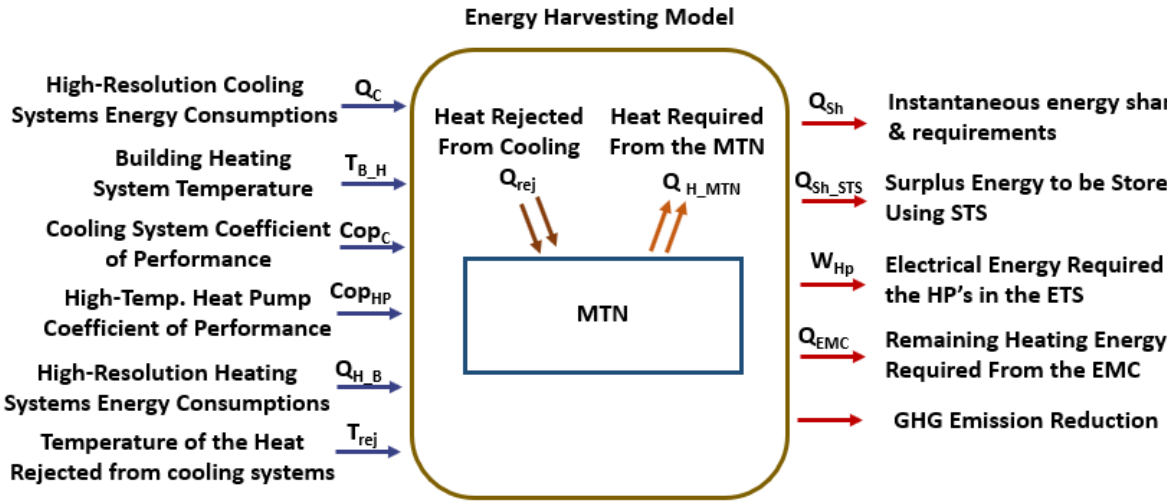

Figure 2-2: Thermal energy sharing model inputs and outputs.

The simultaneous energy sharing between buildings (Q_{Sh}) is defined as the minimum between the heat rejected from the buildings' cooling systems (Q_{rej}) at a certain time interval (i) and the heat

required from the MTN (Q_{H_MTN}) at the same time interval (i), as shown in Equation 1. This minimum was specifically selected to avoid an increase in the MTN temperature in the event of extra heat rejection. The heat rejection from cooling systems is calculated based on their cooling loads (Q_c) and coefficients of performance (COP_c), taking into consideration changes in the $COP_{C\text{-}MTN}$ with the MTN temperature (Equation 1a). The heat required from the MTN (Q_{H_MTN}) is evaluated based on the building energy requirements (Q_{H_B}), which is an input to the model, and the electricity (W_{HP}) required by the heat pumps in the energy transfer stations (ETS) at the connection points between each building and the MTN (Equations 1b and 1c).

$$Q_{Sh} = \sum_{i=1}^{n} Min\{[Q_{rej}(i),\ Q_{H\_MTN}(i)\} \quad (1)$$

Where n is the total number of intervals (i) in any calculation period, which could be a day, a month, a season, a year, or any other period.

$$Q_{rej} = \sum_{j=1}^{nB} Q_C(j) * \left(\frac{1}{Cop_c(j)} + 1\right) \quad (1a)$$

Where j is the building number, and nB is the total number of buildings in the ICE node.

$$Q_{H\_MTN} = (Q_{H\_B} - W_{Hp}) \quad (1b)$$

$$W_{Hp} = \left(\frac{Q_{H\_B}}{Cop_{Hp}}\right) \quad (1c)$$

The heat rejection from the cooling systems and the heat required from the MTN for heating-dominant buildings will not be the same at different time intervals. Sometimes, the energy rejected from the cooling systems is higher than the energy required from the MTN; at other times, the heating energy required by the MTN is higher than the heat rejected from the cooling system. The positive difference in the first case is the surplus energy rejected to the MTN (Q_{rej_s}), as shown in Equation 2. This surplus rejection can be stored or rejected into the surrounding environment using different resources in the EMC, such as thermal storage tanks or a cooling tower, respectively.

When the difference between the rejected heat to the MTN and the heat required from the MTN is negative, Equation 3 can be used to determine the remaining heat energy that should be delivered to the MTN (Q_{H_rem}) from heating sources within the EMC, such as thermal storage, CHP, or backup boiler.

$$Q_{rej\_s} = \sum_{i=1}^{n}[Q_{rej}(i) - Q_{H\_MTN}(i)] \quad if > 0 \qquad (2)$$

$$Q_{H\_rem} = \sum_{i=1}^{n}[Q_{rej}(i) - Q_{H\_MTN}(i)] \quad if < 0 \qquad (3)$$

Equation 4 calculates the amount of energy that must be stored in a short-term thermal storage tank each day (Q_{Sh_STS}). In this equation, the amount of energy to be stored in short-term storage and used each day is defined as the minimum of both the sum of surplus heat rejected to the MTN each day and the sum of the remaining heat required from the MTN during the same day.

$$Q_{Sh\_STS} = Min[\sum_{i=1}^{d} Q_{rej\_s}(i), \sum_{i=1}^{d} Q_{H\_rem}(i)] \qquad (4)$$

Where *d* is the number of time intervals, *i*, in a day. To consider short-term storage for *k* number of days, the value, *d*, should be replaced by (*k* . *d*).

The remaining MTN heat requirement after energy sharing is covered by other resources in the EMC and can be calculated as shown in Equation 5.

$$Q_{EMC} = Q_{H\_MTN} - [Q_{Sh} + Q_{Sh\_STS}] \qquad (5)$$

Not only does an ICE-Harvest system change the amount of heat energy required (Q_{EMC}) compared to stand-alone systems (Q_{H_B}), but it also changes the overall electricity requirement. In the ICE-Harvest system, electricity usage increases due to the use of a lift heat pump in the ETS (W_{HP}), and it also fluctuates due to variance in the coefficients of performance of the existing buildings' cooling systems as they are integrated with the MTN. Equation 6 calculates the difference in

cooling system electricity consumption (W_{C_Var}) for a stand-alone business-as-usual system (BAU) and an ICE-Harvest system with an MTN.

$$W_{C\_Var}(i) = [Q_C(i) * (\frac{1}{Cop_{c-MTN}(i)} - \frac{1}{Cop_c(i)})] \quad (6)$$

Where $COP_{c\text{-}MTN}(i)$ is the coefficient of performance of the cooling systems in an integrated energy system at different MTN temperatures, and $COP_c(i)$ is the coefficient of performance of the same cooling systems in a conventional stand-alone system. The overall electricity requirement ($E_{ICE\text{-}Harvest}(i)$ in an integrated energy system can be calculated via Equation 7,

$$E_{ICE\text{-}Harvest}(i) = E_{BAU}(i) + W_{HP}(i) + W_{C\_Var}(i) \quad (7)$$

Where $E_{BAU}(i)$ is the overall electricity consumption in the business-as-usual system (BAU).

GHG emissions were calculated for both the ICE-Harvest ($GHG_{ICE\text{-}Harvest}$) and stand-alone BAU (GHG_{BAU}) systems. In both cases, GHG emissions will come from using natural gas for heating, as well as from the grid emission factor associated with importing electricity from the grid. Following Canada's 2018 National Inventory Report [27], Equations 8 and 9 use natural-gas-combustion-related CO_2 emissions of 0.1872 tonnes/MWh, and multiply this figure by the amount of heat required in both the BAU and ICE-Harvest systems to calculate their respective GHG emissions. Conversely, calculating GHG emissions from imported electricity depends on the fuel sources used to generate electricity. Maxime et al. [27] defined the hourly emission factor, *EF(i)*, as the ratio of GHG emissions produced by a grid's fossil-fuel-based plants to the total electricity generated in a given hour, *(i)* (Equation 10). Using these formulas, the emissions associated with the imported electricity will equal the amount of electric energy at each time interval *E(i)* multiplied by the *EF*, as shown in Equation 11.

$$GHG_{Heating\_BAU} = [\sum_{i=1}^{n} Q_{H\_B}(i)] * 0.1872 \quad (8)$$

$$GHG_{Heating_{ICE\_Harvest}} = [\sum_{i=1}^{n} Q_{EMC}(i)] * 0.1872 \quad (9)$$

$$EF\ (i) = \frac{GHG\ emissions\ from\ fossil\ fuel\ plants(i)}{Total\ electricity\ generated\ in\ the\ grid\ (i)} \quad (10)$$

$$GHG_{Elec.} = \sum_{i=1}^{n} [E(i) * EF(i)] \quad (11)$$

In the next section, an application of the energy-harvesting model will be presented for a specific ICE-Harvest node in Ontario, Canada.

2.3. Application for the Thermal Energy Sharing Model

2.3.1. Buildings Node Specification and Load Profiles:

The Canadian province of Ontario has many potential locations for integrated energy communities. The node selected for this study consists of four buildings: two refrigeration/cooling-dominant buildings (an ice hockey arena and a library with an IT server), and two heating-dominant buildings (recreation centers with a swimming pool and recreation activities). The building demand is unique for each building based on historical electricity demand in 5 min intervals and disaggregated cooling demand from the electricity 5 min interval smart meter over a full-year period (2017). The disaggregated heat demand is based on measured monthly gas data consumption along with 5 min interval weather dependent algorithm to increase the resolution of natural gas consumption. The supplied energy always meets the demand, but the energy shared between buildings changes depending on availability. The building supply temperature and heat recovery temperatures are the same for each building. The BAU energy system used in the ice hockey arena is an ammonia refrigeration system, while the IT server and other buildings utilize electric chillers to meet their space-cooling needs. The coefficient of performance (COP) of refrigeration for the ammonia refrigeration system was based on its actual performance under

specific operation conditions (ranging from 3.7 to 2.6 at condenser temperatures between 25 and 40°C), while the COP of the electric chillers was based on manufacturer datasheets (ranging from 5.5 to 4.3 at condenser temperatures between 25 and 40°C). The cooling systems of all buildings release waste heat into the environment through cooling towers. The average temperature of the water entering the cooling tower for heat rejection is approximately 25°C in the winter (October 1st to April 30th) and 35°C during the summer (May 1st to September 30th). The heating-distribution systems in all four buildings use gas-fired equipment that requires a heat-supply temperature source of approximately 60°C. Figure 2-3 shows the daily aggregated thermal and electrical energy consumption of the four buildings in the node. It should be noted that, while the figures depict a daily summary of the data for the sake of simplicity, a five-minute interval analysis was used in all of the calculations upon which the results are based.

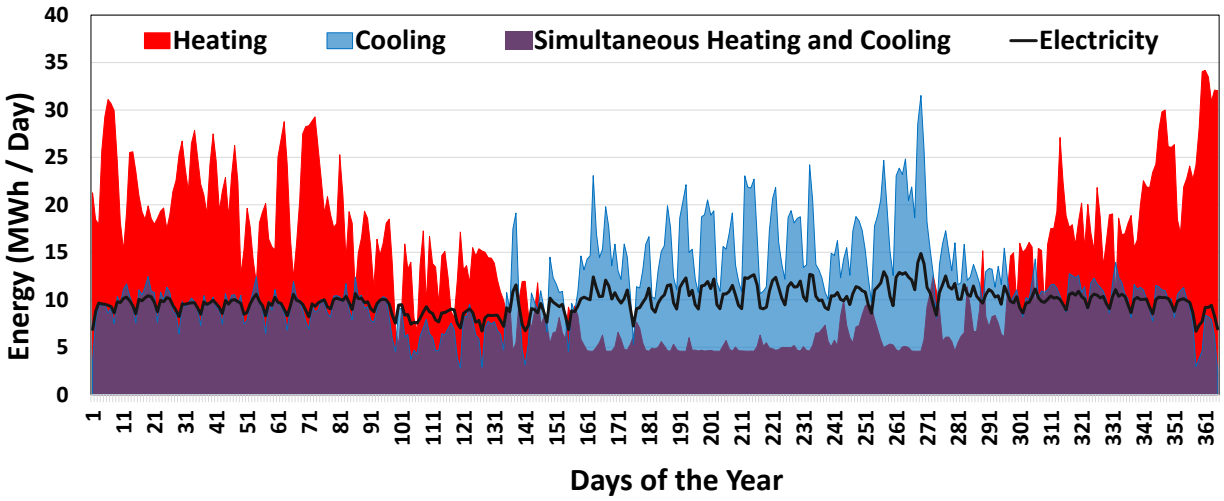

Figure 2-3: Daily sum energy consumption of the existing conventional system for 4 buildings.

Although the thermal energy consumption of this node is almost balanced over the course of a year, with annual heating and cooling energy consumption values of 4882 MWh/year and 4278 MWh/year respectively, the consumption of heating energy in winter is higher than cooling energy consumption, with the inverse occurring in summer. Figure 2-3 suggests that this node has a high

potential for energy sharing, as the node has a concurrent cooling and heating requirement at many times throughout the year.

2.3.2. Thermal Energy Sharing Model Results and Discussion

The model was then applied to the specified ICE node, which uses a low-temperature MTN to connect its constituent buildings. Each building is outfitted with lift heat pumps, which deliver heat from the low-temperature MTN to the higher temperature buildings' heating distribution systems. Each building is equipped with a harvesting heat exchanger, which is used to capture heat and transfer it to the MTN when required; these exchangers are installed on each building's cooling equipment rejection devices, which are situated prior to the heat rejection system (e.g., cooling tower). The lift pumps' coefficient of performance was based on manufacturer data [28] at the specific operating temperature. The following methods were used in the following order to meet the buildings' heating requirements: simultaneous energy sharing (Q_{sh}); energy sharing using short-term storage (Q_{STS}); transferring heat to the MTN from the equipment in the EMC; and using electrical energy to power the heat pumps. Figure 2-4 presents a stacked daily profile of the sum of these heating resources over a full year. In this figure, the electrical energy required by the heat pump is shown separately for both the daytime (7 a.m. to 7 p.m.) and nighttime (7 p.m. to 7 a.m.) periods.

The results in Figure 2-4 show that a large portion (~48%) of the node's heating requirements is covered by simultaneous energy sharing of approximately 2360 MWh/year. In addition to simultaneous sharing, approximately 12% of the buildings' daily heating requirements are met through the use of short-term thermal storage to overcome the intra-day mismatch between waste heat and heating requirements. Approximately 17.5% of the buildings' heating requirements are

also covered by EMC resources. Figure 2-5 shows a comparison of the heating required by the conventional BAU systems and the supplemental heating required by the MTN from the EMC in the integrated systems. The remaining 22.5% of the buildings' yearly heating requirements are supplied by using electricity to drive the ETS heat pumps, which increase the low-grade heat energy from the MTN to the temperature required by the building's heating systems. The heating energy covered by different resources is summarized in Table 2-1.

Table 2-1

Heating energy covered by different resources of the total node heating requirements

Simultaneous energy sharing	2360 MWh/year (48% of heating demands)
Energy sharing using short-term storage	575 MWh/year (12% of heating demands)
Supplemental heating requirement from EMC	850 MWh/year (17.5% of heating demands)
ETS heat pumps electricity	1097 MWh/year (22.5% of heating demands)

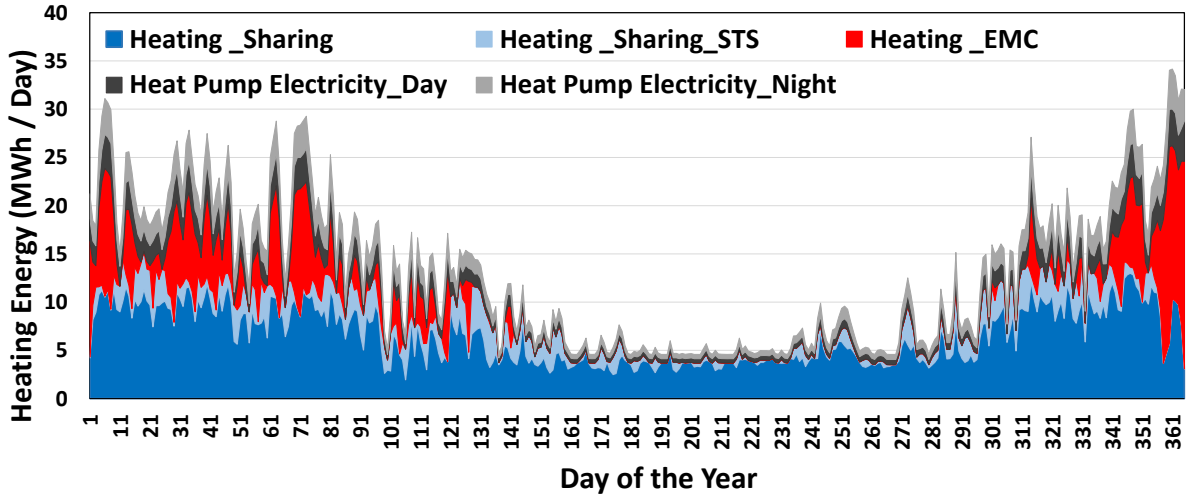

Figure 2-4: Integrated system daily heating energy covered from different resources.

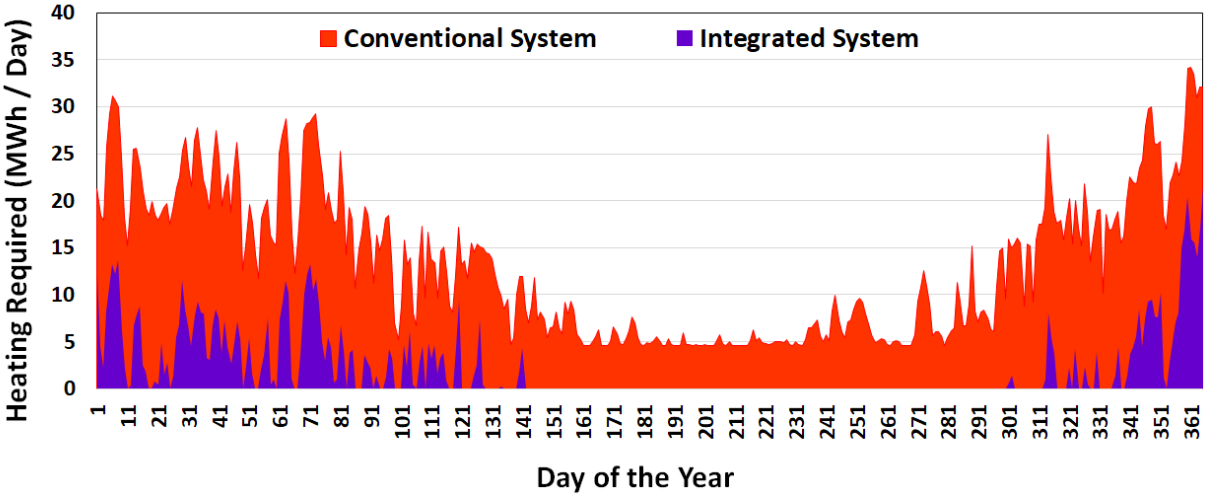

Figure 2-5: Supplemental heating energy requirement of the integrated system compared to the conventional system.

Figure 2-6 shows a stacked daily profile comparing the energy consumption of the BAU system and the integrated system with a heat pump during both the daytime and nighttime periods. Although the total yearly electrical energy consumption increased by around 30%, approximately 24.5% of this increase was due to heating demands during winter. The remaining 5.5% of the electrical energy required by the heat pumps was for the summer months, with only a 2% increase during the daytime when peak electrical demand occurs. Thus, there is only a minimal increase in peak electricity demand during the summer.

Equations 8 and 9 were used to calculate the GHG emissions for the remaining heat energy required from the EMC, and the total heat required from the conventional heating system, respectively. Since the examined node is located in Ontario, Canada, the GHG emissions from the imported electricity, which depends on the grid's fuel source [29], were calculated using the hourly Ontario electricity grid GHG emissions factor (*EF*), as shown in Equation 11. Figure 2-7 presents a comparison of the daily GHG emissions produced by the BAU and integrated systems. As can be seen, the integrated system produces approximately 730 fewer tonnes of GHGs compared to the conventional stand-alone system annually, which represents a decrease of 74%. This substantial reduction is due to the 82.5% reduction in heating energy required from the EMC. Additionally, the GHG emissions factor is very low during the winter, as most of Ontario's electrical energy comes from non-fossil fuel energy resources. Although the integrated system's GHG emissions are impacted by the EMC's heating energy requirements, these requirements are much lower during the summer. However, the EF for the electricity produced during this time is higher, especially during peak times, as shown in the dotted rectangular area in Figure 2-7.

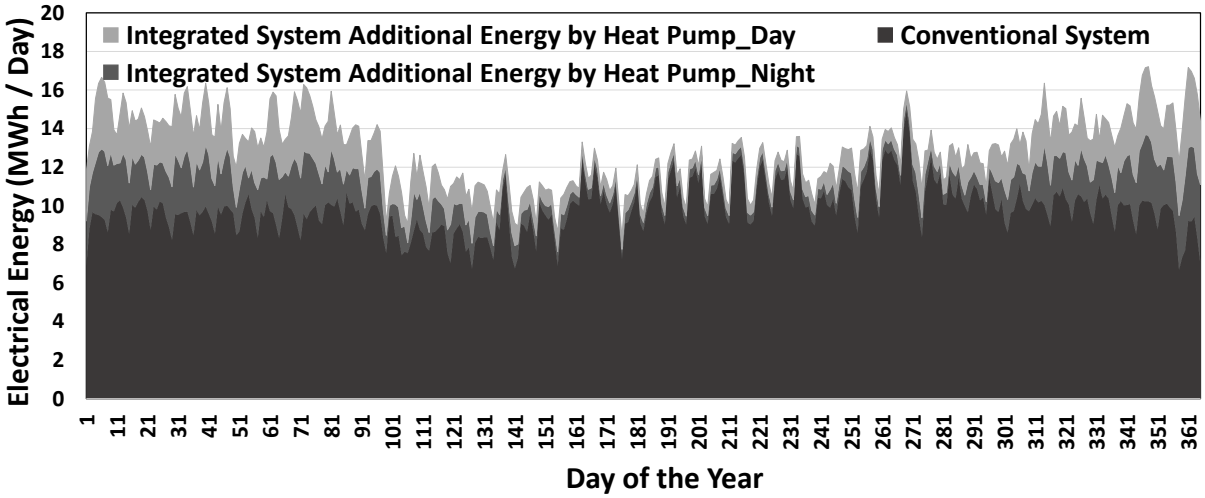

Figure 2-6: Electrical energy requirement of the integrated system compared to the conventional system.

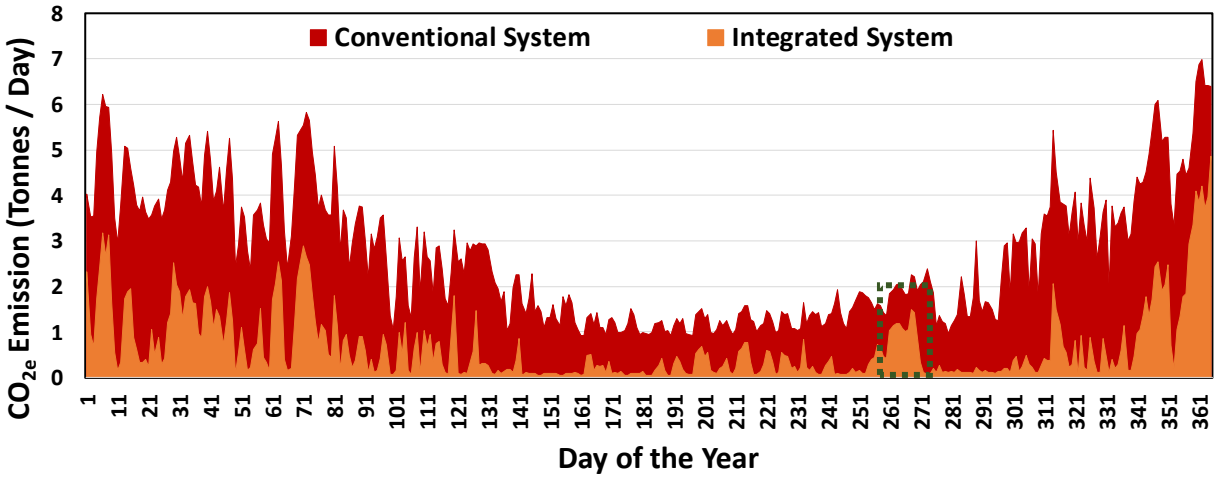

*Figure 2-7: **CO_{2e}** emissions of the integrated system compared to the conventional system.*

2.3.3. Effect of Thermal Network Temperature on Energy Utilization

The MTN works as a sink for the buildings' cooling and refrigeration systems, as it receives the waste heat rejected from these systems. However, the MTN also works as a heat source for the ETS heat pumps that supply heat to the buildings' heating-distribution systems. Varying the MTN temperature will positively affect the performance of one of these systems, and negatively affect the performance of the other. The COPs of a cooling system, whether it is refrigeration or space

air conditioning, are a function of the heat source and sink temperatures as presented in Appendix A. As the MTN represents the sink temperature for the cooling system. The MTN temperature is selected to be at 5°C Lower than the rejection temperature (T_{rej}) of the cooling systems ($T_{MTN}=T_{rej}$ –5) to allow a direct exchange between the rejection and the MTN. Hence increasing the MTN temperature will require a corresponding increase in the rejection temperature of the cooling system and reduce the cooling systems' coefficient of performance as shown in Appendix, Figure 2.A1, and Figure 2.A2 which leads to more electricity consumption—a negative effect during periods of peak electrical demand. Conversely, for the ETS heat pumps that lift the temperature of the rejected heat to be used toward the heating of the buildings, the MTN represents the heat source. The higher the MTN temperature the higher the COP as shown in Appendix Figure 2.A3, which reduces their electricity consumption—a positive effect during periods of peak electrical demand. In this section, the effect of MTN temperature on energy consumption and GHG emissions is discussed in terms of seasonality, as the ratio of heat rejection from cooling systems to the heating requirements of buildings' systems reverses from season to season. The above-described thermal energy sharing model was used to investigate how MTN temperature influences the ICE-Harvest system performance criteria. Different MTN temperatures from 10°C to 40°C, adjusted in increments of 5°C, were used in the thermal energy sharing model with an input load resolution of five-minute intervals. The results indicated that changes in the MTN temperature resulted in corresponding changes to the thermal equipment's coefficients of performance. Figure 2-8 presents the total seasonal amount of Q_{sh}, Q_{Sh_STS}, and Q_{EMC} for each MTN temperature for both the winter (left) and summer periods (right).

Similarly, the thermal energy sharing model was used to calculate the electrical energy consumption of the buildings' heat pumps and the change in the electrical energy consumption of

the BAU's cooling systems. Figure 2-9 shows the effect of the MTN temperature on the amount of electrical energy increased by the heat pump, the change in the electrical energy required by the cooling system, and the overall change in the electricity consumption relative to the BAU system for both winter (left) and summer (right) seasons. Figure 2-10 presents a summary effect of the MTN temperature on the change in the overall electrical energy consumption and reduction of GHG emissions relative to the conventional system in both seasons.

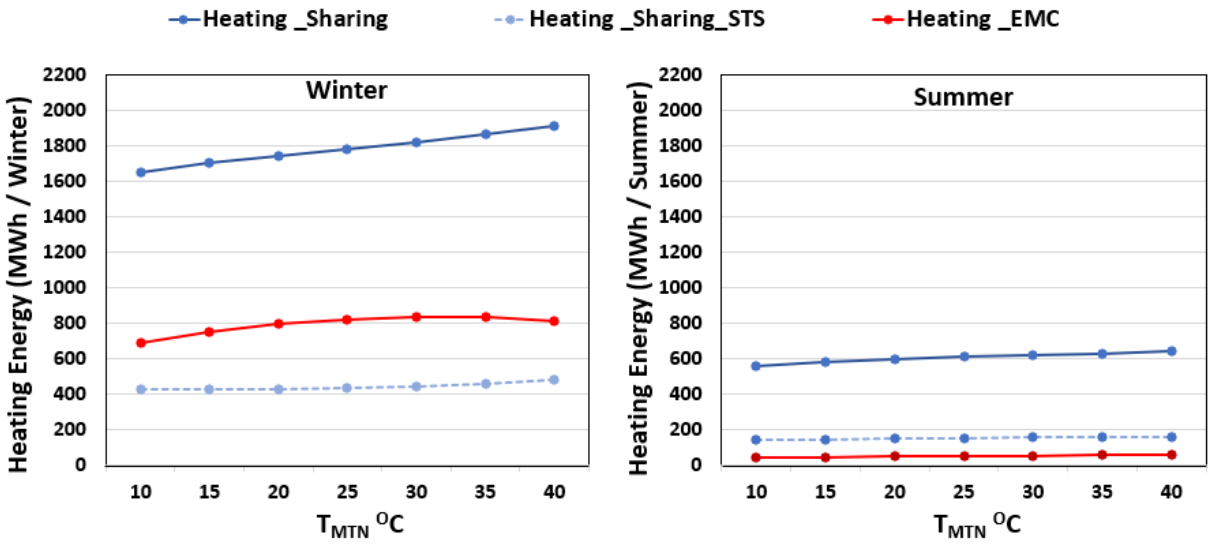

Figure 2-8: Heating energy covered from different resources at different MTN temperatures for the winter (left) and summer (right) seasons.

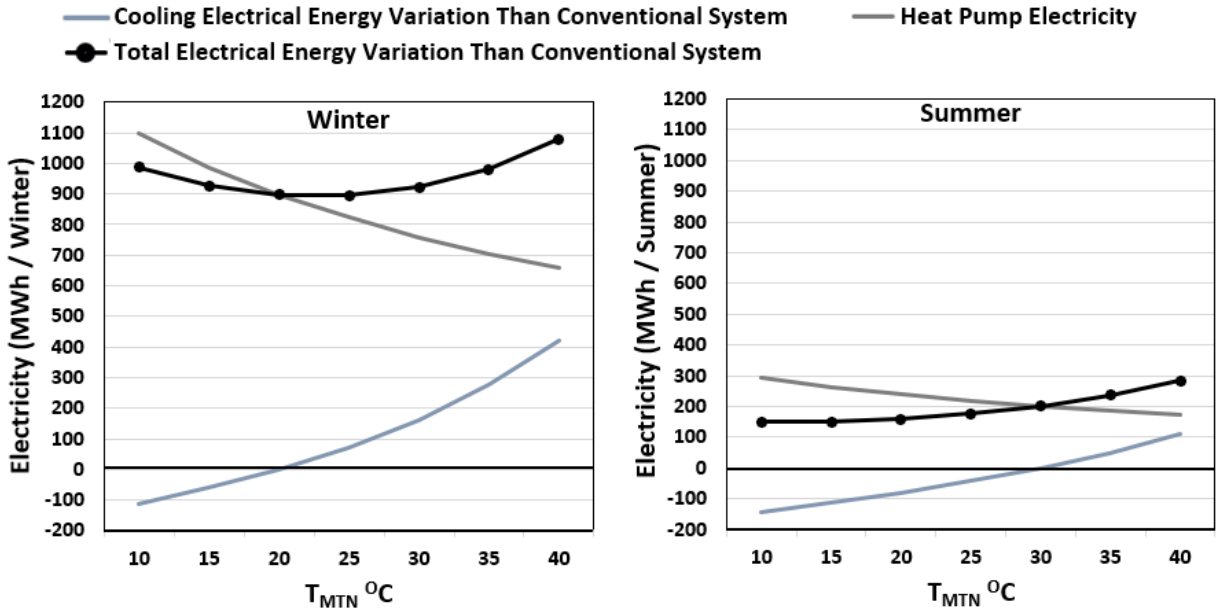

Figure 2-9: Effect of the MTN temperature on the electricity consumption of cooling and heating systems relative to the BAU systems for the winter (left) and summer (right) seasons.

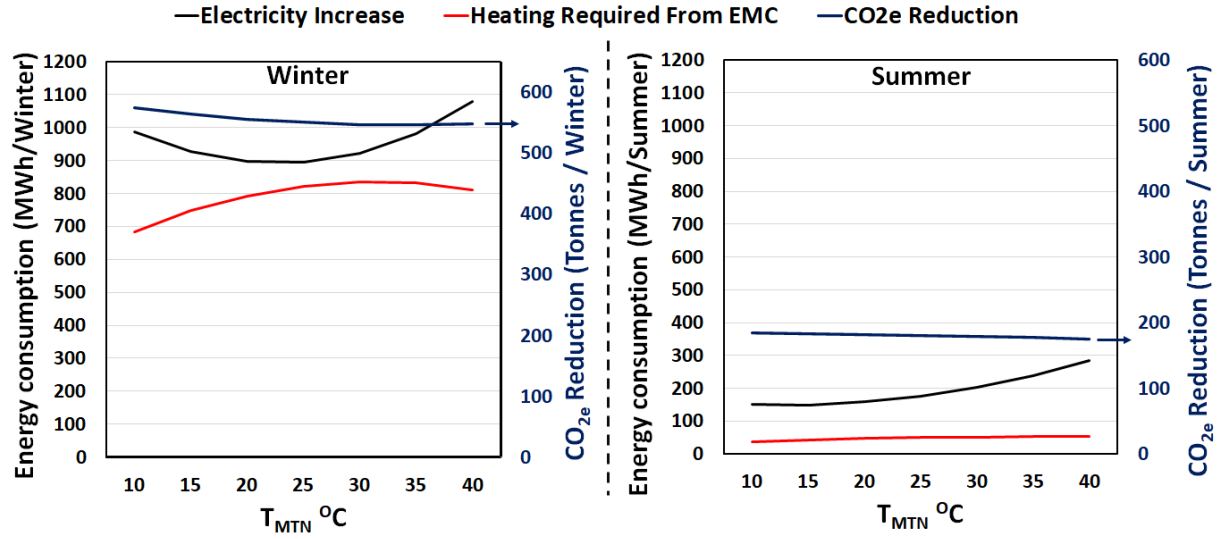

Figure 2-10: Summary curve showing the heat required from the EMC, the extra electrical energy required, and reductions in GHG emissions relative to the BAU case for winter (left) and summer (right) seasons.

The results depicted in Figure 2-8, Figure 2-9, and Figure 2-10 indicate that the selection of a fixed seasonal MTN temperature (T_{MTN}) will depend on the dominant load requirements. In the winter, when heating energy requirements are higher than the cooling demand, the use of MTN temperatures below 20°C will result in better refrigeration equipment performance and, hence, less

cooling-related electrical energy consumption; in contrast, heat pumps will consume more electrical energy during this period, leading to an overall increase in electrical energy consumption. However, the use of a T_{MTN} range of 20°C to 25°C results in approximately constant overall energy consumption, as the decrease in the heat pumps' electricity usage is nearly balanced by the increase in the cooling system's electricity usage. As the T_{MTN} is increased above 25°C, the resultant increased electrical energy consumption by the cooling system becomes dominant and once again increases the overall electricity consumption. In summer, when heating energy requirements are very low compared to cooling energy requirements, raising the T_{MTN} above 20°C reduces the performance of the cooling systems, thereby increasing the total electrical energy consumption. However, this increase in total electricity consumption is low compared to the winter season, as the heat pump requirement is relatively lower during the summer months.

Moreover, during the summer, the heat rejected from the cooling systems is several times higher than the MTN heating requirement. To reject this extra heat through systems such as cooling towers or dry coolers, the rejection temperature must be higher than the ambient sink; this poses a challenge, as the ambient sink of the buildings in this case study can reach or exceed 35°C during the summer. While GHG emissions depend on both electricity usage from fossil fuel sources and heating requirements, however they are mostly affected by heating. Thus, GHG emissions are reduced slightly with lower T_{MTN} in winter and remain almost constant during the summer. In summary, the results presented in this section show that the most energy efficient seasonal fixed operating MTN temperature ranges for this node are 20°C to 25°C during the winter and 20°C or less during the summer.

To determine whether using a fixed seasonal thermal network temperature or one that varies on a smaller time period (e.g., daily) will result in more efficient electricity consumption in the

integrated system, the effect of changing the T_{MTN} on a daily basis over the winter was investigated, as this season had the highest electricity use (Figure 2-10). For this investigation, the T_{MTN} was selected each day based on achieving minimum electricity consumption. Figure 2-11 shows the relationship between the selected T_{MTN} at minimum electricity consumption and the daily energy ratio between the heat rejected from the cooling systems and the MTN heating requirements (Q_{H_MTN}/Q_{rej}). Figure 2-11 also shows that the T_{MTN} ranges will be low, between 10°C and 15°C, at low Q_{H_MTN}/Q_{rej} ratios (less than 0.7). At a balanced ratio (from 0.7 to 1.3), the T_{MTN} will be at a medium temperature, from 20°C to 25°C, with most days in this balanced node falling within this balanced range. At energy ratios between 1.3 and 2.5, the T_{MTN} ranges from 30-35 °C, while the T_{MTN} climbs to 40°C or higher at Q_{H_MTN}/Q_{rej} ratios of 2.5 or more. However, this study did not consider T_{MTNs} above 40°C, as this is the maximum temperature at which the modeled refrigeration systems equipment can reject heat. The thermal load data used for this study consisted of buildings with diverse cooling and heating loads, which enabled a high degree of thermal energy sharing in all seasons. For heating-dominated ICE-Harvest nodes with less thermal load diversity (e.g., where most days have high Q_{H_MTN}/Q_{rej} ratios), using a heat pump on the rejection side of the cooling system to raise the rejection temperature could allow for higher MTN temperature and higher heating COPs, thus lower electricity consumption. Moreover, by controlling the electricity usage during each hour via changing the MTN temperature, it is possible to add dispatchable electrical load and use carbon-free sources in the grid, such as nuclear and renewables, that would otherwise be shut off during surplus generation times. Modeling the impacts of such a high-resolution MTN temperature with an hourly MTN temperature control strategy is recommended to be considered in future work. A comparison between the cost and economic performance of the ICE-Harvesting system and the conventional system could be investigated in future work as well.

Table 2-2 provides a comparison of electricity consumption at fixed seasonal temperatures and variable daily T_{MTN} temperatures selected to achieve minimum electricity consumption during the winter season. As the results show, the electricity consumption for the variable daily T_{MTN} (831 MWh) is 7% lower than the electricity consumption for the best constant seasonal T_{MTN} (895 MWh).

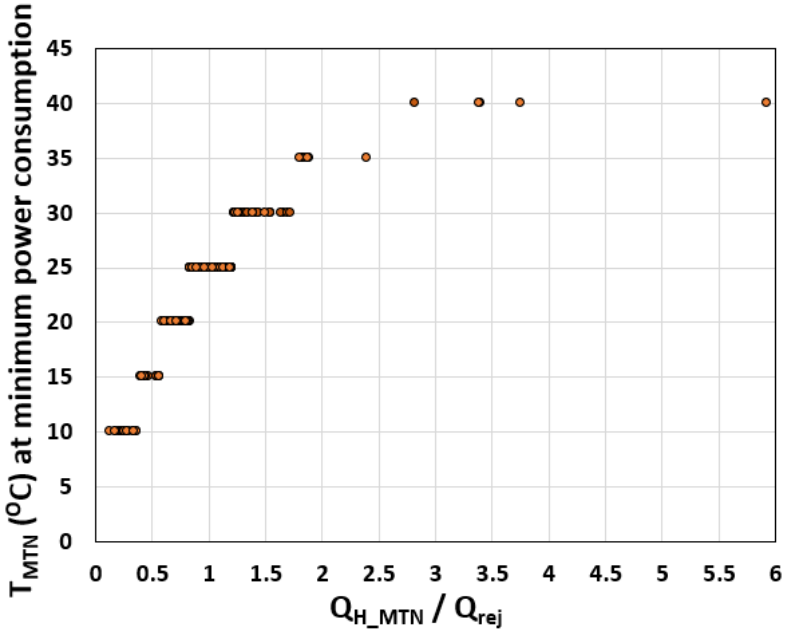

Figure 2-11: MTN temperatures for winter season days selected for minimum electricity consumption.

Table 2-2
Electrical energy increase at different MTN temperatures relative to the BAU systems during the winter season.

MTN Temperature (T_{MTN})	Winter season electrical energy increase
10 °C	988 MWh
15 °C	928 MWh
20 °C	897 MWh
25 °C	895 MWh
30 °C	921 MWh
35 °C	980 MWh
40 °C	1081 MWh
Daily MTN temperature selected for minimum electricity consumption	831 MWh

2.4. Conclusion

This investigation studies a thermal energy sharing model that can provide a real-time characterization of the potential benefits of integrating and harvesting energy within a community of buildings. The proposed model allows engineers to: estimate the amount of rejected heat from cooling and refrigeration systems that can be collected and used to heat other buildings in the node; determine the proper timing and quantity of electricity used by the heat pumps necessary in low-temperature MTNs; and reduce both GHG emissions and the energy required from the EMC relative to BAU conventional stand-alone systems.

The model was applied to a community node of four buildings—two heating-dominated buildings and two cooling-dominated buildings—with diverse thermal loads in Ontario, Canada. The results of this case study showed that the model is capable of providing a high-resolution evaluation of energy consumption and GHG emissions in an integrated energy system relative to a BAU system. The model showed that, over the course of a year, the use of an ICE-Harvest system along with balanced thermal load requirements would reduce this node's GHG emissions by 74% and supplemental heating requirements by approximately 82% compared to the BAU system. Although this approach led to a 30% increase in yearly electrical energy consumption, this increase was very modest during peak electrical periods during the summer; indeed, most of this increase took place during winter, where in Ontario the winter peak is typically several thousand MW lower than the summer peak.

This study also investigated how the performance of the ICE system was affected by using a fixed seasonal MTN temperature. For the seasonally balanced node, the results indicated that the MTN temperature had only a minor effect on GHG emissions, as the major source of emissions reduction was energy sharing between buildings. The analysis also showed that the dominant load mode was

the main factor driving the MTN temperature. During the winter season, when the heating load is dominant, the best energy utilization and emissions performance are achieved at an MTN temperature between 20-25^{o}C. During summer, when the cooling load is dominant, the best performance is achieved at a fixed seasonal MTN temperature of 20^{o}C or lower. Finally, the effect of varying the MTN temperature to achieve minimum electricity consumption on a daily basis over the winter was investigated and found to be better by over 7% of the best seasonal fixed MTN temperature with respect to electrical efficiency.

Acknowledgments

This work was supported by the Natural Sciences and Engineering Research Council of Canada [CRDPJ 509219-2017] and the Ontario Centre of Excellence [27851]. The authors would also like to acknowledge the McMaster Energy Research Cooperative partners for their contributions: HCE Energy Inc., GridSmartCity, GeoSource Energy Inc., s2e Technologies Inc., Siemens Canada Limited, Enbridge Gas Inc., and Alectra Utilities Corporation.

Appendix A

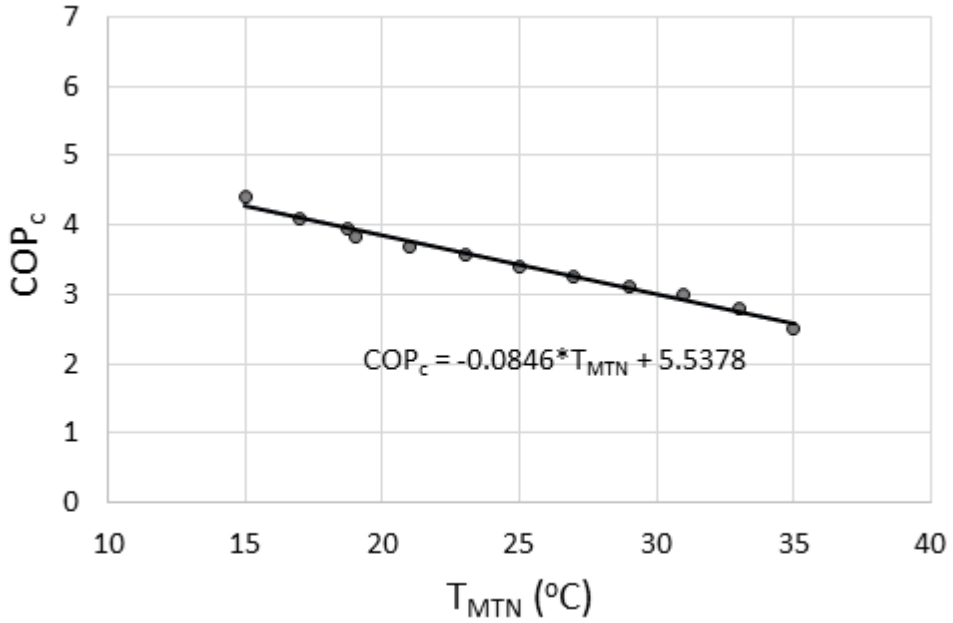

Figure 2.A1: Ammonia refrigeration system COP at different MTN temperatures with evaporator temperature -9°C

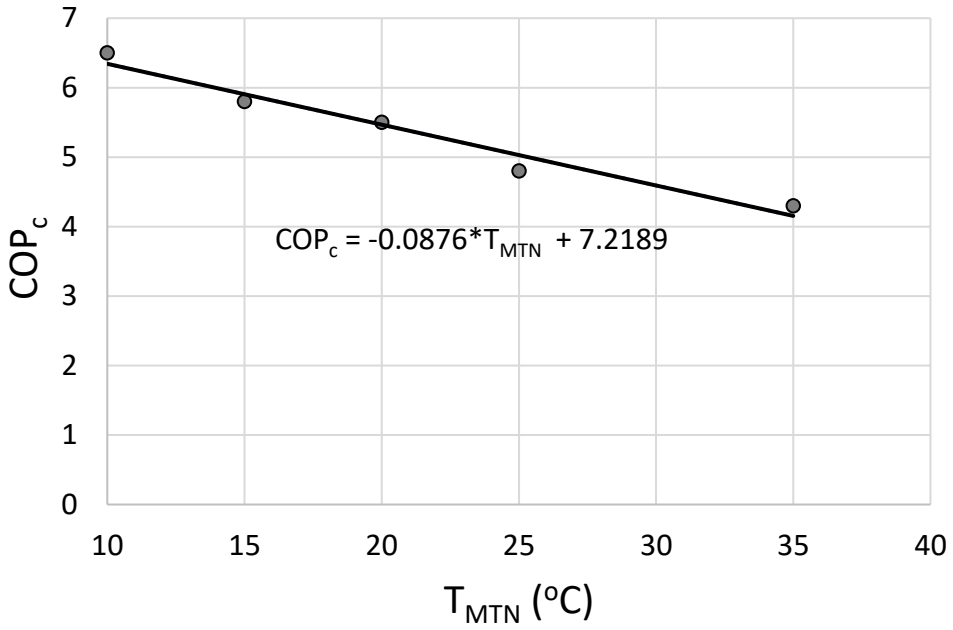

Figure 2.A2: Electric chiller COP at different MTN temperatures with evaporator temperature 10°C

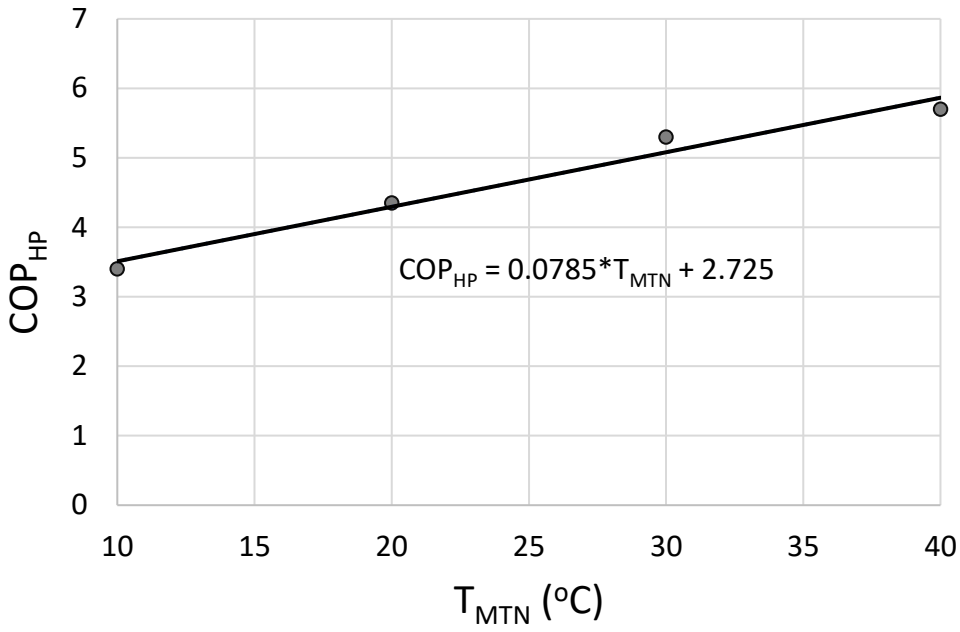

Figure 2.A3: Heat pump COP at different MTN temperatures with condenser temperature 65°C

References

[1] International Energy Agency (IEA), "Towards a zero-emission, efficient, and resilient buildings and construction sector," *Global Status Report*, 2017. [Online]. Available: www.globalabc.org.

[2] "Canada's 4th Biennial Report to the United Nations Framework Convention on Climate Change (UNFCCC)," 2020.

[3] National Research Council of Canada, "National Energy Code of Canada for Buildings 2017," p. 335, 2017.

[4] D. H. Nall, "Integration of refrigeration and HVAC in grocery stores," *ASHRAE J.*, vol. 59, no. 1, pp. 48–54, 2017.

[5] V. Minea, "Supermarket refrigeration system with completely secondary loops," *ASHRAE J.*, vol. 49, no. 9, p. 40+, 2007.

[6] K. Ebrahimi, G. F. Jones, and A. S. Fleischer, "Thermo-economic analysis of steady state waste heat recovery in data centers using absorption refrigeration," *Appl. Energy*, vol. 139, pp. 384–397, 2015, doi: 10.1016/j.apenergy.2014.10.067.

[7] L. Riahi, C. Martinez, P. Lapuente, R. Savickas, Z. Chen, and Š. Prieskienis, "Waste for heating and cooling : How district energy tranforms losses into gains," UN environment, Paris, 2017.

[8] H. Lund *et al.*, "4th Generation District Heating (4GDH). Integrating smart thermal grids into future sustainable energy systems.," *Energy*, vol. 68, pp. 1–11, 2014, doi: 10.1016/j.energy.2014.02.089.

[9] L. T. Cooper, "An Evaluation of District Energy Systems in North America : Lessons Learned from Four Heating Dominated Cities in the U . S . and Canada," pp. 60–72, 2012.

[10] B. Rezaie and M. A. Rosen, "District heating and cooling: Review of technology and potential enhancements," *Appl. Energy*, vol. 93, pp. 2–10, May 2012, doi: 10.1016/J.APENERGY.2011.04.020.

[11] H. Lund *et al.*, "The status of 4th generation district heating: Research and results," *Energy*, vol. 164, pp. 147–159, 2018, doi: 10.1016/j.energy.2018.08.206.

[12] H. Lund, N. Duic, P. A. Østergaard, and B. V. Mathiesen, "Future district heating systems and technologies: On the role of smart energy systems and 4th generation district heating," *Energy*, vol. 165, pp. 614–619, 2018, doi: 10.1016/j.energy.2018.09.115.

[13] J. Ziemele, A. Gravelsins, A. Blumberga, and D. Blumberga, "Combining energy efficiency at source and at consumer to reach 4th generation district heating: Economic and system dynamics analysis," *Energy*, vol. 137, pp. 595–606, 2017, doi: 10.1016/j.energy.2017.04.123.

[14] C. Flynn and K. Sirén, "Influence of location and design on the performance of a solar district heating system equipped with borehole seasonal storage," *Renew. Energy*, vol. 81, pp. 377–388, 2015, doi: 10.1016/j.renene.2015.03.036.

[15] F. Bünning, M. Wetter, M. Fuchs, and D. Müller, "Bidirectional low temperature district energy systems with agent-based control: Performance comparison and operation optimization," *Appl. Energy*, no. October, pp. 502–515, 2018, doi: 10.1016/j.apenergy.2017.10.072.

[16] S. Buffa, M. Cozzini, M. D. Antoni, M. Baratieri, and R. Fedrizzi, "5th generation district heating and cooling systems : A review of existing cases in Europe," *Renew. Sustain. Energy Rev.*, vol. 104, no. October 2018, pp. 504–522, 2019, doi: 10.1016/j.rser.2018.12.059.

[17] J. von Rhein, G. P. Henze, N. Long, and Y. Fu, "Development of a topology analysis tool for fifth-generation district heating and cooling networks," *Energy Convers. Manag.*, vol. 196, no. November 2018, pp. 705–716, 2019, doi: 10.1016/j.enconman.2019.05.066.

[18] S. Boesten, W. Ivens, S. C. Dekker, and H. Eijdems, "5Th Generation District Heating and Cooling Systems As a Solution for Renewable Urban Thermal Energy Supply," *Adv. Geosci.*, vol. 49, pp. 129–136, 2019, doi: 10.5194/adgeo-49-129-2019.

[19] B. Talebi, P. A. Mirzaei, A. Bastani, and F. Haghighat, "A review of district heating systems: Modeling and optimization," *Front. Built Environ.*, vol. 2, no. October 2016, pp. 1–14, 2016, doi: 10.3389/fbuil.2016.00022.

[20] C. Reidhav and S. Werner, "Profitability of sparse district heating," *Appl. Energy*, vol. 85, no. 9, pp. 867–877, 2008, doi: 10.1016/j.apenergy.2008.01.006.

[21] T. Nuytten, B. Claessens, K. Paredis, J. Van Bael, and D. Six, "Flexibility of a combined heat and power system with thermal energy storage for district heating," *Appl. Energy*, vol. 104, pp. 583–591, 2013, doi: 10.1016/j.apenergy.2012.11.029.

[22] R. Rogers, V. Lakhian, M. Lightstone, and J. S. Cotton, "Modeling of Low Temperature Thermal Networks Using Historical Building Data from District Energy Systems," *Proc. 13th Int. Model. Conf. Regensburg, Ger. March 4–6, 2019*, vol. 157, pp. 543–550, 2019, doi: 10.3384/ecp19157543.

[23] R. Z. Pass, M. Wetter, and M. A. Piette, "A thermodynamic analysis of a novel bidirectional district heating and cooling network," *Energy*, vol. 144, pp. 20–30, 2018, doi: 10.1016/j.energy.2017.11.122.

[24] M. Wirtz, L. Kivilip, P. Remmen, and D. Müller, "5th Generation District Heating: A novel design approach based on mathematical optimization," *Appl. Energy*, vol. 260, no. July 2019, p. 114158, 2020, doi: 10.1016/j.apenergy.2019.114158.

[25] M. Wahlroos, M. Pärssinen, J. Manner, and S. Syri, "Utilizing data center waste heat in district heating – Impacts on energy efficiency and prospects for low-temperature district heating networks," *Energy*, vol. 140, pp. 1228–1238, 2017, doi: 10.1016/j.energy.2017.08.078.

[26] B. Sullivan, M. Lightstone, and J. Cotton, "A Comparison of Different Heating and Cooling Energy Delivery Systems and The Integrated Community Energy and Harvesting System in Heating Dominant Communities," (MSc thesis) Mcmaster University, 2020.

[27] M. St-Jacques, S. Bucking, and W. O'Brien, "Quantification of high temporal and spatial

scale GHG emissions from electricity generation: method and case study," *eSim 2018*, vol. 66, no. January 2019, pp. 2008–2013, 2018.

[28] "High temperature heat-pump with PUREtec HFO refrigerant," *Carrier*, 2018. [Online]. Available: https://www.carrieraircon.co.uk/wp-content/uploads/com.pdf.

[29] "The Independent Electricity System Operator (IESO) of Ontario's power system." [Online]. Available: https://www.ieso.ca/en/Power-Data/Data-Directory.

Chapter 3

The Impact of Clustering Strategies to Site Integrated Community Energy and Harvesting Systems on Electrical Demand and Regional GHG Reductions

The impact of clustering strategies to site integrated community energy and harvesting systems on electrical demand and regional GHG reductions

Ahmed Abdalla[1], Saber Mohamed[1], Kelton Friedrich[1], Scott Bucking[2], James S. Cotton[1*],

[1]McMaster University, Department of Mechanical Engineering, Hamilton, Ontario, Canada

[2]Carleton University, Department of Civil and Environmental Engineering and the Azrieli School of Architecture and Urbanism, Ontario, Canada

*Corresponding Author: cottonjs@mcmaster.ca

Abstract

The current work examines the Integrated Community Energy and Harvesting system (ICE-Harvest), an integration of thermal and electrical distributed energy resources. The system prioritizes the harvesting of community waste energy resources—for example, residual heat rejected from cooling processes and peak electricity fossil-fuel fired generators, as well as energy from curtailed clean grid electricity resources—to help in satisfying the heating demands of commercial and residential buildings. As such, ICE-Harvest systems provide a solution that can minimize greenhouse gas emissions from high-energy-consumption buildings in cold-climate regions such as North America and Northern Europe. The current work focuses on where to locate these systems and introduces different clustering methods for integrated energy systems that focus on thermal load diversity among buildings in each cluster. In the first technique, buildings with the highest amount of rejected heat from their cooling systems (anchor buildings) are clustered with nearby high heating demands buildings to create a large opportunity for harvesting wasted energy however, buildings not located close to anchor buildings are clustered using density-based clustering methods. The energy harvesting capabilities of this technique are compared to those provided by full DB clustering without specifying the anchor buildings, as well as to full density-

based clustering with a post-processing step in which the nearest anchor building is added to each cluster. The selected clustering method also demonstrates the grid level potential of the ICE-Harvest systems to impact greenhouse gas emissions, heating, and electricity consumption by presenting a reduced model for the ICE-Harvest system that can be applied to any number of clusters on a municipal or provincial/state scale. Specifically, the model is applied to a database of 14,832 high-energy-consumption buildings with the potential for forming 1,139 clusters in the province of Ontario, Canada. The results of this case study reveal that density-based clustering with post processing resulted in the largest emission reduction per unit piping network length of 360 t CO_2eq /km/year. In addition, the use of ICE-Harvest systems can displace the energy required from the gas-fired heating resources by 11 TWh, accounting for over 70% of the clusters' total heating requirements. This results in a 1.9 Mt CO_2eq reduction in overall sites' emissions, which represents around 60% of the clusters' emissions.

Keywords: *Thermal energy sharing, Integrated energy system, Density-based clustering, Energy harvesting, City scale impact.*

Abbreviations

5GDHCS	Fifth Generation District Heating and Cooling System
AEF	Average Emission Factor
BAU	Business as usual
CHP	Combined Heat and Power
CO_2e	Carbon Dioxide Equivalent
COP	Coefficient of Performance
DB	Density-Based
DER	Distributed Energy Resources
DHS	District Heating Systems
EAC	Equivalent Annual Cost

EMC	Energy Management Center
ETS	Energy Transfer Station
HHP	Heating Heat Pump
HRHP	Heat Recovery Heat Pump
ICE	Integrated Community Energy
IESO	Independent Electricity System Operator
LHD	Linear Heat Density
LTS	Long-Term Storage
MEF	Marginal Emission Factor
OPTICS	Ordering Points to Identify the Clustering Structure
PV	Photovoltaic
STS	Short-Term Storage
SOM	Self-Organizing Map
TTD	Terminal Temperature Difference

Nomenclature

Q	Heat flow rate [kW]
T	Temperature [°C]
L	Length [m]
W	Electric work [kW]
E	Electricity demand [kW]

Subscripts

a	Relating to the maximum allowable value
B	Relating to a building
boiler	Relating to the boiler
C	Relating to a cooling load
CHP	Relating to a CHP
Conv	Relating to the conventional system
H	Relating to a heating process

HP	Relating to a heat pump
min	Minimum allowed or expected value
nB	Number of buildings
T	Relating to the total number
rej	Heat rejection from cooling systems
Sh	Related to thermal energy sharing

3.1. Introduction

The Paris Agreement [1], which has been ratified by the 55 countries responsible for around 55% of global greenhouse gas (GHG) emissions, was implemented with the goal to keep global temperatures from rising more than 1.5^{o}C above pre-industrial levels [2]. One of the key challenges as presented in the United Nations' Global Status Report 2017 is the building operation and construction sectors which accounts for 36% of global end-energy consumption and 39% of carbon dioxide (CO2) emissions [3]. In cold-climate countries, most of these emissions are produced by building heating demands. Fortunately, harvesting waste energy resources such as heat rejected from cooling processes and peak electricity fossil-fuel-fired generators, and electrical grid curtailed carbon-free energy (e.g., nuclear and renewable), can reduce heating-related GHG emissions, while still providing the required levels of utility service [4]–[6].

This introduction is organized as follows, sections (1.1 and 1.2) examine the previous attempts to harvest buildings' waste heat, as well as address the wasted energy resources in the electrical grid. Integrated energy between buildings to increase energy harvesting and reduce energy waste has gained attention in the last few decades however, their potential for mass implementation has not been explored. Section 1.3 presents different integrated energy systems. Following that, section 1.4 presents the different clustering techniques that were used in the literature to group buildings

in integrated energy systems. The research gaps and the scope of this study are discussed in section 1.5.

3.1.1. Building waste heat and thermal energy sharing

Buildings are classified as either cooling-dominated or heating-dominated depending on their energy profiles integrated over the course of a year [4]. Cooling-dominated buildings are characterized by high process cooling throughout the year (i.e., refrigeration and air conditioning) such as grocery stores, ice rinks, IT servers, and data centers. The cooling systems in such buildings produce large amounts of waste heat, which is usually released into the environment through heat-rejection equipment. In contrast, heating-dominated buildings are buildings with higher heating requirements, such as residential towers and hotel buildings.

Many strategies for harvesting waste energy from cooling-dominated buildings have been documented in the literature, including the use of heat-recovery systems to harvest wasted energy within the same building. Minea et al, [7] examined the recovery of refrigeration system heat rejection to meet the space heating demands in a supermarket, founding that 30% of the rejected heat can be recovered. Escriva et al., [11] studied recovering heat rejected from supermarkets' refrigeration systems in the UK which covers 62% of the heating energy requirements and results in over 50% GHG emissions savings. Nall [8] offered a guide for different ways to reduce the energy consumption of grocery stores by 50% through heat recovery from their refrigeration systems. In another study on an ice rink, Piché et al., [9] found that harvesting the heat rejected from the air-cooled condenser of the rink refrigeration system can lead to 60% savings in heating energy consumption.

Murphy et al., [9] examined recovering waste heat between two buildings of a data center and a residential building via a simultaneous heating and cooling heat pump. Although the study results in large energy savings exceeding 50% of the overall buildings' energy demand, the methodology is only applicable to space cooling and heating This approach is not applicable to process refrigeration systems which are considered as a major source of waste heat. For example, around 60% of grocery stores' end energy use is for refrigeration systems [10], [11] which ultimately ends up as cooling process waste heat.

To provide better energy harvesting opportunities, the focus has recently switched towards employing thermal networks to capture and redistribute waste thermal energy within a group of buildings with different energy demands. For example, Pass et al., [12] analyzed the energy demands of some Germain cities' buildings and demonstrated that the optimum combination of building archetypes in terms of energy savings is the one that results in a yearly cooling to heating demand ratio of one (i.e. a balanced thermal energy demand), with such buildings as a hospital with a grocery store. The results showed that using a low-temperature thermal distribution network with that balanced loads maximizes the benefits of energy harvesting. Wahlroos et al., [13] conducted a simulation on a case study in Finland where up to 60 MW of waste heat from a data center was captured and used as an energy source in a low-temperature DH system thermal network. Abdalla et al. [4] presented an energy sharing model wherein a group of buildings with diverse energy demands was connected with a microthermal network to form a thermally balanced cluster. Their findings in that balanced demand case study showed that the proposed energy sharing system was able to satisfy about 80% of the cluster's heating demands, resulting in around a 72% reduction in GHG emissions.

3.1.2. Electrical grid waste energy resources

There are two major waste energy resources from electricity grids. Some electrical grids with a large ratio of carbon-free generation capacity curtail energy production for frequency regulation during periods when carbon-free generation potential exceeds demand (off-peak periods). However, during periods of high demand and low availability of clean resources (peak periods), most grids use dispatchable centralized natural gas plants to meet the electricity demand. Unfortunately, the efficiency of these plants is low typically around 42%, and most of the fuel energy is wasted as heat loss [14].

Most developed countries have been increasing the use of carbon-free technologies in their electricity generation systems such as nuclear and renewable resources (e.g., solar, wind, and hydro). However, the increased prominence of renewable resources has resulted in greater mismatches between generation and demand, as well as the further curtailment of clean resources. According to the 2018 Energy Conservation Progress Report [15], Ontario, Canada, increased its use of carbon-free resources for electricity generation in the last 10 years from about 2 GW to almost 13 GW but this increase was also accompanied by an increase in the annual curtailed electricity from 1 TWh to about 10 TWh. Similarly, in 2016, around 20 TWh of wasted heat from the Ontario grid was due to the usage of centralized natural gas plants at peak periods.

This increase in curtailed electricity caused by the surplus generation of carbon-free resources during off-peak periods creates numerous challenges to the electrical grid. Elsewhere, Olauson et al., [16] concluded that greater system flexibility is required in Nordic countries' electrical grids due to the imbalance between high-generation and high-demand periods caused by the significant implementation of renewable resources in these grids. Different techniques for increasing system flexibility have been detailed in the literature. For example, Ziegler et al., [17] analyzed using

diverse short-term storage technologies to increase the reliability of renewable resources for 4 different electricity grids in the US. The study estimated that the storage energy capacity cost should be below $20/kWh to be cost competitive. On the other hand, other researchers suggested that long-term storage provides great flexibility to renewable power generation and reduces curtailment with low cost levels [18], [19]. Dowling et al., [18] found that storing large quantities of wind and solar energy via long-term storage (seasonal and multi-year) can lead to a 50% cost reduction compared to wind and solar short-term battery storage system.

Other techniques to add flexibility were focused on the demand side, such as demand-response techniques (i.e., the bidirectional charging of electric cars [20] and incentive-based demand-response programs for heavy industries to allow for flexible loads [21]) which ultimately leads to a loss of productivity of these industries. Integrating thermal and electrical networks can add another flexibility to the electrical grid which will be presented in the next section.

3.1.3. Integrated energy systems

Recently many researchers have been moving towards the integration between thermal and electrical grids via the electrification of heating. The electrification of heating can also enhance electrical grid flexibility while simultaneously reducing fossil fuel usage and GHG emissions; however, the non-dispatchable full electrification of heating in cold-climate countries significantly increases electricity demand [22]. Waite and Modi [22] evaluated the impact of electrification of heating for all US grids via air source heat pumps resulting in a 70% increase in the aggregated electricity peak demand. Similarly, Cooper et al., [23] found that using air source heat pumps in the UK for heating will double the aggregated electricity peak demand.

Inter-building energy harvesting with a thermal network can be an effective approach to reduce the impact of the electrification of heating on the electricity grids. Fifth-generation district heating and cooling (5GDHCS) systems [24] were designed to harvest low-grade heat sources such as cooling processes waste heat and energy produced by renewable sources (e.g., solar, and PV) from neighborhood-sized areas with ultra-low temperature thermal networks (near ambient around 20^{o}C). These systems are based on the use of electric heating using water source heat pumps in each building, which raise the network temperature to meet the heating requirements of the buildings in the cluster. Bünning et al., [25] showed that the application of 5GDHCS for two case studies of balanced and heating dominant neighborhoods leads to an emission reduction of 63% and 26% emissions respectively. Rogers et., [11] modeled 5GDHCS on a case study of nine different building archetypes in Ontario. The system resulted in around 34% reduction in the total energy utilization however, the electricity demand and peak increased by 50% and 100% respectively. The use of unresponsive constant ultra-low temperature thermal networks could lead to higher electricity demand during non-preferable times (peak times) especially on extremely cold winter days [26], [27].

The current study focuses on the Integrated Community Energy and Harvesting System (ICE-Harvest) that harvests buildings' cooling systems and grid waste energy resources while providing better flexibility to the electrical grid via novel network and system operation.

The ICE-Harvest system proposed a smart thermal network operation that allows electric heating only when there is surplus generation from non-fossil-fuel resources on the grid. This proposed operation overcomes the 5GDHCS system's significant dependence on electricity at peak electricity demand periods [5]. In addition, the ICE-Harvest system is designed to harvest wasted energy from multiple resources such as building cooling systems, centralized low-efficiency peak

electrical generators, and curtailed clean-energy resources. The system description is explained in detail in section 2.

3.1.4. Clustering

Previous researchers have employed different methods for clustering district heating systems (DHS), including k-means [28], [29], self-organizing map (SOM) [30], and density-based clustering algorithms [31], [32]. Some of these approaches consider the spatial relationships between buildings, while others include the temporal dimension, which includes the energy demand profile. In DHSs, building clustering approaches mainly aim to group buildings in close proximity with high heating loads in order to reach high Linear Heat Density (LHD), which is defined as the annual heating demand/length of the thermal network connecting the clustered buildings. A higher LHD translates to lower mechanical and thermal losses as well as network costs [33]. Yan et al., [28] performed 2 stage optimization for district energy systems wherein k-means clustering algorithms are performed to divide the district into smaller size sites, then MILP programming is used to optimize the operation and configuration of the buildings in each cluster to minimize the total annual cost. The model was applied to a case study of 20 buildings including schools, hospitals residential, and hotels that results in a 24% saving in the TAC compared to a centralized system. Jafari et al., [30] developed a SOM for clustering with a genetic algorithm to cluster 30 houses based on their energy profiles. Their results showed that clustering buildings with shared energy production technologies (e.g., solar and battery) reduced the system costs by 13%. In a different work, Marquant et al., [31] applied an OPTICS density-based clustering algorithm to different building archetypes. In this study, an optimization problem for each cluster was solved by identifying the building with the highest heating demand as the anchor building of

the cluster. Then, the nearest building to the anchor one was iteratively added to minimize the equivalent annual costs (EAC). Applying this method in a case study of 221 buildings showed that 14.4% of the EAC was saved over individual building systems. Marquant et al. [31] also performed an optimization algorithm on each cluster that aimed for minimizing the GHG emissions instead of the EAC which resulted in the addition of all buildings in each cluster achieving the maximum carbon emissions reduction.

3.1.5. Previous studies gaps and the scope of the present work:

Although different building clustering techniques have been applied for DHSs made up of buildings with certain characteristics, assessing or modifying these techniques and characteristics to fit within integrated electrical and thermal networks with thermal energy sharing was not investigated in previous works. This work presents a comparison of three clustering techniques—namely, the existing spatial clustering technique, a novel technique based on the use of an anchor building, and an upgraded combined technique—to identify the most beneficial technique for energy sharing and GHG emissions reduction.

In addition, the previous works that targeted energy harvesting between buildings were focused on balanced or near thermally balanced demand clusters. The current study includes results from different thermal demand conditions such as heating dominated, cooling dominated, and balanced thermal demands clusters.

The ICE-Harvest system design [5] presents a new opportunity for harvesting waste energy from process cooling and low-efficiency peak natural-gas-fired electrical generators, as well as curtailed clean-energy resources on site. This work demonstrates the potential impact of implementing ICE-Harvest systems at a grid scale on a state/provincial level.

The remainder of this article is structured as follows: The ICE-Harvest system description is explained in section 2. The detailed procedure of the three clustering approaches is described in section 3. Later in the same section, reduced model of the ICE-Harvest system and the parameter selection methodology are described. To compare the clustering methods database of 14832 in Ontario is used as a case study. A detailed description of the case study is presented in section 4. Section 5 presents the comparison results of the different clustering approaches, and the best approach is determined in terms of energy harvesting, network length, LHD, and GHG emissions reduction. Also provided in Section 5 are the impacts of the ICE-Harvest system mass implementation for the resulting clusters on the overall clusters' heating, electricity, and GHG emissions. The limitation of the current work and future studies' recommendations are presented in section 6. Section 7 provides the conclusion of the study.

3.2. ICE-Harvest system description

The ICE-Harvest system connects a group of high-energy-consumption buildings using a Micro-Thermal Network (MTN), as shown in Figure 3-1. The MTN is modeled as a single unidirectional thermal distribution pipe that carries water at a temperature (T_{MTN}). This temperature is adjusted depending on the real-time availability of different thermal resources and the site's current heating and cooling requirements. Each building in the integrated energy cluster has an energy transfer station (ETS) with two heat pumps and two heat exchangers. A set of a heat pump and a heat exchanger connects the MTN to the heat rejection condenser of each building's cooling system, while the other set connects the MTN to the building's heating distribution system (Figure 3-1). The ETS provides the MTN unique flexibility by allowing it to operate within a wide temperature range from about 20^{o}C to 80^{o}C. The MTN operates at an ultra-low temperature level

during off-peak times, thus allowing a direct exchange between the MTN and the cooling system's heat rejection via the ETS heat exchanger. The heating heat pump (HHP) in the ETS is used to raise the MTN Temperature (T_{MTN}) to meet the building heating required temperature. Operating the MTN at an ultra-low temperature level increases the aggregated electricity demand created by the electrification of heating, which is favorable during off-peak periods and aids in harvesting the grid curtailed electricity. During peak periods, the MTN is operated at a higher temperature level to decrease the aggregated electricity demand created by the electrification of heating. In addition, it allows for direct heat exchange between the MTN and the building heating distribution systems. To harvest the heat rejected from building cooling systems in this operating condition, the heat recovery heat pump (HRHP) raises the temperature of the rejected heat above the MTN temperature to allow for direct heat exchange.

The energy management center (EMC) of the ICE-Harvest system is a centralized component that provides the remaining energy requirements of the MTN. This EMC includes a CHP, STS, LTS, and a backup gas fired boiler. The CHP displaces the centralized grid natural gas peak generators by distributing the generation to numerous sites to allow the ICE-Harvest system to harvest their residual heat toward the MTN's heat requirements. In addition, the short-and long term thermal-energy storage technologies are employed to increase the system flexibility for the demand and generation mismatch.

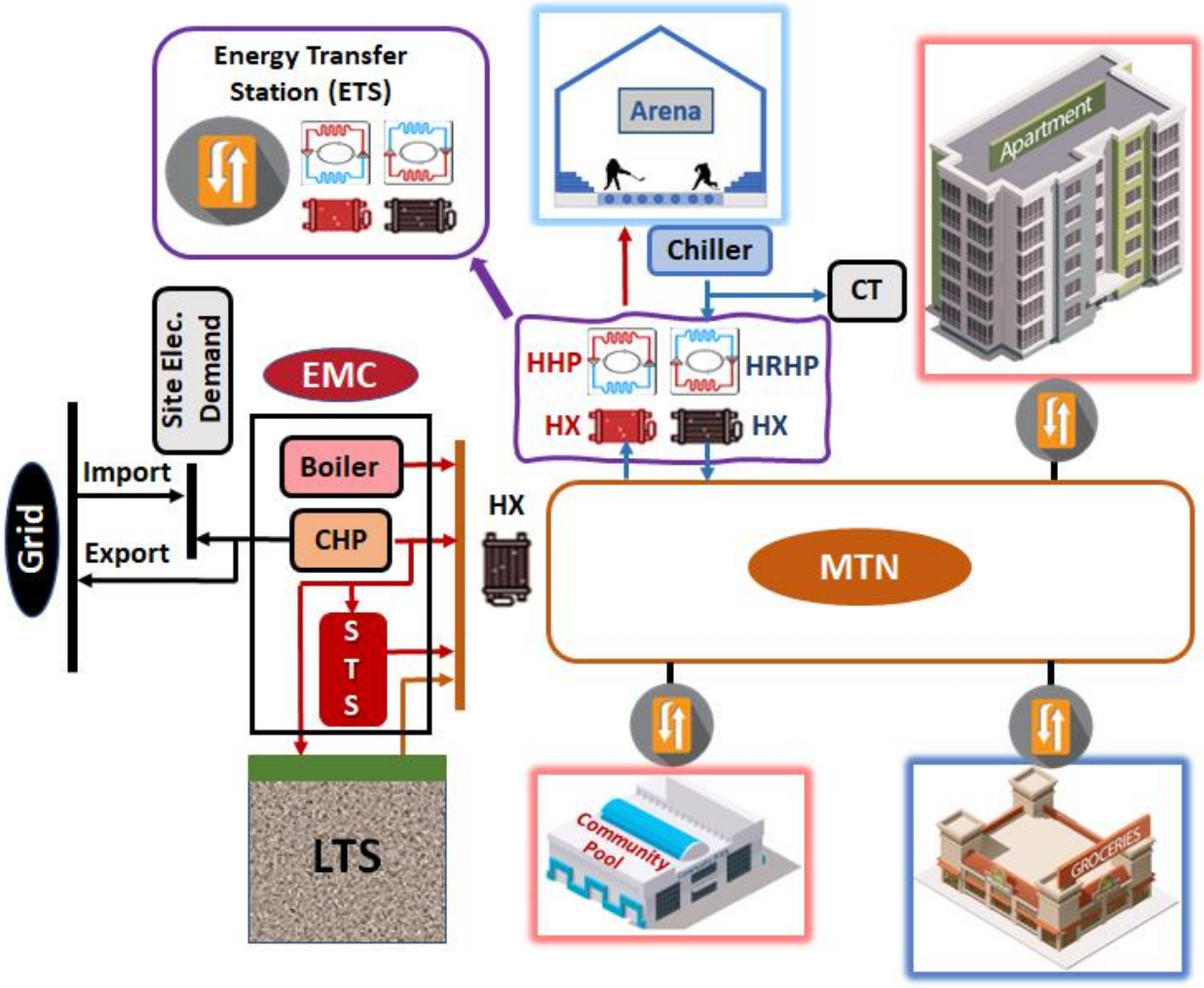

Figure 3-1: Simplified representation of the ICE-Harvest system. Note: the system is not to scale.

3.3. Methodology

This section describes the three different clustering approaches used in this study. In order to facilitate comparison, various parameters are assessed for the clustering strategies to identify the best approach for the integrated energy systems including the reduction of GHG emissions, total piping length, LHD, and thermal losses. Additionally, a simplified ICE-Harvest system model is developed that includes the MTN and the EMC design and operating parameters to evaluate the impacts of the large scale implementation of a fleet of ICE-Harvest systems.

3.3.1 Clustering techniques

The first clustering method (A) is a hybrid technique based on two phases of clustering. First, buildings were clustered around an anchor building (cooling dominated) that is identified in Section 3.1. In this phase, all buildings that are located within 1km distance from the anchor building are clustered to provide a large opportunity for energy sharing. In phase 2, all buildings in the database not used in phase 1 due to being too far from an anchor building (i.e., > 1km) are clustered using the unsupervised machine-learning density-based (DB) algorithm [34]. The DB clusters are created by using a radius of 1km and a minimum of 3 buildings in each cluster.

The second clustering method (B) only employed the unsupervised machine learning DB algorithm without specifying the anchor buildings.

The third method (C) is similar to method B with an extra post-processing step of adding the closest anchor building (within a 1km distance) to increase the energy sharing potential. A visual illustration of the three different clustering methods is presented in Figure 3-2Figure .

Next, a deeper comparison of the three clustering methods was conducted by calculating the shortest piping length, total heating demand, linear heat density (MWh/m.year), and thermal pipe losses for each cluster. The methodology of these models will be presented in section 2.2. Additionally, the reduced thermal energy sharing model [4] was applied to identify the overall energy harvesting potential of each clustering method.

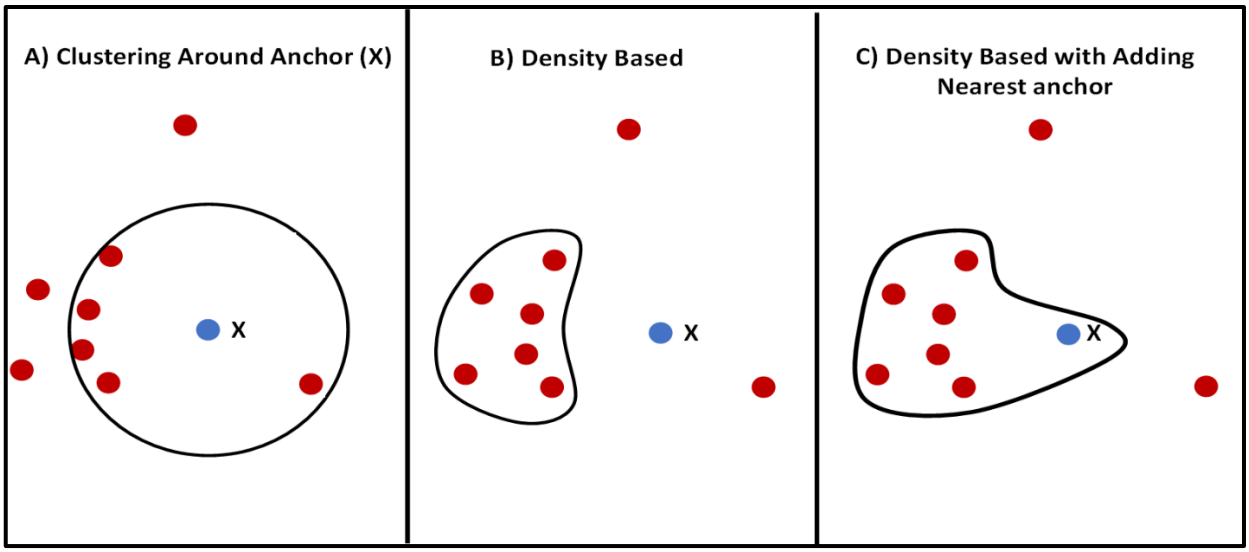

Figure 3-2: Illustration of the three different clustering methods.

3.3.1.1 Clustering constraints

The following constraints were applied to the clusters produced by the three clustering algorithms:

- The maximum allowable MTN length (L_{MTN})

  The maximum MTN length selected is set to be 6 km [5] to avoid large centralized networks with large thermal and mechanical losses, and thermal mass. In addition, the MTN temperature in the ICE-Harvest system change in a wider range than the DHS of around 50^{o}C. The thermal network is designed intentionally to be small in length, in order to keep the water thermal mass sufficiently small to be able to vary the network temperature between 20 and 70^{o}C to provide the ability to fuel switch and as a demand response strategy. Large networks have large thermal masses which is not possible to change the temperature in the time scales needed for grid electricity control and demand management [35]. Small scale networks also feature lower mechanical and thermal losses and lower investment risk. However, as the number of networks in a community increases, these individual networks

could be connected to make a larger district system and increase harvesting potential while being still controlled independently. The metaheuristic Tabu search algorithm [36] was then employed to estimate the shortest MTN length connecting the buildings.

- The maximum allowable CHP size of the cluster

  This constraint is used to avoid centralized, large-capacity clusters with more than 5 MWe of peak electricity demand. Additionally, this constraint helps to "de-risk" the system by lowering the initial capital costs and eliminating the need for significant upgrades to the local distribution grid infrastructure. To apply this constraint before calculating the CHP size, the cluster's maximum allowable heating demand is used to represent the constraint as follows:

  The maximum allowable annual heating energy consumption of the cluster = maximum allowable CHP size * the number of operating hours * the heating-to-electricity ratio of the CHP /CHP average part loading ratio.

  Where: the number of operating hours with high dispatchable loads and high electricity generation from natural gas was used Based on 2017 data in Ontario, of about 3350 hrs [37]; the average heating-to-electricity ratio for the CHP was estimated as 1.2; the average partial loading of the CHP is selected to be 0.667.

  Using these values, a maximum allowable annual heating energy consumption ($Q_{H,a}$) of 30 GWh_{th} was calculated.

Cluster lengths and heating demands should be less than the maximum MTN length and the maximum allowable annual heating energy consumption; if they exceed these values, they will be allocated to smaller clusters using the k-mean algorithm [38]. The clustering method is summarized in Figure 3-3.

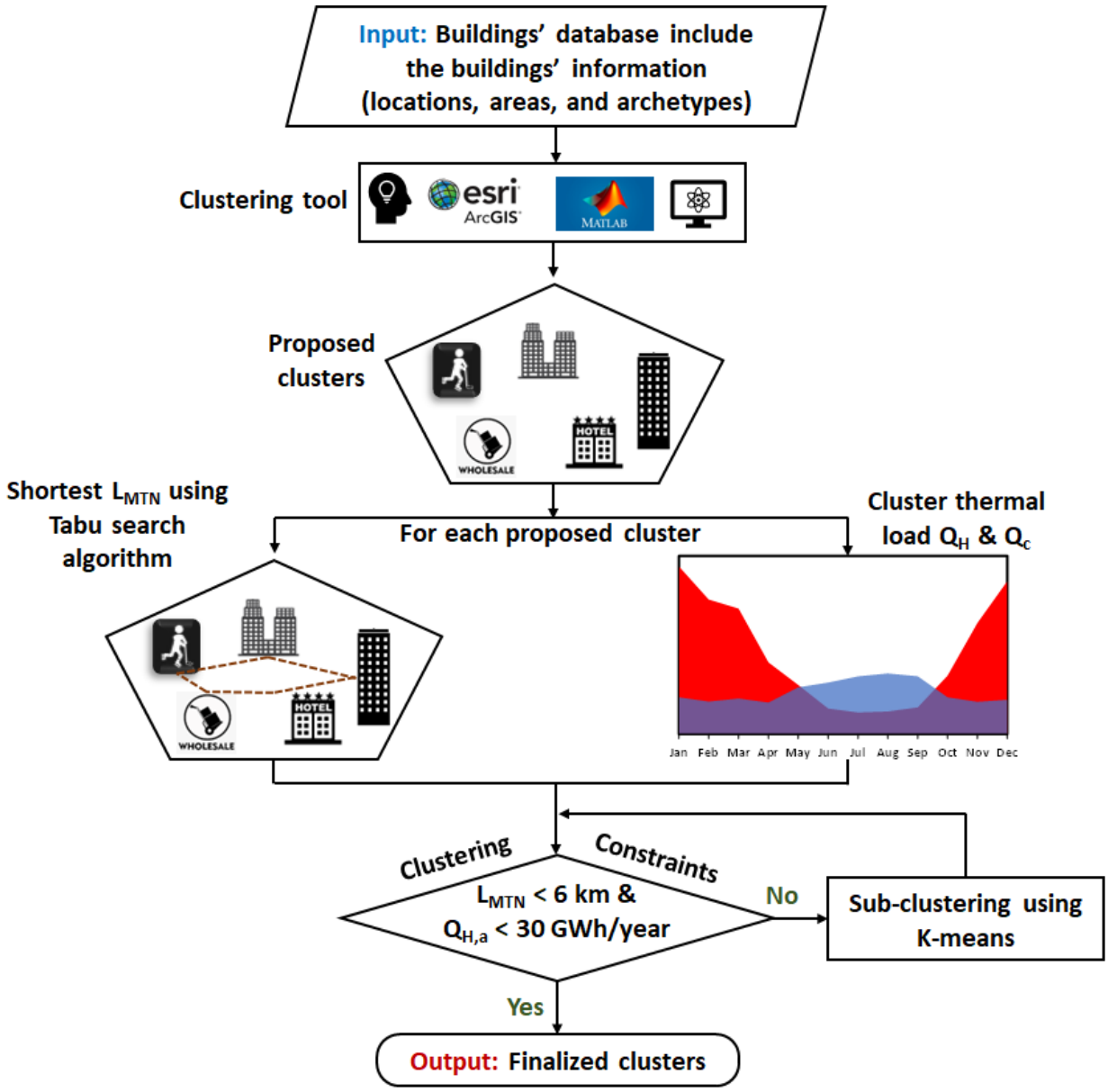

Figure 3-3: Clustering method.

3.3.2. ICE-Harvest system modeling

In this section, a simplified ICE-Harvest model is developed to evaluate the impact of energy harvesting on GHG emissions. The model inputs consisted of the electrical and thermal energy profiles (cooling Q_c, heating Q_H, and electrical demand E_{BAU}) of all buildings in each cluster finalized in the previous step. The current stand-alone business-as-usual system (BAU) for all the

buildings in the database is assumed to use ammonia and electric chillers to meet the buildings' refrigeration and air conditioning demands respectively and a gas-fired boiler to meet their heating demands. Electricity consumed would all be imported to the site from the electrical grid. The reduced ICE-Harvest model's outputs included the MTN's operation temperature at different conditions, the amount of shared heating Q_{sh} via the harvesting of heat rejected from the buildings' cooling systems, the added demand from the MTN's thermal losses, the new heating demand from the EMC, the new electricity demand after using the ETS heat pumps to aid energy sharing, the suitable CHP size (if needed), and the reduction in GHG emissions. The following sections will discuss the model, the applied constraints, and the utilized assumptions in greater detail.

3.3.2.1. Microthermal network modeling

The model presented herein builds on prior work by Abdalla et al. [4]. However, the present model allows the MTN temperature to be varied on an hourly basis via the ETS to run at either 70^{o}C or 20^{o}C. The model was modified to follow the ICE-Harvest system's smart network operation with sharing prioritization as in [5]. The ETS in each building gives the flexibility to use either of these two operational protocols:

A. Using the HRHP to harvest and increase the temperature of heat rejected from the cooling process AND to facilitate direct heat exchange to buildings' heating distribution systems (in case of low MTN temperature of 70^{o}C).
B. Using the HHP to raise the MTN temperature to the buildings' heating distribution systems required temperature AND direct heat exchange to the MTN to harvest the heat rejected from the cooling process (in case of ultra-low MTN temperature of 20^{o}C).

The heating-distribution systems required temperature in all 14832 buildings assumed to be within 60-65^{o}C. The piping system is sized to achieve the maximum energy demands at different MTN operating temperatures with fiberglass insulation thickness based on ASHRAE standard 90.1 [39].

Figure 3-4 presents a flow chart illustrating the decision-making process regarding which MTN temperature to use at each hour. The 70^{o}C setting is selected to allow direct heat exchange with a terminal temperature difference between the MTN and the individual buildings' heating distribution systems. However, the 20^{o}C setting is selected to allow direct heat exchange with a terminal temperature difference (TTD) of at least 5^{o}C between the MTN and the individual buildings' cooling rejection systems (condensers). In the low-temperature setting, (70^{o}C) less electricity is required just to raise the temperature of the heat rejected from cooling systems via HRHP to the network, and the remaining heating requirement by MTN is met via the EMC resources. In contrast, in the ultra-low temperature setting for the MTN, the HHP consumes more electricity to serve the heating demands of the buildings which will lead to more electrification of heating than in the low MTN temperature settings. Thus, the MTN temperature is used to control the amount of electricity-based heating used on an hourly basis. As the flow chart in Figure 3-4 shows, if the grid's centralized peak electricity gas generators are running (i.e., on-peak) at a certain hour, the MTN temperature should be set to low to reduce the electrification of heating; if the generators are not running (i.e., off-peak), the temperature can be set to ultra-low to harvest the grid curtailed carbon-free electricity. Furthermore, during the summer months, it is common for the heat rejected from the cooling systems to be sufficient to satisfy the cluster's heating demands. In this situation, an ultra-low temperature MTN setting is preferred, as it helps to reduce thermal losses. Since the thermal network is short in length, it is considered to have a high linear heat density and the model assumes minor effects of mechanical losses.

3.3.2.2. Harvested heat by sharing

This section provides more detail about the evaluation of the amount of heat harvested by sharing (Q_{sh}), the thermal losses from the MTN, the EMC's new heating demand after sharing, and the new electricity demand after using the ETS heat pumps to aid energy sharing. The heat recovered by harvesting rejected heat at a certain time interval (i), Q_{Sh}, is considered to be the minimum between the summation of the rejected heat and the HRHP work ($Q_{rej} + W_{HRHP}$) and the building's heating requirements minus the HHP work ($Q_{H\_B} - W_{HHP}$) at the same time interval (Equation 1). As shown in Equation 1a, the heat rejected from the cooling system is calculated based on the cooling load (Q_c) and the system's coefficient of performance (COP_c).

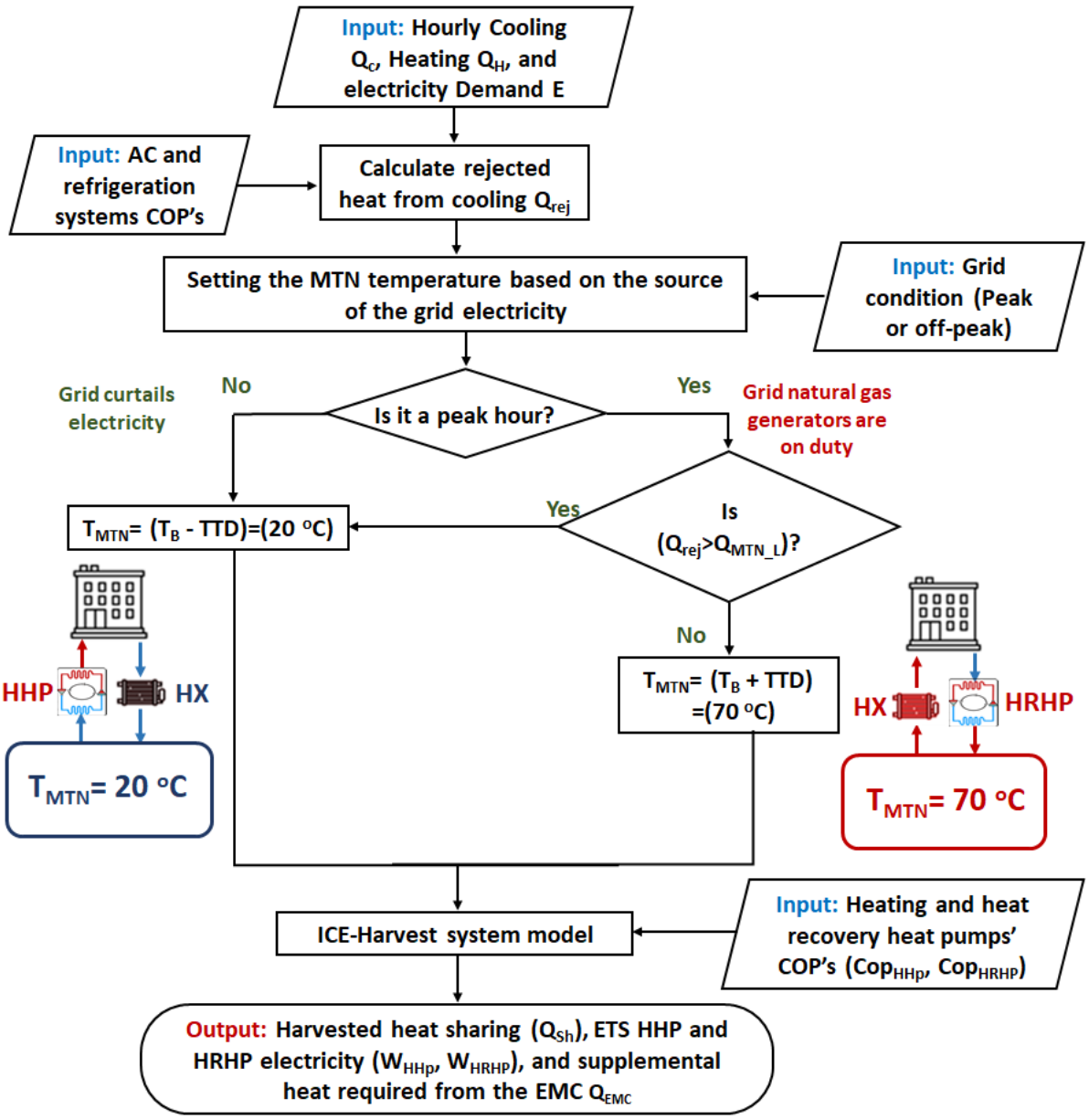

Figure 3-4: MTN Modeling.

The W_{HRHP}=0 when the MTN is set to 20°C, which is lower than the heat rejection temperature (25°C – 35°C) by a 5°C TTD, while a direct exchange happens between the MTN and the rejected heat via the heat exchanger. The W_{HRHP} has a certain value when the MTN is set at 70°C, wherein the HRHP is used to raise the temperature of the heat rejected from the cooling system to be higher than the MTN by a TTD of 5°C to facilitate heat exchange, which is calculated using Equation 1b. The W_{HHP}=0 when the MTN temperature is higher than the building heating system temperature,

and it has a certain value at a lower MTN temperature, which is calculated via Equation 1c. The cluster's total electricity usage is equal to the electricity used by the original BAU plus all of the electricity consumed by the heat pumps, as shown in Equation 2.

$$Q_{Sh} = \sum_{i=1}^{n} \begin{matrix} Min\{[Q_{rej}(i) + W_{HRHP}(i)], \\ [Q_{H\_B}(i) - W_{HHP}(i)]\} \end{matrix} \quad (1)$$

Where *n* is the total number of intervals (*i*) in any calculation period (day/month/year).

$$Q_{rej} = \sum_{j=1}^{NB_T} Q_C(j) * \left(\frac{1}{Cop_c(j)} + 1\right) \quad (1a)$$

$$W_{HRHP} = \begin{cases} \frac{Q_{rej}}{Cop_{HRHP}-1} & if\ T_{MTN} = 70\ °C \\ 0 & if\ T_{MTN} = 20\ °C \end{cases} \quad (1b)$$

$$W_{HHP} = \begin{cases} \frac{Q_{H\_B}}{Cop_{HHP}} & if\ T_{MTN} = 20\ °C \\ 0 & if\ T_{MTN} = 70\ °C \end{cases} \quad (1c)$$

Where *j* is the building number and NB_T is the total number of buildings in the ICE-Harvest cluster.

$$Q_{MTN\_L} = \frac{Q_{H\_B}}{Cop_{HHP}} \quad at \quad T_{MTN} = 20\ °C \quad (2)$$

Where Q_{MTN_L} is the total heat required by the MTN at ultra-low temperature $(T_{MTN} = 20\ °C)$.

The total electricity requirement (E_{Tot}) after harvesting can be calculated via Equation 4,

$$E_{ETS} = W_{HRHP} + W_{HHP} \quad (3)$$

$$E_{Tot} = E_{BAU} + E_{ETS} \quad (4)$$

The heat required from the MTN (Q_{MTN}) is evaluated based on the building's heating requirements (Q_{H_B}) and the ETS heating heat pump work (W_{HP}) (Equation 5).

$$Q_{MTN} = (Q_{H\_B} - W_{HHP}) \quad (5)$$

$$Q_{MTN\_rem} = (Q_{MTN} - Q_{Sh} - W_{HRHP}) \quad (6)$$

Equation 6 is used to determine the remaining heat energy required by the MTN after harvesting. The MTN losses (Q_{Loss}) were calculated using the analytical approach developed by Wallentén [40].

Equation 7 is used to determine the total heat energy that should be delivered to the MTN (Q_{EMC}) from heating sources within the EMC, such as thermal storage, the CHP system, or the backup boiler.

$$Q_{EMC} = (Q_{MTN\_rem} + Q_{Loss}) \quad (7)$$

3.3.2.3. Energy management center modeling

The energy management center (EMC) is a DER integration facility that provides the cluster's remaining energy requirements after sharing in order to maintain the MTN temperature at the desired level. To meet these demands, the EMC utilizes a number of different heating energy resources, including a CHP, which operates as a marginal electricity generator, short-term (STS) and long-term (LTS) thermal energy storage, and a backup boiler. The cluster's electricity demands are met by the CHP and the electrical grid.

The reduced ICE-Harvest model was used to specify the suitable size of the different equipment in the EMC for different regulation scenarios (i.e., no CHP, CHP with no export, and CHP with export to the grid) and a maximum peak cluster electricity demand limit. The size of the CHP in this model starts with no-CHP (CHP size of 0) then it increases in an increment of 250 kW until a maximum limit of peak electricity demand in the cluster in the case of the No-Export, and it is doubled that limit in the With-Export case. The selected CHP size by the model is the maximum size in the specified range that meets the following constraints:

- The annual overall combined electrical and thermal CHP efficiency must be maintained above 65% to adhere to typical regulations set forth by the grid operator [41].
- Since the CHP is only intended to support the system during peak hours, oversizing can be prevented by limiting the incremental increase in the CHP size such that size increases must

be maintained for at least 10% of the CHP's running hours (i.e., if a CHP with a size of 1,000 kW is used for 4,000 hours per year, stepping up the size to 1,250 kW requires the additional 250 kW to be used for at least 400 hours).

The CHP operation methods are constrained as follows:

- The CHP only operates if there is a gas peak generator running on the electrical grid.
- The CHP can operate on a partial load (with min 25%) if the export is not allowed.
- The heat generated from the CHP is primarily used to cover the heat required by the EMC.

The STS is used to cover the daily mismatch between the heat generated by the CHP and the Q_{EMC} requirements, with the STS's size being based on the maximum daily mismatch over the year. The STS is considered a perfectly insulated storage with no losses. The LTS is used after STS to cover the seasonal mismatch between the heat generated by the CHP and the demand from the EMC with assumed efficiency of 50% [42]. The remaining heating requirements are met by the EMC's backup boiler. At each hour, the cluster's electricity import or export from and to the grid is calculated as $E_{Tot} - E_{CHP}$, where a positive number corresponds to import and a negative value to export.

3.3.2.4. GHG emissions calculations

The natural-gas-combustion-related GHG emissions used in this work were calculated based on Canada's 2018 National Inventory Report, which lists CO_2 emissions of 0.1872 t CO_2eq/MWh thermal. The GHG emissions produced by conventional and ICE-Harvest systems were then calculated by multiplying this number by the amount of heat required by a gas-fired boiler, as shown in Equations 8 and 9. Conversely, calculating the GHG emissions from imported electricity depends on the fuel sources that were used to generate it. The average emission factor (AEF) is

the ratio between the GHG emissions produced by the grid's fossil-fuel-based plants and the total electricity generated in a given hour (Equation 10). The GHG for the conventional system is calculated using the AEF in Equation 11.

$$GHG_{B\_Conv} = [\sum_{i=1}^{n} Q_{Boiler\_Conv}(i)] * 0.1872 \quad (8)$$

$$GHG_{B\_EMC} = [\sum_{i=1}^{n} Q_{Boiler\_EMC}(i)] * 0.1872 \quad (9)$$

$$AEF\ (i) = \frac{GHG\ emissions\ from\ fossil\ fuel\ plants(i)}{Total\ electricity\ generated\ in\ the\ grid\ (i)} \quad (10)$$

$$GHG_{E-Conv} = \sum_{i=1}^{n} [E_{Conv}(i) * AEF(i)] \quad (11)$$

The emissions from the additional electricity required by the ETS heat pumps is also calculated using the AEF, as illustrated in Equation 12. However, during peak hours, the increase in electricity consumption due to ETS usage will add marginal GHG emissions due to the use of natural gas generators; as such, it is more appropriate to consider this electricity as being supplied solely from the natural gas generator. Equation 13 is used to evaluate the GHG emissions for what is known as the marginal emission factor. Since the electricity supply is carbon-free during off-peak hours, the GHG emissions from electricity are set to zero.

$$GHG_{E-ETS-AEF} = \sum_{i=1}^{n} [E_{ETS}(i) * AEF(i)] \quad (12)$$

$$GHG_{E-ETS-MEF} = \begin{cases} \sum_{i=1}^{n} [E_{ETS}(i) * \eta_{gen} * 0.1872] & if\ marginal\ gas\ generator\ is\ on \\ 0 & if\ marginal\ gas\ generator\ is\ off \end{cases} \quad (13)$$

Finally, the average electrical efficiency of a centralized peak natural gas generator is assumed to be 42% [43].

3.4. Case study

In order to examine the different clustering techniques and to study the potential of the ICE-Harvest systems, a database of 14,832 for 9 different high-energy-consumption buildings' archetypes in Ontario was collected to examine the clustering methods. Figure 3-5 represents the

selected different archetype and their spatial location on the Ontario map. Field measurement of hourly electricity and monthly heating energy demands for 2000 buildings in Ontario is collected in [5]. To move the resolution of the heating demand from a monthly to an hourly basis, a weather-dependent model was used [5]. For the different building archetypes, the ones that match the Ontario monthly benchmark was chosen as representative building [44]. Based on the building floor area the representative profiles were normalized and used to estimate the energy profiles for the Ontario collected database.

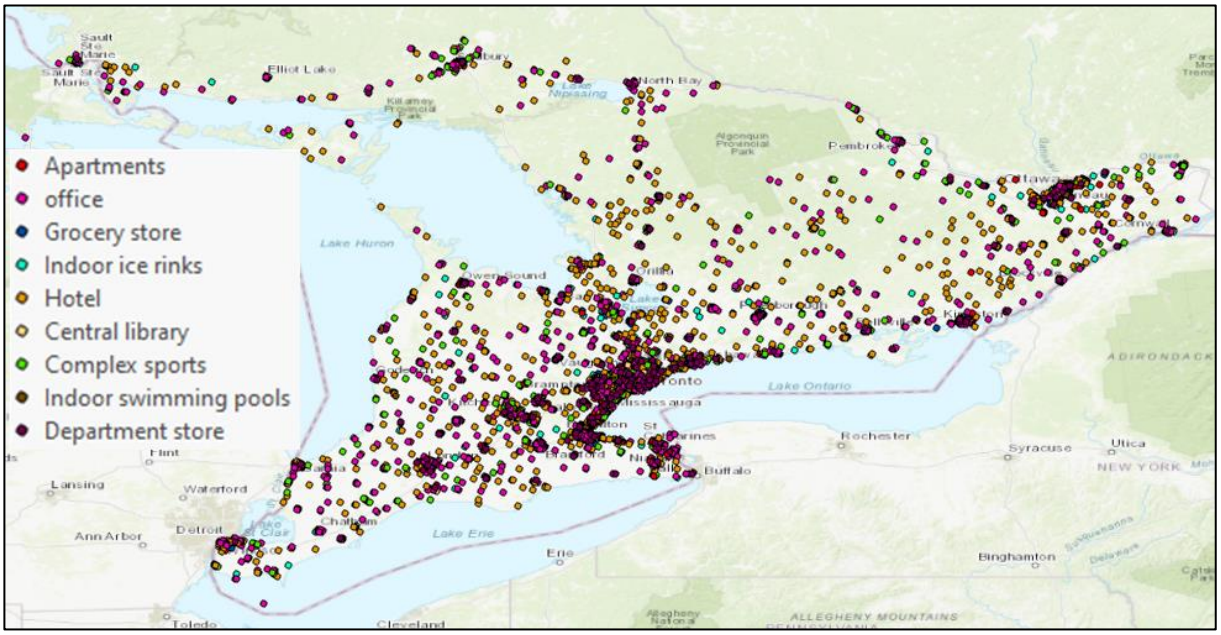

Figure 3-5: Database of high-energy-consumption buildings in Ontario. Buildings are color-coded by archetype.

The representative energy demand profiles of the various archetypes were analyzed. Figure 3-6a shows the annual percentages of cooling and heating demands for each building archetype (i.e., the grocery store has about 72% of the annual thermal energy usage for cooling and 28% for heating). For further analysis, the model presented in [4] is used to calculate the internal energy that could be recovered within the same building as well as the extra heat rejection during the summer and winter seasons (Figure 3-6b). The percentage of these values to the annual heat

rejection is presented in Figure 3-6b for each building archetype. Although the model in [4] was used for a group of buildings, the same model can be used for each building separately by excluding all other buildings from the model. For example, the model equation ($Q_{Sh}= \sum_{i=1}^{n} Min\{[Q_{rej}(i), Q_{H\_B}(i) - W_{HHP}(i)\}$) is used to evaluate the internal energy recovered with n=1 where n is the number of buildings. The buildings that have a large percentage of extra rejected heat during the winter season that was not recovered internally are selected as anchor buildings such as grocery stores, ice arenas, and libraries with IT servers. As such, these building archetypes are considered to be good candidates for integration with other archetypes with high heating demands, such as residential towers, department stores, hotels, swimming pools, and offices. Figure 3-6c presents the remaining heating requirements of each building archetype during the summer and winter seasons after the internal energy recovery. The buildings with large percentages of heat demand after recovery are considered heated dominated buildings. For example, hotel buildings still require around 75% of the heating demand after internal recovery.

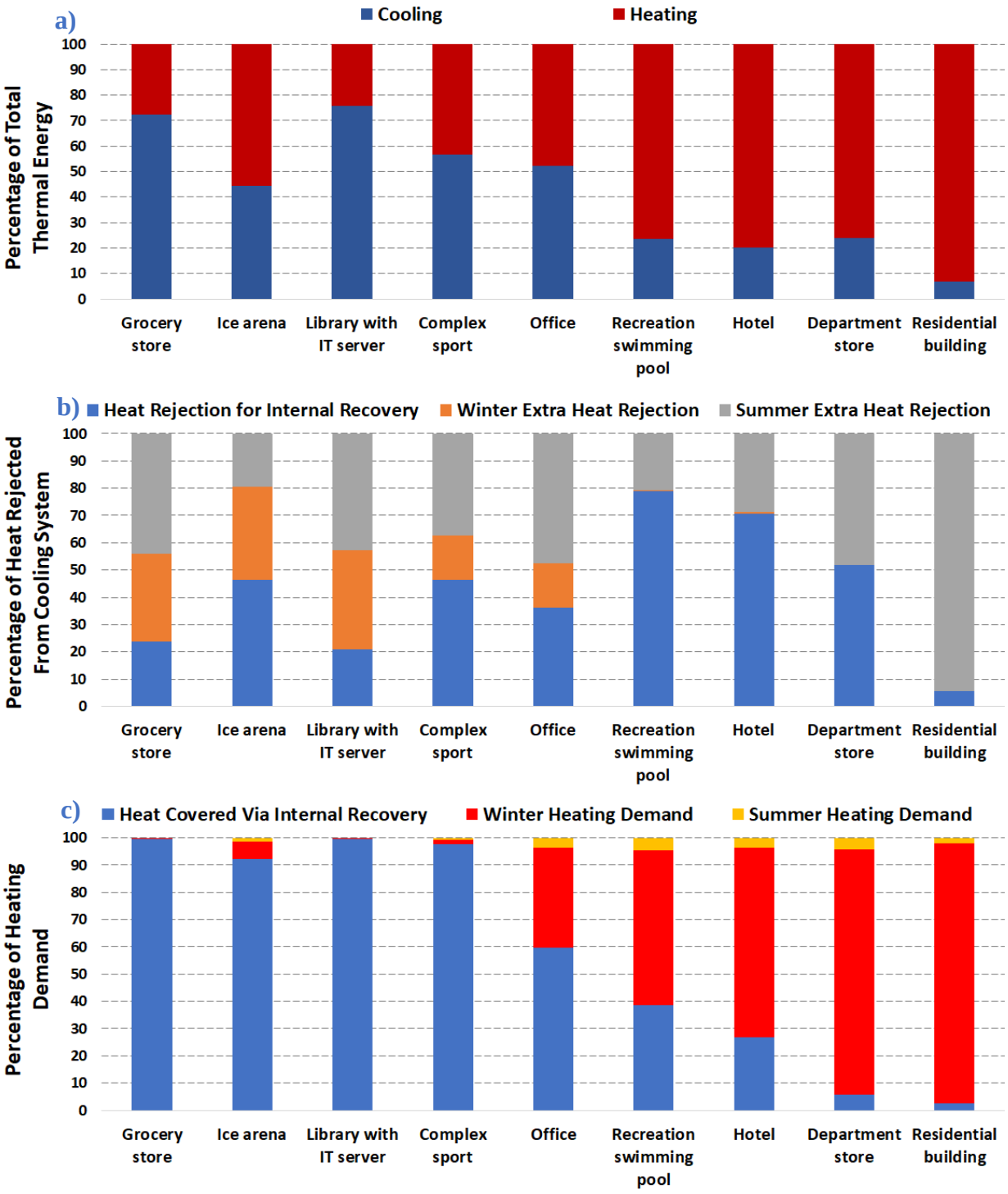

Figure 3-6: Representative thermal-energy demand and energy sharing potential for different building archetypes. a) The annual percentage of the building's cooling and heating demands. b) The annual percentage of internal recovery and the extra heat rejection during the winter and summer seasons to the total heat rejection from the building's cooling system. c) The percentage of the remaining heating requirements of each building during the summer and winter seasons after the internal energy recovery to the annual heating demand.

3.5. Results and Discussion

A comparison between the clustering methods is performed by applying these methods to the identified buildings' database. The results of the comparison include the number of identified clusters, the clusters' energy profile categories, and the physical characteristics such as the piping length and the LHD. In addition, the results present the evaluation criteria such as the amount of energy shared and the reduction in GHG emissions from each clustering method. After identifying the best clustering technique, the potential impacts of using the ICE harvest system for all the clusters' heating, electricity, and GHG emissions are presented.

3.5.1. Clustering results

Applying the three clustering techniques on the database results in 1,196 clusters in method A and 1139 clusters in methods B, and C. The identified clusters that included at least one anchor building are 484, 407, and 452 for methods A, B, and C respectively. Table 3-1 summarizes the results of the different clustering methods. The results show that, while the total heating demands of the clustered buildings in methods A and C are almost identical, method C required approximately 175 km less piping than A, which resulted in a higher linear heat density and lower thermal losses. Table 3-1 shows that method B had the highest LHD and lowest piping losses however, the comparatively smaller number of implemented anchor buildings (630) resulted in about 0.2-0.21 TWh less shared harvested energy and an additional 30,000-40,000 t CO_2eq of the GHG emissions compared to methods A and C. This deficiency in method B is addressed by the modification incorporated in method C. While Method A is simpler and has lower computational costs compared to method C, Method C was selected as the optimal approach, as it resulted in the largest

emissions reduction per unit piping length (360 t CO_2eq /km/year compared with 330 t CO_2eq/km/year in method A, which is equivalent to an improvement of 8.3%).

Table 3-1: Comparison of the results of the three examined clustering methods for the Ontario database.

Clustering Criteria\Clustering Method	A) Clustering Around Anch	B) Density-Base	C) Density-Based with Adding Closest Ancho
Total piping length (km)	2,270	2,010	2,100
Total heating energy consumption (TWh)	15.91	15.76	15.92
Linear heat density (MWh/(m.year))	7.0	7.9	7.6
Total piping losses (TWh)	0.42	0.38	0.40
Energy sharing (TWh)	2.62	2.42	2.63
Number of anchor buildings	703	630	715
Number of clusters with anchor	484	407	452
Total number of clusters	1,196	1,139	1,139
Number of clustered buildings	11,475	11,299	11,384
Number of outliers	3,357	3,533	3,448
GHG emissions reduction (1000 t $CO2_{eq}$)	756	726	762
GHG emissions reduction / total heating (t $CO2_{eq}$ /GWh)	47.5	46	47.9
GHG emissions reduction / total piping leng (t $CO2_{eq}$ /km/year)	332.6	362	363.2

The resulting clusters are categorized into three main types according to the ratio of the cooling demand to the total thermal demand of each cluster as presented in Table 3-2. These categories are:

1- Cooling-dominated clusters

Clusters in this category have a cooling to total thermal demand ratio greater than 50%. Two sub-categories are identified according to the simultaneous heating and cooling demands as shown in figure 7 (purple color). The first sub-category, high-concurrent harvesting clusters, has a high degree of concurrence between cooling and heating demand, thus resulting in high waste-energy harvesting potential. In contrast, the second category, low-concurrent

harvesting clusters have a lower potential for harvesting due to the low concurrence between the cluster's heating and cooling demand as presented in Table 3-2 first and second rows.

2- Balanced-demand clusters

Clusters in this category feature a cooling-to-total thermal demand ratio of between 40-50%. Similar to the previous category, this category consists of high-concurrent and low-concurrent harvesting clusters.

3- Heating-dominated clusters

Heating-dominated clusters are characterized by a cooling to total thermal demand ratio of less than 40%. Heating-dominated clusters can be broken down into three subcategories high-concurrent and low-concurrent harvesting. However, in cold-climate countries it is common for clusters to have a very low cooling to thermal demand ratio (<15%); such clusters are classified as extra-heating-dominated nodes.

Figure 3-7 shows a graphical representation of the monthly cooling (blue), heating (red), and concurrent heating and cooling (purple) demand in each cluster category and subcategory. Although the calculations were done on an hourly basis, the monthly representation was selected for simplicity. The characteristics of each cluster category are presented in Table 3-2, including the percentage of heating demand covered by concurrent sharing (Q_{sh}/Q_H %); the electrification of heating with the ETS heat pumps (E_{ETS}/Q_H %); the remaining heat required from the EMC (Q_{EMC}/Q_H %); the increase in electricity consumption compared to BAU consumption (E_{ETS}/E_{BAU} %); and finally, the percentage of rejected heat from the cooling system that is harvested (Q_{sh}/Q_{rej} %).

The calculated characteristics of each cluster category show that almost all of the heating requirements in high-concurrent cooling-dominated clusters are covered by shared/harvested heat

as well as electricity from the ETS, with almost no heat being required from the EMC (1%). This means that clusters in this category have nearly no need for supplemental boiler heating or the use of a CHP, as most of their heating demands are covered by energy harvesting and electrification of heating. In the low-concurrent cooling-dominated cluster subcategory, the percentage of harvested heat was significantly lower compared to the high-concurrent case, which caused the EMC heating requirement to increase from 1% to 33%.

Conversely, low-concurrent heating-dominated and extra-heating clusters relied on the EMC for 59% and 77% of their heating requirements, respectively. In addition, their electricity usage increased over the BAU case by 35% and 43%, respectively. These results show that these cluster categories are perfectly suited to the use of a CHP in their EMC. As shown in Figure 3-8, 78.5% of the clusters in cold-climate areas fall into the heating-dominated category.

Table 3-2: Harvesting characteristics of the different cluster categories for 1,139 clusters in the province of Ontario.

Cluster Profile		$[Q_C/(Q_C+Q_H)]$ %	(Q_{sh}/Q_H) %	(E_{ETS}/Q_H) %	(E_{ETS}/E_{BAU}) %	(Q_{EMC}/Q_H) %	(Q_{sh}/Q_{rej}) %	No. of clusters	% of total clusters
Cooling Dominant	High Concurrent Harvesting	>50%	66	33	27	1	33	53	13.5
	Low Concurrent Harvesting		37	29	20	33	24	100	
Balanced	High Concurrent Harvesting	(40-50) %	55	30	39	16	51	42	8
	Low Concurrent Harvesting		34	27	24	39	36	50	
Heating Dominant	High Concurrent Harvesting	(15-40) %	37	25	39	38	57	107	35
	Low Concurrent Harvesting		18	22	35	60	50	290	
	Extra Heating	<15%	5	18	43	77	42	493	43.5

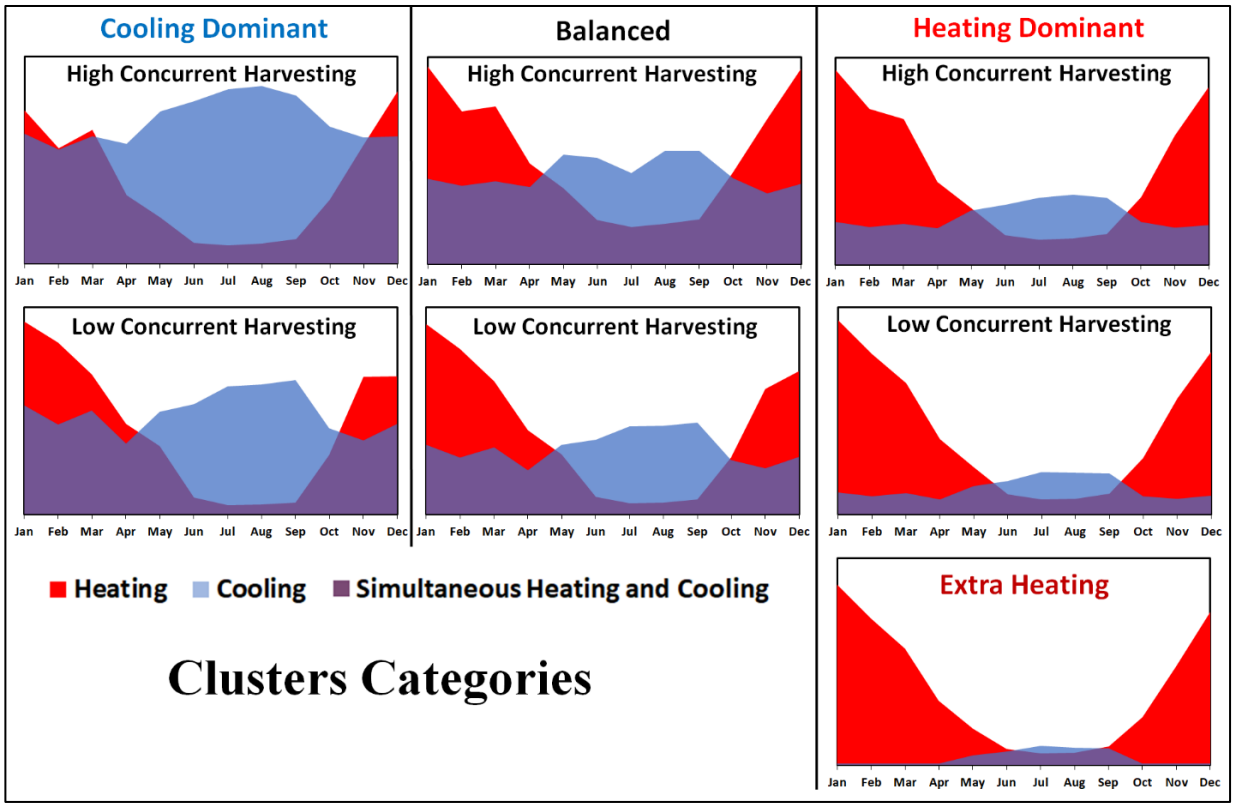

Figure 3-7: Cluster categories according to thermal demand.

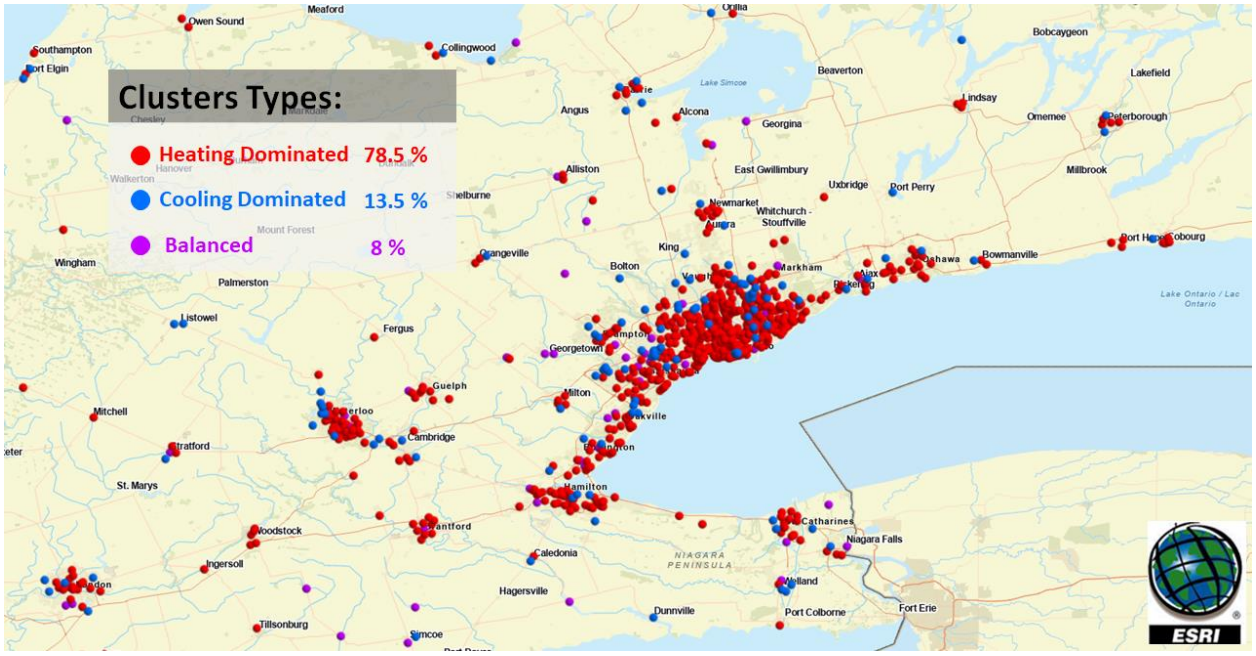

Figure 3-8: Building cluster categories for 1139 clusters in the province of Ontario.

3.5.2. Impacts of mass implementation of ICE-Harvest systems

Integrated energy systems and harvesting can significantly reduce GHG emissions and help address electrical grid challenges caused by mismatches between generation and demand. This latter point is key, as mismatches in generation and demand lead to the use of fossil-fuel generators during peak times and the curtailment of carbon-free electricity during off-peak times. To evaluate this impact, the reduced ICE-Harvest model was applied to 1,139 clusters in Ontario comprising 11,384 buildings with high energy usage and different levels of rejected heat from their cooling systems.

The application of ICE-Harvest systems on all clusters enabled the recovery of almost 41.5% of the rejected heat, which was then used to satisfy the cluster's heating demands (Figure 3-9). Figure 3-9 shows the hourly harvested energy compared to the hourly rejected heat from all buildings.

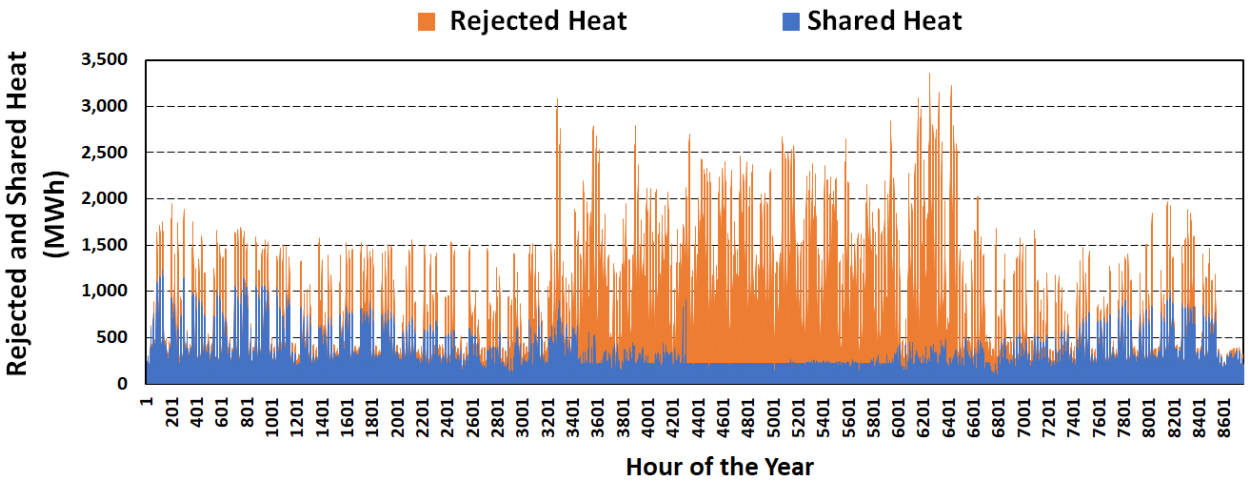

Figure 3-9: The summation of the clusters' hourly harvested heat from the overall clusters' heat rejection for 1,139 clusters in the province of Ontario.

The MTN length and the LHD are important characteristics of the ICE-Harvest system that affects its performance. Figure 3-10 presents a histogram illustration of the MTN length ranges for different clusters. The figure shows that more than 75% of the clusters have an MTN length from 0.5 to 2.5 km. These short piping lengths reduce the infrastructure cost risks as well as the thermal

and mechanical losses during operation. Figure 3-11 shows the LHD for all 1,139 clusters analyzed in this study, along with the thermal loss to heating demand ratio. The cumulative average of this correlation is LHD = 7.6 with a thermal loss of 2.5% of the total heating, which is represented by the red circle in Figure 3-11. In early research, Rosa and Christensen's [33] study on a group of detached houses revealed that a LHD of 0.2 resulted in thermal losses of 20% of the produced heat. The significant difference in thermal losses reported in the present study and Rosa and Christensen's works highlights the importance of clustering high-energy-consumption buildings using the shortest possible MTN.

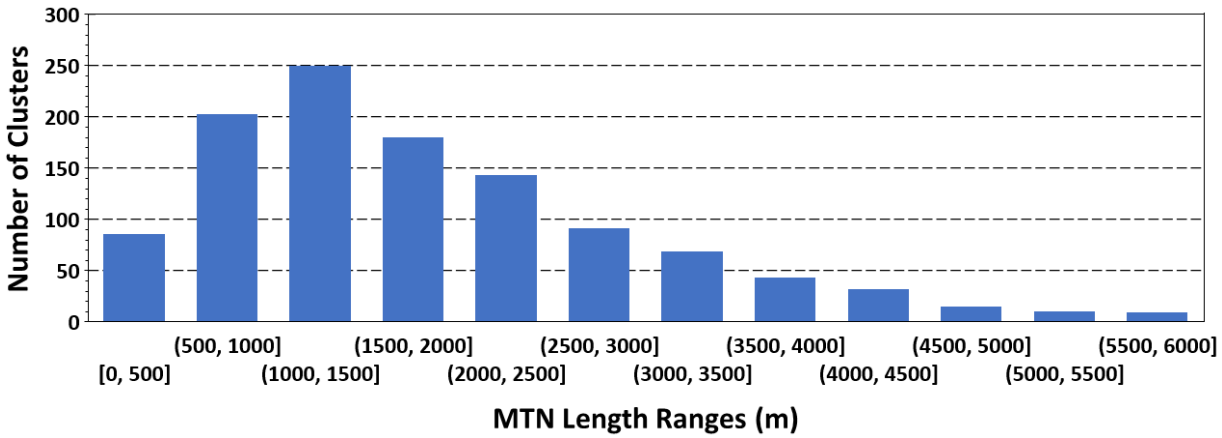

Figure 3-10: Histogram of the range of MTN lengths for 1,139 clusters in the province of Ontario.

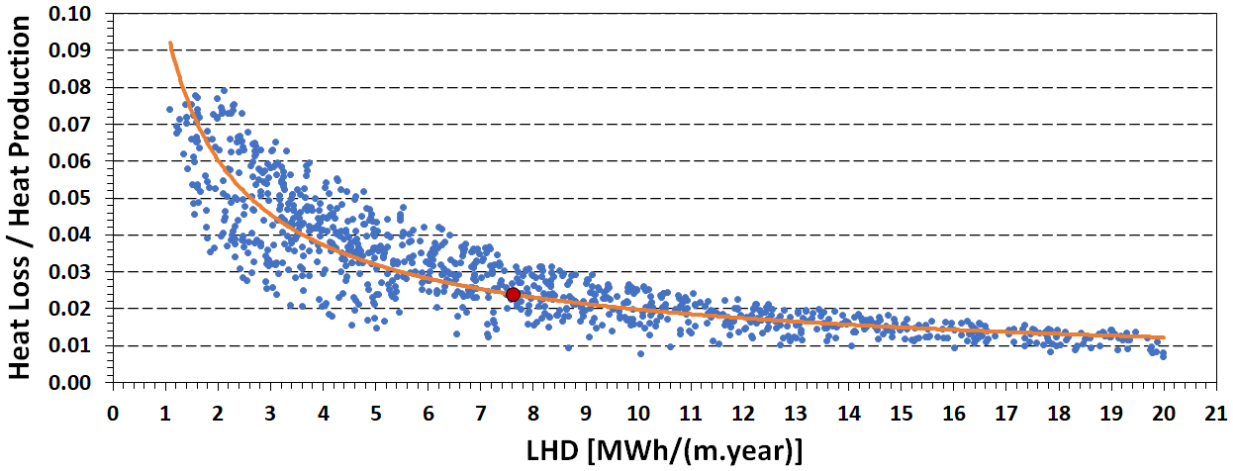

Figure 3-11: Correlation between the thermal loss to heat production ratio and the LHD for 1,139 clusters in the province of Ontario. The red circle represents the accumulative average for all clusters.

The CHPs in the EMC for the 1139 identified clusters are sized according to two different scenarios (No Export and With Export) as mentioned in the methodology. Figure 3-12 presents histograms of the CHP different sizes that were used for each scenario. In the No Export case, almost 75% of the clusters required CHP sizes from 0.25 MW to 1.5 MW. Conversely, over 70% of the clusters in the With Export case required CHPs ranging between 1 MW and 4 MW in size, with about 40% falling within 3 MW and 4 MW. To provide perspective Ontario has a 38.6 GW installed generation capacity that produces around 147.4 TWh/year, whereas the CHPs in the ICE-Harvest

clusters studied have predicted installation and generation capacities of 1.1 GW and 3.3 TWh/year, for the No Export case and 2.1 GW and 6.9 TWh/year, for the With Export case. Around 13.5% of the nodes did not require a CHP; most of these were cooling-dominated and balanced nodes whose heating demands were satisfied using harvested shared energy.

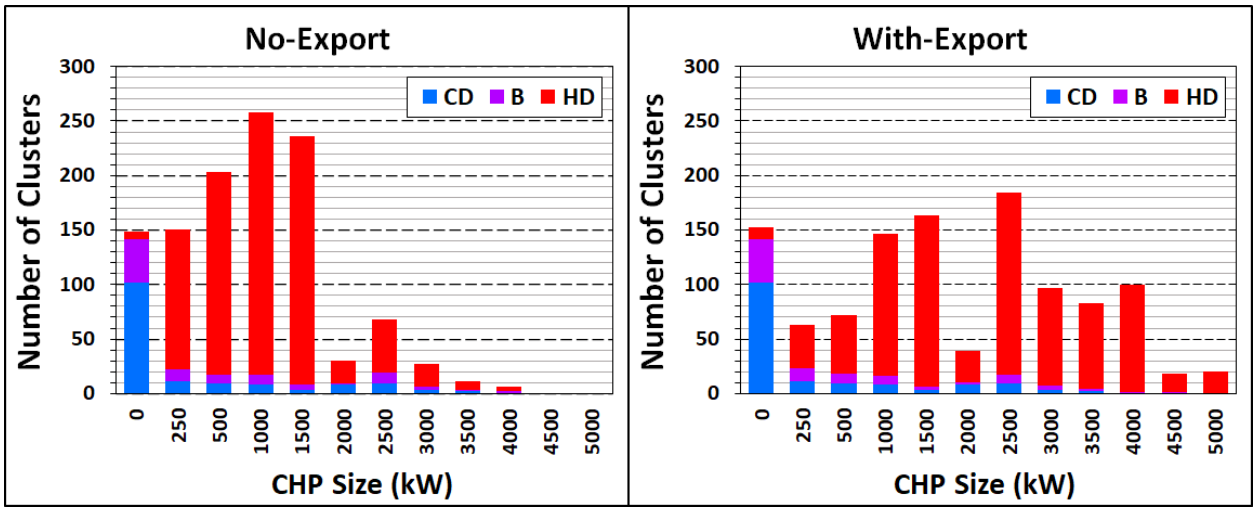

Figure 3-12: CHP size-range histograms for the No Export scenario (left) and the With Export scenario (right) for 1,139 clusters in the province of Ontario.

The heating resources used in integrated energy systems include not only gas-fired boilers, as in the BAU standalone buildings scenario, but also heat harvested from other buildings, CHPs, and ETS heat pumps with the aid of STS and LTS systems. Figure 3-13 illustrates how the heating resources changed between the BAU standalone scenario to the integrated systems in the No Export and With Export scenarios. From Figure 3-13, the following can be concluded:

- The supplemental heat required from boilers in the No Export case is still high, accounting for up to 40% of the heating requirements compared to only 17% in the With Export case. This difference is due to the smaller size of the CHP used in the No Export case.
- The ETS mainly consumes electricity during off-peak times from the grid, where it harvests some of the grid's curtailed electricity (only 19% of ETS electricity consumption occurs during on-peak periods).

- The larger the installed CHP, the higher the size and need for STS and LTS.
- In this study, the LTS losses were assumed to be 50% [42] of the stored energy across the charging and discharging seasons.
- Approximately 2.63 TWh of energy was harvested from rejected waste heat sharing, and another 2.35 and 4.6 TWh of energy was produced by converting centralized peak electricity generators to DER CHPs for the No Export and With Export cases, respectively.

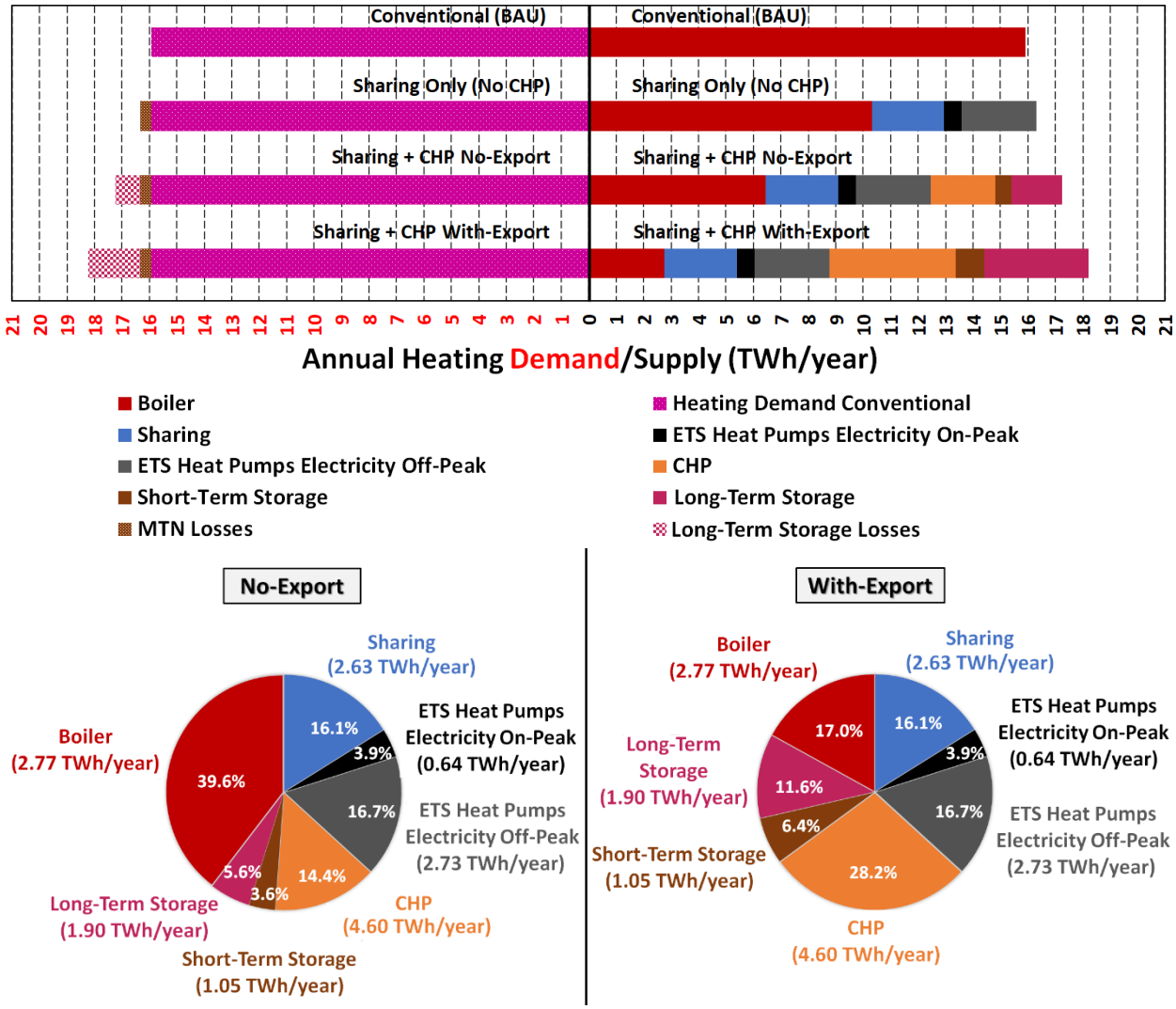

Figure 3-13: Heating resources (supply) and demands in the conventional (BAU), No Export, and With Export scenarios for 1,139 clusters in the province of Ontario.

The implementation of ICE-Harvest systems in all of the clustered nodes significantly impacted the amount of electricity demanded from the grid, not only in terms of overall annual consumption (due to the electrification of heating), but also with respect to on-peak and off-peak maximum hourly electricity demand from the grid (peak hour). DERs that use CHPs as a source of electricity and heat cause peak shaving of the grid on-peak periods demands. Although the model uses hourly data, the results are also presented on a daily timeframe for the sake of simplicity. Figure 3-14 presents a stacked profile showing the system's daily electricity consumption and the different electricity resources that are used to satisfy this demand. Additionally, Figure 3-14 shows consumption during off-peak and on-peak periods for various operation scenarios during 2017. Figure 3-15 presents the total annual electricity consumption (demand) and the different resources used to satisfy it, while Figure 3-16 presents the hourly maximum imported electricity from the grid. Figure 3-14, Figure 3-15, and Figure 3-16 present the relevant data in relation to the following operation scenarios:

Conventional (BAU): Figure 3-14a presents the stacked daily imported electricity from Ontario's grid during off-peak and on-peak periods. As can be seen, currently the electricity peaks during the summer months, when more electricity is required for cooling and less is required for heating. In the BAU case, the hourly maximum imported electricity is almost 2 GW and 1.8 GW during the on-peak and off-peak periods, respectively (Figure 3-16), and the total annual electricity imported from the grid is 4.2 TWh/year during on-peak periods and 5.5 TWh/year during off-peak periods (Figure 3-15).

Sharing only, no CHP: Figure 3-14b presents the daily imported electricity from the grid when sharing with the electrification of heating using the ETS heat pumps is performed and boilers are used to serve the remaining clusters' MTN heating demands (i.e., no CHP is used). In this case,

and due to the use of different MTN temperatures to prevent an increase in electricity consumption, the importing of electricity from the grid mainly increases during the winter months, especially during off-peak times, which aids in the harvesting of curtailed electricity from renewable resources. While the maximum hourly imported electricity in this scenario slightly increased to 2.1 GW during on-peak periods, a larger increase was observed during off-peak times, with consumption rising to 3.2 GW (Figure 3-16). The total annual electricity imported from the grid increased to 4.8 TWh/year and 8.2 TWh/year during on-peak and off-peak periods, respectively (Figure 3-15).

CHP, No Export: The implementation of a CHP to localize production that would otherwise come from peak gas generators on the grid had a significant effect. Since the CHP only runs during on-peak periods, electricity imported from the grid will be lower during these times. Figure 3-14c shows that using CHPs with restricted sizes—to avoid electricity export—will reduce the maximum amount of hourly electricity imported from the grid during on-peak periods by more than 50%; however, imported electricity during off-peak periods will remain the same (Figure 3-16). Furthermore, the total annual electricity imported from the grid dropped from 4.2 TWh/year (BAU case) to 1.5 TWh/year during on-peak periods, while remaining similar during off-peak periods, as the CHP's operation is restricted to these times (Figure 3-15).

CHP, With Export: The use of larger CHPs on site combined with the exporting of electricity had a considerable impact on demand from the electrical grid and subsequent GHG emissions. During on-peak periods, the amount of electricity produced by the CHP exceeds demand, which results in a net export of electricity (Figure 3-14d). The surplus electricity is exported to the grid via the DERs, with waste heat being harvested to satisfy the clusters' heating demands. Figure 3-15 shows that an annual total of 1.2 TWh of electricity is imported from the grid during on-peak

periods, while 3.3 TWh is exported to the grid. Thus, this scenario results in a net export of 2.1 TWh/year.

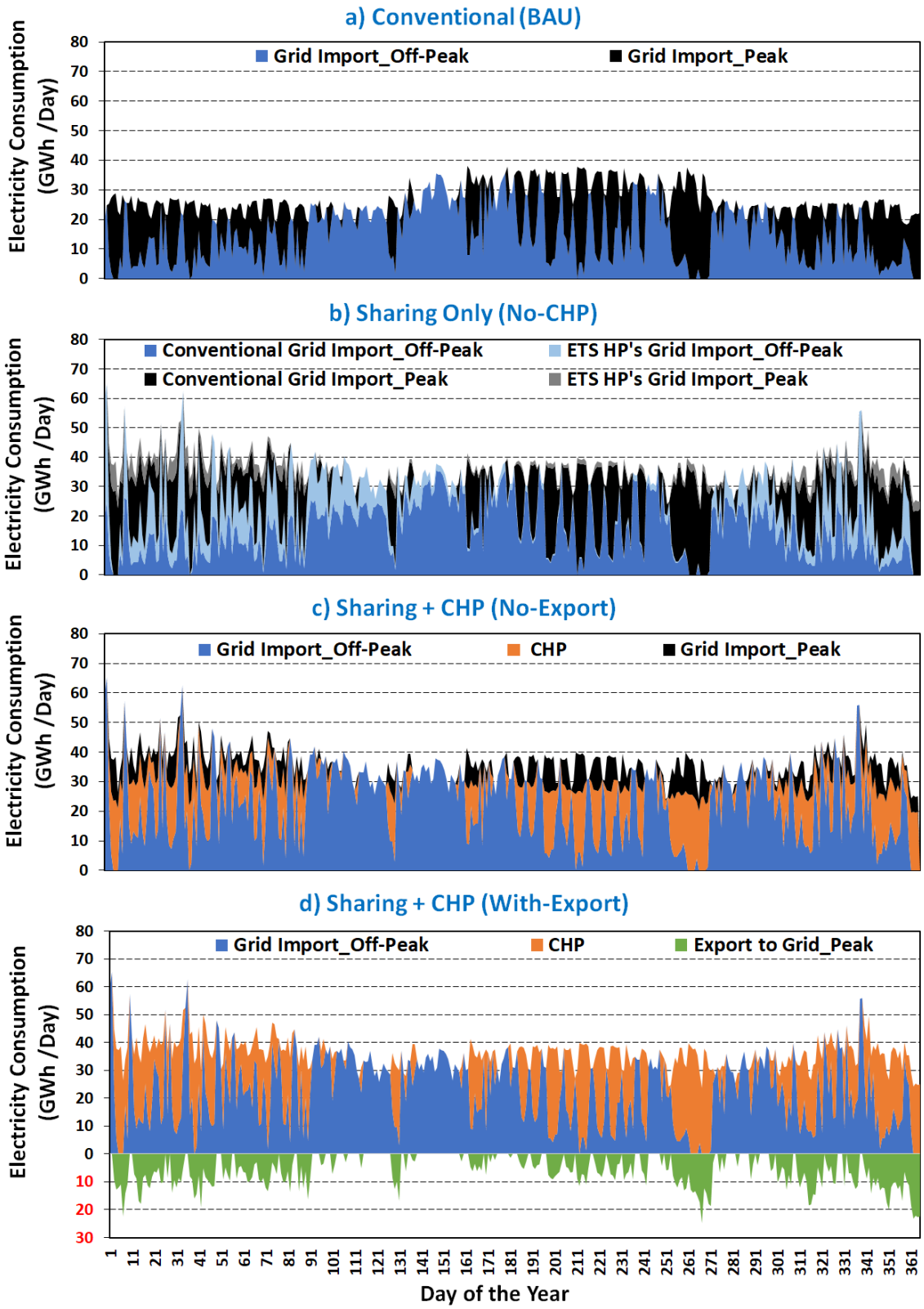

Figure 3-14: Hourly electricity consumption/export over the year for 1,139 clusters in the province of Ontario supplied from different resources for: a) conventional systems; b) ICE-Harvest systems, no CHP; c) ICE-Harvest systems with CHP (No-Export); d) ICE-Harvest systems with CHP (With-Export).

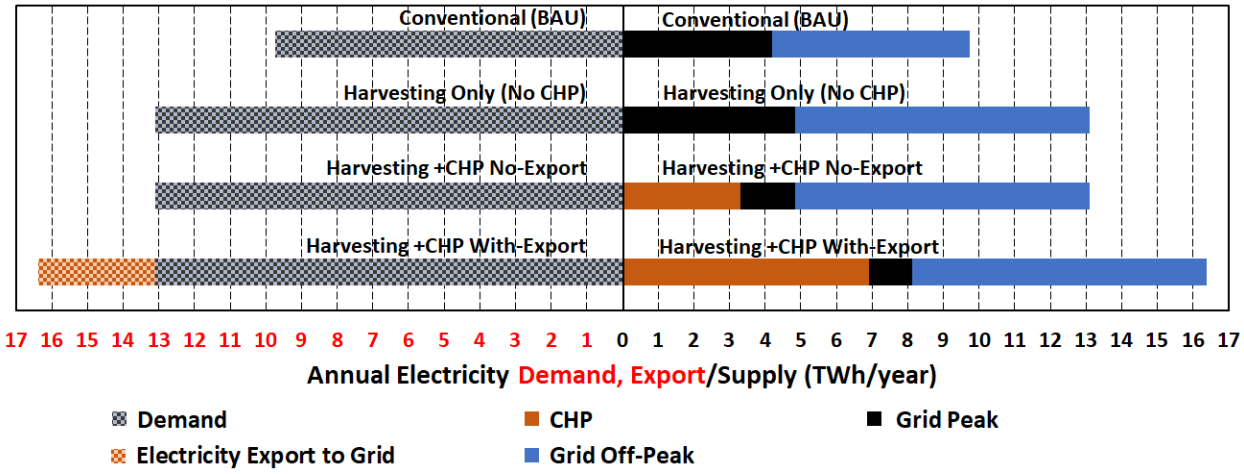

Figure 3-15: Comparison of annual electricity demand and export (left) and supply (right) for the conventional and ICE-Harvest systems with different operating scenarios for 1,139 clusters in the province of Ontario.

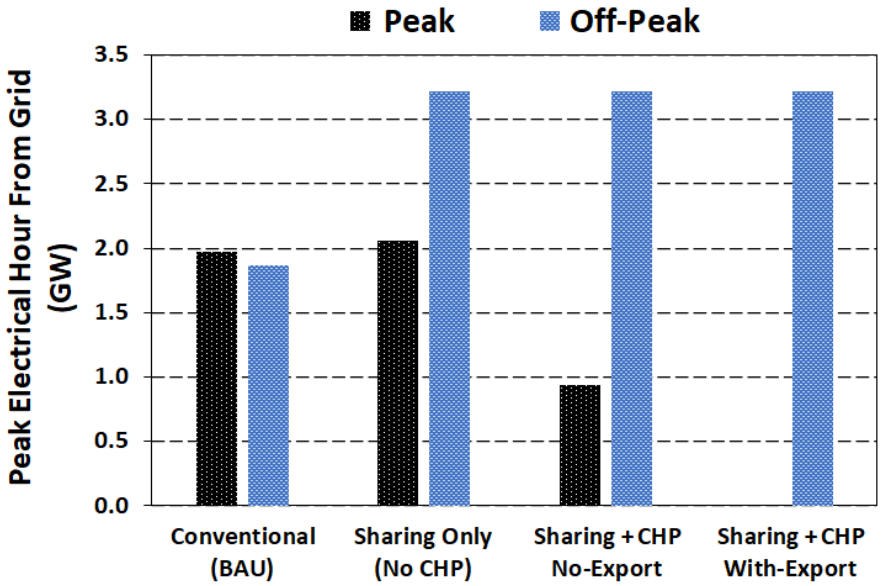

Figure 3-16: The peak hour demand from the grid during On-Peak and Off-Peak times for the conventional systems and the ICE-Harvest systems with different operating scenarios for 1,139 clusters in the province of Ontario.

The application of ICE-Harvest systems with different technologies and scenarios in 1,139 clusters in Ontario reduced GHG emissions by up to 2.3 Mt CO_2eq, or 80% of the clustered buildings' original emissions. Figure 3-17 presents a comparison of the GHG emissions produced by the BAU system and the different ICE-Harvest systems under different operating scenarios. According to Figure 3-17, the buildings in the BAU system produced about 3.2 Mt CO_2eq of GHG emissions,

with nearly 90% of these emissions being produced by the buildings' heating systems (gas-fired boilers).

Sharing only, no CHP: This configuration enabled GHG emissions to be reduced to about 2.4 Mt CO_2eq, or about 25% lower than the BAU case. However, this scenario resulted in higher electricity emissions due to the increase in electricity usage at the ETS for energy harvesting; in this case, the reduction in GHGs was largely due to the use of harvested/shared heat rejected from cooling systems to heat the buildings in the node. This reduces the need for gas-fired boilers to satisfy the remaining heating demand.

Sharing + CHP: Since CHPs displace electricity produced by peak gas-fired electricity generators on the grid, the heat harvested from them is considered a non-additional GHG emission resource. In the No-Export case, the size of the implemented CHPs was limited, which resulted in GHG emissions of 1.9 Mt CO_2eq and 1.4 Mt CO_2eq in the With-Export case compared to 3.2 Mt CO2eq in the BAU case. This reduction is due to the reduced use of boilers on site for heating.

Impact of thermal storage systems: CHPs only run at specific times according to the electrical grid, which means that they may operate during periods of low thermal demand. The use of thermal storage can help overcome such mismatches in resource availability and demand. Applying STS to address hourly and daily mismatches reduced GHG emissions to about 1.8 Mt CO_2eq in the No-Export case and about 1.3 Mt CO_2eq in the With-Export case. However, adding LTS further reduced emissions to about 1.6 and 0.9 Mt CO_2eq for the No-Export and With-Export cases, respectively. The use of thermal energy storage balances the CHPs heat energy generation with the clusters' demands thus reducing GHG emissions.

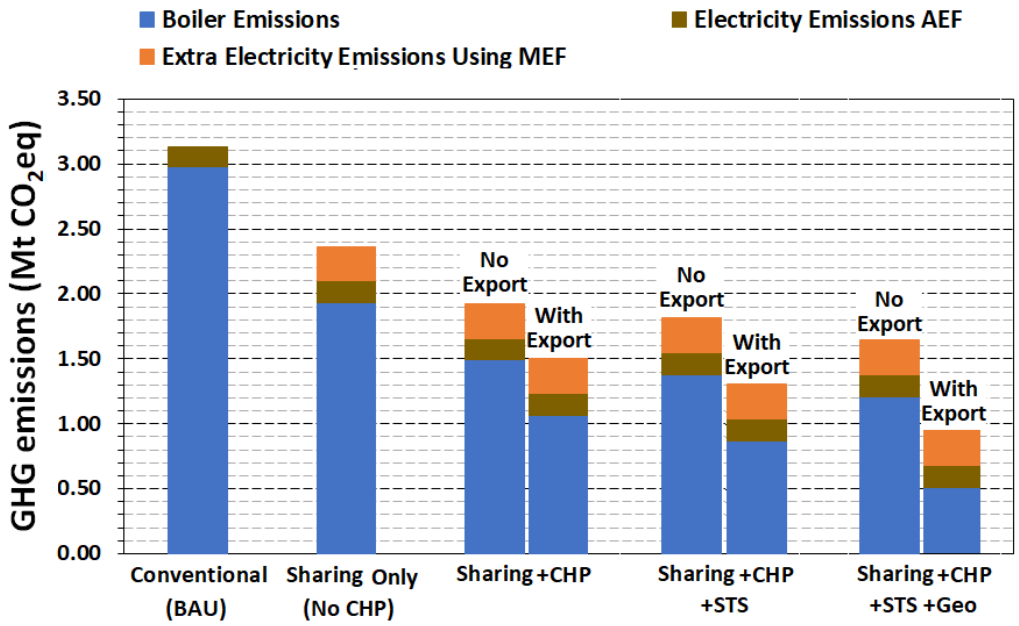

Figure 3-17: Comparison of GHG emissions produced by the conventional system and ICE-Harvest systems under different operating scenarios for 1,139 clusters in the province of Ontario.

3.5.3. Limitations and future recommendations

The present work developed a reduced model for the ICE-Harvest system to evaluate the impact of the mass implementation of the system. A detailed study of the system operation for different cluster categories in the future is recommended. The ICE-Harvest system's MTN operation presented in this study aims to serve the building's space and water heating demands that require a temperature of about 60°C. However, many recent building heating systems start to reduce this temperature by separating space heating and domestic water heating. Further study will be required to investigate the impact of this change on the ICE harvest system design and operation.

Electrification of heating during curtailment periods is one of the key elements of the ICE-Harvest system however, a large portion of the renewable resources are curtailed during the fall and spring seasons which are not captured by the ICE harvest system due to the low heating demands in these

periods. Further upgrading of the system is recommended to maximize the harvesting of these resources perhaps by adding an air source heat pump with the aid of seasonal thermal storage.

The ICE-Harvest system also proposes a solution for mixed generation electrical grids (fossil fuel and carbon-free resources) whereas future grids plan to reach net zero. It is advised that low emissions combined electrothermal systems be investigated as a potential substitute for the natural gas-operated CHP such as fuel cells and small modular reactors.

Investigate the effect of intra-cluster by connecting different ICE-Harvest clusters EMCs and/or networks which could increase waste energy capture and benefit from demand diversity. Finally, cost and life cycle analysis of the ICE-Harvest system for the different cluster categories are recommended to be investigated in the future.

3.6. Conclusion

Harvesting wasted energy provides a great opportunity to minimize GHG emissions, and it can play a key role in the development of entirely carbon-free building energy systems. The ICE-Harvest system captures wasted energy from multiple resources to be used to meet the buildings' heating demands. Two novel clustering techniques for analyzing the city-wide impact of the ICE-Harvest system were developed in the current study. The first method groups the buildings around a pre-defined anchor building within a specified distance. The second method employs density-based (DB) clustering with post processing step that involves including the closest anchor building to each cluster in order to benefit from energy diversity in the connected buildings. Using a database of 14000 buildings in Ontario as a case study the clustering methods are investigated as well as the potential impacts of mass implementation of ICE-Harvest systems. The study's findings led to the following conclusions:

- Clustering buildings with diverse thermal energy demand increase energy harvesting. The DB clustering approach that includes the addition of the closest cooling dominant building to each cluster is the most beneficial, especially in terms of the reduction of GHG emissions and network length.
- Based on the clusters' overall and concurrent cooling-to-heating needs, seven different cluster groups were determined. High levels of simultaneous cooling and heating in high concurrent cluster categories were heated mostly through thermal energy sharing, whereas CHP provided the majority of the recovered heat in the heating dominant clusters.
- With the mass implementation of ICE-Harvest systems, the amount of heating provided by natural gas boilers was significantly reduced by about 8.5 TWh in the No-Export scenario and 11 TWh in the With-Export scenario, which correspond to roughly 54% and 70% of the clusters' overall heating needs, respectively. Moreover, the boiler heating supply can be further reduced by 1.9 TWh using long-term thermal energy storage, which leads to a decrease in carbon emissions of up to 72%.

Acknowledgments

This work was supported by the Natural Sciences and Engineering Research Council of Canada [CRDPJ 509219-2017] and the Ontario Centre of Innovation [27851]. The authors would also like to acknowledge the McMaster Energy Research Cooperative partners for their contributions: HCE Energy Inc., GridSmartCity, GeoSource Energy Inc., s2e Technologies Inc., Siemens Canada Limited, Enbridge Gas Inc., and Alectra Utilities Corporation.

References

[1] United Nations Climate Change, “Paris Agreement - Status of Ratification,” 2017. [Online]. Available: https://unfccc.int/process/the-paris-agreement/status-of-ratification. [Accessed: 09-May-2022].

[2] C. J. Rhodes, “The 2015 Paris Climate Change Conference : COP21,” 2017, vol. 99, no. 2016, pp. 97–104, doi: 10.3184/003685016X14528569315192.

[3] International Energy Agency (IEA), “Towards a zero-emission, efficient, and resilient buildings and construction sector,” *Global Status Report*, 2017. [Online]. Available: www.globalabc.org.

[4] A. Abdalla, S. Mohamed, S. Bucking, and J. S. Cotton, “Modeling of thermal energy sharing in integrated energy communities with micro-thermal networks,” *Energy Build.*, p. 111170, Jun. 2021, doi: 10.1016/j.enbuild.2021.111170.

[5] M. Y. Abdelsalam *et al.*, “Integrated Community Energy and Harvesting Systems: A Climate Action Strategy for Cold Climates,” *Appl. Energy*, 2022.

[6] D. Arvizu *et al.*, *Renewable Energy Sources and Climate Change Mitigation. Special Report of the Intergovernmental Panel on Climate Change*. Cambridge University, 2012.

[7] V. Minea, “Supermarket refrigeration system with completely secondary loops,” *ASHRAE J.*, vol. 49, no. 9, p. 40+, 2007.

[8] D. H. Nall, “Integration of refrigeration and HVAC in grocery stores,” *ASHRAE J.*, vol. 59, no. 1, pp. 48–54, 2017.

[9] O. Piché and N. Galanis, “Thermal and economic evaluation of heat recovery measures for indoor ice rinks,” *Appl. Therm. Eng.*, vol. 30, no. 14–15, pp. 2103–2108, 2010, doi: 10.1016/j.applthermaleng.2010.05.019.

[10] Z. Mylona, M. Kolokotroni, and S. A. Tassou, “Frozen food retail: Measuring and modelling energy use and space environmental systems in an operational supermarket,” *Energy Build.*, vol. 144, pp. 129–143, 2017, doi: 10.1016/j.enbuild.2017.03.049.

[11] Y. Suzuki, Y. Yamaguchi, K. Shiraishi, D. Narumi, and Y. Shimoda, “Analysis and Modeling of Energy Demand of Retail Stores,” *Conf. Int. Build. Perform. Simul. Assoc.*, pp. 14–16, 2011.

[12] R. Z. Pass, M. Wetter, and M. A. Piette, “A thermodynamic analysis of a novel bidirectional district heating and cooling network,” *Energy*, vol. 144, pp. 20–30, 2018, doi: 10.1016/j.energy.2017.11.122.

[13] M. Wahlroos, M. Pärssinen, J. Manner, and S. Syri, “Utilizing data center waste heat in district heating – Impacts on energy efficiency and prospects for low-temperature district heating networks,” *Energy*, vol. 140, pp. 1228–1238, 2017, doi: 10.1016/j.energy.2017.08.078.

[14] “The Independent Electricity System Operator (IESO) of Ontario’s power system.” [Online]. Available: https://www.ieso.ca/en/Corporate-IESO/Media/Year-End-Data.

[15] D. Saxe, "2018 Energy Conservation Progress Report," *Environmental Commissioner of Ontario*, 2018. [Online]. Available: https://www.auditor.on.ca/en/content/reporttopics/envreports/env18/Making-Connections.pdf.

[16] J. Olauson *et al.*, "Net load variability in Nordic countries with a highly or fully renewable power system," *Nat. Energy*, vol. 1, no. 12, 2016, doi: 10.1038/nenergy.2016.175.

[17] M. S. Ziegler *et al.*, "Storage Requirements and Costs of Shaping Renewable Energy Toward Grid Decarbonization," *Joule*, vol. 3, no. 9, pp. 2134–2153, 2019, doi: 10.1016/j.joule.2019.06.012.

[18] J. A. Dowling *et al.*, "Role of Long-Duration Energy Storage in Variable Renewable Electricity Systems," *Joule*, vol. 4, no. 9, pp. 1907–1928, 2020, doi: 10.1016/j.joule.2020.07.007.

[19] O. J. Guerra, J. Zhang, J. Eichman, P. Denholm, J. Kurtz, and B.-M. Hodge, "The value of seasonal energy storage technologies for the integration of wind and solar power," *Energy Environ. Sci.*, vol. 13, no. 7, pp. 1909–1922, 2020, doi: 10.1039/D0EE00771D.

[20] F. Mohammadi, G. A. Nazri, and M. Saif, "A bidirectional power charging control strategy for Plug-in Hybrid Electric Vehicles," *Sustain.*, vol. 11, no. 16, pp. 1–24, 2019, doi: 10.3390/su11164317.

[21] E. A. M. Klaassen, R. J. F. van Gerwen, J. Frunt, and J. G. Slootweg, "A methodology to assess demand response benefits from a system perspective: A Dutch case study," *Util. Policy*, vol. 44, pp. 25–37, 2017, doi: 10.1016/j.jup.2016.11.001.

[22] M. Waite and V. Modi, "Electricity Load Implications of Space Heating Decarbonization Pathways," *Joule*, vol. 4, no. 2, pp. 376–394, 2020, doi: 10.1016/j.joule.2019.11.011.

[23] S. J. G. Cooper, G. P. Hammond, M. C. McManus, and D. Pudjianto, "Detailed simulation of electrical demands due to nationwide adoption of heat pumps, taking account of renewable generation and mitigation," *IET Renew. Power Gener.*, vol. 10, no. 3, pp. 380–387, 2016, doi: 10.1049/iet-rpg.2015.0127.

[24] S. Buffa, M. Cozzini, M. D. Antoni, M. Baratieri, and R. Fedrizzi, "5th generation district heating and cooling systems : A review of existing cases in Europe," *Renew. Sustain. Energy Rev.*, vol. 104, no. October 2018, pp. 504–522, 2019, doi: 10.1016/j.rser.2018.12.059.

[25] F. Bünning, M. Wetter, M. Fuchs, and D. Müller, "Bidirectional low temperature district energy systems with agent-based control: Performance comparison and operation optimization," *Appl. Energy*, no. October, pp. 502–515, 2018, doi: 10.1016/j.apenergy.2017.10.072.

[26] L. Brange, J. Englund, and P. Lauenburg, "Prosumers in district heating networks - A Swedish case study," *Appl. Energy*, vol. 164, pp. 492–500, 2016, doi: 10.1016/j.apenergy.2015.12.020.

[27] R. Rogers, V. Lakhian, M. Lightstone, and J. S. Cotton, "Modeling of Low Temperature Thermal Networks Using Historical Building Data from District Energy Systems," *Proc.*

13th Int. Model. Conf. Regensburg, Ger. March 4–6, 2019, vol. 157, pp. 543–550, 2019, doi: 10.3384/ecp19157543.

[28] Y. Yan, J. Yan, M. Song, X. Zhou, H. Zhang, and Y. Liang, "Design and optimal siting of regional heat-gas-renewable energy system based on building clusters," *Energy Convers. Manag.*, vol. 217, no. May, p. 112963, 2020, doi: 10.1016/j.enconman.2020.112963.

[29] S. Fazlollahi, L. Girardin, and F. Maréchal, "Clustering urban areas for optimizing the design and the operation of district energy systems," *Comput. Aided Chem. Eng.*, vol. 33, no. 2011, pp. 1291–1296, 2014, doi: 10.1016/B978-0-444-63455-9.50050-7.

[30] R. Jafari-Marandi, M. Hu, and O. F. A. Omitaomu, "A distributed decision framework for building clusters with different heterogeneity settings," *Appl. Energy*, vol. 165, pp. 393–404, 2016, doi: 10.1016/j.apenergy.2015.12.088.

[31] J. F. Marquant, R. Evins, L. A. Bollinger, and J. Carmeliet, "A holarchic approach for multi-scale distributed energy system optimisation," *Appl. Energy*, vol. 208, no. May, pp. 935–953, 2017, doi: 10.1016/j.apenergy.2017.09.057.

[32] J. F. Marquant, L. A. Bollinger, R. Evins, and J. Carmeliet, "A new combined clustering method to Analyse the potential of district heating networks at large-scale," *Energy*, vol. 156, pp. 73–83, 2018, doi: 10.1016/j.energy.2018.05.027.

[33] A. Dalla Rosa and J. E. Christensen, "Low-energy district heating in energy-efficient building areas," *Energy*, vol. 36, no. 12, pp. 6890–6899, 2011, doi: 10.1016/j.energy.2011.10.001.

[34] M. Ester, H.-P. Kriegel, J. Sander, and X. Xu, "A Density-Based Algorithm for Discovering Clusters in Large Spatial Databases with Noise," in *Proceedings of the Second International Conference on Knowledge Discovery and Data Mining*, 1996, pp. 226–231.

[35] J. Van Ryn, J. S. Cotton, and M. Lightstone, "Utilizing Micro-Thermal Networks For Energy Demand Response," (MSc thesis) McMaster, 2022.

[36] S. Jayaswal, "A Comparative Study of Tabu Search and Simulated Annealing for Traveling Salesman Problem," Project Report, University of Waterloo, 2014.

[37] "The Independent Electricity System Operator (IESO) of Ontario's power system." [Online]. Available: https://www.ieso.ca/en/Power-Data/Data-Directory.

[38] S. P. Lloyd, "Least Squares Quantization in PCM," *IEEE Trans. Inf. Theory*, vol. 28, no. 2, pp. 129–137, 1982, doi: 10.1109/TIT.1982.1056489.

[39] I. American Society of Heating, Refrigerating and Air-Conditioning Engineers, "Energy standard for buildings except low-rise residential buildings," 2013.

[40] P. Wallentén, "Steady-state heat loss from insulated pipes," *Byggnadsfysik LTH, Lunds Tek. Högskola*, p. 197, 1991.

[41] Association of Power Producers of Ontario, "Renewed interest in Cogeneration – behind the meter." [Online]. Available: https://magazine.appro.org/news/ontario-news/4347-

renewed-interest-in-cogeneration-behind-the-meter-.html.

[42] P. Kandiah and M. Lightstone, “CFD Study of a Large Buried Tank Within a Borehole Field,” M.A.Sc. Thesis, McMaster, 2014.

[43] Ontario Energy Board, “Ontario Wholesale Electricity Market Price Forecast,” 2020. [Online]. Available: https://www.oeb.ca/sites/default/files/rpp-wholesale-electricity-market-price-forecast-20201013.pdf.

[44] Government of Canada, “Natural Resources Canada,” 2020. [Online]. Available: https://oee.nrcan.gc.ca/corporate/statistics/neud/dpa/data_e/databases.cfm.

Chapter 4

The Impact of Thermal Distribution Network Operating Temperature and System Design on Different Communities' Energy Profiles

The impact of thermal distribution network operating temperature and system design on different communities' energy profiles

Ahmed Abdalla[1], Saber Mohamed[1], Kelton Friedrich[1], Scott Bucking[2], James S. Cotton[1*],

[1]McMaster University, Department of Mechanical Engineering, Hamilton, Ontario, Canada

[2]Carleton University, Department of Civil and Environmental Engineering and the Azrieli School of Architecture and Urbanism, Ontario, Canada

*Corresponding Author: cottonjs@mcmaster.ca

Abstract

The use of heat pumps to increase the flexibility of heating networks is critical for overcoming the intermittent nature of renewable energy. This article introduces a novel thermal network operation strategy, referred to as “Smart Network with Peak Control,” which entails adjusting the network temperature to control the peak electricity demand created by the electrification of heating. A comparison between four different operating scenarios—namely, low-temperature (fourth-generation), ultra-low temperature (fifth-generation), smart network (hybrid of low and ultra-low temperatures), and smart network with peak control—is conducted for different sites of different energy profiles. For heating-dominant sites, the application of the smart network and smart network with peak control resulted in 10% lower emissions than the other scenarios. While the peak electricity demand in the smart network scenario was double that of the conventional system, the smart network with peak control scenario was able to counter this effect by adjusting the network temperature. The effects of integrating combined heat and power with different sizes and operating schedules based on the hours of natural-gas peaking generators in mixed electrical grids

were also investigated. The developed model was applied to 1139 sites in Canada, revealing significant carbon emissions reductions of up to 73%.

Keywords: *Thermal distribution networks, Demand response, Electrification of heating, Combined heat and power, Smart grids*

Nomenclature

E	Electricity energy [kW]
H	Pipe depth from the ground surface [m]
K	Thermal conductivity [W/mk]
L	Length [m]
Q	Heat flow rate [kW]
R	Thermal resistance [K/W]
T	Temperature [°C]
W	Electric work (kW]

Subscripts

B	Relating to a building
boiler	Relating to the boiler
C	Relating to a cooling process
ch	Relating to a storage charging
CHP	Relating to a CHP
Conv	Relating to the conventional system
direct	Relating to a CHP direct use
dis	Relating to storage discharging
Elec	Related to electricity
ext	Relating to extra heat from CHP
g	Related to ground
H	Relating to a heating process
HP	Relating to a heat pump

ins	Related to pipe insulation
Los	Related to pipe losses
max	Maximum allowed or expected value
min	Minimum allowed or expected value
rej	Related to heat rejection from cooling systems
rem	Related to remaining heat required
Sh	Related to thermal energy sharing
tank	Relating to thermal storage tank
th	Relating to thermal energy
Tot	Relating to the total value

Abbreviations

1-3GDHS	First Three Generations of District Heating Systems
5GDHCS	5th Generation District Heating and Cooling System
ASHP	Air Source Heat Pump
BHP	Boost Heat Pump
BAU	Business as Usual
Bal	Balanced
BH	Balanced High-Concurrent
BL	Balanced Low-Concurrent
CDD	Cooling Degree Days
CD	Cooling Dominant
CHP	Combined Heat and Power
CH	Cooling High-Concurrent
CL	Cooling Low-Concurrent
CO2e	Carbon Dioxide Equivalent
COP	Coefficient of Performance
DB	Density-Based
DER	Distributed Energy Resources

DHS	District Heating Systems
EMC	Energy Management Center
EoH	Electrification of Heating
ETS	Energy Transfer Station
ExH	Extra-Heating
GHG	Greenhouse Gas
HDD	Heating Degree Days
HD	Heating Dominant
HH	Heating High-Concurrent
HL	Heating Low-Concurrent
HAEF	Hourly Average Emission Factor
HTTN	High Temperature Thermal Network
ICE	Integrated Community Energy
IEA	International Energy Agency
IESO	Independent Electricity System Operator
IPCC	Intergovernmental Panel on Climate Change
LHD	Linear Heat Density
LTTN	Low Temperature Thermal Network
LTS	Long-Term Storage
MEF	Marginal Emission Factor
NG	Natural Gas
PV	Photovoltaic
RHP	Recovery Heat Pump
SMTN	Smart Thermal Network
STS	Short-Term Storage
TN	Thermal Network
TTD	Terminal Temperature Difference
U-LTTN	Ultra-Low Temperature Thermal Network

UN	United Nations
VT	Variable Temperature

4.1. Introduction

The United Nations estimates that 37% of global GHG emissions are the product of building and construction end-energy consumption [1]. In cold-climate countries, most of these emissions are generated by building heating systems, which typically function by burning fossil fuels.

Along with improving the energy efficiency of heating systems, two key strategies have been employed to reduce GHG emissions from the building sector: harvesting waste heat for use in meeting heating demands and electrifying heating using carbon-free resources, such as renewable energy resources.

Recent studies have the benefits of using rejected waste heat harvested from peak natural gas electricity generators and the cooling systems of high-cooling-demand buildings to heat other nearby buildings with high heating demands. To harvest waste heat and share it between buildings, a thermal distribution network is required [2]. The thermal network and energy generator resources (community energy system) can be centralized at a city level or decentralized at a neighborhood level [3]. The centralized approach can require anywhere between 50 to 1000 or more connected kms of piping infrastructure, which can result in thermal losses as large as 30%, especially in low-density cities [4], [5]. In addition, the centralized approach must be implemented during the development of the city itself, as it is both difficult and prohibitively expensive to implement afterward [5]. In contrast, the use of decentralized community energy systems with distributed energy resources (DER) that connect a group of buildings (clusters) via thermal and electrical networks can be more advantageous compared to the centralized approach [6]. A community

energy system consists of two main components: a thermal network (TN) to distribute, harvest, and share thermal energy, and an energy management center (EMC) to provide the site's energy demands thermally and electrically [7]. The temperature of the TN affects its ability to harvest waste heat, as well as the system's thermal losses and its electricity requirements. Buffa et al. [8] provided a detailed overview of both the current generation of direct heating systems (DHS) and earlier generations that functioned via the flow of high-temperature (>90) steam/water through the network by centralized energy systems. The high-temperature thermal networks (HTTN) in the first three generations of district heating systems (1-3GDHS) suffered from significant heat loss, which could often account for up to 30% of the system's heating demand [8]. To address this problem, fourth-generation district heating systems (4GDHS) moved away from the use of HT piping systems in favor of lower temperature (60^{o}C) networks that could still meet space heating and domestic hot water temperature requirements. The subsequent fifth-generation of district heating and cooling system (5GDHCS) [9] networks operate at ultra-low temperatures (5-30^{o}C) that are highly dependent on the electrification of heating via the extensive use of water source heat pumps [10]. One notable drawback of 5GDHCSs is that ultra-low temperature thermal networks (U-LTTN) are prone to high electricity peaks, especially on extremely cold winter days. However, the 5GDHCS's ultra-low operating temperatures and intended use in small-sized networks (i.e., neighborhood size) allows it to harvest low-grade heat sources (i.e., cooling processes, combined heat and power CHP heat rejection, and renewables such as solar thermal) while avoiding the high costs associated with thermal and mechanical losses [11]. The ICE-Harvest system [3] is considered a combination of the 4th and 5th generation DHSs, as it features smart network operation that provides the flexibility to operate at a low temperature (70^{o}C) during peak periods and an ultra-low temperature (20^{o}C) during off-peak periods. Although operating at

ultra-low temperatures during off-peak periods (i.e., periods of surplus carbon-free electricity generation) is favorable for harvesting curtailed electricity, it has a substantial impact on the annual site peak demand, which is typically constrained by the building's electrical connection capacity to the distribution grid infrastructure [3]. For example, Rogers et al. [12] developed a Dymola simulation of a 5GDHCS for nine buildings in Ontario, Canada. Although the proposed method reduced the system's overall energy use by 34%, it also raised its electricity consumption and peak by 50% and 100%, respectively. In another study, Abdelsalam et al. [3] found that the application of an ICE-Harvest system at a balanced site in Ontario, Canada, resulted in approximately 60% savings in carbon emission, but nearly doubled peak electricity demand. Table 4-1 summarizes the differences between the different thermal distribution networks.

Table 4-1: Comparison of different thermal distribution network temperature operation

	1-3GDHS (HTTN)	**4GDHS (LTTN)**	**5GDHCS (U-LTTN)**	**ICE-Harvest (SMTN)**
Thermal network temperature	≥90°C	50-70°C	5-30°C	20-70°C
Thermal losses	High	Medium	Low	Low
Capability for harvesting low temperature waste heat	N/A	Medium	High	High
Thermal network length	Large (City)	Medium (Campus)	Small (neighborhood)	Small (neighborhood)
Electricity demand and peak utilization	-	-	High	High during off-peak hours and low during peak hours

Prior studies focusing on 5GDHCSs employed clusters consisting of buildings with almost equal heating-to-cooling demand ratios [2], [7], [8], [13], [14]; however, the benefits reported in these works cannot be guaranteed for cases with different cluster-load profiles. Abdalla et al. [15] classified cluster thermal demands into 7 categories based on their annual cooling-to-heating consumption ratios, as well as their ratio of cooling-process heat rejection to heating demand.

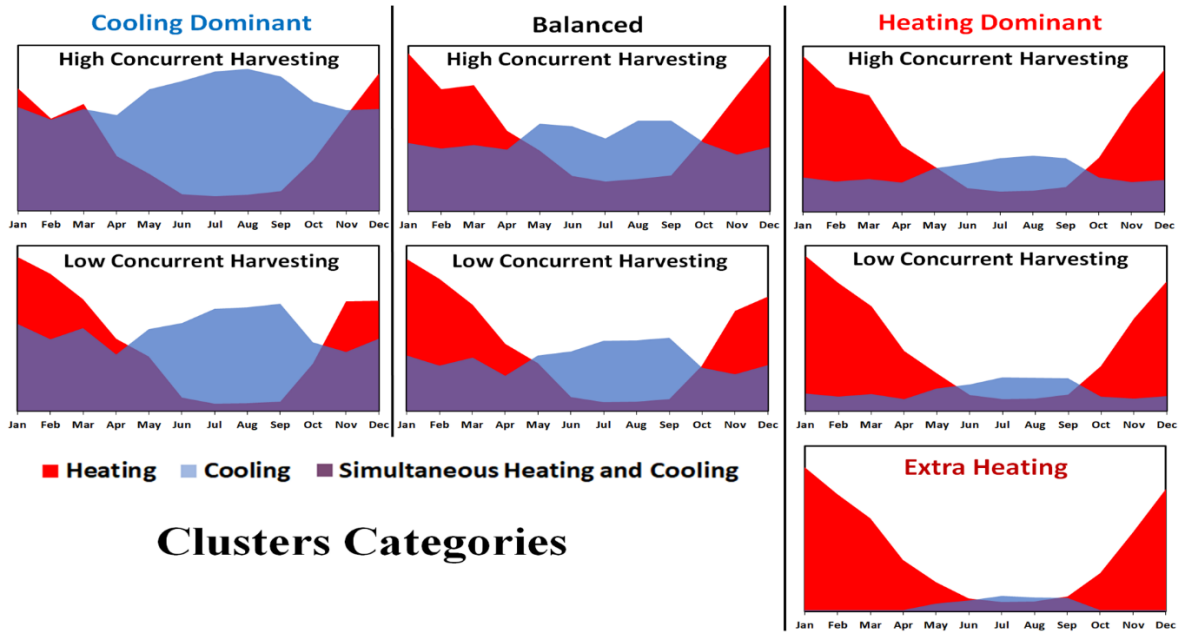

Figure 4-1: Cluster profile categories in Ontario [15].

As shown in Figure 4-1, Abdalla et al. identified 3 major heat-to-cooling ratio categories comprised of 2 to 3 subcategories defined by their simultaneous heat rejection-to-heating ratios. The share of heating accounted for by harvesting cooling process heat rejection, also known as energy sharing [2], increases in proportion to the amount of concurrent cooling and heating demands. Abdalla et al. [15] applied these classification load ratio criteria in a case study set in Ontario, Canada, which is a cold climate region with anywhere between 3000 to over 5000 Heating Degree Days (HDD), much like the northern United States and the Nordic countries [16]–[18]. Almost 80% of the identified clusters in Ontario are heating dominant (HD) with 2500 hours below

0ºC [19], which enables very low COPs for the air source heat pumps (ASHP). The findings indicated that the use of ASHPs in this region significantly increases electricity demand. In a different work, Waite and Modi [20] investigated how the use of ASHPs to electrify heating energy impacted grid levels in all US states. Their findings revealed that this approach resulted in an approximately 70% increase in aggregated peak electricity demands, with demand increasing by more than 100% in 23 states. Elsewhere, Hutty et al. [21] found that the use of ASHPs in a neighborhood of 50 houses caused the electricity peak demand to increase by 2.36 times, which is close to the findings reported in [22], [23]. It is expected that around 80% of clusters in hot-climate regions with more than 3000-5000 cooling degree days (CDD) will fall into the cooling-dominant (CD) category. EoH through the use of heat pumps or the use of low-temperature networks in cold climate regions will result in a significant increase in the peak electricity demands from both the grid and the sites in the network [3], [15]. Thus, there is a need to study how the TN operating conditions impact the different cluster load profiles, and to recommend the optimal operating conditions based on the dominant type of clusters in mass-scale applications, such as at the provincial level.

In addition to selecting the optimal operational scenario for the thermal network, it is critical that the DHS' energy management center (EMC) be designed to integrate the system's thermal and electrical resources to meet the buildings' energy demands. Previous researchers have proposed incorporating different energy resources into the EMC, such as adding CHP to enable the decentralizing of the grid's natural gas generators and using renewables, such as solar photovoltaics (PV). The EMC usually includes on-site CHP as a way of decentralizing the grid's natural gas generators, as the heat produced by these generators can be used to serve the sites' heating demands. This approach is advantageous, as harnessing the CHP heat results in a

significant reduction in cost and GHG emissions. Several electrical grids generate a significant amount of their power from fossil fuels. These fossil fuel resources produce a lot of residual heat that is typically rejected to the environment as waste heat and have a low overall electrical efficiency of roughly 42% [24], [25]. Displacing the fossil fuel generators by on-site CHPs connected to thermal distribution networks allows the heat generated to be used to supply the network heating demand. For example, in Denmark, DHSs provide 60% of household heating energy, with CHP satisfying around 70% [26] of the DHS's heating needs and approximately 50% of the country's electricity needs [27]. The recent proliferation of renewable technologies has resulted in most grids shifting away from fossil fuels and towards more carbon-free electricity generation (e.g., Denmark has been able to attain 47% of its electricity from wind power [28]). As the use of renewable and carbon-free electricity generation continues to grow, the share of natural gas generation will decrease. However, the large increase in renewable energy in the electricity grid with its intermittent behavior led to a challenge for the grid due to the mismatch between the electricity available generation resources times and the demand times. Thus, grids still require flexible generation resources (e.g., natural gas generators) that can be reliably dispatched to supplement renewable generation and provide balance to the electricity grid [29]. In this case, the use of CHP to completely displace the electricity grid is inefficient and may lead to an increase in GHG emissions. Several publications have attempted to develop an optimization model for the design and operation of a CHP distributed-generating system in an urban area setting [30]. In one study, Wang et al. [29] investigated coupling the electricity and heating sector by utilizing a CHP to supply the energy needs of a DHS, while also balancing the electrical grid. Their findings offer a useful roadmap for actions intended to maximize the flexibility potential of CHPs for both lowering the cost of heat and balancing a local energy portfolio. Elsewhere, Yasser et al. [3]

suggested running CHP only during peak periods with highly dispatchable electricity loads in order to offset natural gas generation. However, studies allow the CHP to produce as much electricity as the site needs during peak periods which could lead on a large-scale or a fleet of sites such as city level to higher accumulated generation from the CHP's than the existing grid natural gas usage. For example, carbon-free sources account for around 95% of the electricity generated by Ontario's grid, with only 5% coming from centralized natural gas power plants (10 TWh/year) [31], which is mainly used to meet the dispatchable demands and stabilize the grid. Therefore, for large-scale implementation of CHPs in a fleet of sites (at the city or provincial level), it is critical to set a limit on CHP generation so that the accumulated generation does not exceed the grid's natural gas electricity generation in order to avoid forcing the grid to abandon carbon-free resources.

4.1.1. Contributions of this work

This study introduces a novel operational approach for integrated energy systems on both the network and system sides. On the network side, the current work details a novel "smart network with peak control" strategy wherein the thermal network temperature is variably changed to control increases in peak electricity demand caused by the electrification of heating. Most prior studies focusing on U-LTTNs with the electrification of heating have consisted of case studies based on the energy profiles of specific sites, mainly balanced sites with a large simultaneous cooling and heating demand. In contrast, this work investigates how different thermal network temperature operations and design conditions impact the different site load profiles. This investigation will provide a more detailed understanding of the integrated energy system's capabilities in each situation and how the studied factors affect electricity demand and peak, as well as GHG emissions. On the system side, the current work introduces a new CHP operation. The proposed

operational approach links the site utilization and electrical grid operation for a fleet of sites at the provincial level. Prior studies have focused on optimizing CHP size and operation for a certain site for economic and environmental purposes without considering the cumulative impact of CHPs on the electrical grid for a fleet of sites at the provincial scale. The current study investigates the cumulative impact of different CHP sizes and operating schedules based on site utilization and different grid operations. Different operational scenarios for different grid's natural gas operating schedules will also be considered. The cumulative CHP electricity generation for a fleet of sites is linked to the electrical grid where the CHP generation is set not to exceed the grid peaking natural gas generation at each period.

4.2. Methodology

4.2.1. System description and operation

The integrated energy system uses a one-pipe thermal network that connects a group of high-energy-consumption buildings with diverse thermal energy demands via an energy transfer station ETS. The ETS includes heating heat pumps and heat exchangers that enable thermal energy exchange between the network and the buildings' heating distribution systems. The thermal network satisfies the heating energy requirements for the buildings, while the cooling energy is supplied separately for each building. The heat rejected from the buildings' cooling systems is utilized as a heat source for the network, known as thermal energy sharing [32], via the ETS, which redirects the excess residual heat to the ambient via heat rejection equipment (i.e., cooling towers). The remaining heat energy required to control the network temperature is supplied by a local energy management center (EMC). A comparison of three different ETS configurations is presented in Figure 4-2, with four different thermal network operation scenarios.

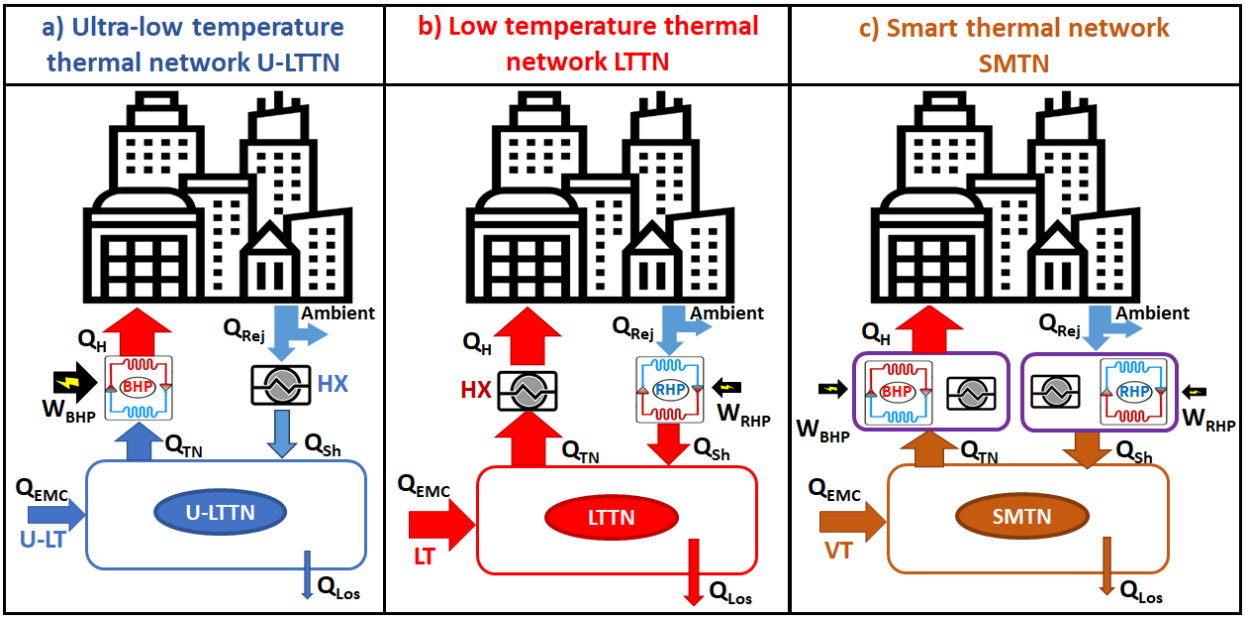

Figure 4-2: Thermal network operating scenarios: a) Ultra-Low Temperature; b) Low Temperature; c) Smart.

The four scenarios, which vary in terms of the thermal network operating temperature, are defined as follows:

Ultra-low-temperature thermal network (U-LTTN)

In this scenario, the network operates at a constant low temperature similar to the 5GDHCS (~20^{o}C) to allow direct exchange between the network and the low-grade heat rejected from the cooling systems (Q_{Sh}) via a heat exchanger (Figure 4-2a). The remaining heating energy required by the network is supplied by the EMC (Q_{EMC}). A boost heat pump (BHP) is used to increase the temperature of the energy provided by the network (Q_{TN}) to the buildings' required temperature (assumed to be 50-65^{o}C) plus a terminal temperature difference TTD of at least 5^{o}C, which results in a final temperature of about 70^{o}C.

Low-temperature thermal network (LTTN)

Here, the network operates at a constant temperature of 70^{o}C, which is suitable for the building heating distribution systems. A recovery heat pump (RHP) is used to raise the lower-temperature

heat rejected from process cooling up to the network temperature TTD (~5^{o}C) to allow for direct exchange, as shown in Figure 4-2b.

Smart thermal network (SMTN): a binary range-controlled temperature-modulating thermal network

In this scenario, the network temperature is set to operate at an ultra-low temperature (20^{o}C) during off-peak hours and a low temperature (70^{o}C) during peak periods. This configuration (Figure 4-2c) can be considered a hybrid binary operation between low and ultra-low temperatures. Operating at an ultra-low temperature requires a high EoH during off-peak hours, thus harvesting the curtailed electricity via the BHP, while increasing the network temperature during peak periods eliminates the use of electricity for EoH. The TN at each site is sized to form a microthermal network of less than 5km to minimize its thermal mass and allow for temperature changes within approximately 1 hour [33]. The heat rejected from the building's cooling processes can be directed either into the atmosphere or for heat recovery with the thermal network. This can be achieved with a direct exchange during ultra-low temperature TN operation or via the RHP during low-temperature TN operation [3].

Smart thermal network (SMTN) with peak control: a range-controlled temperature-modulating thermal network

In the previous scenario, operating the system at an ultra-low temperature during off-peak periods can significantly increase electricity peak demand at certain hours. Peak control allows the network temperature to be continuously controlled between 20-70^{o}C during off-peak periods. While any control value is possible from zero to max EoH, an arbitrary value was selected for demonstration purposes. The model in this study only allows a limited increase of around 30% over the BAU

peak to avoid large increases in site peak electricity demand. The lowest network temperature that meets this constraint is selected, thus benefiting from EoH while maintaining the system's feasibility.

To avoid large centralized networks that require a significant upfront investment, the thermal network is relatively short—less than 5 kilometers—compared to district heating systems. Moreover, small-scale networks have less mechanical and thermal loss as well as less investment risk [8]. The thermal network is purposefully made to have a short length in order to maintain a water thermal mass that is small enough to change the TN temperature between ultra-low level of about 20°C and a higher level of around 70°C (i.e., 50°C range) within 1 hour time interval [33].

The EMC contains different resources to supply the network heating requirements, as well as the site's electricity needs such as CHP that is backed by the electricity grid and natural gas boilers to fulfill the demands depending on the CHP size and operation schedule. The CHP is set to only operate at peak periods to displace electrical grid natural gas peaking generators where the heat generated is used to provide the heating requirements of the thermal network to maintain or increase its temperature. In addition, the EMC also includes short and long-term thermal storage systems to provide flexibility to the system and overcome the mismatch between the CHP generation and demands. These models are compared to the business as usual (BAU) case, which uses grid import for electricity and a natural-gas-fired boiler for heating. In this scenario, heating energy is separated from electricity, and there is no harvesting of residual heat from cooling processes.

4.2.2. Mathematical modeling:

The modeling relations presented in this section fall into two main categories: the modeling equations for the thermal network and the ETS, and the modeling and sizing parameters and constraints of the EMC equipment. Following that, the method for calculating GHG emissions is presented. Flowcharts that describe the modeling steps are presented in Appendix A. Modeling was done with Matlab software, and the model was verified against a Dymola dynamic simulation conducted by Van Ryn [33] (see Appendix B). The model uses the following hypothesis:

- The model neglects the temperature variation along the network length at each time step, this is due to the small length of the TN compared to the DHS networks, and the EMC equipment is sized to maintain a maximum temperature difference of 10^{o}C over the TN at the largest load.
- Since short thermal networks have low pumping power [7], [34], the relatively small pumping power is neglected in the model.
- The thermal network temperature can be changed between 20^{o}C and 70^{o}C in an hour via the available resources in the EMC. This controlling ability is due to the small thermal mass of the network [33].
- For simplification and to show the impact on large-scale applications, CHP operation parameters are estimated based on energy balance. The model assumes that the dynamic parameters' fluctuations can be managed by the thermal energy storage systems.
- In order to quantify the effects of its large-scale implementation, the LTS model is simplified in this study, with no further constraints attached to the charging and discharging rate and real-time efficiency.

4.2.2.1. Mathematical modeling of the thermal network and energy transfer station

The energy recovered via thermal energy sharing in all TN operation scenarios can be evaluated using Equation 1. This equation is generalized, which makes it valid in all operation scenarios with setting values for different network operating conditions. The minimum is used to only use the amount of heat required by the network in times of larger heat rejection than the network heating requirements to avoid the increase in the TN temperature while the extra rejection is emitted to the ambient from each building separately.

$$Q_{Sh} = \sum_{i=1}^{n} \begin{matrix} Min\{[Q_{Rej}(i) + W_{RHP}(i)]\,, \\ [Q_H(i) - W_{BHP}(i)]\} \end{matrix} \quad (1)$$

Here, *n* is the total number of intervals (*i*) in any calculation period (day/month/year).

All parameters are dependent on the TN temperature, which can be set between an ultra-low temperature level lower than the rejection $(T_{rej} - TTD)$ to a higher temperature (T_H) than the building heating distribution system requirements $(T_B + TTD)$. The first is to allow for a direct exchange between the heat rejection from the buildings' cooling systems while the latter is to allow for a direct exchange between the network and the building heating distribution system [35]. The thermal network operating range is shown in Equation 2.

$$(T_{rej} - TTD) \leq T_{TN} \leq (T_B + TTD) \quad (2)$$

The heat rejection from the cooling processes is calculated based on the second law of thermodynamics as a function of the coefficient of performance of the cooling equipment (COP_C), as shown in Equation 3. The COP_C of an ammonia refrigeration system is selected for the refrigeration systems in ice arenas and grocery stores, as it is the most commonly used system in Canada. In addition, an air-cooled chiller is selected for use in air conditioning systems using the COPs employed in [32].

Similarly, the work of the heat pumps is calculated in Equations 4 and 5 as a function of the heat pumps' COPs. The COPs of the heating heat pumps change with the network temperature, and the values are set following the water-cooled heat pump COPs listed on the data sheet for the Nordic heat pumps used in [3].

$$Q_{Rej} = \sum_{j=1}^{NB_T} Q_C(j) * \left(\frac{1}{Cop_c(j)} + 1\right) \quad (3)$$

$$W_{RHP} = \begin{cases} \frac{Q_{Rej}}{Cop_{RHP}-1} & if\ T_{TN} \geq T_H + TTD \\ 0 & if\ T_{TN} \leq T_{TN} - TTD \end{cases} \quad (4)$$

$$W_{BHP} = \begin{cases} 0 & if\ T_{TN} \geq T_H + TTD \\ \frac{Q_H}{Cop_{BHP}} & if\ T_{TN} \leq T_{TN} - TTD \end{cases} \quad (5)$$

In the above equations, NB_T is the total number of buildings connected to the network and j is the counter of each building number.

Equation 6 presents the incremental electricity results from EoH via the ETS heat pumps. The overall electricity consumption (E_{Tot}) after harvesting is evaluated via Equation 7 [2], which sums up the BAU electricity and the ETS heat pump electricity consumption.

$$E_{ETS} = W_{RHP} + W_{BHP} \quad (6)$$

$$E_{Tot} = E_{BAU} + E_{ETS} \quad (7)$$

The heat required from the TN (Q_{TN}) is determined based on the building's heating requirements (Q_H) and the ETS heating heat pump work (W_{BHP}) (Equation 8) by applying the first law of thermodynamics [35].

$$Q_{TN} = (Q_H - W_{BHP}) \quad (8)$$

Thermal network scenarios of operation

In the U-LTTN scenario, the $W_{RHP} = 0$ and the $W_{BHP} \neq 0$. The recovery heat pump is not needed in this configuration because the network operates at an ultra-low temperature (T_{TN}=20^{o}C), which allows the network to capture the low-grade waste heat rejected from the cooling processes directly using a heat exchanger, while EoH is achieved by using a boost heat pump to raise the temperature

of the heat supplied by the network to the temperature required by the buildings' heating distribution systems.

Conversely, in the LTTN scenario, the $W_{RHP} \neq 0$ (unless there is no heat to be recovered from the cooling systems) and the $W_{BHP} = 0$. The network temperature is higher than the buildings' required temperature (T_{TN}=70°C), allowing a direct exchange without the need to boost the network temperature i.e. $W_{BHP} = 0$. In this case, a recovery heat pump is used to increase the rejected heat from process cooling to a temperature higher than that required by the network by a TTD of 5°C.

The SMNT scenario can be considered a combination of the two previous scenarios. In this scenario, the SMNT runs as a U-LTTN during off-peak hours ($W_{RHP} = 0$ and $W_{BHP} \neq 0$) to enable more EoH via the BHP, which in turn boosts the total heating required from the network (Q_{TN}) to the building's required temperature while using less heating energy from the EMC. During peak periods, the SMNT operates as an LTTN ($W_{RHP} \neq 0$ and $W_{BHP} = 0$), thus allowing direct exchange between the network and the building heating distribution systems. Here, high heating from the EMC and RHP can be used to boost the Q_{rej} to the TN.

The SMTN with peak control scenario adds a limitation such that the network temperature is controlled to ensure the BHP and RHP electricity consumption does not exceed the peak electricity of the site within a certain threshold, which in this case is set to be 30% higher than the BAU peak. This approach allows the network temperature to be decreased during off-peak hours to a level selected based on the electricity consumption. Thus, during certain hours, the network temperature can be set to a level that exceeds the cooling system's heat rejection temperature but is lower than the building heating requirements, as shown in Equation 2. During these hours, both the BHP and

RHP operate simultaneously to exchange the energy with the TN, with a minimum temperature difference of 10°C across the heat pumps being set as a constraint.

Thermal network pipe sizing and thermal loss calculations:

The network's piping system is sized to meet the largest energy requirements at various TN operating temperatures and uses insulation material consisting of fiberglass in accordance with the regulations specified by ASHRAE standard 90.1 [36]. The network losses (Q_{Los}) are evaluated using the analytical approach developed by Wallentén [37], who developed a series of analytical models for different pipe configurations, including insulated single pipes, double pipes, and embedded pipes. The heat transfer problems were solved at the zero, first, and second orders for each configuration using the multipole approach. The thermal losses are calculated using a second-order solution for a single insulated pipe. The network heat loss and the relationship's defining parameters are evaluated in Equations 9, 10, and 11 using the model developed in [37].

$$Q_{Los}(i) = \frac{(T_{TN}(i) - T_g(i))}{R_{Los}} \tag{9}$$

$$R_{Los} = \frac{1}{2\pi K_g}\left(\begin{array}{c}\ln\left(\frac{R_o}{R_i}\right) + \propto + \left[1 + \frac{1}{2}\frac{(1+\propto)}{(1-\propto)}\frac{(1+2\propto)}{(1-2\propto)}\left(\frac{R_o}{2H}\right)^2 - \frac{3}{2}\frac{(1-2\propto)}{(1+2\propto)}\left(\frac{R_o}{2H}\right)^4\right] * \\ \left[1 - \left(\left(\frac{2H}{R_o}\right)^2 - 3\frac{(1-2\propto)}{(1+2\propto)}\left(\frac{R_o}{2H}\right)^2\right)\frac{(1+\propto)}{(1-\propto)} - \frac{(1-2\propto)}{(1+2\propto)}\left(\frac{R_o}{2H}\right)^4\right]^{-1}\end{array}\right) \tag{10}$$

$$\alpha = \frac{k_g(T_{TN} - T_{gs})}{k_{ins}}\ln\left(\frac{R_o}{R_i}\right) \tag{11}$$

Where R_{Los} is the thermal resistance from the pipe to the ground, k_g is the ground thermal conductivity, k_{ins} is the pipe insulation's thermal conductivity, T_{TN} is the TN water temperature, T_g is the ground surface temperature, H is the buried pipe depth, R_o is the outer radius of the pipe insulation, R_i is the outer radius of the pipe, and α is a dimensionless thermal resistance parameter.

The ground thermal conductivity is set at 2 W/mK [38]. For simplicity, the model neglects the temperature variation along the network length. The TN is buried 1.5 m below the ground surface and the TN diameter is selected for different clusters based on a maximum flow velocity of 1.5 m/s. An energy balance across the TN is used to calculate the remaining energy needed from the EMC to keep the network temperature at the prescribed setpoint. as presented in Equation 12 [35].

$$Q_{EMC} = (Q_{TN} - Q_{Sh} - W_{RHP} + Q_{Los}) \quad (12)$$

4.2.2.2. Energy management center

As the current study investigates the effect of using different equipment in the EMC to supply the energy required by the network, multiple designs were evaluated. In the first design, the EMC only included heating energy supply equipment—in this case, a natural gas boiler, which is the most common system used in Canada—with electricity demand being met by the electricity grid. In the second design, a CHP is integrated into the EMC to serve as a priority source of heat when running and is set to operate only during peak periods in order to decentralize the central electrical grid's peaking natural gas generator. In addition, short-term thermal energy storage is coupled with CHP to mitigate the short-term mismatch between CHP generation and the network demand, while long-term seasonal storage is employed to address the mismatch over the seasonal periods. The CHP is sized using an iterative method, with a minimum size of 0 kW_e and a maximum size of twice the site's electricity peak with a step change of 250 kW_e. In sizing the CHP and the STS for each cluster, some constraints are applied, including:

- The minimum allowed annual combined heat and power efficiency for the CHP is 65%.

- The maximum allowed hourly export of electricity from a site to the grid is restricted to not exceeding the site's peak electricity to avoid the need for costly grid infrastructure improvements.
- The total electricity generated by all CHPs across all sites is limited at any given hour so as not to surpass the amount of electricity produced by the grid's natural gas peaking plants.
- The STS is sized to cover the maximum daily mismatch between the excess heat from the CHP and the heat required by the EMC.

The amount of heat generated by the CHP that is directly used to satisfy the EMC's heat energy requirements ($Q_{CHP_{direct}}$) is evaluated via Equation 13 [3]. This amount is the minimum between the CHP capacity and the required heat by the EMC at each time interval.

$$Q_{CHP_{direct}}(i) = Min[Q_{CHP}(i), Q_{EMC}(i)] \quad (13)$$

CHP heat generation and the heat required from the EMC by the TN will not be the same at different time intervals; that is, sometimes, CHP heat generation will be higher than the energy required by the TN and vice versa. The positive difference in the first case is the excess heat generation from the CHP ($Q_{CHP_{ext}}$), as shown in Equation 14 [3]. When the difference between CHP heat generation and the heat required by the EMC is negative, Equation 15 [3] is applied to determine the remaining heat energy that must be transferred from the EMC resources rather than the CHP to the TN ($Q_{EMC_{rem}}$). The thermal storage element's main function is to store excess heat produced by the CHP when $Q_{CHP_{ext}}(i) > 0$ and discharge it when $Q_{EMC_{rem}}(i) > 0$.

$$Q_{CHP_{ext}}(i) = \begin{cases} Q_{CHP}(i) - Q_{EMC}(i) & ,if\ Q_{CHP}(i) > Q_{EMC}(i) \\ 0 & ,if\ Q_{CHP}(i) \leq Q_{EMC}(i) \end{cases} \quad (14)$$

$$Q_{EMC_{rem}}(i) = \begin{cases} |Q_{CHP}(i) - Q_{EMC}(i)| & ,if\ Q_{CHP}(i) < Q_{EMC}(i) \\ 0 & ,if\ Q_{CHP}(i) \geq Q_{EMC}(i) \end{cases} \quad (15)$$

The model then calculates the charging rate ($Q_{STS_{ch}}$) based on the comparison between $Q_{CHP_{ext}}$ and the storage maximum energy capacity ($Q_{STS,max}$). The excess heat generated from the CHP at any given time is charged to STS as long it does not exceed the storage maximum capacity; if the excess heat exceeds the STS's maximum capacity, the STS will only charge up to its capacity. The amount of energy that can be charged at any time interval is calculated via Equation 16 [3]. Similarly, during discharge, the storage discharges heat to meet the remaining heat required by the EMC, as presented in Equation 17 [3]. The amount of heat stored in the STS tank at any time interval is calculated using Equation 18 [3].

$$Q_{STS_{ch}}(i) = \begin{cases} Q_{STS_{max}} - Q_{STS_{tank}}(i-1) & ,if\ Q_{STS_{tank}}(i-1) + Q_{CHP_{ext}}(i) \geq Q_{STS,ma} \\ Q_{CHP_{ext}}(i) & ,if\ Q_{STS_{tank}}(i-1) + Q_{CHP_{ext}}(i) < Q_{STS,ma} \end{cases} \quad (16)$$

$$Q_{STS_{dis}}(i) = \begin{cases} Q_{STS_{tank}}(i) & ,if\ Q_{EMC_{rem}}(i) \geq Q_{STS_{tank}}(i) \\ Q_{EMC_{rem}}(i) & ,if\ Q_{EMC_{rem}}(i) < Q_{STS_{tank}}(i) \end{cases} \quad (17)$$

$$Q_{STS_{tank}}(i) = \begin{cases} Q_{STS_{tank}}(i-1) + Q_{STS_{ch}}(i) & ,at\ charging\ state \\ Q_{STS_{tank}}(i-1) - Q_{EMC_{rem}}(i) & ,at\ discharging\ state \\ Q_{STS_{tank}}(i-1) & ,at\ idle\ state \end{cases} \quad (18)$$

As a preliminary sizing approach, the STS is sized to cover the maximum daily mismatch between the excess heat from the CHP and the heat required by the EMC (Equation 19) similar to [2]. The maximum capacity ($Q_{STS,max}$) of the largest STS usage on a peak day for a given year is tracked, and the STS capacity is sized to satisfy this demand. For simplicity, the model assumes a perfect insulated tank with infinite charging and discharging rates.

$$Q_{STS,max} = Max\left(\sum_{1}^{365} Min\left[\sum_{i=1}^{24} Q_{CHP_{ext}}(i), \sum_{i=1}^{24} Q_{EMC_{rem}}(i) \right] \right) \quad (19)$$

Over the course of a year, a large portion of CHP heat generation is wasted due to low heating demands during the summer season. As such, the model also investigates the impacts of adding

seasonal long-term storage (LTS) to cover seasonal mismatches between the sites' CHP production and the demands of individual sites. The potential impact of using LTS is calculated using Equation 20 [39]. The amount of energy used from the LTS is considered the minimum between the required and the available annual heating energy. The model does not account for the dynamic behavior of the storage. The surplus heat generated from CHP that is not stored in STS can be stored in LTS. For simplicity and to show the large-scale impact of the LTS, the model replaces the losses term for LTS with efficiency (η_{LTS}). Two different LTS efficiencies are used: 50% as in geo-storage [39], and 100%, as in a perfectly insulated tank to show the ideal limit.

$$Q_{LTS} = Min\begin{pmatrix} \sum_{i=1}^{8760} [\mathrm{Q}_{\mathrm{CHP}_{\mathrm{ext}}}(i) - Q_{STS_{ch}}(i)] * \eta_{LTS}, \\ \sum_{i=1}^{8760} \left[\mathrm{Q}_{EMC_{\mathrm{rem}}}(i) - Q_{STS_{dis}}(i)\right] \end{pmatrix} \quad (20)$$

After servicing the system's heating demands via CHP heat, STS, and LTS, the remaining required heating energy is provided by a natural gas boiler in the EMC. Equation 21 is used to determine the heating energy covered by the boiler via applying heat balance over the EMC.

$$Q_{boiler} = (Q_{EMC} - Q_{CHP_{direct}} - Q_{STS_{dis}} + Q_{LTS}) \quad (21)$$

The CHP operation is set to follow the electricity produced by gas on the grid, with CHP electricity generation ($\mathrm{E}_{\mathrm{CHP}}$) being used to service the site's demand. When CHP production is lower than the site demands, the remaining electrical demand is satisfied via power imported from the grid ($\mathrm{E}_{\mathrm{Import}}$). Conversely, when CHP production exceeds the site's demand, the excess generation is exported to the grid ($\mathrm{E}_{\mathrm{Export}}$). Equations 22 and 23 [3], [40] are used to evaluate the amount of imported and exported electricity. On the other hand, while the generated heat is used to service the site's demand, some of this heat is not utilized, especially in the case of large-capacity CHPs. Thus, the CHP is sized to meet a specified minimum overall annual efficiency with the aid of STS.

The minimum value of the overall CHP efficiency is evaluated via Equation 24 (must be greater than or equal to 65% to meet Ontario regulations) [41].

$$E_{Import}(i) = \begin{cases} E_{Tot}(i) - E_{CHP}(i) & ,if\ E_{CHP}(i) < E_{Tot}(i) \\ 0 & ,if\ E_{CHP}(i) \geq E_{Tot}(i) \end{cases} \quad (22)$$

$$E_{Export}(i) = \begin{cases} |E_{Tot}(i) - E_{CHP}(i)| & ,if\ E_{CHP}(i) > E_{Tot}(i) \\ 0 & ,if\ E_{CHP}(i) \leq E_{Tot}(i) \end{cases} \quad (23)$$

$$\eta_{CHP} = \frac{\sum_{i=1}^{8760}[Q_{CHP_{direct}}(i) + Q_{STS_{dis}}(i) + E_{CHP}(i)] * 100}{\sum_{i=1}^{8760}[Q_{CHP}(i) + E_{CHP}(i)]} \quad (24)$$

4.2.2.3. GHG emissions calculations

The GHG emissions from the natural gas boiler (GHG_{boiler}) are calculated via Equation 25 based on the boiler efficiency (η_B), which is assumed to be 85%, and the CO_2 emissions for each MWh of thermal energy, which are set to 0.1872 t CO_2eq/MWh based on Canada's 2018 National Inventory Report [42]. The GHG emissions for the electrical side are calculated using Equation 26 and the BAU electricity consumption, which is based on the grid hourly average emission factor (HAEF) in accordance with the method presented in [43]. The HAEF [43] is calculated using Equation 27. However, the GHG emissions for incremental increases in electricity demand by the ETS heat pumps during peak periods are calculated with the assumption that the incremental value is entirely generated by natural gas generators on the grid at an efficiency (η_{gen}) of 42%, as presented in Equation 28. This results in 445 tonnes of CO_{2e}/GWhe [25].

$$GHG_{boiler} = [\sum_{i=1}^{n} Q_B(i)]/\eta_B * 0.1872 \quad (25)$$

Where Q_{boiler} is the heat supplied by the boiler in MWh.

$$GHG_{E-BAU} = \sum_{i=1}^{n}[E_{BAU}(i) * HAEF(i)] \quad (26)$$

$$HAEF\ (i) = \frac{GHG\ emissions\ from\ fossil\ fuel\ plants(i)}{Total\ electricity\ generated\ in\ the\ grid\ (i)} \quad (27)$$

$$GHG_{E-ETS} = \begin{cases} \sum_{i=1}^{n}\left[E_{ETS}(i)/\eta_{gen} * 0.1872\right] & if\ marginal\ gas\ generator\ is\ on \\ 0 & if\ marginal\ gas\ generator\ is\ off \end{cases} \quad (28)$$

Since the CHP heat serves to decentralize the natural gas electricity resources, it is considered as being zero emission to avoid double counting. The CHP's distributed electricity emissions are assumed to be the same as those of the central grid peaking natural gas generators it is displacing. Since the distributed CHP is displacing central grid peaking natural gas generators, there are no CHP site emissions; the site CHP emissions are included either in the grid hourly average emission factor, or as a marginal emission factor for the incremental electricity consumption, just like the central grid peaking natural gas generators emissions.

4.2.3. Case study

The database used in this study includes the energy profiles for the 1139 clusters in Ontario collected in [15]. These clusters comprise 14832 high-energy-consumption buildings representing 9 different archetypes, including residential towers, hotels, grocery stores, and ice arenas. The study used a semi-supervised clustering approach called "density based with adding the nearest anchor building". In this algorithm, the density based clustering algorithm is first applied to the database to identify the closest cooling-dominant building in each cluster within a specified distance, with the identified buildings subsequently being connected to the cluster to maximize thermal energy sharing. In this study, the resulting clusters were categorized as either cooling, balanced, or heating dominant based on their annual cooling-to-heating demand ratio. Each category consisted of two subcategories—high and low concurrent harvesting—which were defined by the thermal energy sharing percentage. Notably, the heating-dominant category contained a third, extra-heating subcategory, thus resulting in 7 total subcategories (Figure 4-1).

The average profile for each of the 7 categories was calculated to study how the different TN operation scenarios impacted the different cluster load categories. This was achieved via the following steps:

1 First, the four network operating scenarios were modeled using the average cluster of each of the 7 cluster's subcategories.

2 Second, the impact of integrating CHP was modeled for all 1139 clusters in the database using the most beneficial scenario in each of the four network operating scenarios, and the effects of this integration on each of the three main cluster categories (CD, Bal, and HD) were analyzed.

3 The overall impact of different CHP operating hours on GHG emissions is calculated using the grid natural gas peaking power plants for two years of operation: 2016, which had a high number of peak hours (93% of the year), and 2017 which had a low number of peak hours (38% of the year).

4 Finally, the impact of changing the CHP minimum allowed efficiency at all sites with and without LTS, as well as overall CHP sizes, was assessed.

4.3. Results and discussion

A comparison of the four network operating scenarios was performed by applying the above-described methods to the 7 cluster categories. The results of the comparison provided insight into the network thermal losses vs. the LHD, the electricity and heating energy consumptions, and the GHG emissions. In addition, the results provide data for evaluation criteria such as the amount of energy shared and the reduction in GHG emissions for each clustering method. After identifying

the best clustering technique, the ICE harvest system's potential impacts with respect to the clusters' heating and electricity needs and GHG emissions are presented.

4.3.1. The impact of the different thermal network operating scenarios for the different categories of clusters

In their case study of Ontario, Canada, Abdalla et al. [15] classified 1139 clusters into 7 categories based on their cooling-to-heating and simultaneous waste heat rejection-to-heating demand ratios (Figure 4-1). The present work examines how the use of different TN operation and design conditions impacts the different cluster load categories in order to better understand the integrated energy system's capabilities in each situation.

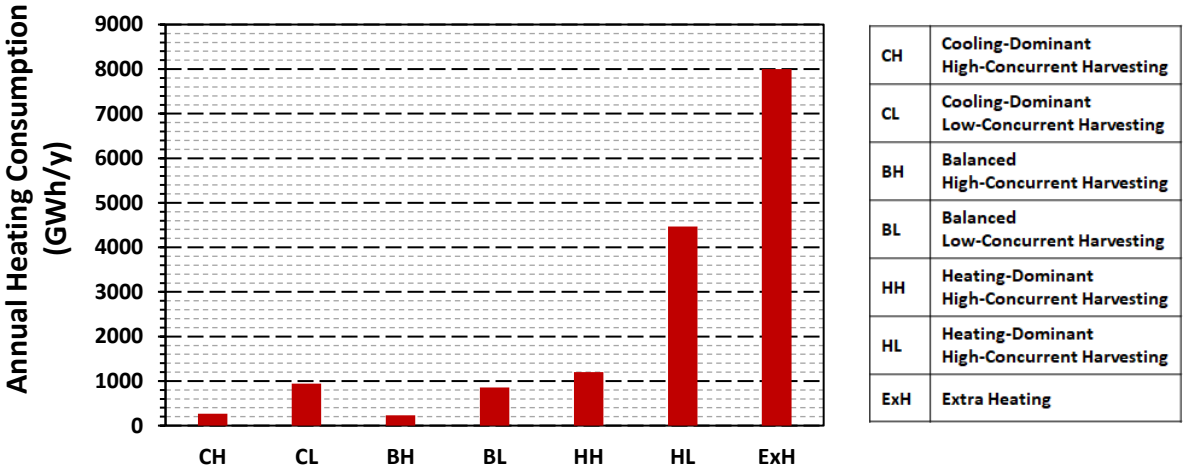

Figure 4-3: Summation of annual heating energy consumption for the different cluster categories.

In the Ontario case, heating-dominated clusters with over 5000 HDDs account for nearly 80% of the total identified sites. The ExH and HL clusters combined account for 85% of the overall heating energy consumption, consuming approximately 8 TWh/year and 4.5 TWh/year, respectively (Figure 4-3). Conversely, the CH and BH clusters had the lowest heating energy consumption at less than 0.25 TWh/y, or around 3% of total consumption. This indicates that the heating dominant clusters, mainly HL and ExH can be selected as representative clusters in cold climate regions.

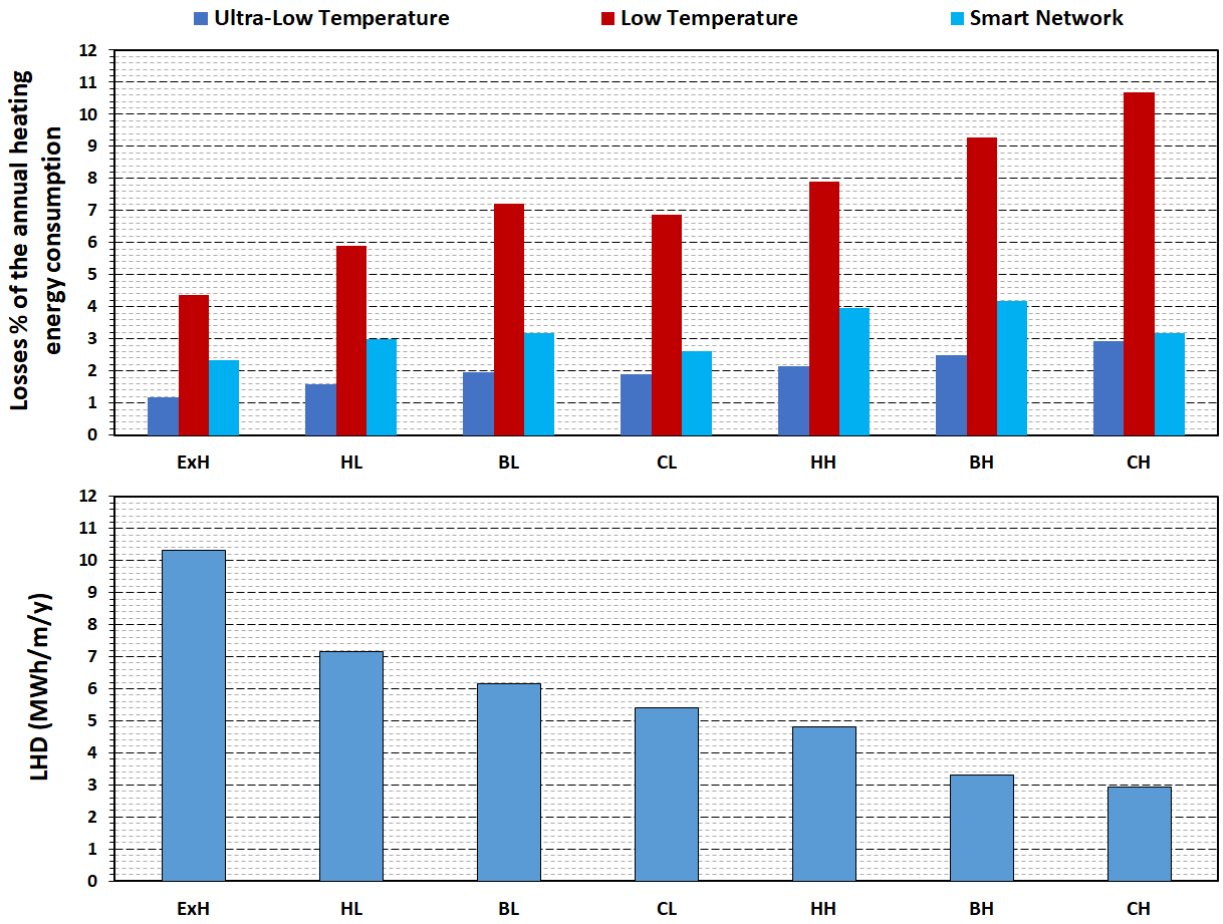

Figure 4-4: (Top) Heat loss % for the different cluster's categories based on network operation scenario. (Bottom) Comparison of cluster's categories with respect to LHD.

The findings indicate that operating temperature and LHD have a significant impact on the network's thermal losses. LHD is used to express the ratio of the total heating energy served per year to the pipe length (MWh/year/m). In Figure 4-4, thermal losses are shown as a ratio of the total network heating for the four TN operating scenarios. As can be seen, the proportion of the total heating that is lost increases alongside the network temperature and LHD; thus, a higher network temperature and a lower LHD will result in higher thermal losses. Heating-dominant cluster sites usually have a higher LHD than the cooling-dominant clusters; for example, the LHD of the ExH-dominated cluster reaches around 10 MWh/m/y compared to 3 MWh/m/y for the CH clusters. With respect to TN temperature, Figure 4 shows that, in the LTTN scenario, the CH

clusters experience approximately 11% loss of the total network heating demand compared to around 4% in the ExH clusters. Notably, the heat loss for the CH cluster in the LTTN operation condition was nearly 4 times greater than in the U-LTTN operating scenario (11% to 3%, respectively). However, in the SMTN operation scenario, the network temperature is alternated between the LTTN and U-LTTN conditions to optimize electricity usage, which enables comparable thermal losses to the U-LTTN cases (i.e., the ExH clusters exhibit thermal losses of over 4% in the LTTN operation case compared to around 1% and 2% in the U-LTTN and SMTN cases, respectively).

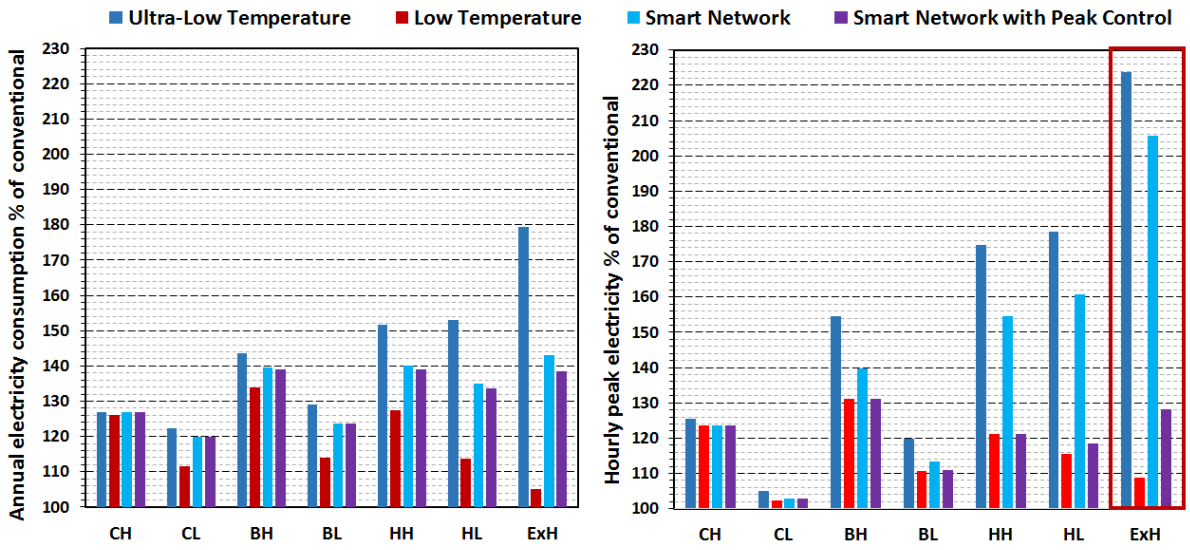

Figure 4-5: Comparison of the annual electricity consumption percentage of the conventional system (left) and peak electricity (right) for different network operation scenarios for an average cluster from each of the 7 categories.

Figure 4-5 presents the impact of the TN temperature operation schedule on the annual electricity consumption and hourly peak demand of each cluster category (results are presented for the average cluster load profile for each category). The impact is shown as the percentage of electrical usage above the BAU case (100%). This extra usage is due to EoH and energy sharing via the ETS heat pumps. Figure 4-5 also shows that the LTTN condition has the lowest impact on electricity consumption and peak in all categories. As the usage of RHP only depends on the heat rejected

from process cooling, the degree of concurrence between cooling and heating will be directly related to electricity consumption and peak in the LTTN case as the case in the BH category (34% consumption and 31% peak increase) and very low impact in the ExH category (5% consumption and 9% peak increase). Although the LTTN condition has the lowest impact on the electricity consumption and peak demand of the clusters, it does not allow for EoH during off-peak hours and it has the highest heat energy loss of the four scenarios. In contrast, the U-LTTN operation scenario has the highest ability to harvest waste heat from the buildings while suffering minimal network losses. Figure 4-5 clearly illustrates the high electrical impact of operating at an ultra-low temperature year round, especially for heating-dominated clusters (dark blue bars). As shown in Figure 4-5 the electricity consumption and peak increased by 80% and 123% higher than the BAU peak in the ExH cluster. This operating scenario increases the electricity consumption at peak and off-peak periods. Unfortunately, increasing electricity consumption during peak periods may raise a significant challenge to the electrical grid, potentially leading to a rise in GHG emissions and operating costs. By using the smart network operation schedule, the TN is set to operate at an ultra-low temperature of 20^{o}C during off-peak periods to maximize the use of clean electricity resources on the grid, and at 70^{o}C during on-peak hours when the central electricity grid employs marginal peak natural gas generators. While this schedule shifts most of the increase in the electrical consumption to clean grid periods in order to harvest the curtailed grid electricity, it also increases the cluster peak demand (light blue). Figure 4-5 shows large peak increases, especially in the heating-dominated clusters, with a 60% increase in the HL clusters and more than double that for the ExH clusters, which is highlighted by the red rectangle. This increase in peak demand at the site either results in large infrastructure costs related to the electricity distribution network or the occupation of a significant share of electrical storage. Smart network operation with peak control

provides the advantage of energy harvesting while minimizing the impact on the electricity peak demand. This is achieved by controlling the TN temperature to increase the network temperature during the site's annual peak electrical demand period to avoid increasing the network's annual peak electricity demand (Purple). Figure 4-6 shows the percentage change in the electricity peak of each of the 1139 clusters operating under the four different TN scenarios in relation to the BAU (100%) condition. The figure clearly shows that, in the U-LTTN scenario, the peak rises to more than twice the BAU peak in around 600 clusters. In contrast, the clusters in the LTTN condition typically showed an increase of less than 20% over the BAU level, with fewer than 10 clusters showing a 40% increase. Although the peak electricity in the SMTN operating scenario is lower than in the LTTN condition for the majority of the clusters, their peak electricity is still relatively high, as around 35% of the clusters (400 clusters) peaked at levels more than double the BAU peak. On the other hand, the SMTN with peak control scenario allows the peak electricity to be set to any desired maximum demand above the BAU level by controlling the network temperature.

A comparison of the four different scenarios with respect to electricity consumption on an hourly resolution for the ExH cluster is presented in Appendix C.

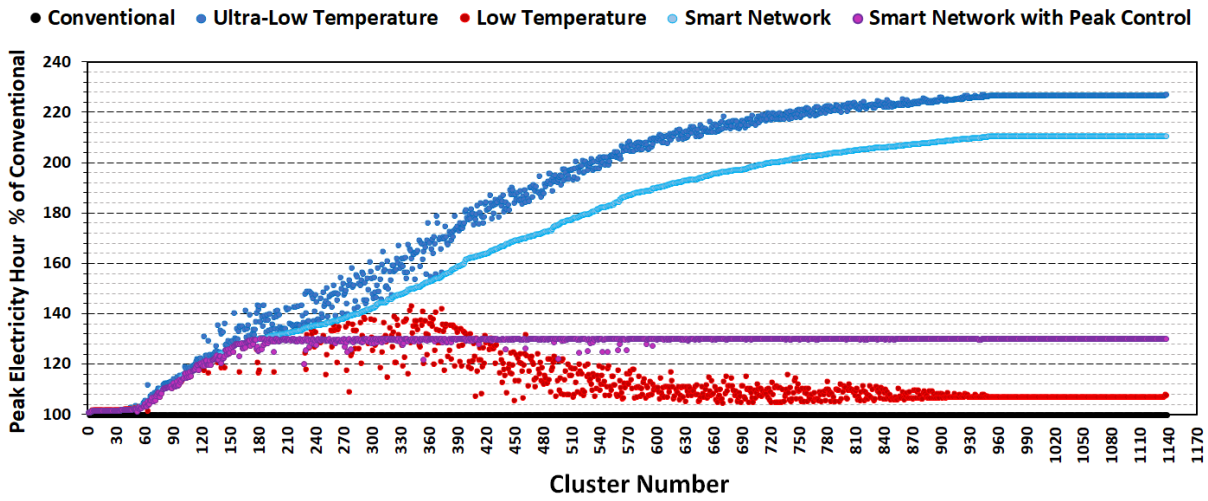

Figure 4-6: Percent change in the electricity peak of each cluster compared to the BAU (100%) for the 1139 clusters operating under the different TN operation scenarios.

The results indicated that the SMTN with the peak control schedule provides the most benefits for the thermal and electrical networks, in addition to enhancing the network's harvesting capability in favorable times, while also minimizing the increase in electricity peak demand from EoH and sharing heat pumps. Because of the flexibility in this scenario, most of these sites may not require battery storage systems, resulting in considerable cost savings.

4.3.1.1. Impact of the TN temperature operation schedule on the total annual GHG emissions for sharing and EoH

Figure 4-7 illustrates the impact of the network temperature operation schedule on the collective annual GHG emissions of the clusters in each load category. As noted earlier, in 2017 the grid utilized natural gas for electricity generation for approximately 38% of the year's hours, whereas in 2016 gas was used to generate electricity for almost 93% of the year's hours. The results are presented with respect to the total GHG emissions (per 1000 tonnes) for all 1139 clusters in all load categories for the different TN operation schedules and as a percentage compared to the BAU case. The network is considered a heat source for the BHP thus the amount of heating required

from the TN is determined by performing an energy balance on the BHP ($Q_H = Q_{TN} + W_{BHP}$). The network heating requirements (i.e., the thermal energy required to maintain the network temperature) are supplied through sharing and by the EMC resources. When the heat rejected from process cooling is high enough to cover the network needs, the network heat (Q_{TN}) can be met by the harvested heat. However, in the case of low heat rejection from cooling processes, as in the heating dominant sites, most of the Q_{TN} is covered by the EMC. Furthermore, as the harvesting potential in these scenarios is very low, the GHG reduction benefits associated with the use of heat pumps for EoH are lost during peak periods. Indeed, cases with low heat rejection from cooling processes are characterized by higher GHG emissions, as the incremental electricity required to power the heat pump is produced by natural gas generators on the grid which are around half as efficient as boilers (42% to 85%, respectively). In 2017, only 35% of the hours were peak hours, which is one of the main reasons for the good reduction in GHG emissions observed for the U-LTTN scenario for cooling and balanced sites, as well as for high concurrent heating sites. On the other hand, most of the 2016 hours were comprised of peak hours, which means that the grid natural gas generators were operational most of the year. In this case, operating the network at a low temperature and electrifying heating increased GHG emissions, as the incremental electricity is produced by a low efficiency natural gas generator. This impact decreases in clusters that attain a large share of their heat from sharing.

Conversely, the low-temperature network reaps very low benefits from the electrification of heating. This operating scenario realizes more reductions in GHG emissions when there are more peak hours, as was the case in 2016. Although LTTN has a slight effect on peak periods by avoiding EoH, it loses the benefits of EoH during off-peak periods when electricity is generated from carbon-free resources (curtailment).

The smart network operation scenario provides greater GHG reduction compared to the two lower-temperature scenarios, as it benefits from the electrification heating during off-peak periods by implementing ultra-low temperature operation and increasing the network temperature during peak hours, thus not allowing EoH during these periods. As shown in Figure 4-5 and Figure C 4-1 the peak electricity consumption more than doubled due to the EoH, especially in the Extra HD clusters (40% of the clusters). The smart network with peak control prevents this from happening by limiting EoH during peak hours. Indeed, the smart network with peak control's impact on GHG emissions is within 1-2% of the smart network operating scenario's, as high peak hours occur relatively infrequently. When the grid's use of gas peak generators is moderate (2017), the harvesting and sharing of rejected waste heat from cooling systems has a large impact on the GHG emissions for all types of load category clusters. The SMTN and the SMTN with peak control operating schedules enabled the greatest reduction in GHG emissions. The site electricity peak control schedule reduces EoH at specific times to prevent a large increase in the site's peak electricity usage. During times of reduced EoH, the SMTN with peak control schedule depends on the use of gas boilers to overcome the difference in heating resources, which is the reason for the slight increase in GHG emissions observed with this schedule compared to the SMTN without site peak control schedule.

If the electricity grid's utilization of natural gas generators is high most of the time, as in the case of 2016, the harvesting and sharing of rejected heat from cooling processes will have an insignificant impact on GHG emissions. The insignificant impact on GHG emissions in such cases is due to the fact that the ETS heat pumps require additional electricity to raise the low-temperature residual heat that is harvested and shared between buildings. This added demand represents a new incremental load, which in 2016 was likely predominantly satisfied via the use of peaking natural

gas generators as marginal generators. Figure 4-5, 4-6, and Figure C 4-1 clearly indicate that the U-LTTN operation schedule has the highest electricity demand from the electrification of heating. The results indicate that the SMNT with site peak control approach offers the greatest benefits with respect to harvesting ability, providing EoH at favorable times, and avoiding the huge increases in site electricity consumption and peak inherent to the other strategies. Significantly, the SMNT with site peak control approach also offers the highest reduction in GHG emissions.

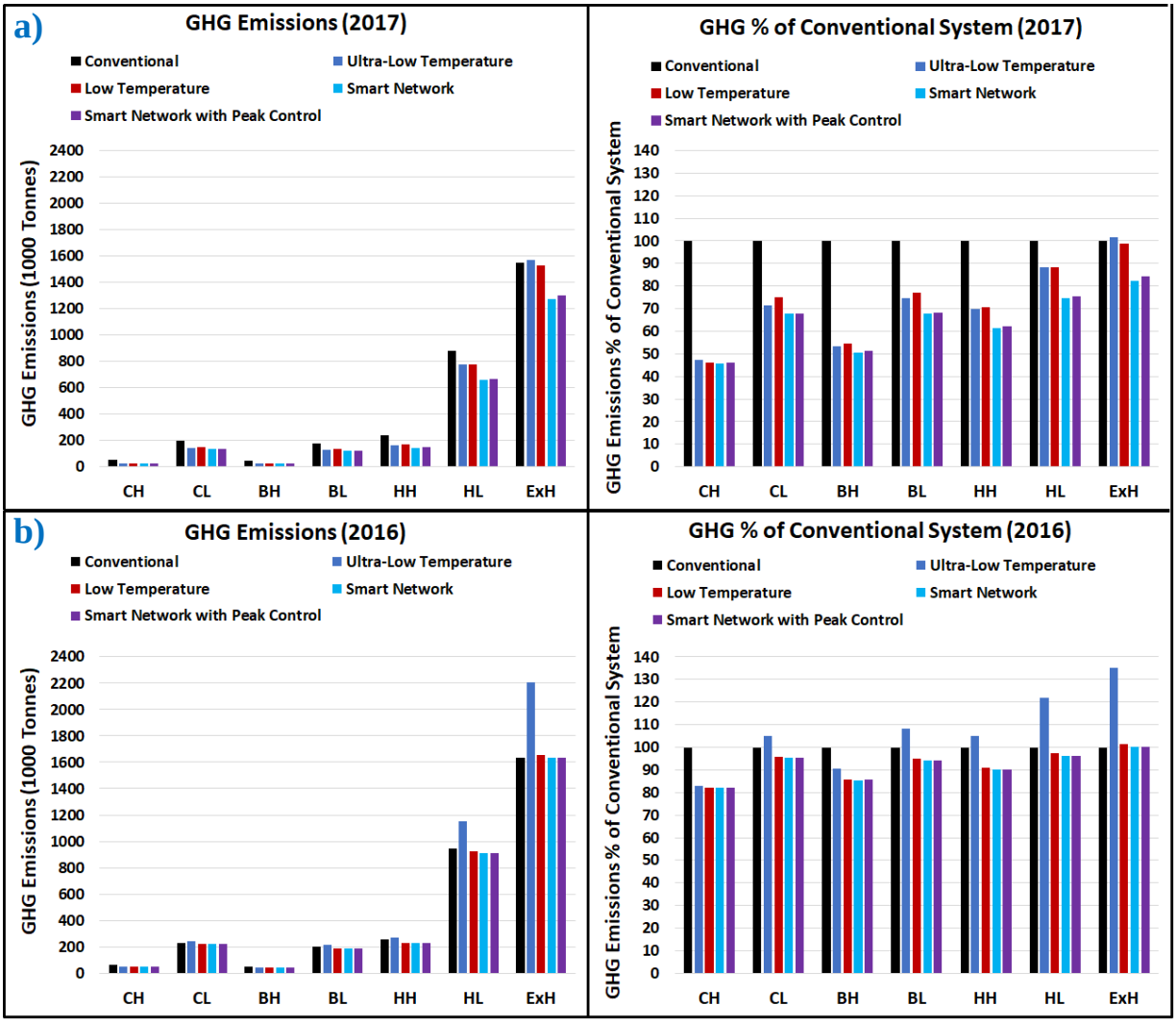

Figure 4-7: Summation of GHG emissions in tonnes for each cluster category and percentage of BAU emissions in two different years of operation, with sharing and EoH. a) 2017, b) 2016.

4.3.2. Impacts of the integration of combined heat and power system

In the previous section, the sharing of waste heat from the cooling process between site buildings was presented as the first resource for serving heating demands, with traditional natural gas boilers supplying the remaining network thermal demand. This section demonstrates the effects of utilizing CHP systems to displace natural gas generators at the site with the aim of harvesting a secondary source of residual heat. This approach is investigated using the SMNT with

site peak control operating schedule, as the results presented in the previous section identified it as offering the greatest number of benefits.

The results presented in this section include the hourly electricity consumption and the energy resources that are used to meet that consumption, as well as their impact on heating requirements and GHG emissions. These results reflect the data for an average cluster of 902 heating-dominant sites, an average cluster of 140 cooling-dominated sites, and an average cluster of 95 balanced sites.

4.3.2.1. Impacts of combined heat and power in an average heating-dominant cluster

The hourly electricity requirements for the average heating-dominant cluster are presented in Figure 4-8a for both the BAU system (black) and the SMNT with site peak control schedule after energy harvesting by the ETS heat pumps (purple). The average heating-dominated cluster has a peak electricity demand of 1.5MWh in the summer and 1.9MWh in the winter. The energy resources employed to service this load are presented on an hourly basis in Figure 4-8b (stack-up curves). These resources include imported electricity from the grid during off-peak hours (carbon-free resources). The dark blue represents the BAU system's electricity consumption, while the light blue represents the extra power used to run the ETS heat pumps during off-peak hours. During peak periods, the electricity required from the grid (black) is almost negligible, as most of the site electrical demands are met by the CHP, which is presented by the orange color (Figure 4-8b). This on-site electricity generation is made possible by the heat generated by the CHP, which is also used to meet the buildings' heating requirements. Any surplus electricity that is generated is exported to the grid at peak times (light green). The dark green area represents the range of electricity the CHP can export to the grid without limiting the CHP electricity production. Since

the hourly basis results for the whole year are too dense to present effectively, the results for three-week periods from different seasons (winter, shoulder, and summer) are presented in Figure 4-10. For the winter period, there are many peak hours wherein the grid meets demand via gas-fired generators; however, these periods involve lower gas consumption compared to the summer period, which causes the CHP to run at partial load most of the time to reduce the electricity exported to the grid and to avoid increasing the GHG emissions from the grid. As shown in Figure 4-10a (winter period), the dark green sections are larger than the light green sections. In the off-peak hours, the site depends on the clean grid for electricity (blue). For the shoulder season period (spring/fall; Figure 4-10b), the grid is carbon-free almost all the time, which means the demand is serviced by electricity imported from the grid and the CHP is usually off. For the summer period (Figure 4-10c), the grid has more peak hours and a larger capacity compared to the winter period. Thus, the CHP is in full load most of the time to serve the site and export as much electricity as possible to the grid (the light green area is larger than the dark green area).

A major difference between running the CHP in the summer and winter is the concurrent heat demand. As shown in Figure 4-9, there is a large heat demand during the winter period, so any heat produced by the CHP will be used immediately or diverted to short-term storage. However, the extra heat produced by the CHP during the summer (green) period requires seasonal storage so it can be used during the winter period, as the heating demand is low in the summer period (Figure 4-9).

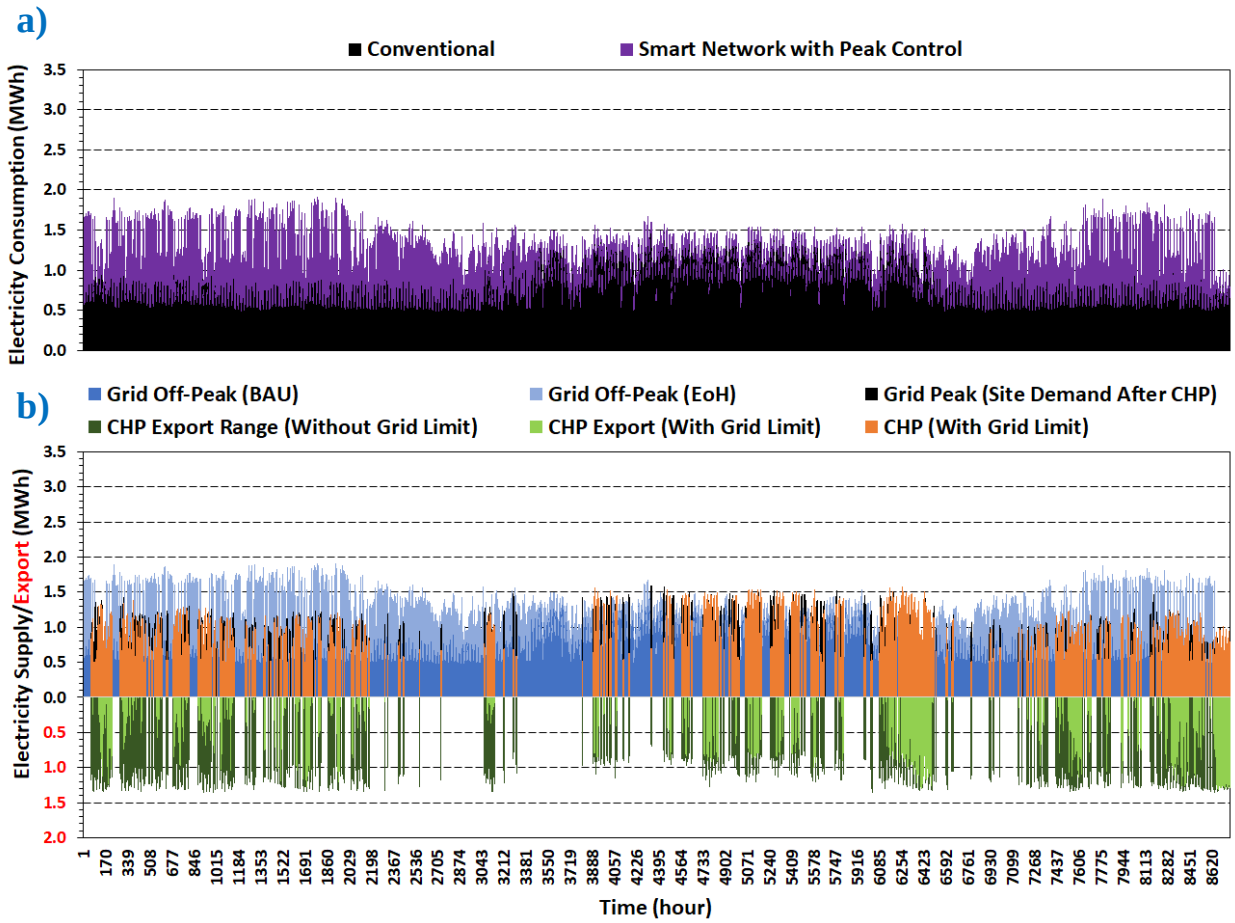

Figure 4-8: (a) Hourly electricity consumption in megawatts and (b) electricity supplied from and exported to the grid for average heating-dominated cluster utilizing a smart network with peak control and conventional systems.

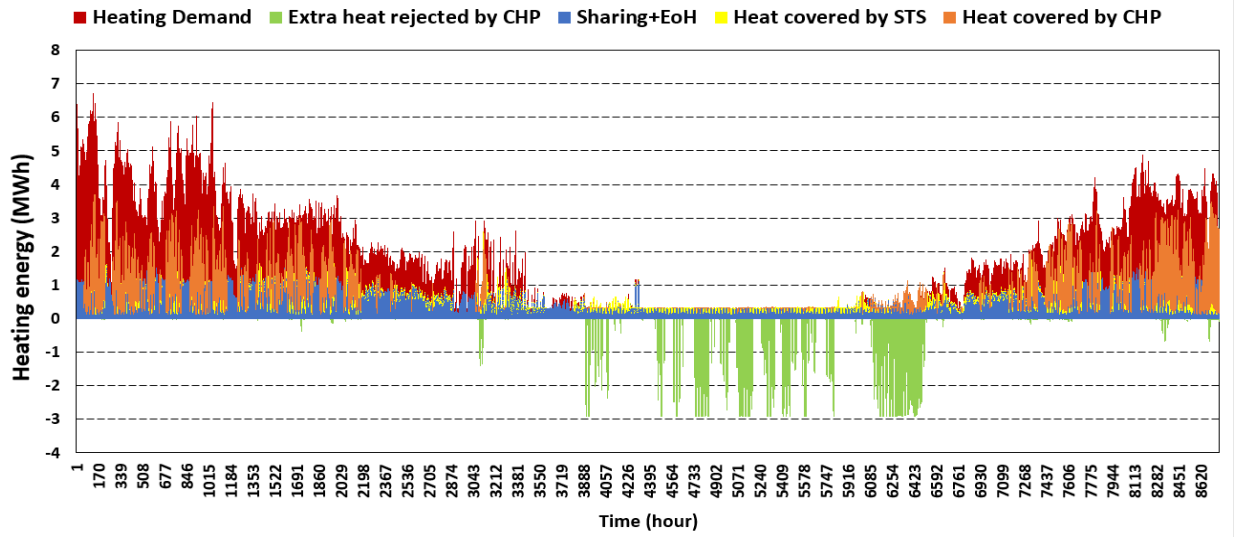

Figure 4-9: Average heating-dominant cluster heating energy consumption covered by different resources and extra heat rejection from CHP.

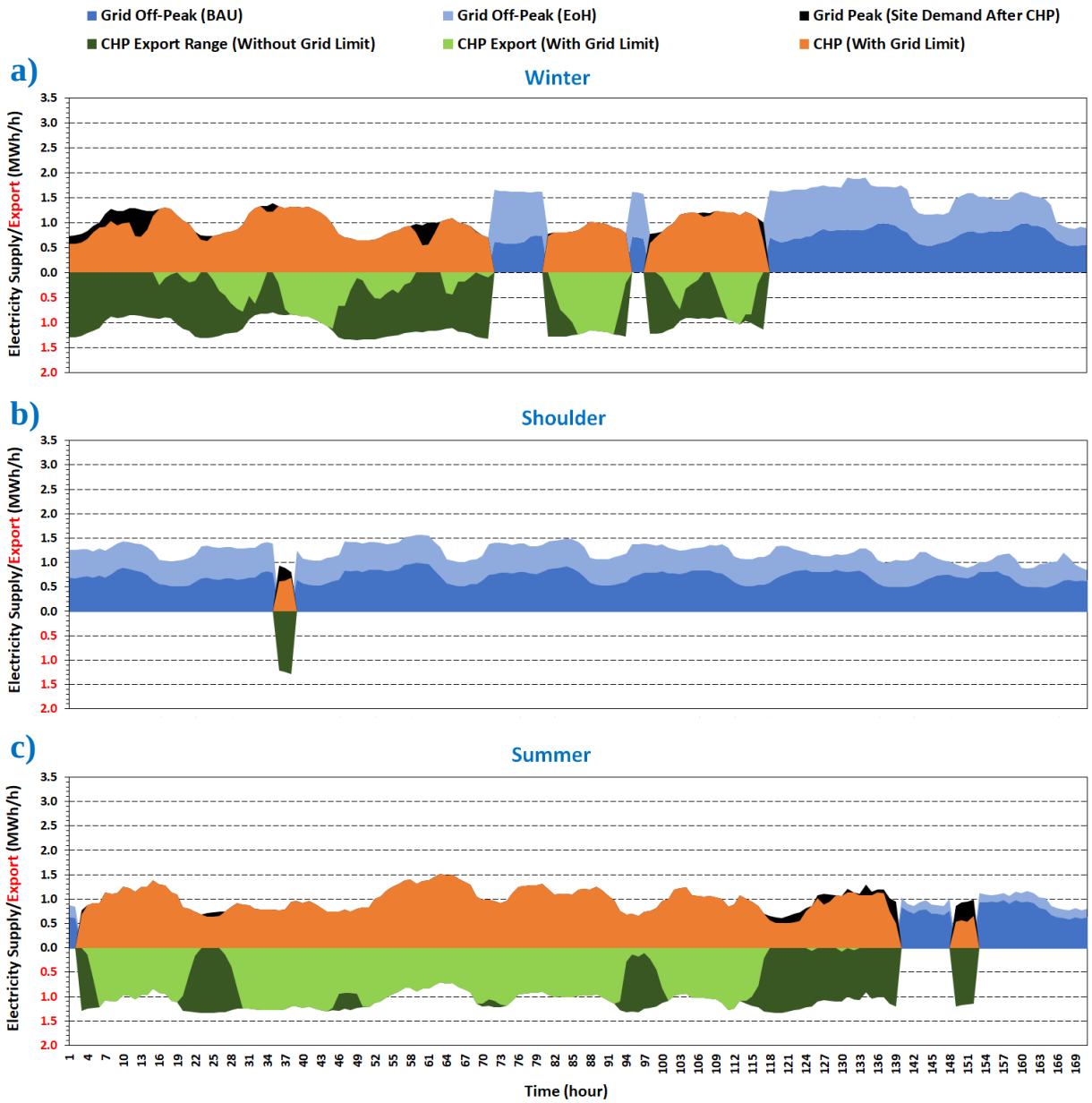

Figure 4-10: Hourly electricity supply and export from different resources for an average heating-dominant cluster over a week for: a) winter period, b) shoulder period with harvesting only (no CHP), and c) summer period.

4.3.2.2. Impacts of combined heat and power in an average balanced-load cluster

The hourly electricity requirements for the average balanced-load cluster are presented in Figure 4-11a for both the conventional BAU system and the smart network with peak control

system (purple). The balanced cluster consumes more electricity than heating-dominant sites due to its large cooling demand. As shown in Figure 4-11a, the average balanced cluster's peak electricity ranges from 2.5 to 3 MWh, which is almost double the peak demand of the average heating-dominated cluster. The results of integrating the CHP to help service this load are presented in Figure 4-11b. Since balanced clusters have relatively smaller heating requirements compared to heating-dominated sites, they typically employ smaller CHPs to avoid wasting the heat they generate. In addition, the use of smaller CHPs results in significantly higher levels of electricity being imported from the grid during peak times (black) compared to the heating-dominated case. For this load category cluster, the CHP generates low levels of electricity during peak hours (orange) and no export electricity is available (no green sections). The week's zoom-in presentations (Figure 4-13) clearly show that the limited CHP size requires more electricity to be imported from the grid during peak periods (black sections).

As shown in Figure 4-12 the heating demand in the winter period is almost fully covered by energy harvested from different resources, such as sharing with EoH and CHP with aid of STS. This results in extra heat produced by the CHP in summer (green) that will go unused, even with seasonal thermal storage.

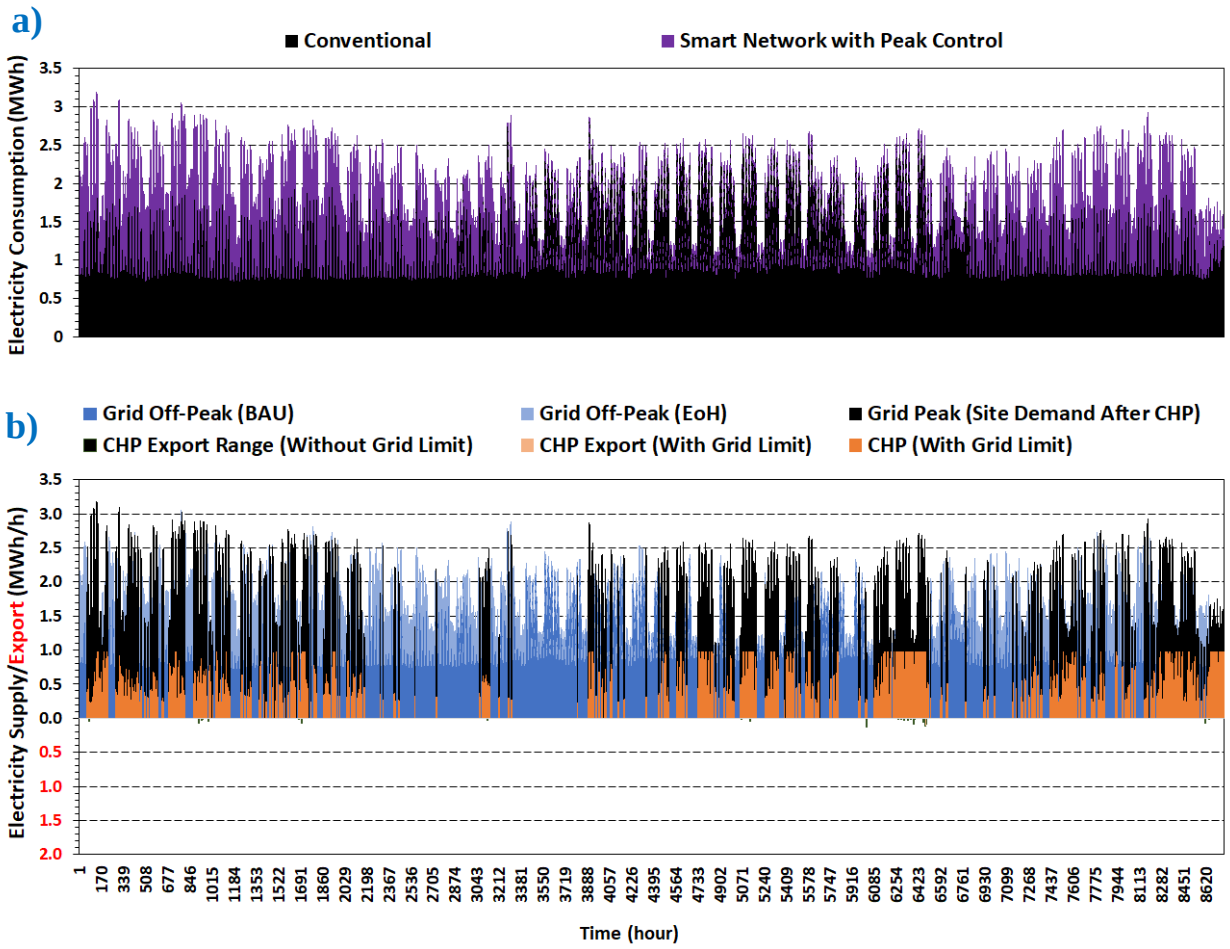

Figure 4-11: (a) Hourly electricity consumption in megawatts and (b) electricity supplied from and exported to the grid for an average balanced cluster utilizing a smart network with peak control and conventional systems

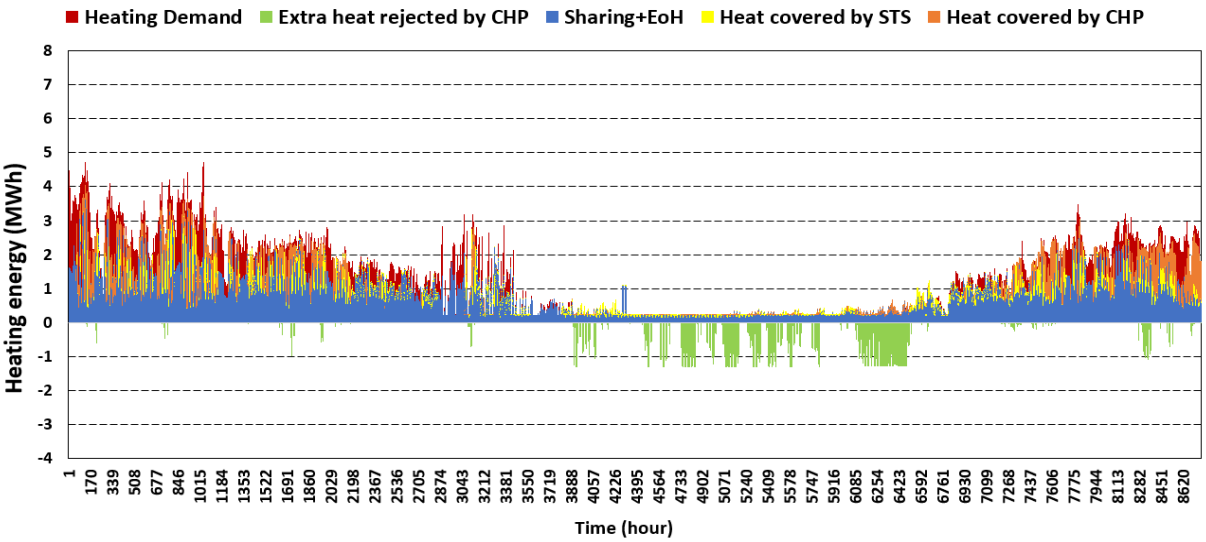

Figure 4-12: Average balanced cluster heating energy consumption provided by different resources and extra heat rejected by the CHP.

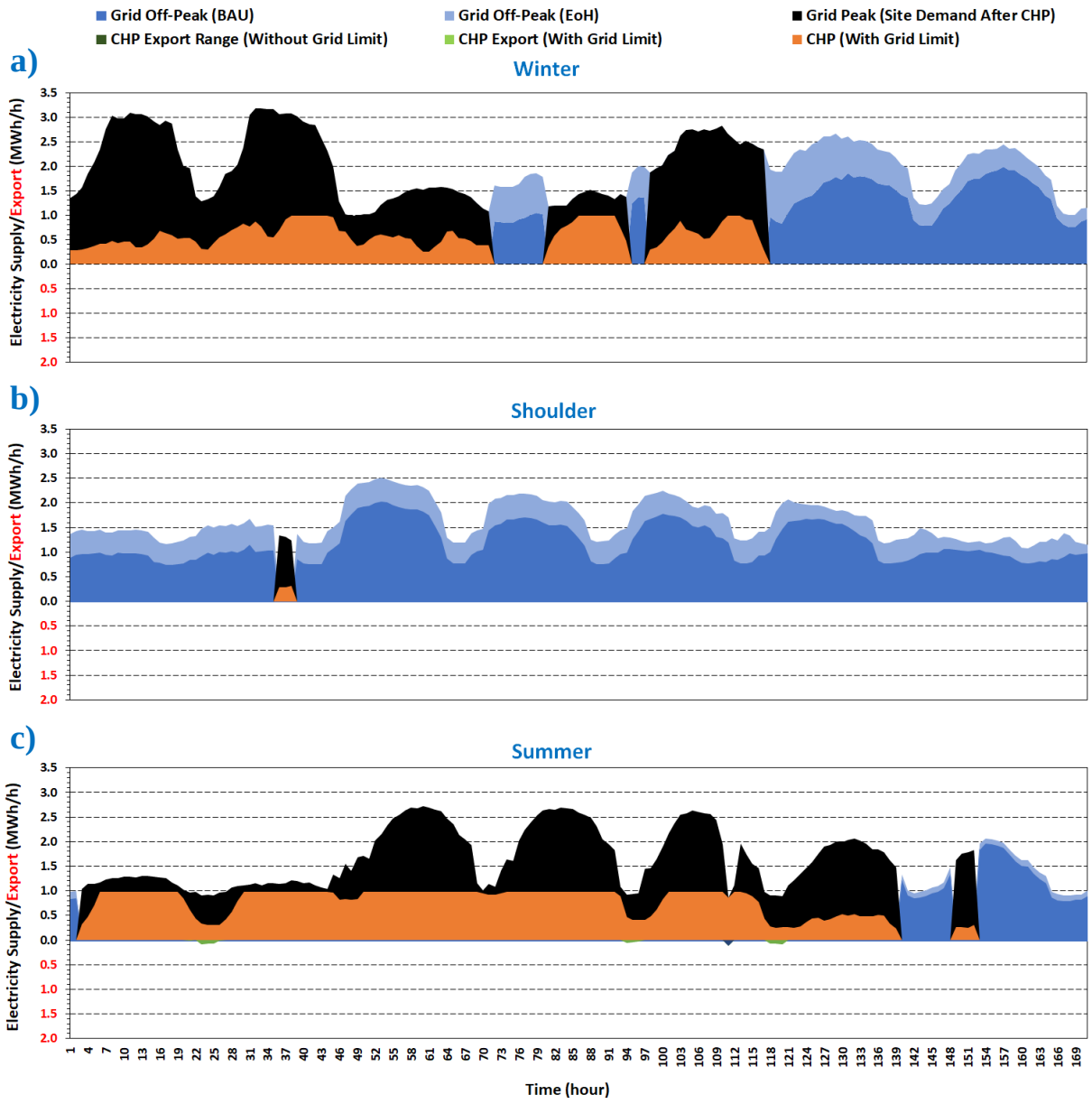

Figure 4-13: Hourly electricity supply and export from different resources for an average balanced cluster for: a) the winter period, b) the shoulder period with harvesting only (no CHP), c) the summer period.

4.3.2.3. Impacts of combined heat and power in an average cooling-dominant cluster

The hourly electricity requirements of an average cooling-dominant cluster are presented in Figure 4-14a. This cluster has a relatively larger cooling demand compared to the heating-dominant site, which results in electricity demand of about 2.5 to 3 MWh. This demand is nearly

double the peak demand in the average heating-dominated site and similar to that of the balanced site. Since cooling-dominated clusters have very low heating demands, they use smaller CHPs compared to the heating-dominant and balanced load clusters to minimize waste heat. Figure 4-14b shows that the majority of the electricity is imported from the grid (black) during peak periods. This explains why the impact of the SMTN system with a CHP is relatively small in this load cluster. As shown in Figure 4-15, the heating demand in cooling-dominant clusters is mostly covered by sharing and there is no need for thermal storage.

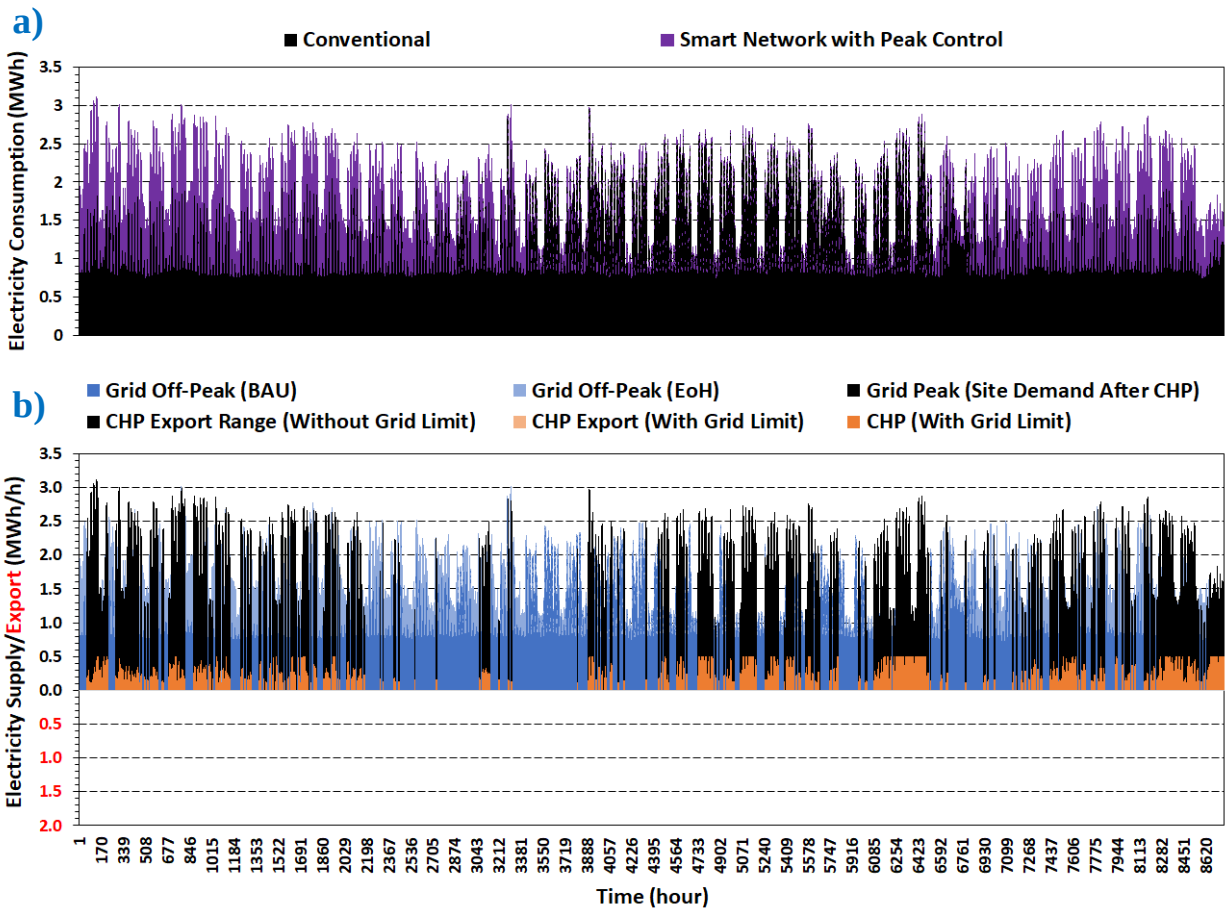

Figure 4-14: (a) Hourly electricity consumption in megawatts and (b) electricity supplied from and exported to the grid for average cooling-dominated cluster utilizing a smart network with peak control and conventional systems

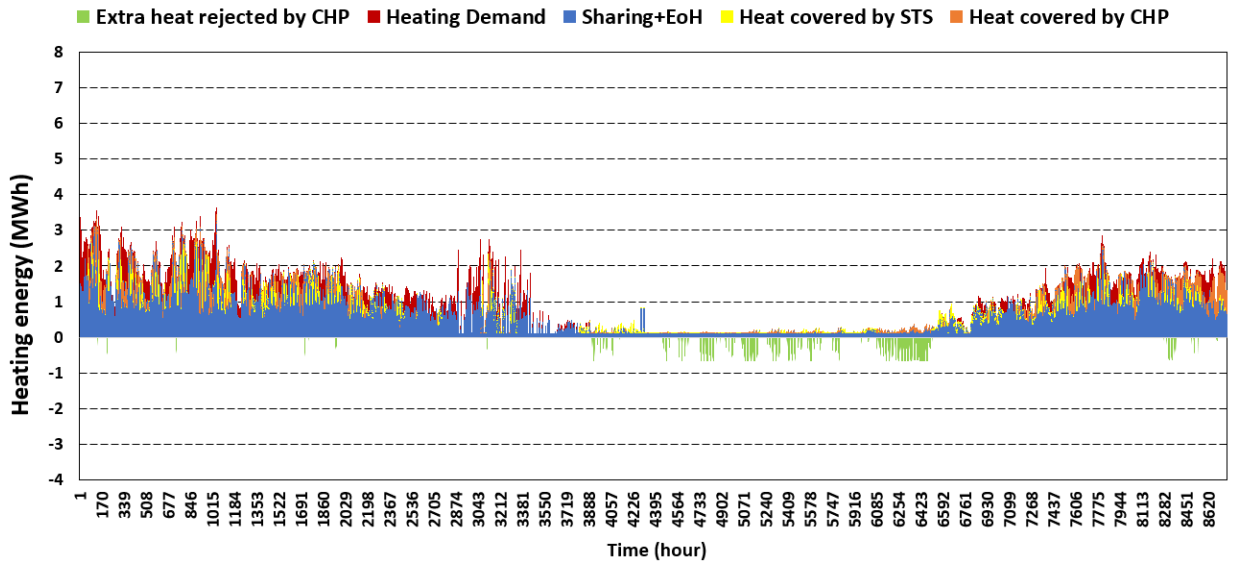

Figure 4-15: Average cooling-dominant cluster heating energy consumption provided by different resources and extra heat rejected by the CHP.

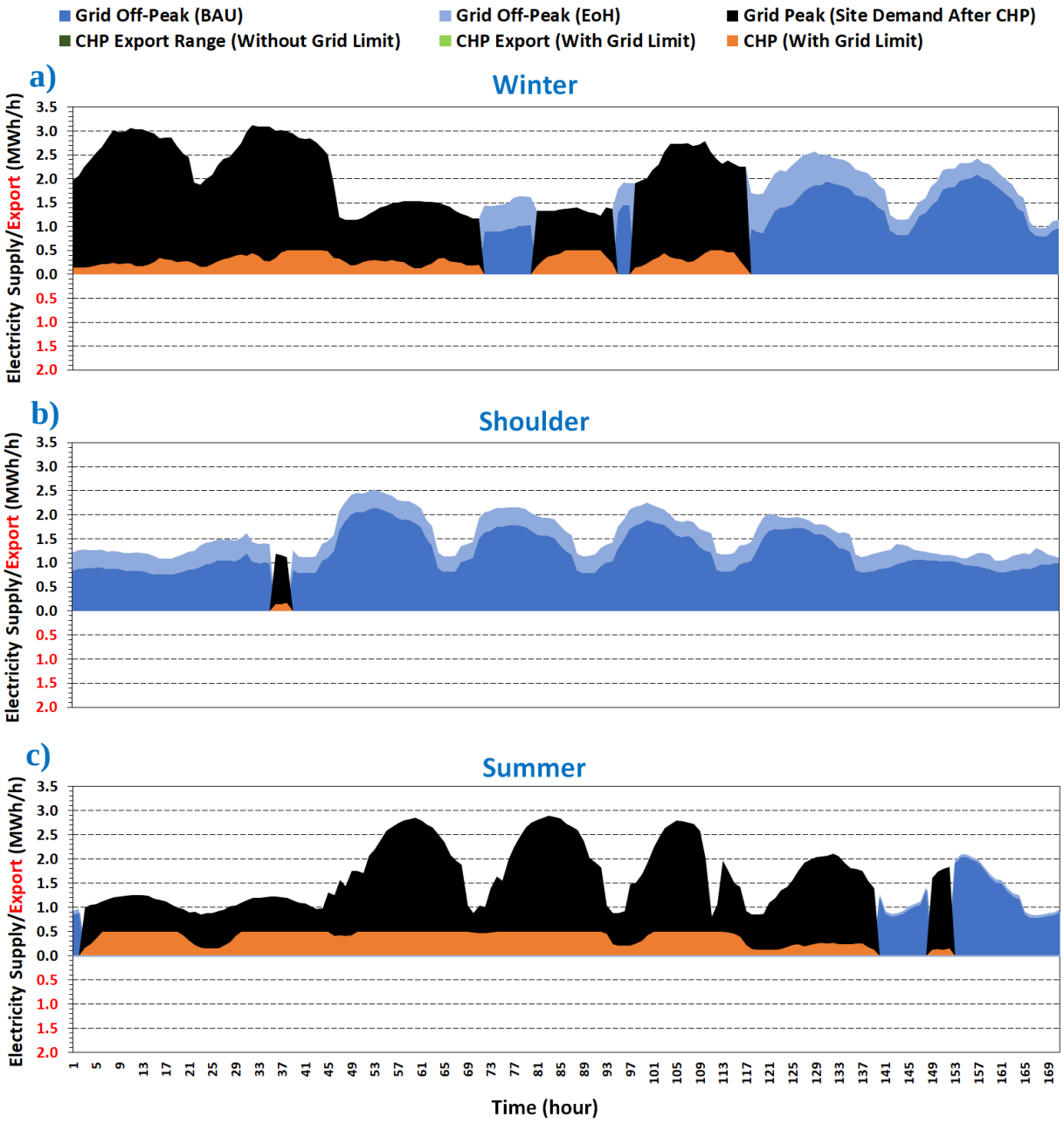

Figure 4-16: Hourly electricity supply and export from different resources for an average cooling-dominant cluster during: a) the winter period, b) the shoulder period with harvesting only (no CHP), c) the summer period.

It can be concluded that, for the majority of heating-dominated clusters, it is better to employ the SMTN system with peak control and CHP to service their high heating demands, although this approach requires more thermal storage, especially seasonal storage. For the majority of balanced and/or cooling-dominated clusters, the need for CHP is very low as there is a large amount of

excess heat from the cooling systems. Using thermal storage systems to harvest the excess heat rejection from cooling during low heating demand and use it to serve heating demands during high demand periods could eliminate the need for the CHP. The focus in balanced and cooling dominated sites shall be targeted toward the cooling demands. Thus, it is better to implement more carbon-free resources on-site that produce electricity but are not primarily associated with heating. Examples of such resources include wind, hydro, and solar PV panels to serve the cooling demand. The next section examines how the GHG emissions of the different clusters are impacted by the allowable minimum CHP efficiency, the electricity grid's different use of peak gas generators, and the use of thermal storage.

4.3.2.4. Impacts of changing the maximum allowable CHP system efficiency

In the previous section, the impact of adding a CHP with a minimum allowable combined heat and power efficiency of 65% was illustrated. This constraint results in the use of a specific CHP capacity to avoid wasting residual heat. It is important to add a sensitivity analysis for this constraint, as the regulations from the grid operator might change from one location to another. While relaxing this constraint by reducing the efficiency to 60% or 55% will result in a CHP with a larger capacity (about 2.2 GW), the CHP will inevitably only run at partial load due to the other constraints in the study related to its sizing. However, increasing this constraint by raising the minimum efficiency to 75% and 80% will enable the use of a smaller-capacity CHP (less than 0.25 GW), as shown on the right side of Figure 4-17. The GHG emissions reduction for the different CHP overall annual efficiencies is presented on the left side of Figure 4-17. As can be seen on the left side of Figure 4-17, there is no significant change in GHG emissions reductions in the case of lower allowable efficiencies; however, a significant change of almost 50% can be observed

between the lower efficiencies and the 65% and 80% cases. The results also show that thermal storage plays an important role in increasing the GHG emissions reductions in most cases, but has limited impact on smaller CHPs, as in the case of the CHPs with 75% and 80% minimum allowable efficiencies.

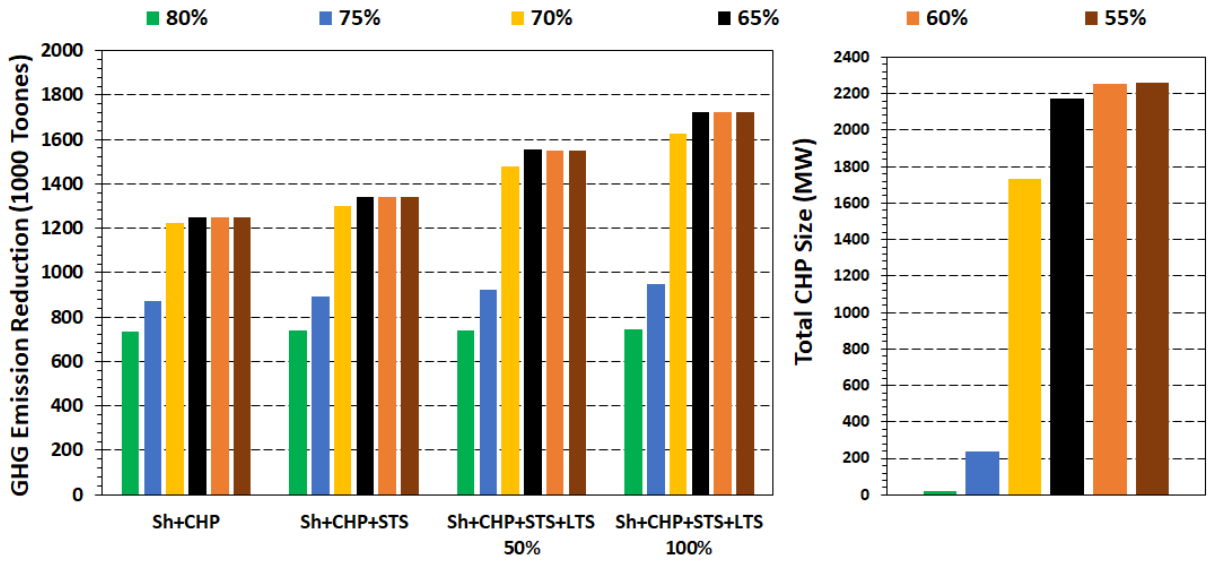

Figure 4-17: GHG emissions with and without thermal energy storage for different minimum overall CHPs efficiencies (left) and overall CHP sizes (right) for 1139 clusters in Ontario.

4.3.2.5. Impacts of different combined heat and power operations for different grid operating schedules

As the CHP is operated to displace the grid's natural gas generators, CHP electricity production shall not exceed the grid's natural gas electricity production in order to avoid displacing carbon-free electrical resources on the grid. The operation of the CHP is dependent on the operating hours of the grid's natural gas generators: a high number of operating hours results in more CHP utilization and less dependency on EoH, whereas a low number of operating hours has the reverse effect. To illustrate the impact of thermal storage on the GHG emissions reductions achievable by the integrated energy systems, the GHG emissions reductions enabled by the different systems were evaluated for all the clusters. Figure 4-18 shows the reduction in GHG

emissions enabled via sharing in conjunction with EoH, by incorporating CHP with STS, and by using LTS for two different years: 2017 (right side) and 2016 (left side). The GHG emissions were calculated based on a case wherein the maximum accumulated hourly CHP electricity production for the 1139 sites is limited to the grid's natural gas generation capacity. Furthermore, to approximate the emission reduction that can be achieved in grids with substantial natural gas output, GHG emissions were computed with no restriction on CHP generation, assuming that the system produces large amounts of natural-gas-generated electricity during peak hours.

In 2017, around 50% of the emissions savings were achieved via sharing and EoH; this percentage was much lower in 2016 as shown in Figure 4-18. The reason for this discrepancy is that, in 2016, only 10% of the annual hours were off-peak with less than half the curtailment compared to 2017, while the NG generators run 90% of the time with double the NG electricity generation. Thus, CHPs ran 90% of the time in 2016 following the grid's natural gas electricity operating schedule. Figure 4-18 shows that the reduction in GHG emissions was greater in 2016 than in 2017, due to the capture of additional high-grade heat from CHP. In 2016, the operation of the CHP without production limits can represent grids with large electricity generation from natural gas. Figure 4-18 (left) shows that, in 2017, the GHG emissions savings were around 55% with approximately 25% resulting from sharing and EoH, 17% provided from CHP with STS, and 17.5% via LTS (12% at 50% efficiency and another 5.5% at 100% efficiency). The results also show a case wherein natural-gas-based electricity production is high during peak hours. Here, the constraint on CHP production no longer affects GHG emission savings. In 2016, the reduction in GHG emissions was mostly dependent on the CHP for the reasons mentioned above, only reaching around 68% with CHP production constraints and approximately 72% in the case of no production limits. These results indicate that using distributed CHPs to displace the grid natural gas generators will enable

significant reductions in GHG emissions in cities where fossil fuel energy sources comprise a large share of the grid's resources. However, in cities where renewable energy accounts for a large share of the grid's resources, dependency on CHPs should be decreased and replaced by EoH via different available technologies.

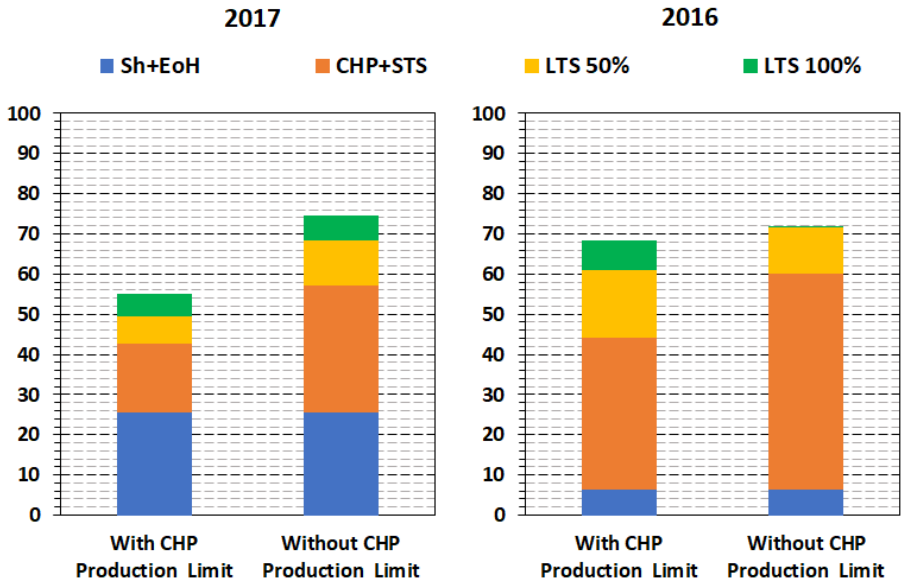

Figure 4-18: CHP emissions reductions from different resources with and without CHP production limitations for the years 2017 (left) and 2016 (right).

4.3.3. Comparison of GHG emission reduction potentials with prior work

This section presents the potential of GHG emissions reduction from the current system compared to previous case studies that employed different technologies and operation conditions. Table 4-2 shows the GHG emission reduction for different case studies in the literature compared to the current work.

Song et. al. [44] investigated the use of an absorption heat pump to heat an LTTN in a community center, resulting in a 25% reduction in GHG emissions. In a medium-sized neighborhood of 137 buildings, Ameri et al. [45] evaluated the use of CHP as a heat supply to an LTTN, which resulted in a 35% decrease in GHG emissions. According to [46] the employment of GSHP, industrial waste heat, and solar in a district heating network can reduce GHG emissions by around 44%. Each of these studies investigated the employment of different types of technology. On the other hand, Wirtz combined a variety of resources with an ultra-low temperature thermal network, resulting in a 56% reduction in GHG emissions. The present system makes use of a range of

resources, including on-site CHP and grid renewables. The recent study offered a novel system operation and technology that may reduce GHG emissions by up to 73% for a fleet of 1139 small-scale sites, which is more than all previous trials. The key reason for the greater GHG emissions reduction than [7] is that the system is connected to the grid, allowing for CHP export and hence more heat to be captured to meet site needs. Additionally, the TN operating scenario proposed in the current work "SMTN with peak control" provides great flexibility to the electrical grid while maintaining the system feasibility via controlling the site's peak demand.

Table 4-2: Comparison of different prior case studies and present work.

Study	Thermal network operating scenario	Thermal network size	Employed technology	GHG emissions reduction % of the BAU emissions
Song et al. [44]	LTTN	Small-scale (Business center)	Absorption heat pump with low temperature geothermal water, natural gas boiler	25%
Ameri et al. [45]	LTTN	Medium-scale (137 buildings)	CHP, natural gas boiler	35%
Abdurafiko et al. [46]	LTTN	City scale (District)	Solar photovoltaics (PV), industrial waste, ground source heat pumps	44%
Wirtz et al. [7]	Bidirectional U-LTTN	Small scale (17 buildings)	CHP, solar photovoltaics (PV), electric boiler, natural gas boiler, low-grade cooling processes residual heat, thermal energy storage systems, battery storage	56%
Present Work	SMTN with peak control	Multiple small-scale (1139 sites include14832 buildings)	micro-CHP, low-grade cooling processes residual heat, connected to a mixed electrical grid.	73%

4.4. Conclusion

This study demonstrates that the operating temperature of the heating distribution network in an integrated energy system significantly impacts its performance and greenhouse gas emissions. To achieve these results, four thermal distribution network operating scenarios were modeled for various community energy profiles, namely: a low-temperature network (fourth-generation); an ultra-low temperature network (fifth generation); a smart network (ICE-Harvest), which is a hybrid system comprising elements of the low and ultra-low systems; and a new operating scenario (smart network with peak control) wherein the peak electricity demand is controlled by changing the network temperature. The findings of this study enable the following conclusions:

Ultra-low temperature thermal network (20^{o}C)

- This case enables the most electrification of heating and the lowest use of gas-fired boilers; it also causes the site electricity peak to more than double for heating-dominant sites.
- Large emissions savings in sites with high simultaneous cooling and heating, such as high concurrent balanced and high concurrent cooling-dominant clusters and with grids characterized by low levels of natural-gas-generation resources and peak hours, as well as high levels of carbon-free electricity generation.
- Can increase the emissions in heating-dominant clusters with grids with high peaking natural gas generator running hours.
- Large electrification of heating during peak and off-peak hours allows the system to benefit from the curtailed electricity resources from the grid. However, the increased electricity demand during peak periods forces the grid to increase electricity generation via natural gas resources, which in turn increases emissions.

Low-temperature thermal network (70°C)

- This case features the lowest use of electrification of heating and the highest use of gas-fired boilers in integrated systems.
- Enables higher GHG emission savings compared to ultra-low temperature systems for sites with low simultaneous cooling and heating, such as low concurrent balanced and heating-dominant clusters, especially those connected to grids with low natural gas resources and high carbon-free electricity generation.
- Low increase in electricity consumption and peak demand, resulting in a low impact on the electricity grid and minor benefits from carbon-free resources curtailed from the grid.

Smart thermal network (70°C during peak and 20°C during off-peak)

- Balances the electricity grid by electrifying heating only during periods of surplus carbon-free electricity generation.
- Increases site electricity peak demand by more than double in heating-dominant sites, which may jeopardize the system's feasibility.
- Provides the greatest carbon emission savings compared to all other operating scenarios.

Smart thermal network with peak control (70°C during peak periods and varying between 20°C and 70°C during off-peak periods)

- Provides the most benefits for both thermal and electrical networks, as it offers good harvesting capability in favorable times and avoids a sizable increase in site electricity peak demand.
- Similar to the smart thermal network operating scenario, this system provides a good balance to the electricity grid by electrifying heating only during periods of surplus carbon-free electricity generation.

- Provides large emission savings that are only slightly lower compared to the smart thermal network operating scenario.

The integration of CHPs affords significant benefits, particularly for heating-dominant sites, especially those connected to grids where a large portion of electricity generation uses natural gas resources. The developed model was implemented on a fleet of 1139 sites with different energy profiles in Ontario, Canada. The results indicated that, for most of the heating-dominated clusters, it is better to employ the smart network with peak control and a CHP on site to serve these clusters' high heating demands, and that this approach further benefits from the use of thermal storage, especially seasonal storage. For the majority of balanced and cooling-dominated clusters, it is better to implement more carbon-free resources that produce electricity but are not associated with heat. Examples of such resources include wind, hydro, and solar photovoltaic panels.

The findings of this study also revealed that CHP size significantly affects carbon emission savings. The CHPs in this study were sized to achieve a minimum overall efficiency ranging between 55% and 80%, with results indicating a significant reduction of approximately 35% for the lower-efficiency ranges (55%-65%) in 2017 with 36% CHP operating hours. The savings nearly doubled in 2016 with 93% of CHP operational hours. In contrast, the greenhouse gas emission savings were very low in the high-efficiency range because the CHPs had to be sized very small to achieve these high efficiencies. Also, short- and long-term thermal storage played a critical role in harvesting residual CHP heat, thus further lowering carbon emissions. Indeed, approximately half the emission savings from CHP residual heat were achieved by short- and long-term thermal storage. In order to achieve net-zero carbon, future work should consider replacing the CHP with low-carbon electrothermal resources, such as micronuclear reactors and fuel cells. It is also recommended that future work investigate additional solutions for harvesting curtailed

electricity during shoulder seasons with low heating demands and moderate outdoor temperatures; such solutions may include the use of air source heat pumps with the aid of thermal storage, especially in heating-dominant sites with low sharing potentials. The scope of this research was limited to waste energy recovery from cooling and refrigeration processes. Therefore, it is recommended that future work explore other waste heat sources (e.g., solar thermal, industrial, sewer water, etc). Finally, the cost and economic performance of the system, as well as a life cycle analysis, should be explored in future work as well.

Acknowledgments

This work was supported by the Natural Sciences and Engineering Research Council of Canada [CRDPJ 509219-2017] and the Ontario Centre of Innovation [27851]. The authors would also like to acknowledge the McMaster Energy Research Cooperative partners for their contributions: HCE Energy Inc., GridSmartCity, GeoSource Energy Inc., s2e Technologies Inc., Siemens Canada Limited, Enbridge Gas Inc., and Alectra Utilities Corporation.

Appendix A

A.1. Thermal network and energy transfer station modeling steps

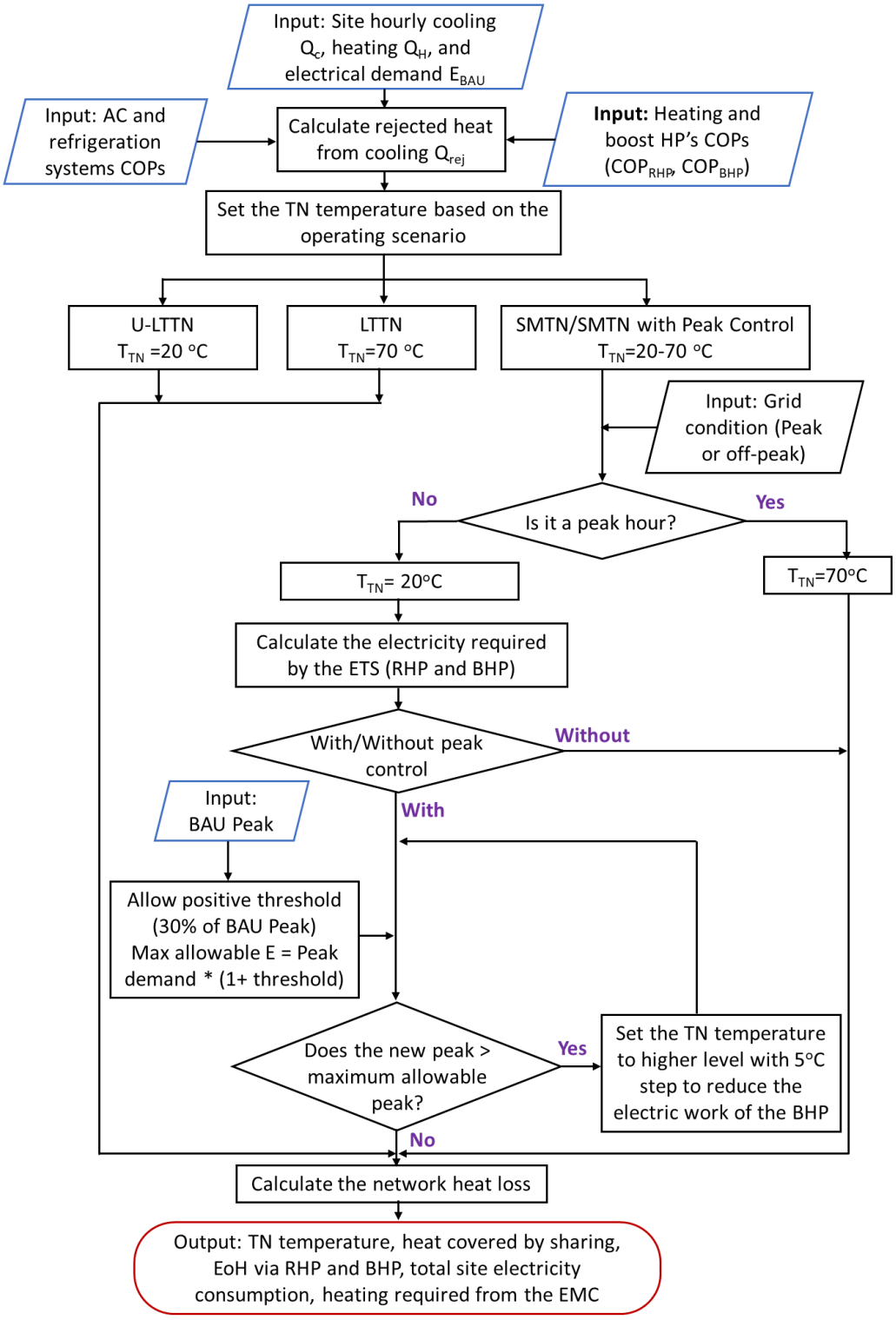

Figure A1: Thermal network and energy transfer station modeling steps

A.2. EMC modeling steps

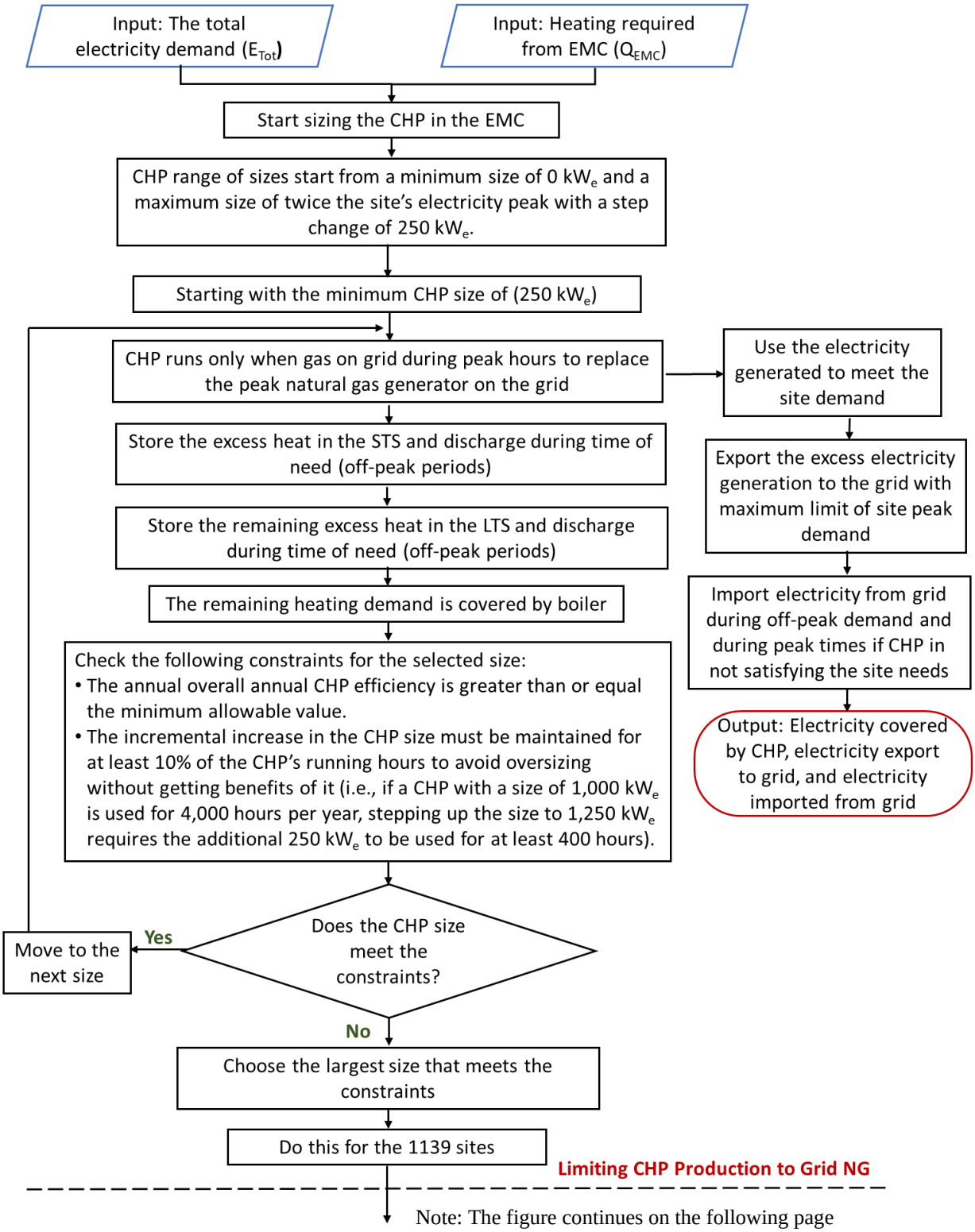

Note: The figure continues on the following page

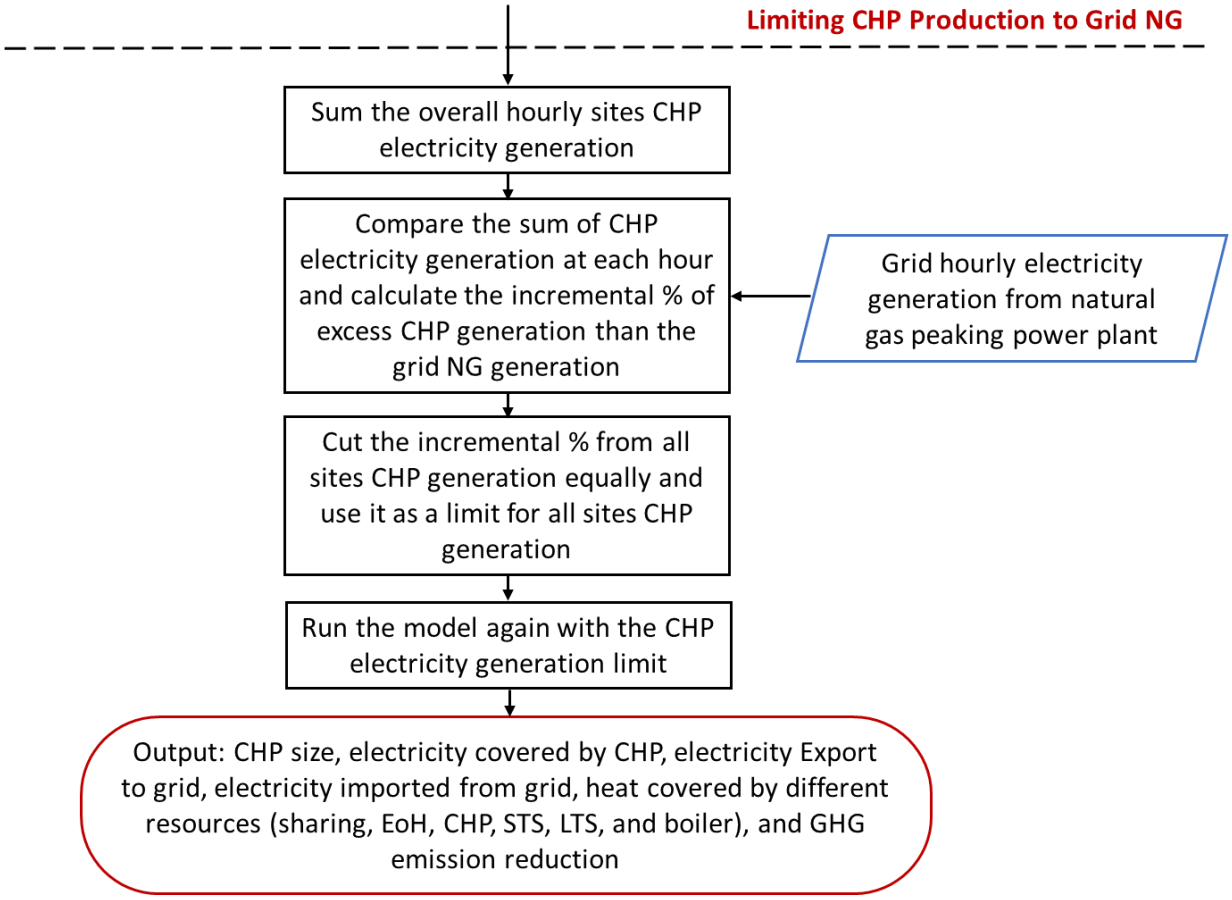

Figure A2: EMC modeling steps

Appendix B

Model verification

The mathematical model used in this current work was developed on Matlab and tested using the hourly resolution data attained via Van Ryn's Dymola model [33]. The Dymola model was run using a 10 minute resolution, with the average hourly results being used for the comparison. The case study includes 5 buildings: an ice arena, a community center, a library with an IT server, a YMCA, and a residential tower. Table B1 lists the buildings' cumulative energy profiles. This site's cooling load accounts for 40% of the overall thermal energy consumption; according to the classifications outlined by Abdallah et al. [15], this site would be categorized as balanced.

Table B1: Total heating and cooling energy.

Demand source	Energy demand [MWh]
Cooling	10,808
Heating	7,341
Electricity	4,918
Heat rejection	8,655

The comparison was performed using a constant network operation temperature of 70^{o}C. The modeling operation and calculations are described in the Methodology section. The results generated by both models were compared, including the amount of heat shared (harvested heat from cooling systems), the network thermal losses, the heat required from the EMC, and the heat covered by the different resources in the EMC, such as the CHP, STS, and boiler. The network used in the model was 900 m long, the CHP size was 3,500 KW_{th}, and the STS size was 1,000 m^3.

Figure B1 shows the annual energy results for the Matlab and the Dymola models. The largest differences between the two models are the quantity of heat loss and the heat required from the EMC. The Matlab model suffered a loss of 278 MWh, accounting for 2.5% of the overall site heating demand; by contrast, the Dymola model only had losses of 175 MWh, which accounted

for 1.6% of the site's overall heating demand. This difference is likely attributable to the type of pipe insulation used in both models. The Matlab model used fiberglass insulation with a thermal conductivity of 0.042 W/mK, while the Dymola model used urethane foam insulation with a 0.022W/mK thermal conductivity. These differences resulted in a larger heating requirement from the EMC resources, mainly the CHP and STS, as shown in Figure B1.

Overall, the models showed good agreement, thus providing confidence in the application of the Matlab model.

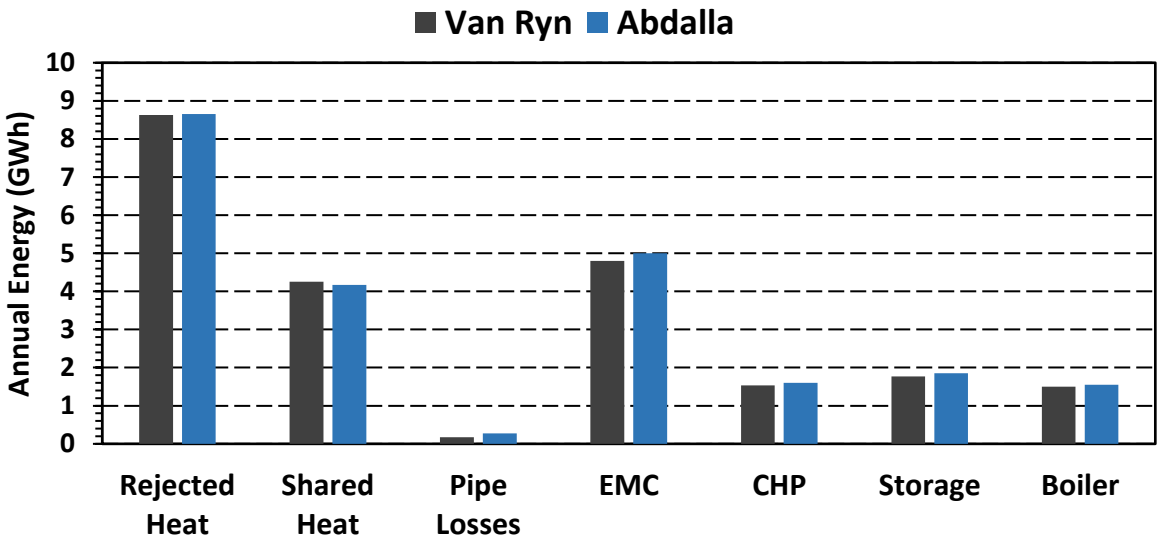

Figure B1: Comparison between the annual energy results from the Matlab model vs. the Dymola model.

Appendix C

This section details the effects of the TN temperature operation schedule on the hourly electricity consumption of an extra heating-dominated cluster, which represents around 45% of the clusters in Ontario. Figure C 4-1 shows a comparison of the hourly electricity consumption for the U-LTTN, LTTN, SMTN, and SMTN with peak control systems versus the BAU system's electricity consumption (black). As can be seen, electricity consumption increased slightly during the summer for all scenarios. This result is due to the fact that heating requirements are very low during the summer, typically only being required for domestic hot water.

In the U-LTTN scenario, the TN heating source consists of harvested residual heat and the EMC gas-fired boiler at low temperatures. Boost heat pumps are used to increase the network temperature to meet the temperature requirements of the buildings' heating distribution systems. The boost heat pump runs continuously during peak and off-peak hours, which results in a significant increase in electricity consumption during these times. This case entails the largest use of EoH and the lowest usage of natural-gas-fired boilers. As shown in Figure C 4-1a, the site peak electricity rose to more than twice that of the conventional system in this operating scenario.

Conversely, the LTTN scenario had the lowest EoH year-round (Figure C 4-1b), as the network operates at a higher temperature than the building heating requirements, thus allowing for a direct exchange of heat without the need for a BHP. The increased electrical demand in this scenario comes from the RHP, which raises the temperature of heat rejected from the buildings' cooling systems and exchanges it with the network. Although electricity consumption also increases significantly in the SMTN scenario (Figure C 4-1c), this increase happens only during off-peak periods when the network runs at ultra-low temperatures. During peak hours, the SMTN runs as an LTTN to reduce EoH. Although the large rise in electricity consumption during off-peak periods is favorable for harvesting carbon-free resources curtailed from the grid, the site electricity peak demand increased to 4.4MW, just over double the conventional system peak (2.12MW). As a result, large infrastructure upgrades in the distribution grid or a larger share of battery storage are necessary. In the SMTN with peak control scenario (Figure C 4-1d), electricity consumption increased during off-peak periods similar to the SMTN scenario, but the increase is always limited to ensure peaks do not surpass 2.75 MW, which is 30% higher than the BAU peak. The 30% limit was set as an arbitrary value that can vary from the conventional peak to a maximum value equal

to the U-LTTN peak. This limitation in the electricity usage for heating is replaced by a gas-fired boiler; however, this only happens in extremely cold weather hours.

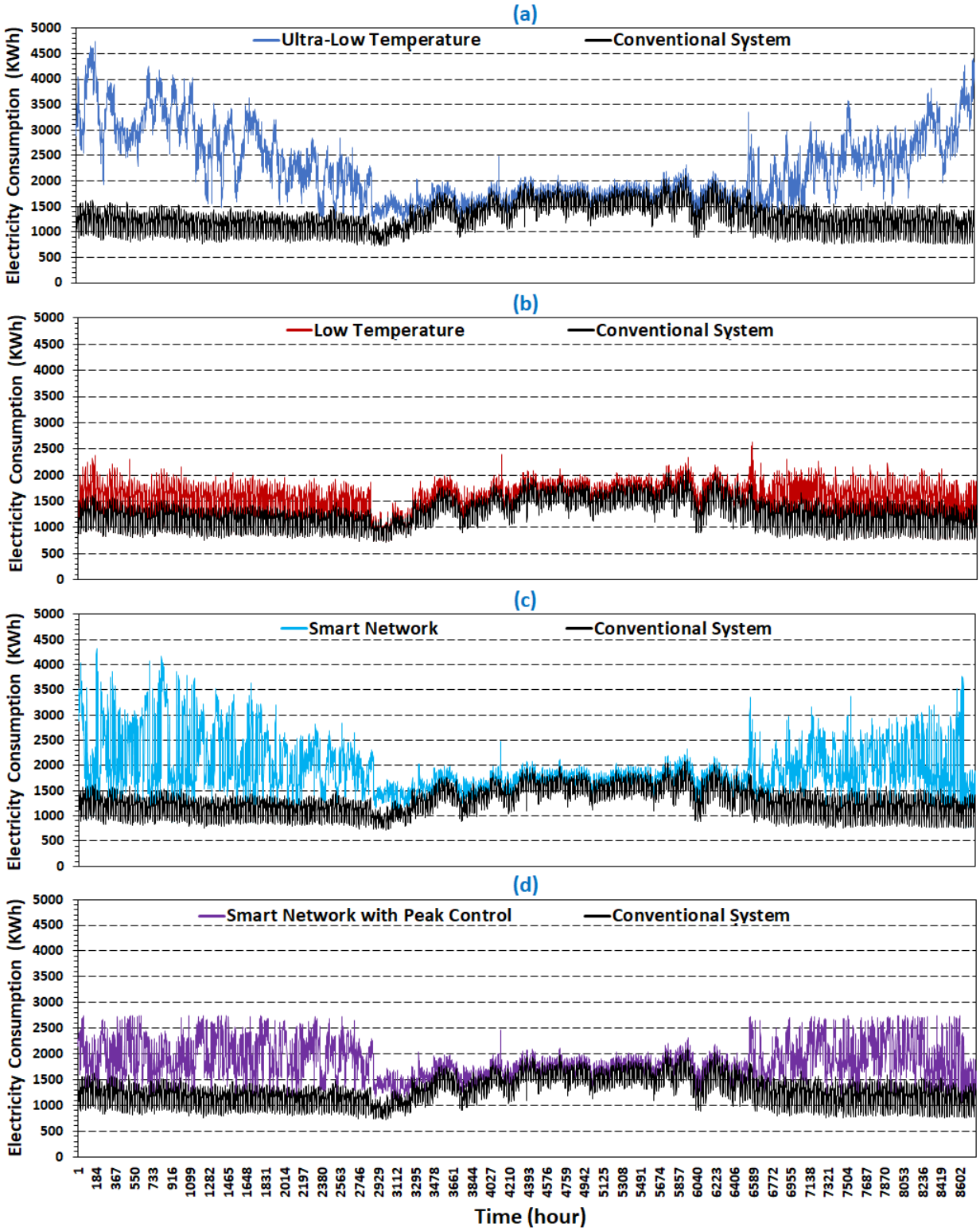

Figure C 4-1: Hourly electricity consumption compared to the BAU electricity consumption for an extra heating-dominated cluster: a) U-LTTN*; b) LTTN; c) SMTN; (d) SMTN with peak control.*

References

[1] International Energy Agency (IEA), "Towards a zero-emission, efficient, and resilient buildings and construction sector," Global Status Report, 2017. [Online]. Available: www.globalabc.org.

[2] A. Abdalla, S. Mohamed, S. Bucking, and J. S. Cotton, "Modeling of thermal energy sharing in integrated energy communities with micro-thermal networks," Energy Build., vol. 248, p. 111170, Jun. 2021, doi: 10.1016/j.enbuild.2021.111170.

[3] M. Y. Abdelsalam et al., "Integrated Community Energy and Harvesting Systems: A Climate Action Strategy for Cold Climates," Appl. Energy, 2022.

[4] "European Commission"District heating system of the municipality of Bucharest"." [Online]. Available: https://ec.europa.eu/commission/presscorner/detail/fr/ip_21_762.

[5] S. Werner, "International review of district heating and cooling," Energy, vol. 137, pp. 617–631, 2017, doi: 10.1016/j.energy.2017.04.045.

[6] F. Bouffard and D. S. Kirschen, "Centralised and distributed electricity systems," Energy Policy, vol. 36, no. 12, pp. 4504–4508, Dec. 2008, doi: 10.1016/J.ENPOL.2008.09.060.

[7] M. Wirtz, L. Kivilip, P. Remmen, and D. Müller, "5th Generation District Heating: A novel design approach based on mathematical optimization," Appl. Energy, vol. 260, no. July 2019, p. 114158, 2020, doi: 10.1016/j.apenergy.2019.114158.

[8] S. Buffa, M. Cozzini, M. D. Antoni, M. Baratieri, and R. Fedrizzi, "5th generation district heating and cooling systems : A review of existing cases in Europe," Renew. Sustain. Energy Rev., vol. 104, no. October 2018, pp. 504–522, 2019, doi: 10.1016/j.rser.2018.12.059.

[9] F. Calise, F. L. Cappiello, M. Dentice d'Accadia, F. Petrakopoulou, and M. Vicidomini, "A solar-driven 5th generation district heating and cooling network with ground-source heat pumps: a thermo-economic analysis," Sustain. Cities Soc., vol. 76, p. 103438, 2022, doi: https://doi.org/10.1016/j.scs.2021.103438.

[10] J. von Rhein, G. P. Henze, N. Long, and Y. Fu, "Development of a topology analysis tool for fifth-generation district heating and cooling networks," Energy Convers. Manag., vol. 196, no. November 2018, pp. 705–716, 2019, doi: 10.1016/j.enconman.2019.05.066.

[11] K. Gjoka, B. Rismanchi, and R. H. Crawford, "Fifth-generation district heating and cooling systems: A review of recent advancements and implementation barriers," Renew. Sustain. Energy Rev., vol. 171, no. October 2022, p. 112997, 2023, doi: 10.1016/j.rser.2022.112997.

[12] R. Rogers, V. Lakhian, M. Lightstone, and J. S. Cotton, "Modeling of Low Temperature Thermal Networks Using Historical Building Data from District Energy Systems," Proc. 13th Int. Model. Conf. Regensburg, Ger. March 4–6, 2019, vol. 157, pp. 543–550, 2019, doi: 10.3384/ecp19157543.

[13] M. Y. Abdelsalam, B. Sullivan, M. Lightstone, and J. S. Cotton, "Integrated Community Energy and Harvesting Systems: A comparative study of a heating dominant building

cluster," Renew. Sustain. Energy Rev., 2022.

[14] R. Z. Pass, M. Wetter, and M. A. Piette, "A thermodynamic analysis of a novel bidirectional district heating and cooling network," Energy, vol. 144, pp. 20–30, 2018, doi: 10.1016/j.energy.2017.11.122.

[15] A. Abdalla, S. Mohamed, F. Kelton, S. Bucking, and J. S. Cotton, "The impact of clustering strategies to site integrated community energy and harvesting systems on electrical demand and regional GHG reductions," Energy Convers. Manag.

[16] Goverment of Canada, "Canada - Heating Degree-Days." [Online]. Available: https://open.canada.ca/data/en/dataset/fd8efb83-b73d-5442-ab60-7987c824f5fd.

[17] U.S. Energy Information Administration (EIA), "Heating degree days (HDD)." [Online]. Available: https://www.eia.gov/energyexplained/units-and-calculators/degree-days.php.

[18] Eurostat, "Heating degree days," 2021.

[19] Current Results, "Toronto Temperatures: Averages by Month," 2022. [Online]. Available: https://www.currentresults.com/Weather/Canada/Ontario/Places/toronto-temperatures-by-month-average.php. [Accessed: 22-Oct-2020].

[20] M. Waite and V. Modi, "Electricity Load Implications of Space Heating Decarbonization Pathways," Joule, vol. 4, no. 2, pp. 376–394, 2020, doi: 10.1016/j.joule.2019.11.011.

[21] T. D. Hutty, N. Patel, S. Dong, and S. Brown, "Can thermal storage assist with the electrification of heat through peak shaving?," Energy Reports, vol. 6, pp. 124–131, 2020, doi: 10.1016/j.egyr.2020.03.006.

[22] Durham Energy Institute and Element Energy, "Insight Report : Domestic Heat Pumps," no. January, pp. 1–26, 2015.

[23] S. J. G. Cooper, G. P. Hammond, M. C. McManus, and D. Pudjianto, "Detailed simulation of electrical demands due to nationwide adoption of heat pumps, taking account of renewable generation and mitigation," IET Renew. Power Gener., vol. 10, no. 3, pp. 380–387, 2016, doi: 10.1049/iet-rpg.2015.0127.

[24] Cortes Currents, "Transmission Grid Loss," 2022. [Online]. Available: https://cortescurrents.ca/transmission-grid-loss/. [Accessed: 24-Oct-2022].

[25] Ontario Energy Board, "Ontario Wholesale Electricity Market Price Forecast," 2020. [Online]. Available: https://www.oeb.ca/sites/default/files/rpp-wholesale-electricity-market-price-forecast-20201013.pdf.

[26] Danish Energy Agency, "Regulation and planning of district heating in Denmark," p. 27, 2016.

[27] ENERGINET, "Environmental report for Danish electricity and CHP for 2017 status year," 2017.

[28] Reuters, "Denmark sources record 47% of power from wind in 2019," 2020. [Online]. Available: https://www.reuters.com/article/us-climate-change-denmark-windpower-idUSKBN1Z10KE.

[29] J. Wang, S. You, Y. Zong, H. Cai, C. Træholt, and Z. Y. Dong, "Investigation of real-time flexibility of combined heat and power plants in district heating applications," Appl. Energy, vol. 237, no. January, pp. 196–209, 2019, doi: 10.1016/j.apenergy.2019.01.017.

[30] A. Franco and M. Versace, "Optimum sizing and operational strategy of CHP plant for district heating based on the use of composite indicators," Energy, vol. 124, pp. 258–271, 2017, doi: 10.1016/j.energy.2017.02.062.

[31] "The Independent Electricity System Operator (IESO) of Ontario's power system." [Online]. Available: https://www.ieso.ca/en/Corporate-IESO/Media/Year-End-Data.

[32] A. Abdalla, S. Mohamed, S. Bucking, and J. S. Cotton, "Modeling of thermal energy sharing in integrated energy communities with micro-thermal networks," Energy Build., p. 111170, Jun. 2021, doi: 10.1016/j.enbuild.2021.111170.

[33] J. Van Ryn, J. S. Cotton, and M. Lightstone, "Utilizing Micro-Thermal Networks for Energy Demand Response," (MSc thesis) McMaster, 2022.

[34] H. Kauko, K. H. Kvalsvik, D. Rohde, N. Nord, and Å. Utne, "Dynamic modeling of local district heating grids with prosumers: A case study for Norway," Energy, vol. 151, pp. 261–271, 2018, doi: 10.1016/j.energy.2018.03.033.

[35] Y. A. Cengel, Thermodynamics: An Engineering Approach, vol. 8, no. 1. 1998.

[36] I. American Society of Heating, Refrigerating and Air-Conditioning Engineers, "Energy standard for buildings except low-rise residential buildings," 2013.

[37] P. Wallentén, "Steady-state heat loss from insulated pipes," Byggnadsfysik LTH, Lunds Tek. Högskola, p. 197, 1991.

[38] C. Miler, "Experimental Evaluation of Thermal Response Tests Performed on Borehole Strings," (MSc thesis) McMaster University, 2020.

[39] P. Kandiah and M. Lightstone, "CFD Study of a Large Buried Tank Within a Borehole Field," M.A.Sc. Thesis, McMaster, 2014.

[40] B. Sullivan, M. Lightstone, and J. Cotton, "A Comparison of Different Heating and Cooling Energy Delivery Systems and The Integrated Community Energy and Harvesting System in Heating Dominant Communities," (MSc thesis) Mcmaster University, 2020.

[41] Association of Power Producers of Ontario, "Renewed interest in Cogeneration – behind the meter." [Online]. Available: https://magazine.appro.org/news/ontario-news/4347-renewed-interest-in-cogeneration-behind-the-meter-.html.

[42] Canada, Library and Archives Canada Cataloguing in Publication Canada Main entry under title: National Inventory Report 1990-2018: Greenhouse Gas Sources and Sinks in Canada. 2019.

[43] M. St-Jacques, S. Bucking, and W. O'Brien, "Spatially and temporally sensitive consumption-based emission factors from mixed-use electrical grids for building electrical use," Energy Build., vol. 224, p. 110249, 2020, doi: 10.1016/j.enbuild.2020.110249.

[44] Z. Song et al., "Integration of geothermal water into secondary network by absorption-heat-

pump-assisted district heating substations," Energy Build., vol. 202, p. 109403, 2019, doi: 10.1016/j.enbuild.2019.109403.

[45] M. Ameri and Z. Besharati, "Optimal design and operation of district heating and cooling networks with CCHP systems in a residential complex," Energy Build., vol. 110, pp. 135–148, 2016, doi: 10.1016/j.enbuild.2015.10.050.

[46] R. Abdurafikov et al., "An analysis of heating energy scenarios of a Finnish case district," Sustain. Cities Soc., vol. 32, pp. 56–66, 2017, doi: 10.1016/j.scs.2017.03.015.

Chapter 5

Conclusions and Recommendations For Future Work

5.1. Conclusions

This research investigates the impact of harvesting residual energy via integrating the electrical and thermal community buildings' energy systems which plays an important role in the decarbonization of heating in the building sector. Increasing the use of renewable energy resources to electricity generation requires more flexible generation resources and demands; this increases the need for a combined thermal and electrical demand management strategy that minimizes the curtailed electricity on the grid and electrifies heating without increasing the electricity peak demand.

The current research **developed an integrated community energy thermal energy sharing model** that can provide a dynamic characterization of the potential benefits of integrating and harvesting energy within a community of any number of buildings. The developed model estimates the amount of rejected heat from cooling and refrigeration systems that can be simultaneously collected and used to heat other nearby buildings in the cluster. It also evaluates the timing and quantity of electricity used by the heat pumps necessary in low-temperature MTNs as well as the reduction of both GHG emissions and the energy required from the EMC relative to BAU conventional stand-alone systems. For an energy balanced community cluster, the model showed that, over the course of a year, the energy harvesting would reduce this node's GHG emissions by 74% and cover approximately 82% of the heating requirements compared to the BAU system.

Selected buildings in integrated community energy clusters are affecting the benefits of integration. **Two novel clustering techniques were proposed and examined in the current work** for Integrated Community Energy and Harvesting systems (ICE-Harvest) that prioritize the harvesting of waste heat rejected from cooling processes to help satisfy the heating demands of

commercial and residential buildings. Clustering around anchor building and density-based (DB) clustering with post-processing by adding the nearest anchor building to each cluster were developed based on the energy diversity in the connected buildings in each cluster. These techniques were examined with the aid of the developed energy sharing model over a large high energy consumption buildings database in Ontario and compared to the commonly used DB clustering technique in the literature. The results of this case study reveal that DB clustering with post-processing resulted in the highest GHG reduction per unit piping network length of 360 t CO_2eq /km/year. In addition, this research identified seven different cluster categories based on the total annual and simultaneous cooling-to-heating ratios of each cluster.

The ICE harvest system integrates the thermal and electrical networks to add more flexibility to the electricity grid and schedule the EoH. In addition, it harvests wasted energy from three main different resources, process cooling, surplus carbon-free electricity generation on the electricity grid; and wasted heat from peak gas generators. Current research provides a reduced model for the ICE-Harvest system to study its impact on a fleet of over 1100 clusters of different categories on a municipal or provincial/state scale on the GHG emission and electricity demand from the grid. The use of ICE-Harvest systems on this scale can displace the energy required from the gas-fired heating resources by 11 TWh, accounting for over 70% of the clusters' total heating requirements. This results in a 1.9 Mt CO_2eq reduction in total GHG emissions, which represents around 60% of the clusters' emissions.

Operating conditions of the TN in the integrated community energy systems affect the ability to harvest waste energy and the reduction of GHG emissions. Modeling of four different thermal distribution network operating scenarios was performed in this research for the previously identified different community energy profiles. These operation scenarios include low-temperature

(fourth- generation), ultra-low (fifth generation), a binary range-controlled temperature modulating thermal network (smart network ICE-Harvest), and a range-controlled temperature modulating micro-thermal network (smart network with peak control) which variably change the thermal network temperature to control peak electricity demand caused by electrification of heating. The Ultra-low temperature thermal network shows high emission savings in sites with high simultaneous cooling and heating such as high concurrent balanced and high concurrent cooling dominant clusters, especially with grids of low natural gas generation resources and peak hours as well as high carbon-free electricity generation. It causes a significant increase in the electricity demand in heating dominant clusters during peak periods thus adding a great challenge during peak periods which also increases GHG emissions, especially for the extra heating dominant sites. Conversely, the low-temperature thermal network causes the least usage of electrification of heating and the most usage of gas-fired boilers in integrated systems thus, low effect on the electricity grid as well as slight benefit from the grid curtailed carbon-free resources. This results in the least electricity demand and consumption at all times thus, losses the benefit from electrification of heating during off-peak periods. It has higher GHG emission savings than the ultra-low in heating dominant sites. Smart thermal network operation balances the electricity grid through electrifying heating only during periods of surplus carbon-free electricity generation. Although, this operation results in the most emission savings compared to all other scenarios of operation as it allows EoH only during off-peak periods, it increases the site electricity peak demand to more than double in heating dominant sites. The proposed operating scenario smart network with peak control adds more flexibility to the system. It balances the electricity grid like the smart network scenario. It also results in GHG emission savings slightly lower than the smart thermal network operating scenario, but without the huge increase in site electricity peak demand.

The integration of CHP adds a large benefit especially for heating dominant sites as well as in sites connected to grids with high electricity generation from natural gas resources.

The last model was implemented on the 1139 identified sites with different energy profiles in Ontario, Canada, and the following is concluded:

- For most of the heating-dominated clusters, it is better to employ the SMTN with peak control and CHP on sites to serve the high heating demands- this will require more thermal storage especially seasonally.
- For the majority of balanced and /or cooling-dominated clusters, it is better to implement more carbon-free resources to the electricity grid or on-site that produce electricity but are not associated with heat such as wind, hydro, and solar PV panels.

Another conclusion is that the CHP size and operating hours highly affect the GHG emission saving wherein the CHP in this work were sized to achieve a minimum overall efficiency in the ranges from 55% to 80% with two different operating hours percentages low 36% and high 93% following the NG operating hours in Ontario grid for the years 2017 and 2016 respectively. The results showed a significant reduction of around 35% of the 1139 sites' emissions for the lower efficiencies ranges of 55%-65% with 36% CHP operating hours, where the low efficiencies allow larger sizes of CHPs. And the savings almost doubled for 2016 with 93% CHP operating hours.

On the other hand, the GHG savings is very low in the high-efficiencies range as the CHPs sized to very small sizes in order to achieve these high efficiencies. Also, short and long-term thermal storages play a great role in harvesting the CHP residual heat thus reducing the sites' emissions. The study shows that about half the emission saving of the CHP residual heat is achieved by short and long-term storage.

5.2. Recommendations for Future Work

Investigating the impact of integrating the electrical and thermal community buildings' energy systems on the reduction of GHG emissions and energy harvesting between buildings is challenging. Although the contributions made by the research in this thesis address many of these challenges, there remain several avenues for future research to build upon this work, including:

- Investigating the integration of Air source heat pumps ASHP that operates during periods of moderate outdoor temperature (>5^{o}C) and during shoulder season with thermal storage especially for heating dominant sites and with grids that use high carbon-free electricity generation.
- Investigate the effect of intra-cluster by using a connected energy hub to serve different thermal networks and gain from diversity loads.
- Study the impact of using the TN to operate according to the space heating that requires a heat source in the range of 30-40^{o}C and the small load of domestic heating that requires 60-70^{o}C can be served by an extra heat pump. This might impact the EoH and the system's performance.
- This research was limited to waste energy recovery from cooling and refrigeration processes. It is recommended that other waste heat sources are explored in future research (solar thermal, industrial, sewer water, etc.). Which will also require an upgraded clustering technique.
- According to the case study on Ontario, only 42% of the total waste heat from the sites' cooling processes is harvested. Most of the heat is rejected during the summer season with

low heating demands. Using seasonal storage to harvest this heat is a recommendation for future work.

- The cost and economic performance of the ICE-Harvesting system as well as its life cycle analysis could be investigated in future work.
- Consider adding low emissions combined electrothermal resources in the EMC instead of the natural gas operated CHP such as fuel cells or small modular reactors.